

ISSN 1881-7815    Online ISSN 1881-7823

# **BST**

# **BioScience Trends**

Volume 19, Number 1  
February 2025



[www.biosciencetrends.com](http://www.biosciencetrends.com)



# BST

## BioScience Trends



ISSN: 1881-7815  
Online ISSN: 1881-7823

CODEN: BTIRCZ

Issues/Year: 6

Language: English

Publisher: IACMHR Co., Ltd.

**BioScience Trends** is one of a series of peer-reviewed journals of the International Research and Cooperation Association for Bio & Socio-Sciences Advancement (IRCA-BSSA) Group. It is published bimonthly by the International Advancement Center for Medicine & Health Research Co., Ltd. (IACMHR Co., Ltd.) and supported by the IRCA-BSSA.

**BioScience Trends** devotes to publishing the latest and most exciting advances in scientific research. Articles cover fields of life science such as biochemistry, molecular biology, clinical research, public health, medical care system, and social science in order to encourage cooperation and exchange among scientists and clinical researchers.

**BioScience Trends** publishes Original Articles, Brief Reports, Reviews, Policy Forum articles, Communications, Editorials, News, and Letters on all aspects of the field of life science. All contributions should seek to promote international collaboration.

## Editorial Board

### Editor-in-Chief:

Norihiro KOKUDO  
*National Center for Global Health and Medicine, Tokyo, Japan*

### Co-Editors-in-Chief:

Xishan HAO  
*Tianjin Medical University, Tianjin, China*  
Takashi KARAKO  
*National Center for Global Health and Medicine, Tokyo, Japan*  
John J. ROSSI  
*Beckman Research Institute of City of Hope, Duarte, CA, USA*

Hongen LIAO  
*Tsinghua University, Beijing, China*  
Misao MATSUSHITA  
*Tokai University, Hiratsuka, Japan*  
Fanghua QI  
*Shandong Provincial Hospital, Ji'nan, China*  
Ri SHO  
*Yamagata University, Yamagata, Japan*  
Yasuhiko SUGAWARA  
*Kumamoto University, Kumamoto, Japan*  
Ling WANG  
*Fudan University, Shanghai, China*

### Senior Editors:

Tetsuya ASAKAWA  
*The Third People's Hospital of Shenzhen, Shenzhen, China*  
Yu CHEN  
*The University of Tokyo, Tokyo, Japan*  
Xunjia CHENG  
*Fudan University, Shanghai, China*  
Yoko FUJITA-YAMAGUCHI  
*Beckman Research Institute of the City of Hope, Duarte, CA, USA*  
Jianjun GAO  
*Qingdao University, Qingdao, China*  
Na HE  
*Fudan University, Shanghai, China*

### Proofreaders:

Curtis BENTLEY  
*Roswell, GA, USA*  
Thomas R. LEBON  
*Los Angeles, CA, USA*

### Editorial and Head Office

Pearl City Koishikawa 603,  
2-4-5 Kasuga, Bunkyo-ku, Tokyo 112-0003, Japan  
E-mail: [office@biosciencetrends.com](mailto:office@biosciencetrends.com)

# BioScience Trends

## Editorial and Head Office

Pearl City Koishikawa 603, 2-4-5 Kasuga, Bunkyo-ku,  
Tokyo 112-0003, Japan

E-mail: [office@biosciencetrends.com](mailto:office@biosciencetrends.com)  
URL: [www.biosciencetrends.com](http://www.biosciencetrends.com)

## Editorial Board Members

Girdhar G. AGARWAL  
(Lucknow, India)

Hirotsugu AIGA  
(Geneva, Switzerland)

Hidechika AKASHI  
(Tokyo, Japan)

Moazzam ALI  
(Geneva, Switzerland)

Ping AO  
(Shanghai, China)

Hisao ASAMURA  
(Tokyo, Japan)

Michael E. BARISH  
(Duarte, CA, USA)

Boon-Huat BAY  
(Singapore, Singapore)

Yasumasa BESSHO  
(Nara, Japan)

Generoso BEVILACQUA  
(Pisa, Italy)

Shiuan CHEN  
(Duarte, CA, USA)

Yi-Li CHEN  
(Yiwu, China)

Yue CHEN  
(Ottawa, Ontario, Canada)

Naoshi DOHMAE  
(Wako, Japan)

Zhen FAN  
(Houston, TX, USA)

Ding-Zhi FANG  
(Chengdu, China)

Xiao-Bin FENG  
(Beijing, China)

Yoshiharu FUKUDA  
(Ube, Japan)

Rajiv GARG  
(Lucknow, India)

Ravindra K. GARG  
(Lucknow, India)

Makoto GOTO  
(Tokyo, Japan)

Demin HAN  
(Beijing, China)

David M. HELFMAN  
(Daejeon, Korea)

Takahiro HIGASHI  
(Tokyo, Japan)

De-Fei HONG  
(Hangzhou, China)

De-Xing HOU  
(Kagoshima, Japan)

Sheng-Tao HOU  
(Guanzhou, China)

Xiaoyang HU  
(Southampton, UK)

Yong HUANG  
(Ji'ning, China)

Hirofumi INAGAKI  
(Tokyo, Japan)

Masamine JIMBA  
(Tokyo, Japan)

Chun-Lin JIN  
(Shanghai, China)

Kimitaka KAGA  
(Tokyo, Japan)

Michael Kahn  
(Duarte, CA, USA)

Kazuhiro KAKIMOTO  
(Osaka, Japan)

Kiyoko KAMIBEPPU  
(Tokyo, Japan)

Haidong KAN  
(Shanghai, China)

Kenji KARAKO  
(Tokyo, Japan)

Bok-Luel LEE  
(Busan, Korea)

Chuan LI  
(Chengdu, China)

Mingjie LI  
(St. Louis, MO, USA)

Shixue LI  
(Ji'nan, China)

Ren-Jang LIN  
(Duarte, CA, USA)

Chuan-Ju LIU  
(New York, NY, USA)

Lianxin LIU  
(Hefei, China)

Xinqi LIU  
(Tianjin, China)

Daru LU  
(Shanghai, China)

Hongzhou LU  
(Guanzhou, China)

Duan MA  
(Shanghai, China)

Masatoshi MAKUUCHI  
(Tokyo, Japan)

Francesco MAROTTA  
(Milano, Italy)

Yutaka MATSUYAMA  
(Tokyo, Japan)

Qingyue MENG  
(Beijing, China)

Mark MEUTH  
(Sheffield, UK)

Michihiro Nakamura  
(Yamaguchi, Japan)

Munehiro NAKATA  
(Hiratsuka, Japan)

Satoko NAGATA  
(Tokyo, Japan)

Miho OBA  
(Odawara, Japan)

Xianjun QU  
(Beijing, China)

Carlos SAINZ-FERNANDEZ  
(Santander, Spain)

Yoshihiro SAKAMOTO  
(Tokyo, Japan)

Erin SATO  
(Shizuoka, Japan)

Takehito SATO  
(Isehara, Japan)

Akihito SHIMAZU  
(Tokyo, Japan)

Zhifeng SHAO  
(Shanghai, China)

Xiao-Ou SHU  
(Nashville, TN, USA)

Sarah Shuck  
(Duarte, CA, USA)

Judith SINGER-SAM  
(Duarte, CA, USA)

Raj K. SINGH  
(Dehradun, India)

Peipei SONG  
(Tokyo, Japan)

Junko SUGAMA  
(Kanazawa, Japan)

Zhipeng SUN  
(Beijing, China)

Hiroshi TACHIBANA  
(Isehara, Japan)

Tomoko TAKAMURA  
(Tokyo, Japan)

Tadatoshi TAKAYAMA  
(Tokyo, Japan)

Shin'ichi TAKEDA  
(Tokyo, Japan)

Sumihito TAMURA  
(Tokyo, Japan)

Puay Hoon TAN  
(Singapore, Singapore)

Koji TANAKA  
(Tsu, Japan)

John TERMINI  
(Duarte, CA, USA)

Usa C. THISYAKORN  
(Bangkok, Thailand)

Toshifumi TSUKAHARA  
(Nomi, Japan)

Mudit Tyagi  
(Philadelphia, PA, USA)

Kohjiro UEKI  
(Tokyo, Japan)

Masahiro UMEZAKI  
(Tokyo, Japan)

Junming WANG  
(Jackson, MS, USA)

Qing Kenneth WANG  
(Wuhan, China)

Xiang-Dong WANG  
(Boston, MA, USA)

Hisashi WATANABE  
(Tokyo, Japan)

Jufeng XIA  
(Tokyo, Japan)

Feng XIE  
(Hamilton, Ontario, Canada)

Jinfu XU  
(Shanghai, China)

Lingzhong XU  
(Ji'nan, China)

Masatake YAMAUCHI  
(Chiba, Japan)

Aitian YIN  
(Ji'nan, China)

George W-C. YIP  
(Singapore, Singapore)

Xue-Jie YU  
(Galveston, TX, USA)

Rongfa YUAN  
(Nanchang, China)

Benny C-Y ZEE  
(Hong Kong, China)

Yong ZENG  
(Chengdu, China)

Wei ZHANG  
(Shanghai, China)

Wei ZHANG  
(Tianjin, China)

Chengchao ZHOU  
(Ji'nan, China)

Xiaomei ZHU  
(Seattle, WA, USA)

(as of February 2025)

**Editorial**

- 1-9            **Serum proteomics reveals early biomarkers of Alzheimer's disease: The dual role of *APOE-ε4*.**  
*Ya-nan Ma, Ying Xia, Kenji Karako, Peipei Song, Wei Tang, Xiqi Hu*

**Review**

- 10-30        **The glamor of and insights regarding hydrotherapy, from simple immersion to advanced computer-assisted exercises: A narrative review.**  
*Yaohan Peng, Yucong Zou, Tetsuya Asakawa*
- 31-52        **Post-stroke dysphagia: Neurological regulation and recovery strategies.**  
*Xinyue Li, Minmin Wu, Jiongliang Zhang, Donghui Yu, Yuting Wang, Yumeng Su, Xiangyu Wei, Xun Luo, Qing Mei Wang, Luwen Zhu*
- 53-71        **From light to insight: Functional near-infrared spectroscopy for unravelling cognitive impairment during task performance.**  
*Na Liu, Lingling Yang, Xiuqing Yao, Yaxi Luo*
- 72-86        **Growth and differentiation factor 15: An emerging therapeutic target for brain diseases.**  
*Yingying Zhou, Lei Dou, Luyao Wang, Jiajie Chen, Ruxue Mao, Lingqiang Zhu, Dan Liu, Kai Zheng*

**Original Article**

- 87-101      **Intestinal microbiota distribution and changes in different stages of Parkinson's disease: A meta-analysis, bioinformatics analysis and *in vivo* simulation.**  
*Tingyue Jiang, Yu Wang, Wenxin Fan, Yifan Lu, Ge Zhang, Jiayuan Li, Renzhi Ma, Mengmeng Liu, Jinli Shi*
- 102-115     ***N*<sup>5</sup>-((perfluorophenyl)amino)glutamine regulates BACE1, tau phosphorylation, synaptic function, and neuroinflammation in Alzheimer's disease models.**  
*Jun-Sik Kim, Yongeun Cho, Jeongmi Lee, Heewon Cho, Sukmin Han, Yeongyeong Lee, Yeji Jeon, Tai Kyoung Kim, Ju-Mi Hong, Jeonghyeong Im, Minshik Chae, Yujeong Lee, Hyunwook Kim, Sang Yoon Park, Sung Hyun Kim, Joung Han Yim, Dong-Gyu Jo*
- 116-124     **Plasma extracellular vesicle pathognomonic proteins as the biomarkers of the progression of Parkinson's disease.**  
*Chien-Tai Hong, Chen-Chih Chung, Yi-Chen Hsieh, Lung Chan*
- 125-139     **Multimodal optimal matching and augmentation method for small sample gesture recognition.**  
*Wenli Zhang, Bo Liu, Tingsong Zhao, Shuyan Qie*



# Serum proteomics reveals early biomarkers of Alzheimer's disease: The dual role of *APOE-ε4*

Ya-nan Ma<sup>1</sup>, Ying Xia<sup>1</sup>, Kenji Karako<sup>2</sup>, Peipei Song<sup>3,\*</sup>, Wei Tang<sup>2,3</sup>, Xiqi Hu<sup>1,\*</sup>

<sup>1</sup> Department of Neurosurgery, Haikou Affiliated Hospital of Central South University Xiangya School of Medicine, Haikou, China;

<sup>2</sup> Department of Surgery, Graduate School of Medicine, The University of Tokyo, Tokyo, Japan;

<sup>3</sup> National Center for Global Health and Medicine, Tokyo, Japan.

**SUMMARY:** Alzheimer's disease (AD), the leading cause of dementia, significantly impacts global public health, with cases expected to exceed 150 million by 2050. Late-onset Alzheimer's disease (LOAD), predominantly influenced by the *APOE-ε4* allele, exhibits complex pathogenesis involving amyloid-β (Aβ) plaques, neurofibrillary tangles (NFTs), neuroinflammation, and blood-brain barrier (BBB) disruption. Proteomics has emerged as a pivotal technology in uncovering molecular mechanisms and identifying biomarkers for early diagnosis and intervention in AD. This paper reviews the genetic and molecular roles of *APOE-ε4* in the pathology of AD, including its effects on Aβ aggregation, tau phosphorylation, neuroinflammation, and BBB integrity. Additionally, it highlights recent advances in serum proteomics, revealing *APOE-ε4*-dependent and independent protein signatures with potential as early biomarkers for AD. Despite technological progress, challenges such as population diversity, standardization, and distinguishing AD-specific biomarkers remain. Directions for future research emphasize multicenter longitudinal studies, multi-omics integration, and the clinical translation of proteomic findings to enable early detection of AD and personalized treatment strategies. Proteomics advances in AD research hold the promise of improving patient outcomes and reducing the global disease burden.

**Keywords:** Alzheimer's disease (AD), *APOE-ε4*, proteomics, neuroinflammation, blood-brain barrier (BBB), multi-omics

## 1. Introduction

Alzheimer's disease (AD) is the most common cause of dementia, accounting for approximately 80% of all dementia cases worldwide (1). This neurodegenerative disorder is primarily characterized by a gradual decline in cognitive function, accompanied by memory impairment, reduced language skills, and spatial disorientation. Currently, around 55 million people globally are affected by dementia, and this number is expected to exceed 150 million by 2050, placing a significant burden on society and healthcare systems (2). Late-onset Alzheimer's disease (LOAD) is the most prevalent form of AD and its incidence rises sharply in individuals over the age of 65, posing a major public health challenge globally (3).

The exact cause of AD is not yet fully understood, but research has indicated that its pathogenesis involves a range of complex biological processes, including the deposition of amyloid-β (Aβ) plaques, the formation of neurofibrillary tangles (NFTs), neuroinflammation, and neuronal loss (4). Current Aβ-targeted therapeutic strategies have made some progress in slowing disease

progression, but their efficacy remains limited (5). Therefore, identifying new potential therapeutic targets and biomarkers is crucial to the early diagnosis of and intervention in AD.

In recent years, the rapid development of proteomics technology has enabled researchers to reveal the biological characteristics that precede the onset of LOAD by analyzing circulating proteins in individual body fluids (6,7). Proteomics studies specifically focus on identifying early warning signals of the disease by analyzing biomarkers in blood and cerebrospinal fluid (CSF), even allowing for interventions before clinical symptoms manifest (8). However, most existing proteomic studies are limited to small-scale cross-sectional research and lack validation in large prospective cohorts. Notably, the genetic factors for AD, and especially the influence of the apolipoprotein E (*APOE*) gene, have been widely confirmed to be closely associated with LOAD onset (9).

Among the three main *APOE* gene alleles (ε2, ε3, ε4), the ε4 allele is the strongest risk factor for LOAD (10). Studies have shown that about 25% of the general

population carries the *APOE-ε4* allele, whereas over 50% of AD patients are *APOE-ε4* carriers (11). The risk of developing LOAD for *APOE-ε4* carriers is three times higher than that in the general population, and for homozygotes, the risk can be as high as 12 times (4). The relationship between *APOE-ε4* and LOAD has been extensively studied, but how *APOE-ε4* specifically regulates the protein networks related to AD remains a key focus of current research. Identifying *APOE-ε4*-dependent and independent molecular characteristics is crucial for a deeper understanding of the mechanisms underlying AD. Moreover, proteomic analyses hold promise for providing new potential biomarkers for early diagnosis and personalized treatment of AD while offering insights into the role of *APOE-ε4* in disease progression.

## 2. Background and challenges of AD

### 2.1. Pathogenesis of AD

The pathological mechanisms of AD are diverse and complex, primarily involving the formation of Aβ plaques, abnormal phosphorylation of tau protein, synaptic dysfunction, mitochondrial damage, and neuronal death (4). The two hallmark pathological changes are the formation of Aβ plaques in the brain and the aggregation of hyperphosphorylated tau protein, which forms NFTs. These pathological phenomena lead to damage and death of neurons, ultimately disrupting neural networks and resulting in cognitive and functional decline.

In addition to Aβ and tau protein pathology, chronic inflammation and oxidative stress are also considered key factors in the progression of AD. In particular, neuroinflammation has emerged in recent years as a significant mechanism influencing AD onset and progression. Microglia, the immune cells of the central nervous system, become activated in response to Aβ and tau pathology, triggering inflammatory responses that further exacerbate neuronal damage (12).

These pathological mechanisms play critical roles in the progression of AD, but not all patients follow the same disease patterns. Recent research has revealed that AD exhibits significant genetic heterogeneity and phenotypic diversity, with genetic factors playing a crucial role in its onset and progression (13). Among these, the ε4 allele of the *APOE* gene has been recognized as one of the strongest genetic risk factors associated with AD.

### 2.2. Genetic association of APOE with AD

The *APOE* gene, located on chromosome 19, encodes APoE, which plays a key role in lipid metabolism and transport. There are three major alleles of *APOE*: ε2, ε3, and ε4. The ε4 allele significantly increases the

risk of LOAD. Individuals carrying one copy of the ε4 allele have a threefold increased risk of developing AD compared to the general population, while individuals with two copies (homozygotes) have up to a twelvefold increased risk (14). In contrast, the *APOE-ε2* allele has a protective effect, reducing the risk of AD.

The mechanism of APOE's influence is primarily through its effects on the deposition and clearance of Aβ (15). Research has suggested that the *APOE-ε4* allele may promote the aggregation and deposition of Aβ in the brain, accelerating neurodegenerative changes (16). Moreover, *APOE-ε4* carriers often have impaired blood-brain barrier (BBB) function, exacerbating the accumulation of Aβ in the brain. In addition, *APOE-ε4* may interfere with synaptic function and neuronal plasticity by affecting cholesterol and lipid metabolism, exacerbating the pathology of AD.

Although the risk associated with *APOE-ε4* has been extensively studied, its precise impact on protein regulation processes and its specific role in LOAD remains incompletely understood. Notably, the effects of *APOE-ε4* vary significantly among individuals, suggesting complex interactions between genetic and environmental factors. Thus, further understanding of the *APOE-ε4*-dependent and independent protein characteristics will provide new insights into the pathogenesis of LOAD and inform the development of personalized therapeutic strategies.

### 2.3. Proteomics in AD

Proteomics is a technology that enables large-scale analysis of protein expression, modification, and interactions, revealing key biological processes. In recent years, proteomics has been widely used in AD research, particularly in identifying proteins in blood and CSF that may be associated with the risk of AD. By uncovering disease-related molecular features, proteomic studies provide important clues for understanding the mechanisms of AD pathogenesis.

Several studies have found that circulating protein levels in serum are highly correlated with the pathological processes of AD. Certain proteins in the blood can reflect neuronal damage or inflammatory states in the brain, making them potential biomarkers for the disease. However, most existing studies are primarily cross-sectional, with small sample sizes and lacking longitudinal follow-up data. Therefore, identifying protein characteristics that change over the long term before the onset of AD, and particularly those dependent or independent of *APOE-ε4*, holds significant scientific value.

## 3. Mechanistic association of *APOE-ε4* with AD

The *APOE* gene is one of the most extensively studied genetic risk factors in AD research. Located on

chromosome 19, it encodes ApoE, which plays a crucial role in lipid metabolism, primarily by regulating the transport and distribution of cholesterol and lipids to maintain brain function. Among *APOE* alleles, the  $\epsilon 3$  allele is the most common neutral genotype,  $\epsilon 2$  is thought to have some protective effects, and  $\epsilon 4$  significantly increases the risk of LOAD.

### 3.1. Function of *APOE-ε4* in AD

ApoE is a lipoprotein that functions mainly in the brain and peripheral tissues. Its primary role is to transport, metabolize, and store lipids by binding to lipids, cholesterol, and their receptors (17). Lipid metabolism in the brain is critical to maintaining neuronal function, synaptic plasticity, and cell membrane integrity. During neuronal regeneration and repair, ApoE facilitates the transport of cholesterol and phospholipids, assisting in membrane repair and neuronal regeneration (17) (Figure 1). ApoE's function is essential to maintaining brain health and neuronal plasticity.

The impact of different *APOE* alleles on ApoE function varies. Compared to *APOE-ε3*, ApoE encoded by the *APOE-ε4* allele is less efficient in lipid transport and metabolism, particularly in the brain, where its ability to clear Aβ is significantly reduced (18). The accumulation and deposition of Aβ is a hallmark of the pathology of AD, and the presence of *APOE-ε4* contributes to increased Aβ accumulation, exacerbating the progression of AD.

### 3.2. *APOE-ε4* and Aβ metabolism

The influence of *APOE-ε4* on Aβ metabolism is one of the primary mechanisms by which it increases the risk of AD. The production and clearance of Aβ are crucial processes for maintaining the dynamic balance of Aβ levels in the brain, and different *APOE* alleles play an important regulatory role in this process. Studies have shown that the clearance rate of Aβ is significantly lower in *APOE-ε4* carriers compared to those with *APOE-ε3* or  $\epsilon 2$  alleles (19).

ApoE encoded by *APOE-ε4* plays a key role in promoting Aβ deposition (Figure 1). ApoE binds directly to Aβ, forming insoluble complexes that promote the aggregation of Aβ in the brain. Compared to *APOE-ε3* and *APOE-ε2*, *APOE-ε4* more readily accelerates the deposition of Aβ around blood vessels and neurons, forming characteristic Aβ plaques (18). Significant interactions between ApoE4 and Aβ have been observed in primary immortalized astrocytes, making protein aggregation complexes more likely (20).

*APOE-ε4* not only promotes Aβ deposition but also significantly reduces its clearance efficiency. The clearance of Aβ primarily relies on phagocytosis, lipoprotein-mediated transport, and translocation across the BBB (21). Soluble oligomeric forms of Aβ42

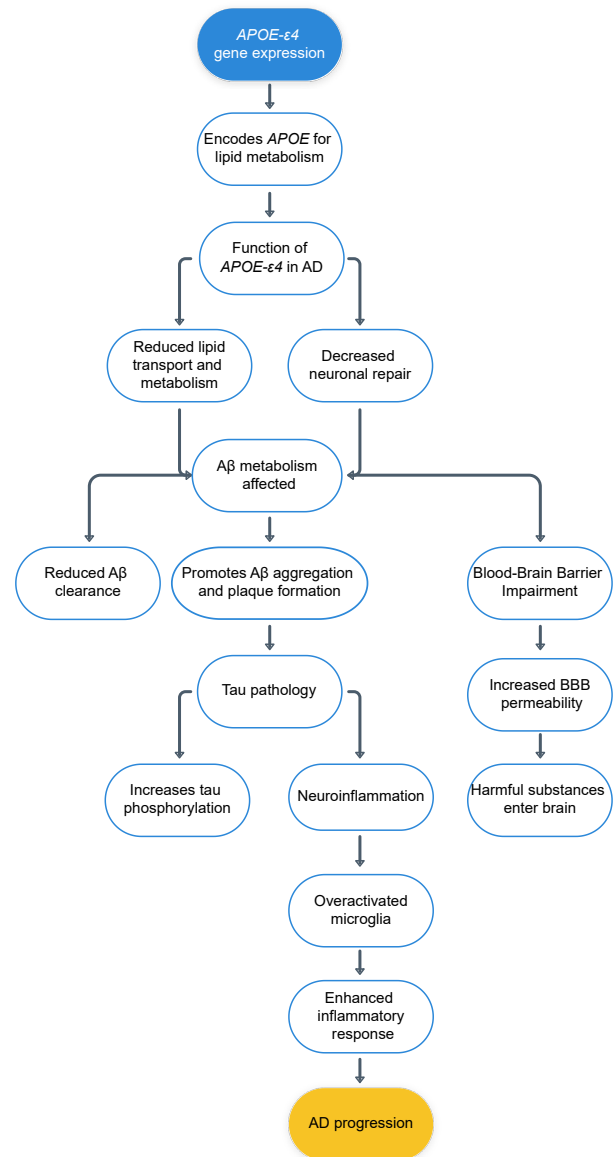


**Figure 1. The mechanistic impact of *APOE-ε4* on Alzheimer's disease development.** Abbreviations: AD, Alzheimer's disease; BBB, blood-brain barrier.

(including dimers, trimers, and small oligomers) are typically cleared through systemic circulation. Compared to *APOE ε3/ε3* carriers, *APOE ε4/ε4* carriers exhibit higher levels of Aβ oligomers. Prolonged exposure to Aβ42 dimers and trimers can lead to progressive dendritic spine loss and hippocampal synapse reduction (22,23). Low-density lipoprotein receptor-related protein 1 (LRP1) plays an essential role in Aβ clearance, and ApoE4 enhances Aβ production by accelerating LRP-mediated amyloid precursor protein (APP) endocytosis (24,25). Moreover, *APOE-ε4* carriers have a weaker BBB, with Aβ aggregates being cleared by pericytes through LRP1/ApoE interactions, a process that ApoE4 disrupts, resulting in impaired translocation of Aβ from the brain to peripheral circulation, further exacerbating Aβ accumulation in the brain (26,27). Additionally, *APOE-ε4* inhibits the phagocytic and degradative

abilities of microglia to clear A $\beta$ , further contributing to A $\beta$  accumulation. Collectively, these factors lead to earlier A $\beta$  deposition in *APOE- $\epsilon$ 4* carriers.

### 3.3. *APOE- $\epsilon$ 4* and tau pathology

In addition to its role in A $\beta$  metabolism, *APOE- $\epsilon$ 4* also significantly impacts the phosphorylation and aggregation of tau protein, another key pathological hallmark of AD (28). Tau protein is a component of neuronal microtubules and plays a crucial role in maintaining cytoskeletal stability. However, abnormally phosphorylated tau protein forms NFTs, another hallmark of the pathology of AD.

Studies have shown that tau protein phosphorylation and aggregation are more severe in the brains of *APOE- $\epsilon$ 4* carriers (28). This may be due to the indirect effects of *APOE- $\epsilon$ 4* on lipid metabolism and synaptic function, which promote pathological changes in tau protein (29) (Figure 1). Moreover, neuroinflammatory responses in the brains of *APOE- $\epsilon$ 4* carriers exacerbate the progression of tau pathology (30). Particularly in the hippocampus, tau pathology is significantly more pronounced in *APOE- $\epsilon$ 4* carriers, which is closely associated with accelerated cognitive decline (31).

### 3.4. *APOE- $\epsilon$ 4* and the BBB

*APOE- $\epsilon$ 4* affects not only A $\beta$  and tau metabolism but also has a significant impact on the integrity of the BBB (26). The BBB is essential for maintaining central nervous system homeostasis by preventing harmful substances from entering the brain. *APOE- $\epsilon$ 4* carriers tend to have diminished BBB function, characterized by a reduced capillary basement membrane area and increased thrombinogen concentrations in the microvascular walls and perivascular nerve membranes that accelerate breakdown of the BBB (32-34). This breakdown allows peripheral toxins and inflammatory factors to more easily enter the brain, exacerbating the pathology of AD.

Studies have also found that impaired BBB function in *APOE- $\epsilon$ 4* carriers further decreases the efficiency of A $\beta$  clearance, creating a vicious cycle that accelerates the progression of AD (35) (Figure 1). Therefore, BBB disruption is considered a key mechanism by which *APOE- $\epsilon$ 4* promotes the development of AD *via* multiple pathways.

### 3.5. *APOE- $\epsilon$ 4* and neuroinflammation

Neuroinflammation is a critical pathological mechanism in the progression of AD. ApoE protein is typically synthesized by microglia and astrocytes. *APOE- $\epsilon$ 4* promotes excessive activation of microglia and astrocytes, intensifying inflammation in the brain. Microglia, as the immune cells of the central nervous system, play a key role in responding to A $\beta$

pathology. There is a higher risk of A $\beta$  deposition in *APOE- $\epsilon$ 4* carriers, and the toxicity of A $\beta$  plaques is also significantly enhanced. A $\beta$  aggregation triggers neuroinflammatory responses, leading to neuronal death (36). In *APOE- $\epsilon$ 4* carriers, however, microglial function shifts from A $\beta$  clearance to pro-inflammatory responses, further damaging neurons (37). ApoE4 induces neuroinflammation by activating the pro-inflammatory prostaglandin E2 (PGE2) pathway or inhibiting the triggering receptor expressed on myeloid cells 2 (TREM2) pathway (38).

In addition, *APOE- $\epsilon$ 4* regulates the release of inflammatory factors, promoting the infiltration of more immune cells into the brain and further exacerbating neuroinflammation (Figure 1). Compared to ApoE3 mice, ApoE4 mice exhibit significantly increased levels of TNF- $\alpha$  and IL-6 in the brain (30). ApoE4 increases the expression of inflammatory factors in human astrocytes (30). This excessive inflammatory response accelerates A $\beta$  and tau pathology progression. ApoE4 can also activate the cyclosporin A-matrix metalloproteinase-9 (CypA-MMP9) pathway, leading to neuronal loss and synaptic disruption (39). Additionally, ApoE4 induces the activation of Ca<sup>2+</sup>-dependent phospholipase A2 (cPLA2), affecting the arachidonic acid (AA) signaling cascade that is typically associated with chronic brain inflammation (40). Neuroinflammation plays a particularly important role in the early stages of AD in *APOE- $\epsilon$ 4* carriers.

### 3.6. Individual variability in *APOE- $\epsilon$ 4*

*APOE- $\epsilon$ 4* is widely considered to be a key risk factor for AD, but not all *APOE- $\epsilon$ 4* carriers develop AD. In fact, approximately 24% of *APOE- $\epsilon$ 4* carriers do not develop AD during their lifetime (41). This suggests that the effects of *APOE- $\epsilon$ 4* may depend on other genetic, environmental, and lifestyle factors (42) (as shown in Figure 2). Studies have shown that lifestyle interventions such as a healthy diet, regular physical activity, maintaining cognitive engagement, and managing cardiovascular health may help reduce the risk of AD in *APOE- $\epsilon$ 4* carriers (43-47). Additionally, the influence of other genes, individual immune status, and sex differences also affect AD risk in *APOE- $\epsilon$ 4* carriers (48). Compared to male ApoE4 mice, primary microglia from female ApoE4 mice have higher levels of IL1b, TNF- $\alpha$ , IL6, and NOS2 (49). A study has suggested that female have a higher incidence of AD than males (50). The *APOE4* allele similarly increases the risk of amyloid abnormalities in both male and female, but its impact on tau is more significant in female (50). However, another study has suggested that sex differences in dementia risk may partially depend on age and/or geographic region (51). A recent meta-analysis found no significant differences in the relationship between *APOE- $\epsilon$ 4* and AD between males and females, but between the ages of 55



Figure 2. Risk factors for Alzheimer's disease (AD)

and 70, females had a higher risk of AD associated with *APOE-ε4* than males (52). Thus, *APOE-ε4* is thought to have its most potent effects during this age range. Whether the impact of *APOE-ε4* is dependent on sex hormones such as estrogen remains unclear (53).

#### 4. Serum proteomic characteristics of AD and future directions

The rapid development of proteomics has opened new avenues for studying complex neurodegenerative diseases such as AD. Serum proteomics, in particular, offers unique advantages in discovering new biomarkers and understanding disease mechanisms. Given that blood is relatively easy to obtain and reflects dynamic changes in systemic diseases, serum proteomic characteristics hold great potential for early diagnosis and research into the pathology of AD.

Recent studies have shown that proteins in the serum may reflect pathological changes in the brain and CSF, even before clinical symptoms appear. Therefore, identifying serum proteomic features associated with AD, and especially those dependent or independent of the *APOE-ε4* genotype, provides new perspectives for early diagnosis, understanding the molecular mechanisms of the disease, and developing personalized treatment strategies.

##### 4.1. Serum proteins as early biomarkers

The early stages of AD, and particularly the asymptomatic phase or mild cognitive impairment (MCI) stage, represent a critical window for therapeutic intervention. Early intervention has the potential to slow or reverse disease progression, but there is a lack

of biomarkers that are able to accurately diagnose AD in this stage. Serum proteomics research, through large-scale screening, can identify proteins that exhibit abnormal levels years or even decades before AD clinical symptoms manifest.

In different stages of the pathology of AD, levels of specific proteins in the serum change significantly. For example, proteins associated with neuronal damage, inflammatory responses, and metabolic dysregulation have been found to be abnormally expressed even in the preclinical stages of AD. These proteins could not only serve as early biomarkers for AD but also reflect the core pathological processes of neurodegenerative diseases.

A recent longitudinal analysis of serum proteomes in 5,294 participants identified 329 proteins associated with AD, some of which were linked to *APOE-ε4*-dependent pathways while others were linked to independent pathways (54). Notably, some *APOE-ε4*-independent proteins, such as glycoprotein non-metastatic protein B (GPNMB), netrin 1 (NTN1), SPARC-related modular calcium binding 1 (SMOC1), and spondin 1 (SPON1), displayed a high degree of consistency with AD-related proteins in the brain and CSF. This suggests that these proteins may reflect early neuronal pathway changes and could be used as early biomarkers for predicting and diagnosing AD.

##### 4.2. The significance of *APOE-ε4*-dependent and independent protein characteristics

Research has found that the serum proteomic characteristics of AD patients can be divided into two categories based on *APOE-ε4* carrier status: dependent and independent. *APOE-ε4*-dependent protein characteristics primarily reflect pathological processes related to lipid metabolism, Aβ metabolism, and neuroinflammation regulated by *APOE-ε4*. For example, *APOE-ε4*-dependent proteins such as ARL2, S100A13, and TBCA are closely related to AD, and levels of their expression are significantly influenced by the *APOE-ε4* genotype (54). AD-related changes in these proteins are more pronounced in *APOE-ε4* carriers, suggesting that they may serve as biomarkers specific to *APOE-ε4* carriers and help to identify early cases of AD in this high-risk group.

In contrast, *APOE-ε4*-independent proteins reflect broader neuronal dysfunction and metabolic abnormalities and are potentially indicative of a wider range of AD patients. Proteins such as GPNMB, NTN1, SMOC1, and SPON1 are closely associated with neuronal survival, synaptic function, and extracellular matrix changes. These proteins exhibit similar pathological patterns in the serum, CSF, and brain tissue (54). This consistency suggests that these proteins could become universal biomarkers across different *APOE* genotypes, allowing for broader AD detection and monitoring.

Moreover, the discovery of *APOE-ε4*-independent protein characteristics offers new insights for treating AD in non-*APOE-ε4* carriers. The specificity and broad applicability of these protein markers suggest that they have significant potential for personalized treatments in the future. By combining different sets of protein characteristics, scientists could better identify individual risk and tailor personalized treatment plans.

#### 4.3. Limitations and challenges of proteomics

Proteomics research has brought new hope to AD diagnosis and treatment, but several limitations and challenges remain. First, most current proteomics studies focus on specific populations, and particularly Nordic populations. Whether these findings can be generalized to other populations, and especially those with different racial, geographic, and lifestyle backgrounds, needs to be validated further. Differences in population genetics and environmental exposure may significantly affect protein expression. Therefore, future studies should include more diverse populations to ensure the generalizability of findings.

Second, proteomics technology itself presents certain technical challenges. Different proteomic platforms vary in sensitivity, specificity, and methods of data processing, leading to potential inconsistencies between studies. For example, protein levels measured using different platforms may display different patterns of association across cohorts (55,56). Therefore, to improve the reproducibility and consistency of studies, standardizing experimental protocols and methods of data analysis in proteomics research is essential.

Moreover, proteomics studies have revealed many potential biomarkers associated with AD, but further research is needed to determine whether these biomarkers can accurately differentiate AD from other types of dementia. Biomarkers of AD may overlap with other neurodegenerative diseases, such as Parkinson's disease and Lewy body dementia. Therefore, identifying proteins that can specifically distinguish AD is crucial.

#### 4.4. Directions for future research

To overcome the current limitations and further advance the early diagnosis and personalized treatment of AD, further studies are needed.

##### 4.4.1. Large-scale, multicenter prospective cohort studies

To enhance the generalizability of their findings, future studies should involve multicenter collaborations that include populations of different races, geographic backgrounds, and age groups in prospective cohort studies. This approach will help identify proteomic biomarkers that are common across various ethnic and cultural groups and reveal the impact of environmental

and lifestyle factors on protein characteristics.

##### 4.4.2. Longitudinal studies and dynamic monitoring

As a slowly progressing disease, AD's pathological process may evolve over several decades. Therefore, longitudinal studies are essential for revealing the temporal dynamics of proteomic characteristics. Long-term follow-up studies will enable researchers to better understand changes in protein levels and identify proteins that are abnormal before symptoms appear, improving the accuracy of early diagnosis.

##### 4.4.3. Integration of proteomics with multi-omics

Single -omics studies often cannot fully capture the complexity of diseases. Future research should integrate proteomics with other -omics, such as genomics, metabolomics, and transcriptomics, to create more comprehensive molecular network models. This multi-omics approach can reveal interactions between different biomolecules, providing deeper insights into the pathogenesis of AD and new avenues for personalized treatment.

##### 4.4.4. Personalized treatment strategies

Future research should focus on developing personalized treatment strategies based on proteomic characteristics. By identifying specific proteomic profiles in patients, and particularly *APOE-ε4*-dependent and independent proteins, researchers can design precise interventions for different risk groups. For instance, therapies targeting Aβ and neuroinflammation may be developed for *APOE-ε4* carriers, while treatments focused on neuronal protection and metabolic regulation could be tailored for non-*APOE-ε4* carriers.

##### 4.4.5. Clinical translation of novel biomarkers

Although many protein markers have been discovered to be associated with the risk of AD, extensive work is still required to use these biomarkers clinically. Future studies should focus on validating these markers in clinical settings and developing simple, accurate, and cost-effective detection tools for widespread use in routine medical practice.

## 5. Conclusion

In conclusion, the use of serum proteomics in AD research holds great promise, not only offering new solutions for early diagnosis and risk prediction but also laying the foundation for the development of personalized treatments. As technological advances continue and research goes further in depth, the clinical translation of proteomic biomarkers will help to improve

the quality of life for patients and alleviate the significant public health burden of AD worldwide.

Study of AD is reaching a new milestone, where the integration of proteomics, genetics, and other multi-omics technologies will enable scientists to better understand the complexity of the disease and provide a solid scientific basis for the development of new therapeutic approaches. Future research should focus on further validating these biomarkers in clinical settings and exploring how to integrate them into existing healthcare systems with the ultimate goals of early detection of, precise intervention in, and personalized treatment for AD.

**Funding:** This work was supported by a grant from the National Natural Science Foundation of China (No. 82460268) and the Hainan Province Clinical Medical Research Center (No. LCYX202410, LCYX202309) and Grants-in-Aid from the Ministry of Education, Science, Sports, and Culture of Japan (24K14216).

**Conflict of Interest:** The authors have no conflicts of interest to disclose.

## References

- Deng Y, Wang H, Gu K, Song P. Alzheimer's disease with frailty: Prevalence, screening, assessment, intervention strategies and challenges. *Biosci Trends*. 2023; 17:283-292.
- Wang C, Song P, Niu Y. The management of dementia worldwide: A review on policy practices, clinical guidelines, end-of-life care, and challenge along with aging population. *Biosci Trends*. 2022; 16:119-129.
- Andrade-Guerrero J, Santiago-Balmaseda A, Jeronimo-Aguilar P, Vargas-Rodríguez I, Cadena-Suárez AR, Sánchez-Garibay C, Pozo-Molina G, Méndez-Catalá CF, Cardenas-Aguayo MD, Diaz-Cintra S, Pacheco-Herrero M, Luna-Muñoz J, Soto-Rojas LO. Alzheimer's disease: An updated overview of its genetics. *Int J Mol Sci*. 2023; 24:3754.
- Andronie-Cioara FL, Ardelean AI, Nistor-Cseppento CD, Jurcau A, Jurcau MC, Pascalau N, Marcu F. Molecular mechanisms of neuroinflammation in aging and Alzheimer's disease progression. *Int J Mol Sci*. 2023; 24:1869.
- Ma YN, Hu X, Karako K, Song P, Tang W, Xia Y. Exploring the multiple therapeutic mechanisms and challenges of mesenchymal stem cell-derived exosomes in Alzheimer's disease. *Biosci Trends*. 2024. doi: 10.5582/bst.2024.01306.
- Dammer EB, Ping L, Duong DM, Modeste ES, Seyfried NT, Lah JJ, Levey AI, Johnson ECB. Multi-platform proteomic analysis of Alzheimer's disease cerebrospinal fluid and plasma reveals network biomarkers associated with proteostasis and the matrisome. *Alzheimers Res Ther*. 2022; 14:174.
- Sun YY, Wang Z, Huang HC. Roles of ApoE4 on the pathogenesis in Alzheimer's disease and the potential therapeutic approaches. *Cell Mol Neurobiol*. 2023; 43:3115-3136.
- Bhalala OG, Watson R, Yassi N. Multi-omic blood biomarkers as dynamic risk predictors in late-onset Alzheimer's disease. *Int J Mol Sci*. 2024; 25:1231.
- Mauch DH, Nagler K, Schumacher S, Goritz C, Muller EC, Otto A, Pfrieger FW. CNS synaptogenesis promoted by glia-derived cholesterol. *Science*. 2001; 294:1354-1357.
- Gouveia Roque C, Phatnani H, Hengst U. The broken Alzheimer's disease genome. *Cell Genom*. 2024; 4:100555.
- Gharbi-Meliani A, Dugravot A, Sabia S, Regy M, Fayosse A, Schnitzler A, Kivimaki M, Singh-Manoux A, Dumurgier J. The association of APOE epsilon4 with cognitive function over the adult life course and incidence of dementia: 20 years follow-up of the Whitehall II study. *Alzheimers Res Ther*. 2021; 13:5.
- Fruhwrth S, Zetterberg H, Paludan SR. Microglia and amyloid plaque formation in Alzheimer's disease - Evidence, possible mechanisms, and future challenges. *J Neuroimmunol*. 2024; 390:578342.
- Gatz M, Reynolds CA, Fratiglioni L, Johansson B, Mortimer JA, Berg S, Fiske A, Pedersen NL. Role of genes and environments for explaining Alzheimer disease. *Arch Gen Psychiatry*. 2006; 63:168-174.
- Corder EH, Saunders AM, Strittmatter WJ, Schmechel DE, Gaskell PC, Small GW, Roses AD, Haines JL, Pericak-Vance MA. Gene dose of apolipoprotein E type 4 allele and the risk of Alzheimer's disease in late onset families. *Science*. 1993; 261:921-923.
- 2020 Alzheimer's disease facts and figures. *Alzheimers Dement*. 2020; 10. doi: 10.1002/alz.12068.
- Mouchard A, Boutonnet MC, Mazzocco C, Biendon N, Macrez N, Neuro CEBNN. ApoE-fragment/Abeta heteromers in the brain of patients with Alzheimer's disease. *Sci Rep*. 2019; 9:3989.
- Hauser PS, Narayanaswami V, Ryan RO. Apolipoprotein E: From lipid transport to neurobiology. *Prog Lipid Res*. 2011; 50:62-74.
- Hashimoto T, Serrano-Pozo A, Hori Y, *et al*. Apolipoprotein E, especially apolipoprotein E4, increases the oligomerization of amyloid beta peptide. *J Neurosci*. 2012; 32:15181-15192.
- Serrano-Pozo A, Qian J, Monsell SE, Betensky RA, Hyman BT. APOE epsilon2 is associated with milder clinical and pathological Alzheimer disease. *Ann Neurol*. 2015; 77:917-929.
- Kara E, Marks JD, Roe AD, Commins C, Fan Z, Calvo-Rodriguez M, Wegmann S, Hudry E, Hyman BT. A flow cytometry-based *in vitro* assay reveals that formation of apolipoprotein E (ApoE)-amyloid beta complexes depends on ApoE isoform and cell type. *J Biol Chem*. 2018; 293:13247-13256.
- Mok KK, Yeung SH, Cheng GW, Ma IW, Lee RH, Herrup K, Tse KH. Apolipoprotein E epsilon4 disrupts oligodendrocyte differentiation by interfering with astrocyte-derived lipid transport. *J Neurochem*. 2023; 165:55-75.
- Shankar GM, Li S, Mehta TH, Garcia-Munoz A, Shepardson NE, Smith I, Brett FM, Farrell MA, Rowan MJ, Lemere CA, Regan CM, Walsh DM, Sabatini BL, Selkoe DJ. Amyloid-beta protein dimers isolated directly from Alzheimer's brains impair synaptic plasticity and memory. *Nat Med*. 2008; 14:837-842.
- Shankar GM, Bloodgood BL, Townsend M, Walsh DM, Selkoe DJ, Sabatini BL. Natural oligomers of the Alzheimer amyloid-beta protein induce reversible synapse

- loss by modulating an NMDA-type glutamate receptor-dependent signaling pathway. *J Neurosci.* 2007; 27:2866-2875.
24. Tachibana M, Holm ML, Liu CC, *et al.* APOE4-mediated amyloid-beta pathology depends on its neuronal receptor LRP1. *J Clin Invest.* 2019; 129:1272-1277.
  25. Ma Q, Zhao Z, Sagare AP, Wu Y, Wang M, Owens NC, Verghese PB, Herz J, Holtzman DM, Zlokovic BV. Blood-brain barrier-associated pericytes internalize and clear aggregated amyloid-beta42 by LRP1-dependent apolipoprotein E isoform-specific mechanism. *Mol Neurodegener.* 2018; 13:57.
  26. Moon WJ, Lim C, Ha IH, Kim Y, Moon Y, Kim HJ, Han SH. Hippocampal blood-brain barrier permeability is related to the APOE4 mutation status of elderly individuals without dementia. *J Cereb Blood Flow Metab.* 2021; 41:1351-1361.
  27. Pietrzik CU, Busse T, Merriam DE, Weggen S, Koo EH. The cytoplasmic domain of the LDL receptor-related protein regulates multiple steps in APP processing. *EMBO J.* 2002; 21:5691-5700.
  28. Kang SS, Ahn EH, Liu X, Bryson M, Miller GW, Weinschenker D, Ye K. ApoE4 inhibition of VMAT2 in the locus coeruleus exacerbates Tau pathology in Alzheimer's disease. *Acta Neuropathol.* 2021; 142:139-158.
  29. Barthelemy NR, Li Y, Joseph-Mathurin N, *et al.* A soluble phosphorylated tau signature links tau, amyloid and the evolution of stages of dominantly inherited Alzheimer's disease. *Nat Med.* 2020; 26:398-407.
  30. Iannucci J, Sen A, Grammas P. Isoform-specific effects of apolipoprotein E on markers of inflammation and toxicity in brain glia and neuronal cells *in vitro*. *Curr Issues Mol Biol.* 2021; 43:215-225.
  31. Salami A, Adolfsson R, Andersson M, Blennow K, Lundquist A, Adolfsson AN, Scholl M, Zetterberg H, Nyberg L. Association of APOE varepsilon4 and plasma p-tau181 with preclinical Alzheimer's disease and longitudinal change in hippocampus function. *J Alzheimers Dis.* 2022; 85:1309-1320.
  32. Zipser BD, Johanson CE, Gonzalez L, Berzin TM, Tavares R, Hulette CM, Vitek MP, Hovanesian V, Stopa EG. Microvascular injury and blood-brain barrier leakage in Alzheimer's disease. *Neurobiol Aging.* 2007; 28:977-986.
  33. Stannard AK, Riddell DR, Sacre SM, Tagalakis AD, Langer C, von Eckardstein A, Cullen P, Athanasopoulos T, Dickson G, Owen JS. Cell-derived apolipoprotein E (ApoE) particles inhibit vascular cell adhesion molecule-1 (VCAM-1) expression in human endothelial cells. *J Biol Chem.* 2001; 276:46011-46016.
  34. Salloway S, Gur T, Berzin T, Tavares R, Zipser B, Correia S, Hovanesian V, Fallon J, Kuo-Leblanc V, Glass D, Hulette C, Rosenberg C, Vitek M, Stopa E. Effect of APOE genotype on microvascular basement membrane in Alzheimer's disease. *J Neurol Sci.* 2002; 203-204:183-187.
  35. Zhou X, Shi Q, Zhang X, Gu L, Li J, Quan S, Zhao X, Li Q. ApoE4-mediated blood-brain barrier damage in Alzheimer's disease: Progress and prospects. *Brain Res Bull.* 2023; 199:110670.
  36. Tai LM, Ghura S, Koster KP, Liakaite V, Maienschein-Cline M, Kanabar P, Collins N, Ben-Aissa M, Lei AZ, Bahroos N, Green SJ, Hendrickson B, Van Eldik LJ, LaDu MJ. APOE-modulated Abeta-induced neuroinflammation in Alzheimer's disease: Current landscape, novel data, and future perspective. *J Neurochem.* 2015; 133:465-488.
  37. Krasemann S, Madore C, Cialic R, *et al.* The TREM2-APOE pathway drives the transcriptional phenotype of dysfunctional microglia in neurodegenerative diseases. *Immunity.* 2017; 47:566-581 e569.
  38. Li X, Montine KS, Keene CD, Montine TJ. Different mechanisms of apolipoprotein E isoform-dependent modulation of prostaglandin E2 production and triggering receptor expressed on myeloid cells 2 (TREM2) expression after innate immune activation of microglia. *FASEB J.* 2015; 29:1754-1762.
  39. Anderson EL, Williams DM, Walker VM, Davies NM. Little genomic support for Cyclophilin A-matrix metalloproteinase-9 pathway as a therapeutic target for cognitive impairment in APOE4 carriers. *Sci Rep.* 2022; 12:1057.
  40. Duro MV, Ebricht B, Yassine HN. Lipids and brain inflammation in APOE4-associated dementia. *Curr Opin Lipidol.* 2022; 33:16-24.
  41. Wang YY, Ge YJ, Tan CC, Cao XP, Tan L, Xu W. The proportion of APOE4 carriers among non-demented individuals: A pooled analysis of 389,000 community-dwellers. *J Alzheimers Dis.* 2021; 81:1331-1339.
  42. 2022 Alzheimer's disease facts and figures. *Alzheimers Dement.* 2022; 18:700-789.
  43. Di Marco LY, Marzo A, Munoz-Ruiz M, Ikram MA, Kivipelto M, Ruefenacht D, Venneri A, Soininen H, Wanke I, Ventikos YA, Frangi AF. Modifiable lifestyle factors in dementia: A systematic review of longitudinal observational cohort studies. *J Alzheimers Dis.* 2014; 42:119-135.
  44. Wang HX, Karp A, Winblad B, Fratiglioni L. Late-life engagement in social and leisure activities is associated with a decreased risk of dementia: A longitudinal study from the Kungsholmen project. *Am J Epidemiol.* 2002; 155:1081-1087.
  45. Wang HX, Xu W, Pei JJ. Leisure activities, cognition and dementia. *Biochim Biophys Acta.* 2012; 1822:482-491.
  46. Staff RT, Hogan MJ, Williams DS, Whalley LJ. Intellectual engagement and cognitive ability in later life (the "use it or lose it" conjecture): Longitudinal, prospective study. *BMJ.* 2018; 363:k4925.
  47. Najjar J, Ostling S, Gudmundsson P, Sundh V, Johansson L, Kern S, Guo X, Hallstrom T, Skoog I. Cognitive and physical activity and dementia: A 44-year longitudinal population study of women. *Neurology.* 2019; 92:e1322-e1330.
  48. Zhang YR, Yang L, Wang HF, Wu BS, Huang SY, Cheng W, Feng JF, Yu JT. Immune-mediated diseases are associated with a higher incidence of dementia: A prospective cohort study of 375,894 individuals. *Alzheimers Res Ther.* 2022; 14:130.
  49. Mhatre-Winters I, Eid A, Han Y, Tieu K, Richardson JR. Sex and APOE genotype alter the basal and induced inflammatory states of primary microglia from APOE targeted replacement mice. *Int J Mol Sci.* 2022; 23:9829.
  50. Altmann A, Tian L, Henderson VW, Greicius MD, Alzheimer's Disease Neuroimaging Initiative I. Sex modifies the APOE-related risk of developing Alzheimer disease. *Ann Neurol.* 2014; 75:563-573.
  51. Chene G, Beiser A, Au R, Preis SR, Wolf PA, Dufouil C, Seshadri S. Gender and incidence of dementia in the Framingham Heart Study from mid-adult life. *Alzheimers Dement.* 2015; 11:310-320.
  52. Neu SC, Pa J, Kukull W, *et al.* Apolipoprotein E genotype

- and sex risk factors for Alzheimer disease: A meta-analysis. *JAMA Neurol.* 2017; 74:1178-1189.
53. Yaffe K, Haan M, Byers A, Tangen C, Kuller L. Estrogen use, APOE, and cognitive decline: Evidence of gene-environment interaction. *Neurology.* 2000; 54:1949-1954.
54. Frick EA, Emilsson V, Jonmundsson T, *et al.* Serum proteomics reveal APOE-epsilon4-dependent and APOE-epsilon4-independent protein signatures in Alzheimer's disease. *Nat Aging.* 2024; 4:1446-1464.
55. Sattlecker M, Kiddle SJ, Newhouse S, *et al.* Alzheimer's disease biomarker discovery using SOMAscan multiplexed protein technology. *Alzheimers Dement.* 2014; 10:724-734.
56. Sattlecker M, Khondoker M, Proitsi P, Williams S, Soininen H, Kloszewska I, Mecocci P, Tsolaki M, Vellas B, Lovestone S, Dobson RJ. Longitudinal protein changes in blood plasma associated with the rate of cognitive decline

in Alzheimer's disease. *J Alzheimers Dis.* 2016; 49:1105-1114.

Received November 17, 2024; Revised January 14, 2025; Accepted January 19, 2025.

*\*Address correspondence to:*

Xiqi Hu, Department of Neurosurgery, Haikou Affiliated Hospital of Central South University Xiangya School of Medicine, Haikou, China 570208.

E-mail: 218302048@csu.edu.cn

Peipei Song, National Center for Global Health and Medicine, Tokyo, Japan 162-8655.

E-mail: psong@it.ncgm.go.jp

Released online in J-STAGE as advance publication January 23, 2025.

# The glamor of and insights regarding hydrotherapy, from simple immersion to advanced computer-assisted exercises: A narrative review

Yaohan Peng<sup>1</sup>, Yucong Zou<sup>2</sup>, Tetsuya Asakawa<sup>3,\*</sup>

<sup>1</sup>Key Laboratory of Plateau Hypoxia Environment and Life and Health, Xizang Minzu University, Xianyang, Shaanxi, China;

<sup>2</sup>Department of Rehabilitation, Zhuhai Hospital of Integrated Traditional Chinese & Western, Zhuhai, Guangdong, China;

<sup>3</sup>Institute of Neurology, National Clinical Research Center for Infectious Diseases, the Third People's Hospital of Shenzhen, Shenzhen, Guangdong, China.

**SUMMARY:** Water-based therapy has been gaining attention in recent years and is being widely used in clinical settings. Hydrotherapy is the most important area of water-based therapy, and it has distinct advantages and characteristics compared to conventional land-based exercises. Several new techniques and pieces of equipment are currently emerging with advances in computer technologies. However, comprehensive reviews of hydrotherapy are insufficient. Hence, this study reviewed the *status quo*, mechanisms, adverse events and contraindications, and future prospects of the use of hydrotherapy. This study aims to comprehensively review the latest information regarding the application of hydrotherapy to musculoskeletal diseases, neurological diseases, and COVID-19. We have attempted to provide a "take-home message" regarding the clinical applications and mechanisms of hydrotherapy based on the latest evidence available.

**Keywords:** water-based therapy, hydrotherapy, rehabilitation, neurorehabilitation, musculoskeletal diseases

## 1. Introduction

Water-based therapy, also referred to as "spa therapy," is akin to land-based therapy and includes a spectrum of potentially efficacious modalities using water or mud. Water-based therapy, which usually includes hydrotherapy, aqua therapy, and balneotherapy, is commonly used along with other therapies, including land-based exercises and massage, in clinical practice. Hydrotherapy, also termed "aquatic therapy," is an important area of water-based rehabilitation. It was started by Charles Leroy Lowman in 1911, who used therapeutic tubs to treat patients with spasticity, and is widely used for rehabilitation purposes (1). Contrary to land-based exercises, movement in water is influenced by the physical properties of water, such as density, specific gravity, hydrostatic pressure, buoyancy, viscosity, and thermodynamics, and hence is associated with special effects. The main advantages of hydrotherapy are: *i*) it provides a safer exercise environment than land-based therapies because of the lower risk of falls (2). Because of the low psychological burden of falling, patients can focus on exercise, thereby enhancing the effects of balance and stability training. *ii*) Owing to the buoyant

nature of water, the burden of body weight on the joints of the lower limbs is alleviated, thereby reducing the strain on the knees, ankles, and hips (3). Appropriate training, including range of motion in these joints, gentle strength building, and gait training, can have a better efficacy. *iii*) Movement in water requires the person to overcome water resistance, which increases the effort associated with exercise. Therefore, exercises such as deep-water running might be more efficacious than those performed on land (3). Hydrotherapy enhances respiratory and cardiopulmonary functions because of the hydrostatic pressure exerted on the thorax (4). *iv*) Stimuli associated with water *per se*, including water temperature and flow, may contribute to the effects of physical therapy. *v*) Community-based hydrotherapy encourages patients. For example, the mandatory communication required during hydrotherapy can benefit children with communication disorders. Communicating with the coach, therapist, or other patients might potentially benefit children with autism (5). For individuals who have difficulty walking, a lower risk of falls (compared to land-based walking exercises) may enhance their self-confidence. A well-organized hydrotherapy course is helpful to encourage individuals to build momentum and keep training. In

addition to conventional athletic rehabilitation (6,7) and neurorehabilitation (8), hydrotherapy is widely used to relieve pain associated with labor (9,10) and a battery of diseases including knee osteoarthritis (KOA) (2), vascular diseases (11,12), pediatric disorders (13,14), chronic diseases such as hypertension (15), obesity and type 2 diabetes (16), and chronic obstructive pulmonary disease (4,17). Due to its characteristics, hydrotherapy can be used in several situations: *i)* For older adults with balance problems because of the lower associated risk of falls. A systematic review by Shariat *et al.* included 385 participants in 15 trials to investigate the efficacy of hydrotherapy in improving balance in older adults (18). They concluded that hydrotherapy had a positive impact on dynamic balance in the elderly population. *ii)* For obese patients with disorders of the lower joints, the buoyancy of water can relieve the burden on the knees, ankles, and hips. Lim *et al.* conducted a randomized controlled trial (RCT) to compare the efficacy of aquatic exercise and land-based exercise in treating obesity in obese patients with KOA, and they reported that aquatic exercise was more efficacious in reducing body fat since the patients could exercise more due to less pain (19). *iii)* For children, since most children enjoy playing in water. Lai *et al.* evaluated the efficacy of hydrotherapy in children with cerebral palsy and found that children undergoing pediatric aquatic therapy had better Physical Activity Enjoyment Scale scores compared to the control group post-treatment (20).

Several insightful reviews have discussed the applications and mechanisms of hydrotherapy from various perspectives. Becker summarized the marked physiologic changes associated with hydrotherapy as well as its clinical applications in rehabilitation in 2009 (1). Later, in 2020, Becker further summarized the applications of hydrotherapy in neurological diseases (8). These two articles are landmark papers on hydrotherapy. Torres-Ronda *et al.* reviewed the properties of water and their applications in training (21). They focused on the muscle damage and soreness following exercise in athletes. Mooventhan and Nivethitha reviewed the impacts of hydrotherapy on various physical systems (22). This was the first review to comprehensively summarize the application of hydrotherapy to the whole body. In addition, several systematic reviews have evaluated the efficacy and safety of hydrotherapy in different diseases. Bartels *et al.* reported small, short-term, and clinically relevant effects of hydrotherapy on OA-related pain, disability, and quality of life (QOL) in patients with knee and hip OA (23,24). Reger *et al.* conducted a review that investigated the effectiveness of hydrotherapy in treating cancer, but they failed to reach a concrete conclusion because of the heterogeneous results (25). These reviews have provided useful insights regarding the clinical use of hydrotherapy from different perspectives. Hydrotherapy is commonly practiced in clinical settings, but the comprehensive reviews

are limited and hydrotherapy-related mechanisms in particular are still not completely understood. Hence, the aim of the current review was to present updated information related to hydrotherapy. We have attempted to provide "take-home messages" regarding the clinical applications and mechanisms of hydrotherapy based on the latest evidence available.

## 2. The underlying mechanisms of hydrotherapy

Mechanisms of hydrotherapy are not yet completely understood. The temperature of water is known to play a vital role in terms of those mechanisms. Different water temperatures can trigger different physiological reactions (22). Cold water centralizes the circulating blood to perfuse major organs, which can help reduce lymphedema and heal chronic wounds with analgesic and antiphlogistic effects (25). Warm water induces vasodilation, which can relieve vascular spasm and relax muscles. Warm water also relieves hypertension and chronic pain. Thus, cold water immersion (CWI), warm water immersion, and contrast water therapy are selected based on different clinical scenarios and seasons (Table 1). Whole-body cryotherapy (WBC), namely short exposure (2–4 min) to very cold air (–100°C, –150°F) has been reported to ameliorate muscle soreness (26) and muscle pain (27) due to harsh training through alleviation of systemic inflammation and repair of muscle damage. A study by Driller and Leabeater has demonstrated that the recovery effects of CWI are comparable to those of WBC; however, CWI can more easily be conducted (7). A study focusing on balneotherapy reported that balneotherapy might reduce several proinflammatory cytokines such as TNF- $\alpha$  and IL-1 $\beta$  and increase anti-inflammatory molecules such as IGF-1 growth factor particularly in musculoskeletal diseases (28). Thus, anti-inflammatory action might be regarded as a significant mechanism of hydrotherapy.

Currently, neurotransmitter-related mechanisms of hydrotherapy are attracting attention (29). Peripheral serotonin levels are thought to be associated with a spectrum of neuromuscular diseases *via* development and resolution of immunity/inflammation-related mechanisms (29). However, a series of experiments by an Italian laboratory found no significant differences in 5-HT platelet transporter levels in participants who had undergone thermal balneotherapy (30,31). The dopaminergic pathway has been found to be involved in the pathophysiology of OA, and a dysfunction in systemic or local dopaminergic system has been found to be associated with several inflammatory diseases. Some researchers have hypothesized that immunomodulation of dopamine might contribute to the mechanisms by which spa therapy treats OA (29). However, only one study in Japan reported enhanced serum dopamine levels in healthy participants after a 15-minute hydrotherapy session (32).

**Table 1. Selection of an appropriate temperature protocol for hydrotherapy**

| Items                          | Cold water   | Warm water   | Alternating between warm and cold water          |
|--------------------------------|--|--|--|
| <b>Commonly used protocol</b>  | Cold water immersion   | Warm water immersion                                     | Contrast water therapy                           |
| <b>Recommended temperature</b> | 11–15°C (50–59 °F)   | 38–40°C (100–104 °F)                                     | Alternating between cold and warm                |
| <b>Duration</b>                | 11–15 min  | ≥10 min  | ≥10 min  |
| <b>Physiological reactions</b> | Increases: Activity of the sympathetic nervous system metabolic rate, heart rate, systolic blood pressure and diastolic blood pressure, plasma noradrenaline and dopamine, diuresis<br>Decreases: Plasma cortisol renin levels | Opposite effects of cold water in the column on the left | Depends on the duration of warm/cold immersion   |
| <b>Physiological effects</b>   | Increases: Local anesthetic effects<br>Decreases: Local metabolic rate and edema, nerve conduction velocity, muscle blood flow, and muscle spasm   | Opposite effects of cold water in the column on the left | Depends on the duration of warm/cold immersion   |
| <b>Clinical applications</b>   | Muscle fatigue and soreness, chronic wounds  | For relaxation   | Used as an acute post-exercise recovery strategy |

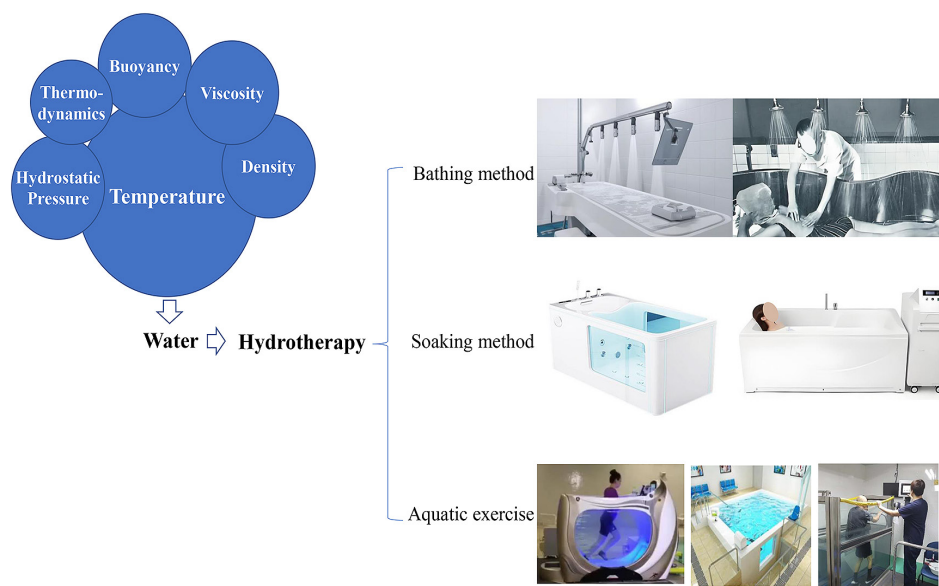


**Figure 1.** Methods based on treatment modalities used in hydrotherapy.

Overall, evidence concerning mechanisms of hydrotherapy is insufficient and further study is warranted.

### 3. Modality

Based on treatment modalities, hydrotherapy can be categorized into bathing methods, soaking methods, and aquatic exercise therapy. In brief, bathing methods are similar to a shower and refer to slowly streaming water that is maintained at an appropriate temperature over the body or using a water jet with appropriate pressure to vertically stream water over body parts. Bathing methods

differ from the common shower since parameters such as water temperature and pressure can be controlled. Soaking methods use soaking equipment such as a bathtub. Either the full body or part of the body is immersed in water at certain temperatures and the water might be medicated. Aquatic exercise therapy refers to conducting exercise therapy in an aquatic environment (Figure 1).

Techniques for hydrotherapy can include either a conventional approach or special techniques. Conventional approaches refer to conducting conventional land-based exercise in an aquatic environment, such as a pool or a special tank (Figure 1). Special techniques

include several approaches specifically developed for hydrotherapy, such as Ai Chi (1), the Halliwick method (33), the Bad Ragaz Ring therapy (34), and WATSU (WaterShiatsu) (35). These approaches should be selected after considering the pathophysiology and the goals of rehabilitation. For example, the Halliwick method is particularly recommended for patients with physical or learning difficulties (33). These individuals are trained to engage in water activities, moving and swimming

independently in water. The main techniques commonly used in hydrotherapy are listed in Table 2.

#### 4. Clinical applications of hydrotherapy

The most common application of hydrotherapy is for sports-related rehabilitation or post-exercise recovery among athletes (21,36). However, considering the aim of this review, we shall focus on the clinical applications of

**Table 2. Commonly used hydrotherapy techniques and their applications**

| Methods   | Advantages   | Weaknesses   | Applications                                       |
|---|--|--|--|
| <b>Conventional approaches</b>                        |  |  |  |
| Aquatic obstacle training                             | Mainly trains the initiation of movement; good for gesture failure and freezing of gait in patients with PD.   | Only suitable for patients with mild-moderate PD (Hoehn & Yahr stage 2–3); Requires certain walking ability; Involves a risk of falls.           | PD, Stroke.  |
| Aquatic treadmill                                     | Safe and easy to use; Can be used to evaluate multiple functions simultaneously.   | Requires expensive equipment, has modest efficacy compared to other training programs.   | Athletic rehabilitation, obesity, PD, SCI, Stroke. |
| YMCA arthritis  | Improvement of stability and compensatory effects.   | Only suitable for females.   | Arthritis.   |
| Group warm water therapies, Aqua aerobics, Water yoga | Good for improvement of communication between patients and boosting self-confidence of patients.   | In terms of compliance, males and younger people are worse compared to females and older people.   | Arthritis, ASD, neuromuscular disease, obesity.    |
| Deep-water running, Aqua jogging                      | Interesting; Good for improvement of cardiopulmonary function and regional cerebral blood flow.  | Involves a risk of falls, not good for improvement of cognitive function.  | Inactive elderly people, obesity, arthritis.       |
| Dual-task training                                    | Good for training the motor cortex and basal ganglia; helpful for formulating a walking training strategy, training for body coordination and motor execution.       | Requires a certain level of ability to walk independently; modest improvement of cognitive function.   | PD, stroke.  |
| <b>Special techniques</b>                             |  |  |  |
| Ai Chi  | Interesting, and readily accepted by most patients; Allows training in static and dynamic balance simultaneously; Good for training if respiratory function is good. | Only suitable for patients with a certain level of balance (score greater than 3 on Item 2 of the Berg Balance Scale). Very deep-water is risky. | Arthritis, PD, spine and fracture.                 |
| Halliwick   | Interesting, and readily accepted by most patients; One-on-one training format; Balance and independence are taught.   | Mainly used for children; Certain levels of understanding and communication are required.  | ASD, CP, MS, PD, Stroke.                           |
| Bad Ragaz Ring method                                 | May result in a satisfactory efficacy when combined with proprioceptive neuromuscular facilitation exercises.  | Commonly used for early rehabilitation.  | Arthritis, Chronic low back pain, Stroke.          |
| WATSU   | Uses the meridian and acupoint theory of traditional Chinese medicine; Can provide physical and spiritual relaxation; marked alleviation of pain.                    | Efficacy is markedly affected by water temperature; passive rehabilitation; patients cannot gain full activity.                                  | ASD, FS, MS, neuromuscular disease, PD, obesity.   |

ASD: autism spectrum disorder, Ai Chi: Taichi in the water, CP: cerebral palsy, FS: fibromyalgia syndrome, MS: multiple sclerosis, PD: Parkinson's disease, SCI: spinal cord injury, WATSU: WaterShiatsu, pressure finger massage in the water, YMCA: Young Men's Christian Association.

hydrotherapy for rehabilitation of patients with various diseases.

#### 4.1. Musculoskeletal diseases

Over the past few decades, mounting evidence supports the contention that hydrotherapy is beneficial at improving the symptoms of musculoskeletal diseases such as OA (29,37,38), fibromyalgia (39-43), inflammatory arthritis (44), exercise-induced muscle damage (45), juvenile idiopathic arthritis (JIA) (46), ankylosing spondylitis (AS) (47,48), low back pain (LBP) (49,50), and musculoskeletal pain (51,52). Hydrotherapy also relieves musculoskeletal pain associated with hemophilia (53,54), and helps in recovery after joint surgery (55,56). Primary benefits of hydrotherapy include: *i*) redistribution and enhancement of the blood supply along with the oxygen supply of the musculoskeletal system; *ii*) alleviation of pain, since pain is the main symptom associated with several musculoskeletal diseases such as KOA (57); *iii*) relief of an inflammatory reaction. Several studies have reported that hydrotherapy can reduce proinflammatory cytokines and increase anti-inflammatory cytokines (28,58); *iv*) suppression of the activity of the sympathetic nervous system by reducing noradrenaline levels and blocking nociceptors (58).

##### 4.1.1. Osteoarthritis

Lower limb osteoarthritis (OA), and KOA in particular, is a very prevalent condition since the joints of the lower limb are complex and vulnerable. Hydrotherapy plays an important role as a part of comprehensive OA treatments (59). Several previous studies have documented the efficacy of hydrotherapy in treating KOA. A meta-analysis by Dong *et al.* compared the efficacy of hydrotherapy to that of land-based exercises in treating KOA (60). They reported that there were no significant differences in the efficacy of hydrotherapy and land-based exercise in terms of pain relief, physical function, and QOL. Better compliance and levels of satisfaction were observed with hydrotherapy; however, it was found to have modest efficacy at improving the activities of daily living (ADL). Another study found that hydrotherapy was effective at alleviating pain and improving physical function, muscle strength of knee extension, and walking ability in individuals with KOA (61). A recent study that used Bad Ragaz Ring therapy in hot spring water to treat KOA reported that the Western Ontario and McMaster Universities OA index scores were better for the hydrotherapy group in terms of pain, stiffness, and function (62). Duan *et al.* reported that hydrotherapy might have only a short-term efficacy in treating OA-related pain, physical function, stiffness and athletic ability that did not persist as of a long-term follow-up (63). Another study conducted on women

suffering from KOA in Europe yielded different results. According to that study, intensive aquatic resistance training program only resulted in a mild short-term amelioration of knee stiffness but no short- or long-term amelioration of pain, physical function, or QOL (64). A plausible interpretation of the heterogeneity of the aforementioned studies might be the variations in the recruiting of patients, treatment conditions, and small sample sizes. Well-designed, large, and multicenter RCTs can provide more robust evidence regarding the efficacy of hydrotherapy in treating OA.

##### 4.1.2. Fibromyalgia

Fibromyalgia is another well-documented musculoskeletal disease that is treated with hydrotherapy. Fibromyalgia is associated with hyperalgesia and deficient pain inhibition that might be induced by hyperactivity of the hypothalamic–pituitary–adrenal axis and dysfunction of dopamine (65). Hong-Baik *et al.* found that elevated levels of proinflammatory cytokines such as IL-1 $\beta$ , IL-6, IL-8, and TNF- $\alpha$  in patients with fibromyalgia were reduced by hydrotherapy (58). Hence, they concluded that low chronic inflammation might contribute to the mechanisms of fibromyalgia and might be alleviated by hydrotherapy. Although the definition and classification of and the diagnostic criteria for fibromyalgia remain controversial, "relief of pain" is the main consideration in treating patients suspected to be suffering from fibromyalgia. Hydrotherapy is therefore considered and used to treat fibromyalgia. Hydrotherapy might modulate the hyperactive hypothalamic–pituitary–adrenal axis, activate the thermal receptors and mechanoreceptors, and suppress the nociceptors, helping to alleviate pain (66) and thereby ameliorate related symptoms such as sleep disturbance (40). Ai Chi has been reported to be the most effective method of treating fibromyalgia, and particularly for improvement of sleep quality (40). Earlier in 2009, Calandre *et al.* compared the efficacy of Ai Chi and stretching and found that Ai Chi significantly alleviated fibromyalgia-related symptoms and improved sleep quality while stretching only ameliorated the psychological well-being of the enrolled patients (67). A recent study has confirmed the efficacy of hydrotherapy in improving sleep quality, alleviating pain, and improving QOL in patients with fibromyalgia (40). Two studies that compared the efficacy and safety of hydrotherapy to land-based exercise for fibromyalgia have reported similar results, and they found hydrotherapy to be superior to land-based exercise, in terms of both pain control and improvement of sleep quality (41,68). In addition, social pressure is closely associated with fibromyalgia (69), and its prevalence is higher in females (70). Hydrotherapy is reportedly useful at reducing social pressure and improving muscle strength (at least 20%) and functional capacity in women (71-73). However, hydrotherapy

has not been found to be superior to other treatments like mat Pilates (74) and a health education program (75) in female patients with fibromyalgia. Nevertheless, hydrotherapy remains a valuable treatment modality for alleviating the symptoms of fibromyalgia.

#### 4.1.3. Fracture

Hydrotherapy is commonly used for the post-surgical rehabilitation of fractures and is used during both fixation as well as during convalescence. Deep-water running (DWR) has recently gained popularity for rehabilitation of fractures and osteoporosis in the lower limbs. When patients are training in a pool with 70% of their body immersed in water, submerged at shoulder level, and feet touching the pool bottom, the buoyancy of the water reduces the vertical ground reaction forces, thereby diminishing joint load and minimizing the potential risk of injury to the musculoskeletal system (76). Open-chain movement, which cannot be performed on land, is possible in an aquatic environment. DWR enables patients to exercise more. It also enables more complicated movements and a wider range of movements. Moreover, DWR is effective at maintaining cardiorespiratory function (76). In addition, DWR reduces the patients' fear of falling and enables them to experience the feeling of accomplishment.

Hydrotherapy activates bone formation biomarkers, suppresses bone resorption biomarkers, and improves bone metabolism, facilitating bone calcification and reconstruction (77). Exercise in water has been found to stimulate neuromuscular excitability, establish synaptic links, enhance nerve innervation rate, and restore muscle strength and muscle tone (78). In addition, hydrotherapy helps to reduce the likelihood of fragility fractures in the elderly by improving bone density and gait stability (79,80). Taken together, hydrotherapy can confer neuromuscular, psychological, and cardiorespiratory benefits that are recommended for patients with fractures, and elderly patients with osteoporosis-related fractures in particular.

#### 4.1.4. Anterior cruciate ligament injury

Anterior cruciate ligament (ACL) injury is not rare among basketball and football players who usually indulge in rotating, variable, and opposing motions. ACL injury markedly affects the competitive level of athletes. Only 65% athletes have been reported to return to the same competitive level after undergoing ACL reconstruction surgery (81,82). Thus, selection of a worthwhile rehabilitation protocol that can rapidly restore knee joint function and minimize movement limitations is inevitable but challenging. Hydrotherapy plays a unique role in the rehabilitation of an ACL injury (83). Again, thanks to the property of buoyancy, water helps to reduce the weight-bearing load for patients

undergoing post-surgical rehabilitation of an ACL injury. Pressure exerted on the knee joints can be adjusted by changing the level of immersion. With immersion to the neck, pressure on the knee is approximately 15 pounds, while immersion up to the symphysis pubis, umbilical region, and xiphoid regions results in knee pressure that is approximately 60%, 50%, and 40% of body weight, respectively (1). Water temperature is beneficial for producing and recruiting motor units. Hydrostatic pressure may alleviate tissue edema by promoting venous and lymphatic return (84). In the event of sudden onset pain, the drag force and turbulence of water can promptly decelerate limb movement, thereby reducing the risk of a repeat injury due to fall in comparison to exercise on land. The aquatic environment helps patients to maintain their balance by reducing the proprioceptive deficit in the flexion of the knee. Moreover, hydrotherapy helps to enhance the strength of the quadriceps and hamstring muscles, leading to a substantial reduction in reliance on the unaffected leg (85). A hybrid rehabilitation protocol that includes gymnasium, aquatic, and field exercises was reported to be helpful at enabling athletes to return to competition following rehabilitation for 90 days (86). Hajouj *et al.* found that alternately walking forward and backward on a foam roll in a pool promoted neuromuscular coordination and proprioception efficiency, helping after ACL reconstruction (87). So *et al.* reported on the significance of an aquatic treadmill (ATM) after ACL reconstruction (88). When participants ran at a cadence of 110 steps per minute, there was marked neuromuscular activation of the biceps femoris muscle in the stance phase and rectus femoris in the swing phase, potentially improving knee stability and protecting the ACL. Moreover, an increase in the depth of water was accompanied by a corresponding increase in muscle activity. All of this evidence supports the contention that hydrotherapy can yield positive outcomes in rehabilitation of an ACL injury. Selection of an appropriate rehabilitation protocol with appropriate use of auxiliary equipment, such as a foam roller and ATM, might play a crucial role in achieving satisfactory efficacy following an ACL injury.

#### 4.2. Neurological diseases

Neurorehabilitation is also an important area of modern rehabilitation medicine. Hydrotherapy is widely used in the rehabilitation of neurological diseases such as stroke (89-99), Parkinson's disease (PD) (100), multiple sclerosis (MS) (101-103), and dementia in adults, along with cerebral palsy (CP) (14) and autism spectrum disorder (ASD) (5) in children. Other than these widely reported diseases, hydrotherapy is also mentioned for treatment of conditions like migraines (104) and Rett syndrome (105). Hydrotherapy usually is performed as a part of the rehabilitation protocol, and it might have better efficacy when combined with conventional

physiotherapy. Moritz *et al.* reported that a combination of hydrotherapy and physiotherapy might be useful at overcoming activity limitations in stroke, but not in PD and other neurological diseases (106). In terms of the direct influence of hydrotherapy on the central nervous system (CNS), no new findings other than those from Becker were available, according to whom: *i)* hydrotherapy can increase regional cerebral blood flow (rCBF) due to enhanced cardiac output; and *ii)* hydrotherapy positively impacts the autonomic nervous system in a significant manner, including suppression of sympathetic activity and maintenance of sympathovagal balance (8). The complex neural mechanisms impacted by hydrotherapy warrant further study.

#### 4.2.1. Stroke

Stroke is the second leading cause of death and the third leading cause of disability (107). Post-stroke rehabilitation is known to markedly improve the clinical outcomes of stroke (108). To achieve a satisfactory clinical outcome including good ADL, QOL, and the ability to return to the community, a proper post-stroke rehabilitation plan that provides early, active, and sustained intensive training is indispensable. Hydrotherapy is no exception. Apart from conventional land-based post-stroke rehabilitation, hydrotherapy offers added advantages. Like conventional land-based rehabilitation, hydrotherapy provides motor and sensory stimuli, induces neuronal plasticity, and improves motor function along with static and dynamic balance in individuals suffering from a stroke (109). Therefore, hydrotherapy has been widely used as an adjuvant therapy in clinical settings. Hydrotherapy constitutes a coherent rehabilitation protocol for stroke patients combined with conventional rehabilitation methods since mounting evidence has shown that use of hydrotherapy in combination with other rehabilitation methods results in better rehabilitation than use of hydrotherapy alone (106).

Hemiplegia is the most predominant neurological deficit in stroke patients. Hence, overcoming hemiplegia is the first crucial task for both land- and water-based rehabilitation modalities. Cronin *et al.* evaluated the efficacy of hydrotherapy in reducing hyperreflexia in seven stroke patients with hemiplegia, and they found that water immersion for a short amount of time (5 min, 33°C) significantly reduced peripheral reflex excitability in patients as well as in healthy controls (110). Reduction of hyperreflexia in hemiplegic limbs is significant for post-stroke rehabilitation. Cronin *et al.* speculated that immersion for a longer amount of time might be required to have a persistent effect. Hence, water immersion is recommended for rehabilitation in hemiplegic stroke patients. Bei *et al.* compared the effects of hydrotherapy in combination with conventional post-stroke rehabilitation on the recovery of lower limb

dysfunction in hemiplegic patients suffering from a first stroke (89). They found that early aquatic exercise results in better balance, walking performance, and limb coordination (*vs.* conventional rehabilitation). Special equipment specially developed for hemiplegic patients is required for hydrotherapy with better efficacy. Pereira *et al.* developed special buoyancy cuffs for aquatic exercise used in post-stroke patients with hemiplegia (96). This equipment was found to modify gait kinematics, which might play a positive role in aquatic exercise training.

The most commonly used hydrotherapy method in post-stroke rehabilitation is aquatic exercise training involving active therapeutic movement, which is known to improve the functions of the lower limbs. Mounting evidence indicates that ATM facilitates enhanced balance, muscle strength and function of the lower limbs, and cardiopulmonary function (8). Saleh *et al.* conducted an RCT to compare the effects of rehabilitation using ATM and conventional land-based training on balance and gait in patients with chronic stroke, and they found that ATM improved isometric paretic knee flexor and knee extensor strength (111). ATM training was found to have better efficacy at improving balance and gait functions in these patients. Later, a study involving subacute stroke patients by Lee *et al.* compared the results of ATM and conventional land-based training (112). They found that ATM improved maximal isometric strength in the knee flexors and extensors (*vs.* land-based training) and concluded that ATM improved isometric muscle strength in the lower limbs. As with the application of ATM to other diseases, the important parameters are water temperature, water depth, walking speed, and duration. Parfitt *et al.* investigated the effects of ATM using different parameters, and they found that rCBF and heart rate (HR) improved with a longer time and faster speed on the treadmill (113). The ATM group had greater improvement of rCBF and a lower overall HR (*vs.* land-based training). Deeper water immersion may further lower the HR. Parfitt *et al.* concluded that ATM led to greater rCBF improvement, which contributed to optimizing the shear stress-mediated adaptation of the cerebrovasculature. Besides ATM, other hydrotherapy methods such as Ai Chi and Halliwick have also been used for post-stroke rehabilitation. A series of RCTs by Sagrario and Cruz compared the efficacy of Ai Chi to land-based rehabilitation and the combined use of Ai Chi and land-based rehabilitation (114-116). They found that Ai Chi and the combination group had better pain relief and amelioration of dysfunctions of balance (static and dynamic) and gait. These improvements contributed to a better QOL. The group receiving combination treatment had more improvement. Importantly, Rafsten *et al.* pointed out that Ai Chi helped to improve self-confidence and resilience and ameliorate post-stroke depression (117). Zhang *et al.* reported that the combination of the Halliwick method and ATM had better efficacy (*vs.* land-based rehabilitation) in terms of increasing

muscle strength and ameliorating muscle co-contraction without increasing spasticity in patients with subacute stroke (118). The aforementioned evidence demonstrates that hydrotherapy is an effective option for post-stroke rehabilitation, although a combination of hydrotherapy and conventional land-based rehabilitation might result in better efficacy.

#### 4.2.2. PD

PD is the second leading neurodegenerative disease (NDD) and has been a global concern. Patients with PD commonly suffer from motor and non-motor symptoms that markedly impact their daily life. Early and timely rehabilitation can significantly improve the ADL and QOL of patients with PD (119). Considering the pathophysiological characters of PD, several issues should be taken into account when devising a rehabilitation protocol for a patient with PD: *i)* patients with advanced PD commonly suffer from bradykinesia, gesture failure, and freezing of gait (FOG). Balance disturbance is common in patients with PD, so these patients have a greater risk of falls compared to healthy individuals. *ii)* Due to rigidity and bradykinesia, patients with PD find performing certain exercises more strenuous and they have less stamina in rehabilitation training. *iii)* Non-motor symptoms, such as cognitive impairments, mood dysfunction, and weaker executive function, can reduce their compliance with and adherence to the rehabilitation plan. *iv)* Due to the progressive nature of PD, the rehabilitation protocol needs to be adjusted in a timely manner depending on the patient's status and treatments (medication and/or surgery). Hence, as with the selection of a proper assessment task, the principles of objectification, multi-purpose, and simplification (OMS) as proposed in our previous studies (119-121) are also appropriate for the selection/development of a rehabilitation method for patients with PD. Moreover, the development of rehabilitation methods, and particularly for patients with PD, is highly encouraged and practiced (119-121). Hydrotherapy is recommended for PD rehabilitation due to the lower risk of falls and satisfactory efficacy in improving lower limb strength, balance, and gait. However, there are some specific concerns to consider once hydrotherapy is selected for PD rehabilitation: *i)* Water temperature: Currently, heat shock protein (HSP)-related PD mechanisms have garnered a great deal of attention. HSPs are known to be associated with the restoration of damaged proteins, response to inflammation, and tissue injury (122,123). Immersion in warm water can raise the core body temperature and act on HSPs, thereby relieving PD-related symptoms (124). Thus, selection of warm water is reasonable. However, higher pool temperatures ( $\geq 33^{\circ}\text{C}$ ) should be used with caution, since warmer water might be appropriate only for low-intensity training or for patients with advanced PD and

reduced physical capacity. *ii)* Location of hydrotherapy training: Carroll *et al.* reported that patients with PD may benefit from community-based hydrotherapy due to the timely provision of information and encouragement of adherence (125). Access to a rehabilitation location is an important factor due to the physical restrictions on patients with PD. A feasible location might improve the adherence of patients with PD to sustained long-term rehabilitation. *iii)* Long-term program: Hydrotherapy should be regularly and consistently performed due to the progressive and lifelong nature of PD. Bloem *et al.* recommended that hydrotherapy should be performed for at least 12 weeks, twice a week, and for 30–60 minutes at a time as a long-term course (126). *iv)* Protection: Considering the compromised movement of patients with PD, hydrotherapy for patients with PD requires more caution and protection by the therapist or coach. *v)* Individuation: The complex nature of PD symptoms leads to several individual differences among patients. Thus, the rehabilitation protocol should be individually selected depending on the pathophysiological status of the given patient. The main training components should seek to attain the goals of rehabilitation for the patient, and factors such as locomotion performance (127,128), gait (127,129), trunk stabilization and rotation (128), balance (127-130), and QOL (128) should be considered.

Several hydrotherapy methods have been used for PD rehabilitation. Conventional hydrotherapy methods like Ai Chi and Halliwick have been reportedly used in PD rehabilitation. Kurt *et al.* reported that Ai Chi improved balance, mobility, motor ability, and QOL in patients with PD (128). Moreover, Ai Chi had a better efficacy compared to land-based rehabilitation in patients suffering from mild to moderate stages of PD. In a pilot study, Terrens *et al.* reported that Halliwick alleviated balance dysfunction in patients with PD, and they recommended Halliwick as a safe treatment for patients with PD (130). Furthermore, several rehabilitation tasks originally performed on land were modified to be performed in water. Dual-task aquatic training is used for comprehensive training of patients with PD. Performing dual-task training in water may improve walking capacity and lead to better body adjustments and better motor skills, along with a reduced risk of falls. An RCT by da Silva and Israel compared the efficacy of dual-task aquatic training to a control group (not exercising), and they found that patients undergoing dual-task aquatic training had better functional mobility, gait, and balance (127). Recently, the same group investigated the efficiency of dual-task aquatic training in improving the motor symptoms, ADL, and QOL in patients with PD. They found that dual-task aquatic training can improve motor functions and ADL; however, a combination of aquatic and land-based dual-task training was recommended (131). Aquatic obstacle training (AOT) is developed for treating FOG. FOG is a common symptom in advanced PD, which is closely associated with the

risk of falls and QOL. Hydrotherapy is frequently recommended for rehabilitation of patients with FOG, because an aquatic environment can provide substantial stimuli for both central sensorimotor integration and peripheral muscle activity (132). Zhu *et al.* conducted an RCT to compare the efficacy of rehabilitation of AOT and Halliwick method in patients with PD and FOG (129). They found that after 6 weeks of training, AOT had a better efficacy with regards to gait and balance than the Halliwick method in these patients. However, another study found no significant differences in outcomes of motor-cognitive rehabilitation between land-based training and land-based training + hydrotherapy in patients with PD and FOG (133). The study therefore concluded that hydrotherapy was not associated with more benefits for motor-cognitive rehabilitation. A recent study designed a sequential multimodal rehabilitation protocol, namely sequentially performing water- and land-based exercises for 12 weeks, for patients with PD (134). The study found that this multimodal protocol markedly improved balance, ADL, and motor functions in these patients. Moreover, hydrotherapy and land-based rehabilitation are complementary therapies, and their combination might result in better efficacy. Sleep disturbance is an important non-motor symptom in PD (135). Loureiro *et al.* conducted an RCT comparing the efficacy of PD rehabilitation using conventional land-based training and land-based training + WATSU (136). They found that land-based training + WATSU had better efficacy in improving sleep quality and QOL in patients with PD.

#### 4.2.3. MS

MS is a chronic progressive demyelinating disease involving the CNS. MS-related symptoms involve a spectrum of neurologic deficits, involving cognitive impairments, fatigue, symptoms of cranial nerve palsy (diplopia, visual field deficits, dysphonia, and dysphagia, *etc.*), paresthesia, dysfunctions of gait and balance, ataxia, spasticity, walking disorder, and bowel and bladder disorders. Mental and mood disorders are not rare. The ADL and QOL of patients are markedly influenced by these complex and individual symptoms. However, there is currently no specific treatment or definitive cure for MS. Other than medication, neurorehabilitation plays a significant role in the treatment of MS, and exercise training is the most effective non-pharmacological treatment for MS (103). The goals of rehabilitation include alleviation of functional disorders and improvement of ADL and QOL. All forms of physiotherapy, namely exercise rehabilitation, kinesiotherapy, massage, and certainly hydrotherapy, can be used for rehabilitation of MS. Mechanisms involved in MS rehabilitation are not completely understood. According to the literature, the neurorehabilitation-related mechanisms offer: *i)*

Benefits of neuroplasticity: Bonzano *et al.* found that appropriate rehabilitation including voluntary movement of the upper limbs resulted in changes in the white matter microstructure and improved motor performance in patients with MS (137). In a resting-state functional nuclear magnetic resonance imaging (fMRI) study, Pareto *et al.* found that effective cognitive rehabilitation could lead to improved patterns of brain synchronization and resting-state networks along with amelioration of cognitive function in patients with MS (138). Bahmani *et al.* had reported that effective hydrotherapy could enhance neurotransmitter levels (139). In a review, Shariat *et al.* reported that an imbalance in brain-derived neurotrophic factor (BDNF) played a role in the pathophysiology of MS (140). Hydrotherapy could alleviate MS-related fatigue by elevating BDNF levels. Evidence from the aforementioned research indicates that effective neurorehabilitation exercise may have positive effects on the brain and alleviate neurological deficits. *ii) Modulation of the peripheral and CNS immunomodulatory responses:* A study by Souza *et al.* found that effective exercise suppressed the production of proinflammatory cytokines and upregulated regulatory T cell markers in spleen cells. Moreover, exercise reduced the permeability of the blood-brain barrier and limited the transmigration of autoreactive T cells to the CNS in animal models of autoimmune encephalomyelitis (141). In addition, exercise reportedly affected remyelination, neuroinflammation, microglia, astrocytes, and infiltrating immune cells in MS (142). MS is an autoimmune inflammatory disease, so the mechanisms of neurorehabilitation might be affected by protective regulation of the inflammatory response. *iii) Regulation of the dysbiosis of the gut microbiota:* Barone *et al.* reported that neurorehabilitation caused the modulation of the MS-related dysbiosis of gut microbiota by supplementing beneficial short-chain fatty acid producers and suppressing pathobionts (143). The study noted, along with improvement of physical performance and alleviation of fatigue, a reduction in proinflammatory lymphocytes, inflammatory markers (such as proinflammatory IL-17), and circulating lipopolysaccharide levels.

As rehabilitation treatment for MS, hydrotherapy has been used for management of fatigue (140,144,145), balance (140,145), spasticity (144,146), and QOL (144,147). Hydrotherapy has been recommended for relieving spasticity in MS since it can suppress the activity of gamma neurons, inhibit afferent impulses, and have relaxing and analgesic effects (101). A study by Amedoro *et al.* indicated that a combination of hydrotherapy and conventional land-based physical therapy may have a better efficacy in MS rehabilitation (102). Shariat *et al.* conducted a systematic review and found that hydrotherapy is effective at relieving fatigue and improving balance in patients with MS (140). Bahmani *et al.* found that hydrotherapy is helpful at

improving sexual function in women with MS (139). Gurpinar. *et al.* compared the efficacy of hydrotherapy in the form of Halliwick and aquatic plyometric exercise (APE) in patients with MS. They noted significant improvement in the limits of stability and hand dexterity in both groups; however, the Halliwick method had better efficacy in terms of hand dexterity and overall limits of stability (*vs.* APE). Both Halliwick and APE are recommended for MS rehabilitation because of their safety and efficacy (148). A RCT involving women with MS concluded that hydrotherapy significantly improved functional capacity, balance, and fatigue in those subjects (145). All of these previous studies verified the value of hydrotherapy in MS rehabilitation. Hao *et al.* compared the effects of seven different exercise modalities (hydrotherapy, aerobic exercise, yoga, Pilates, virtual reality (VR) exercise, whole-body vibration exercise, and resistance exercise) on balance function and functional walking ability in patients with MS (149). They reported that hydrotherapy significantly reduced the Timed-Up-and-Go Scores, indicating a significant improvement in functional walking ability. The authors contended that hydrotherapy is superior to conventional land-based exercise and might be the best method to improve functional walking ability in patients with MS.

#### 4.2.4. Dementia

Dementia has become a major public health concern with the aging of the global population. Age-related frailty is closely associated with various physiological or pathophysiological changes, including age-related hearing loss (150), accumulation of pathogenetic proteins like  $\beta$ -amyloid ( $A\beta$ ) (151), and  $\alpha$ -synuclein (152), dysbiosis of gut microbiota (153), and dementia (150). Alzheimer's disease (AD), the leading NDD, is the most common type of dementia (154). Thus far, there is no specific medication to cure dementia or even to reverse its progression (155). Several studies have confirmed the positive effects of aerobic activities performed on land as well as in the water on the improvement of cognition function (156,157), even in subjects with AD (156); nonetheless, the benefits that rehabilitation has on dementia, and particularly on mild cognitive impairment (MCI) and early dementia, remains controversial. Tortora *et al.* conducted a dementia-specific rehabilitation program focusing on strength, balance, physical activity, and ADL involving 365 patients with early dementia or MCI, but they noted no improvement in terms of ADL, physical activity, or QOL (158). According to a recent study by Antonenko *et al.*, cognitive training with concurrent brain stimulation did not ameliorate symptoms in patients with cognitive impairments (159). In contrast, several recent studies reported that VR-based cognitive rehabilitation was effective at treating patients with MCI (158,160). The available evidence regarding hydrotherapy is insufficient. Kim *et al.* found that both

hydrotherapy and land-based exercise increased serum  $A\beta$  and HSP27 and decreased pulse wave velocity in 40 older healthy women (161). Their results provided a working basis of hydrotherapy's potential to prevent NDDs. Becker and Lynch reported the first case of a 54-year woman with advanced AD who underwent 17 hydrotherapy sessions in 19 weeks (1 hour per day) in a warm water therapy pool, following which, her cognitive functions improved (162). A subsequent review by Becker mentioned the application of hydrotherapy to dementia, but no robust evidence was provided (8). Henwood *et al.* conducted an aquatic exercise program for residential aged adults with dementia for 12 weeks (163). They noted significant improvements in the skeletal muscle index and lean mass, but dementia-related behavioral and psychological symptoms and ADL only tended to improve ( $p = 0.06$ ).

Overall, studies verifying the efficacy of hydrotherapy in treating dementia are insufficient, which might be due to the difficulties associated with conducting such studies. Medical personnel are usually reluctant to provide hydrotherapy to patients with cognitive impairments since it is risky and laborious. The study by Becker required two persons. Moreover, a situation in which patients cannot clearly communicate with the staff might result in a failure to identify a potentially dangerous situation in a timely manner. In addition, difficulty in accessing the hydrotherapy location, and/or poor economic conditions may curtail hydrotherapy for subjects with dementia. Nonetheless, studies verifying the efficacy and safety of hydrotherapy in treating dementia are warranted.

#### 4.2.5. CP

CP is the most common lifelong movement disability in children (164), and it markedly influences the ADL and QOL of children. It is not progressive but improvement is rare in clinical practice. CP mainly affects gross motor skills, walking ability, spasticity, gait and balance, and it leads to compromised cardiorespiratory function, particularly in children, due to the lack of exercise. Mounting evidence indicates that CP-related symptoms can be markedly alleviated by rehabilitation exercises. Accordingly, children and adults (children who have grown up with CP) require regular rehabilitation (165), which involves therapeutic training including land-based exercises, muscle strengthening, stretching, balance training, task-oriented functional training, and hydrotherapy (166). Over the past 20 years, hydrotherapy has been used for CP rehabilitation (8). The physical properties of water, such as buoyancy and its comfortable temperature, can confer several benefits and allow many difficult tasks to be attempted. Immersion in warm water at 33°C–35°C can reduce spasticity in children with CP (167). Moreover, exercise in water is interesting and relaxing for many children (children like to play in

water) (167). Hence, hydrotherapy is readily accepted by children and parents.

In contrast to conventional land-based rehabilitation, hydrotherapy has the following advantages: *i*) Hydrotherapy is effective at improving gross motor skills. Akinola *et al.* conducted a 10-week hydrotherapy program involving 30 children with spastic CP who were divided into a hydrotherapy group and a control group. Both groups performed stretching and functional training exercise. The control group performed rehabilitation on land while the hydrotherapy group performed exercises in the water (28°C–32°C). After the intervention (10 weeks, twice per week), all domains of gross motor skills except walking, running, and jumping had significantly improved in the hydrotherapy group, and results for the hydrotherapy group were considered to be significantly better than those for the control group (164). Treatments like swimming (168) and the ten-point Halliwick program (14,169,170) are commonly used for CP rehabilitation and have demonstrated good efficacy at improving gross motor skills. *ii*) Hydrotherapy is useful at managing spasticity. Adar *et al.* compared the efficacy of hydrotherapy and land-based exercises in 32 children with CP (168). The hydrotherapy program included aquatic exercises (33°C, 60 min, five times per week for six weeks) and aerobic exercises (slow walking or swimming, 25 min). The study found that hydrotherapy had the same efficacy as land-based exercise for spasticity management and improvement of motor dysfunction. Hydrotherapy resulted in a better QOL. A Pakistan-based study also found that hydrotherapy in a pool (32°C–34°C, twice a week, 32 weeks) resulted in amelioration of spasticity and improvement in gross motor skills in children with CP (171). *iii*) Hydrotherapy helps to enhance cardiorespiratory function. Due to the hydrostatic pressure in an aquatic environment, fluids are driven from the extremities toward the central cavity, which results in the compression of the thorax, an increase in the respiratory load, and ultimately results in a subsequent increase (approximately 30%–60%) in cardiac output (172,173). Thus, hydrotherapy offers significant benefits in terms of enhancing cardiopulmonary function. This is especially beneficial for children with CP, who have compromised cardiorespiratory function due to lack of exercise. *iv*) Other than physical benefits, hydrotherapy can result in psychological improvements. Hydrotherapy is interesting and relaxing; this is helpful at relieving stress regarding the disease and training for children and parents. Moreover, exercise in the water allows the children to try difficult movements that cannot otherwise be performed on land, which has a positive influence on their self-confidence. Communication in the swimming pool with the therapist/coach or wardmates positively impacts their psychological states. Other than these advantages, a handful of studies have reported that hydrotherapy was efficacious at improving aerobic capacity (174), body fat,

core strength, and bone mineral density (175).

However, the available research on CP-related hydrotherapy has several limitations that prevent the obtaining of more robust evidence. Most of the aforementioned studies were conducted using small sample sizes. In addition, important domains, such as CP-related pain, were seldom mentioned. Immersion in hot water is known to be helpful at relieving pain in infants (176). Hydrotherapy is also suitable for the management of chronic pain in patients with CP (177). However, no study has evaluated hydrotherapy's feasibility at alleviating CP-related pain thus far. Studies addressing these issues are highly anticipated.

#### 4.2.6. ASD

ASD refers to a spectrum of genovariation-based neurodevelopmental disorders characterized by impairments in social communication, limited interests, and repetitive stereotyped behaviors. Barriers in social communication might prevent patients with ASD from participating in sports and exercises, thereby reducing their athletic activities. Conversely, motor impairments can cause problems in social communication, thereby forming a vicious circle (178). Previous evidence had indicated that improvement in motor ability *via* exercise interventions not only improved motor outcomes but also reduced impairments in behavior, cognition, and deficits in social communication (178). The mechanisms for this are not completely understood. Breaking the vicious circle involving motor impairment and deficits in social communication might be a plausible explanation. Based on this "vicious circle" theory, the application of hydrotherapy to ASD could confer two benefits: *i*) Direct effects by ameliorating behaviors as a direct result of hydrotherapy itself. Exercise or immersion in warm water is comfortable and enjoyable for most children. Hydrotherapy is helpful at reducing their stress and nervousness. Hydrotherapy can create opportunities for communication, such as inevitable communication with the therapist/coach and communication with other children undergoing training. Moreover, children with ASD reportedly need strong sensory stimulation. Exercise in the water involves a response to water pressure, and this strong sensory stimulation might result in a "calming effect," thereby improving their capacity to interact and communicate with other people (179). *ii*) Indirect effects involve the improvement of their motor skills, which might indirectly benefit their social communication. In addition, children with ASD usually suffer from sleep disturbance, which might be associated with elevated levels of circulating IL-1 $\beta$  and TNF- $\alpha$  (180). Hydrotherapy can reduce serum IL-1 $\beta$  and TNF- $\alpha$  levels, improving sleep quality (181). Sourvinos *et al.* reported that hydrotherapy is effective at improving language skills in children with ASD (182).

Thus far, the hydrotherapy programs for ASD,

such as the Halliwick method, sensory exposure, iCan Swim, multi-systemic aquatic therapy (CI-MAT), and aquatic versus kata techniques training, are based on "learn-to-swim programs." The Halliwick method plays a crucial role among the aforementioned methods. The Halliwick method has benefits with regards to social communication and behavior in children with ASD. Moreover, these improvements might be further reinforced by communication with fellow trainees or with therapists (183). In addition to social communication, Vodakova *et al.* found that the Halliwick method was effective at improving gross motor skills (33). Thus, hydrotherapy, and particularly the Halliwick method, is beneficial for ASD rehabilitation.

#### 4.3. COVID-19

Over four years have passed since the start of the COVID-19 pandemic. The dangers of the SARS-CoV-2 virus cannot be neglected (184). Indeed, numerous people are suffering from the post-acute sequelae of COVID-19, which are referred to as long COVID (185). Hence, the "application of hydrotherapy to COVID-19" is a topic that should not be ignored. Bailly *et al.* reviewed the potential and feasibility of providing hydrotherapy during the COVID-19 pandemic (186). Antonelli and Donelli discussed the possibility of performing respiratory rehabilitation for post-COVID-19 patients in a spa center (187). A study pointed out that water from a swimming pool is not good for the survival of SARS-CoV-2 virus (188). A research protocol focusing on verification of the efficacy of hydrotherapy for post-COVID-19 children has been published (189). Lucas *et al.* reported a strategy to perform hydrotherapy during the pandemic (190). However, there are few studies that involved actually performing hydrotherapy during the pandemic, which might be attributed to measures such as "lockdowns" and "isolation at home" that were enforced to prevent the epidemic. Moreover, medical staff might be reluctant to conduct these rehabilitation training exercises for fear of being infected themselves.

All of the available studies are related to long COVID. Grishechkina *et al.* reported on the efficacy of a tailored and multidisciplinary rehabilitative program including hydrotherapy in treating patients with long COVID. Neuromotor rehabilitation consisting of aquatic exercises for muscle strength and balance, respiratory exercises, and psychological support were performed by COVID-19 survivors. This tailored and multidisciplinary rehabilitative program was found to prevent the new onset of disabilities over the short term and long term (over 6 months). Moreover, incorporating health resort medicine and balneotherapy into rehabilitation programs can reduce the economic burden on healthcare system (191). Ogonowska-Slodownik *et al.* conducted a RCT to compare the effects of rehabilitation using hydrotherapy and land-based exercise in 74 children with post-COVID

conditions (192). Oxygen uptake values were found to increase in both the hydrotherapy and land-based groups. There were no significant differences in fatigue-related indices. The land-based group had better results with regard to the QOL domain.

The impacts of SARS-CoV-2 infection are known to be systemic. Almost all systems and all organs in the human body can theoretically be affected by COVID-19 (185). Accordingly, various symptoms might manifest due to the dysfunction of a certain system/organ. Hydrotherapy is feasible for rehabilitation of COVID-19-related symptoms, and long COVID-related disabilities and deficits in particular. More studies are expected to investigate this topic.

#### 5. Adverse events and contraindications

Hydrotherapy-related adverse events, and particularly severe adverse events, have rarely been reported. Most of the available studies have reported that "no adverse effects were observed," hydrotherapy-related adverse events cannot be ignored, and this is especially true for patients with certain conditions. Fatigue and exhaustion are the most commonly reported adverse events in patients with cancer after undergoing hydrotherapy (193,194). Short-term edema (193) and increased pain (195) have been sporadically reported in patients with cancer. One study on OA reported that a patient withdrew from hydrotherapy owing to low back pain (196). However, none of these studies reported whether these problems could be attributed to hydrotherapy.

Hydrotherapy is performed in an artificial environment, and the intervention protocol (treatment duration, frequency, *etc.*) and parameters (water temperature, pool size, *etc.*) are strictly managed by the therapist. Excessive hydrotherapy may result in a sports injury, so the therapist should devise an appropriate hydrotherapy protocol while fully considering the physical and pathophysiological state of a given patient to avoid adverse events. Moreover, the establishment of strict but feasible criteria for indications and contraindications of hydrotherapy would help clinicians to select (or exclude) those patients who are suited (or unsuited) to hydrotherapy.

Patients with contraindications to land-based rehabilitation are unsuitable for hydrotherapy. However, hydrotherapy-related contraindications have not yet been comprehensively reported. Based on the available literature and our own experience, several issues should be considered.

*i)* Hydrotherapy-induced infection is the first noteworthy problem because a hydrotherapy pool with a water temperature above 30°C is a favorable environment for microbial growth. Owing to the strict daily management of the water quality of the hydrotherapy pool, the prevalence of hydrotherapy-related infections is extremely low, even in patients with

external fixation who are susceptible to infection. A recent study investigated hydrotherapy-related infections in patients who underwent external fixation, and it found that only 32 of 1,200 sessions (3%) were missed because of secretions or other signs of infection (197). Thus, hydrotherapy-related infection is controllable if the water quality is strictly managed and the participating patients are carefully selected. Hydrotherapy is only suitable for infection-free patients (197). A confirmed infection or signs of infection are contraindications for hydrotherapy.

*ii)* Hydrotherapy-related changes in the blood circulation are another non-negligible problem. That said, temperature and pressure stimuli due to water might improve circulatory function and benefit patients with cardiovascular disease. Water pressure compresses the superficial veins of the extremities, resulting in increased blood volume in the chest, 26–34% of which is allocated to the heart, effectively expanding the functional capacity and hemodynamic parameters of the left ventricle. In addition, warm water (32–34°C) enhances the influence of the parasympathetic nervous system and induces bradycardia, decreased blood pressure, and vascular resistance by stimulating the pressure receptors (198). That said, hydrotherapy may be harmful to patients with heart disease. Meyer and Bücking reported that hydrotherapy induced abnormal mean pulmonary artery pressure and mean pulmonary artery pressure in patients with myocardial infarction and chronic congestive heart failure (199). Left ventricular overload and stroke volume have been noted in patients with severe congestive heart failure. A point worth noting is that many patients still feel good during hydrotherapy, regardless of hemodynamic deterioration (199,200). Accordingly, severe heart conditions such as heart failure and myocardial infarction are contraindications for hydrotherapy.

*iii)* Considering the special aquatic environment, some dermatoses, such as eczema, psoriasis, and chronic pruritus, were put forward as contraindications for hydrotherapy according to a French study (201).

## 6. Concluding remarks

The current study conducted a comprehensive review investigating the clinical applications of hydrotherapy, with a focus on athletic rehabilitation and neurorehabilitation based on the latest available evidence. The aim of this study was to provide updated information to all rehabilitation researchers. Although the application of hydrotherapy extends beyond the diseases discussed in this paper, the take-home messages should benefit those who are engaging in the research/practice of hydrotherapy. Based on the aforementioned insights as well as on our clinical experience thus far, we offer several suggestions that might benefit future research:

*i)* Combining hydrotherapy with other treatments: Mounting evidence cited in this study has corroborated

that the combined use of hydrotherapy and other treatments [land-based exercises, medication, surgery, and other treatments such as direct-current stimulation (202)] has a better efficacy than hydrotherapy alone. Thus, combined therapeutic programs should be designed after considering the pathophysiological state of a given patient so as to reap the maximal benefits.

*ii)* Attention needs to be paid to the barriers associated with participation in hydrotherapy. Compared to conventional land-based exercise, hydrotherapy requires special facilities and a well-trained therapist or coach, making it more expensive and potentially discouraging low-income patients. Thus, the government and the health insurance system should offer added support for hydrotherapy. The location of the hydrotherapy facility must be seriously considered since access to a facility is a determining factor for the patient and his or her family with regards to continuing hydrotherapy. Thus, a hydrotherapy center for geriatric diseases needs to be established in or near where the elderly live or in a geriatric hospital to increase adherence.

*iii)* Development of hydrotherapy-specific assessment tools should be considered. Thus far, almost all outcome measures for hydrotherapy are the same as those used for land-based therapies. However, the environment in the water is quite different from that on the land. Thus, tools that are specific to an aquatic environment need to be developed. The principles of OMS as mentioned for development of PD-related behavioral assessments (119–121) are applicable to the development of those tools.

*iv)* Tasks and equipment in hydrotherapy should be developed in a disease-specific manner. Different diseases have their own pathophysiological characteristics. Thus, disease-specific tasks/equipment might have better efficacy and safety for the patient. When, for example, using an ATM for PD, it should have a lower speed, a task of a shorter duration, and better protection should be provided since patients with PD always have a higher risk of falls than other patients

*v)* Use of the latest computer technologies should be considered in hydrotherapy: With the development of sensors, physiological parameters can be measured in real time (119), which can allow the therapist to ascertain the patient's state and adjust the training exercise in a timely manner. Well-developed motor analysis software with a camera to dynamically capture kinetic motion can help the clinician to understand the motor characteristics of a particular patient and then design a more appropriate training exercise plan. VR-based equipment is also helpful to simulate various training scenarios, thereby improving the exercise. A robot-assisted hydrotherapy system would help to resolve the problem of the dearth of therapists. Miyoshi *et al.* developed a robotic gait trainer that can be used in walking exercises on a treadmill in water, and they found that this equipment improved the effects of both hydrotherapy and land-based treadmill gait training (203). Moreover, artificial

intelligence technology with machine learning could be used to design a rehabilitation program, evaluate the effectiveness of training, and improve the training program. However, there are few studies on these topics. Studies that provide robust evidence regarding the application of computer technologies to hydrotherapy are highly anticipated.

In conclusion, more novel hydrotherapy-related techniques are emerging with advances in science and technology. The value of hydrotherapy should be recognized by more people, including clinicians and patients. Along with land-based rehabilitation, hydrotherapy may lead to a better future.

### Acknowledgements

The authors would like to thank the therapists from Shenzhen Jieshui Medical Technology Co., LTD (<http://jc-rehab.com/en/>) for their useful suggestions.

**Funding:** This work was supported by the Shenzhen High-level Hospital Construction Fund (No.23274G1001).

**Conflict of Interest:** The author has no conflicts of interest to disclose.

### References

1. Becker BE. Aquatic therapy: Scientific foundations and clinical rehabilitation applications. *PM R*. 2009; 1:859-872.
2. Lei C, Chen H, Zheng S, Pan Q, Xu J, Li Y, Liu Y. The efficacy and safety of hydrotherapy in patients with knee osteoarthritis: A meta-analysis of randomized controlled trials. *Int J Surg*. 2024; 110:1711-1722.
3. Adeel M, Lin BS, Chaudhary MA, Chen HC, Peng CW. Effects of strengthening exercises on human kinetic chains based on a systematic review. *J Funct Morphol Kinesiol*. 2024; 9.
4. Xiong T, Bai X, Wei X, Wang L, Li F, Shi H, Shi Y. Exercise rehabilitation and chronic respiratory diseases: Effects, mechanisms, and therapeutic benefits. *Int J Chron Obstruct Pulmon Dis*. 2023; 18:1251-1266.
5. Naumann K, Kernot J, Parfitt G, Gower B, Davison K. Water-based interventions for people with neurological disability, autism, and intellectual disability: A scoping review. *Adapt Phys Activ Q*. 2021; 38:474-493.
6. Palladino L, Ruotolo I, Berardi A, Carlizza A, Galeoto G. Efficacy of aquatic therapy in people with spinal cord injury: A systematic review and meta-analysis. *Spinal Cord*. 2023; 61:317-322.
7. Driller M, Leabeater A. Fundamentals or icing on top of the cake? A narrative review of recovery strategies and devices for athletes. *Sports (Basel)*. 2023; 11.
8. Becker BE. Aquatic therapy in contemporary neurorehabilitation: An update. *PM R*. 2020; 12:1251-1259.
9. Mellado-Garcia E, Diaz-Rodriguez L, Cortes-Martin J, Sanchez-Garcia JC, Piqueras-Sola B, Prieto Franganillo MM, Rodriguez-Blanque R. Hydrotherapy in pain management in pregnant women: A meta-analysis of randomized clinical trials. *J Clin Med*. 2024; 13.
10. Mellado-Garcia E, Diaz-Rodriguez L, Cortes-Martin J, Sanchez-Garcia JC, Piqueras-Sola B, Higuero Macias JC, Rodriguez-Blanque R. Systematic reviews and synthesis without meta-analysis on hydrotherapy for pain control in labor. *Healthcare (basel)*. 2024; 12.
11. Park SY, Kwak YS, Pekas EJ. Impacts of aquatic walking on arterial stiffness, exercise tolerance, and physical function in patients with peripheral artery disease: A randomized clinical trial. *J Appl Physiol (1985)*. 2019; 127:940-949.
12. Bissacco D, Mosti G, D'Oria M, Lomazzi C, Casana R, Morrison N, Caggiati A. Rationale and current evidence of aquatic exercise therapy in venous disease: A narrative review. *Vascular*. 2023; 31:1026-1034.
13. Shariat A, Najafabadi MG, Dos Santos IK, Anastasio AT, Milajerdi HR, Hassanzadeh G, Nouri E. The effectiveness of aquatic therapy on motor and social skill as well as executive function in children with neurodevelopmental disorder: A systematic review and meta-analysis. *Arch Phys Med Rehabil*. 2024; 105:1000-1007.
14. Tapia C, Constanzo J, Gonzalez V, Barria RM. The effectiveness of aquatic therapy based on the Halliwick concept in children with cerebral palsy: A systematic review. *Dev Neurorehabil*. 2023; 26:371-376.
15. Moini Jazani A, Nasimi Doost Azgomi H, Nasimi Doost Azgomi A, Nasimi Doost Azgomi R. Effect of hydrotherapy, balneotherapy, and spa therapy on blood pressure: A mini-review. *Int J Biometeorol*. 2023; 67:1387-1396.
16. Chidambaram Y, Vijayakumar V, Ravi P, Boopalan D, Anandhan A, Kuppusamy M. Does hydrotherapy influence plasma glucose levels in type 2 diabetes? - A scoping review. *J Complement Integr Med*. 2024; 21:14-18.
17. Zhu Z, Muhamad AS, Omar N, Ooi FK, Pan X, Ong MLY. Efficacy of exercise treatments for chronic obstructive pulmonary disease: A systematic review. *J Bodyw Mov Ther*. 2024; 38:106-127.
18. Shariat A, Ghayour Najafabadi M, Ghannadi S, Nakhostin-Ansari A, Hakakzadeh A, Shaw BS, Ingle L, Cleland JA. Effects of aquatic therapy on balance in older adults: A systematic review and meta-analysis. *Eur Geriatr Med*. 2022; 13:381-393.
19. Lim JY, Tchai E, Jang SN. Effectiveness of aquatic exercise for obese patients with knee osteoarthritis: A randomized controlled trial. *PM R*. 2010; 2:723-731; quiz 793.
20. Lai CJ, Liu WY, Yang TF, Chen CL, Wu CY, Chan RC. Pediatric aquatic therapy on motor function and enjoyment in children diagnosed with cerebral palsy of various motor severities. *J Child Neurol*. 2015; 30:200-208.
21. Torres-Ronda L, Del Alcazar XS. The properties of water and their applications for training. *J Hum Kinet*. 2014; 44:237-248.
22. Mooventhan A, Nivethitha L. Scientific evidence-based effects of hydrotherapy on various systems of the body. *N Am J Med Sci*. 2014; 6:199-209.
23. Bartels EM, Lund H, Hagen KB, Dagfinrud H, Christensen R, Danneskiold-Samsøe B. Aquatic exercise for the treatment of knee and hip osteoarthritis. *Cochrane Database Syst Rev*. 2007;CD005523.
24. Bartels EM, Juhl CB, Christensen R, Hagen KB, Danneskiold-Samsøe B, Dagfinrud H, Lund H. Aquatic

- exercise for the treatment of knee and hip osteoarthritis. *Cochrane Database Syst Rev.* 2016; 3:CD005523.
25. Reger M, Kutschan S, Freuding M, Schmidt T, Josfeld L, Huebner J. Water therapies (hydrotherapy, balneotherapy or aqua therapy) for patients with cancer: A systematic review. *J Cancer Res Clin Oncol.* 2022; 148:1277-1297.
  26. Bleakley CM, Bieuzen F, Davison GW, Costello JT. Whole-body cryotherapy: empirical evidence and theoretical perspectives. *Open Access J Sports Med.* 2014; 5:25-36.
  27. Rose C, Edwards KM, Siegler J, Graham K, Caillaud C. Whole-body cryotherapy as a recovery technique after exercise: A review of the literature. *Int J Sports Med.* 2017; 38:1049-1060.
  28. Maccarone MC, Magro G, Solimene U, Scanu A, Masiero S. From *in vitro* research to real life studies: An extensive narrative review of the effects of balneotherapy on human immune response. *Sport Sci Health.* 2021; 17:817-835.
  29. Galvez I, Fioravanti A, Ortega E. Spa therapy and peripheral serotonin and dopamine function: A systematic review. *Int J Biometeorol.* 2024; 68:153-161.
  30. Marazziti D, Baroni S, Giannaccini G, Catena Dell'Osso M, Consoli G, Picchetti M, Carlini M, Massimetti G, Provenzano S, Galassi A. Thermal balneotherapy induces changes of the platelet serotonin transporter in healthy subjects. *Prog Neuropsychopharmacol Biol Psychiatry.* 2007; 31:1436-1439.
  31. Baroni S, Marazziti D, Consoli G, Picchetti M, Catena-Dell'Osso M, Galassi A. Modulation of the platelet serotonin transporter by thermal balneotherapy: A study in healthy subjects. *Eur Rev Med Pharmacol Sci.* 2012; 16:589-593.
  32. Kurabayashi H, Tamura K, Tamura J, Kubota K. The effects of hydraulic pressure on atrial natriuretic peptide during rehabilitative head-out water immersion. *Life Sci.* 2001; 69:1017-1021.
  33. Vodakova E, Chatziioannou D, Jesina O, Kudlacek M. The effect of Halliwick method on aquatic skills of children with autism spectrum disorder. *Int J Environ Res Public Health.* 2022; 19.
  34. Cha HG, Shin YJ, Kim MK. Effects of the Bad Ragaz Ring method on muscle activation of the lower limbs and balance ability in chronic stroke: A randomised controlled trial. *Hong Kong Physiother J.* 2017; 37:39-45.
  35. Schitter AM, Fleckenstein J, Frei P, Taeymans J, Kurpiers N, Radlinger L. Applications, indications, and effects of passive hydrotherapy WATSU (WaterShiatsu)-A systematic review and meta-analysis. *PLoS One.* 2020; 15:e0229705.
  36. Pooley S, Spendiff O, Allen M, Moir HJ. Comparative efficacy of active recovery and cold water immersion as post-match recovery interventions in elite youth soccer. *J Sports Sci.* 2020; 38:1423-1431.
  37. Pesare E, Vicenti G, Kon E, Berruto M, Caporali R, Moretti B, Randelli PS. Italian Orthopaedic and Traumatology Society (SIOT) position statement on the non-surgical management of knee osteoarthritis. *J Orthop Traumatol.* 2023; 24:47.
  38. Zhang X, Xue T, Hou D, Lu C. The efficacy and safety of hydrotherapy in patients with knee osteoarthritis: A protocol for systematic review and meta-analysis. *Medicine (Baltimore).* 2023; 102:e33027.
  39. Calles Plata I, Ortiz-Rubio A, Torres Sanchez I, Cabrera Martos I, Calvache Mateo A, Heredia-Ciuro A, Valenza MC. Effectiveness of aquatic therapy on sleep in persons with fibromyalgia. A meta-analysis. *Sleep Med.* 2023; 102:76-83.
  40. Bravo C, Rubi-Carnacea F, Colomo I, Sanchez-de-la-Torre M, Fernandez-Lago H, Climent-Sanz C. Aquatic therapy improves self-reported sleep quality in fibromyalgia patients: A systematic review and meta-analysis. *Sleep Breath.* 2024; 28:565-583.
  41. Rivas Neira S, Pasqual Marques A, Fernandez Cervantes R, Seoane Pillado MT, Vivas Costa J. Efficacy of aquatic vs land-based therapy for pain management in women with fibromyalgia: A randomised controlled trial. *Physiotherapy.* 2024; 123:91-101.
  42. Carrasco-Vega E, Guiducci S, Nacci F, Bellando Randone S, Bevilacqua C, Gonzalez-Sanchez M, Barni L. Efficacy of physiotherapy treatment in medium and long term in adults with fibromyalgia: An umbrella of systematic reviews. *Clin Exp Rheumatol.* 2024; 42:1248-1261.
  43. Ma J, Zhang T, Li X, Chen X, Zhao Q. Effects of aquatic physical therapy on clinical symptoms, physical function, and quality of life in patients with fibromyalgia: A systematic review and meta-analysis. *Physiother Theory Pract.* 2024; 40:205-223.
  44. Medrado LN, Mendonca MLM, Budib MB, Oliveira-Junior SA, Martinez PF. Effectiveness of aquatic exercise in the treatment of inflammatory arthritis: Systematic review. *Rheumatol Int.* 2022; 42:1681-1691.
  45. Qu C, Wu Z, Xu M, Qin F, Dong Y, Wang Z, Zhao J. Cryotherapy models and timing-sequence recovery of exercise-induced muscle damage in middle- and long-distance runners. *J Athl Train.* 2020; 55:329-335.
  46. Elnaggar RK, Elshafey MA. Effects of combined resistive underwater exercises and interferential current therapy in patients with juvenile idiopathic arthritis: A randomized controlled trial. *Am J Phys Med Rehabil.* 2016; 95:96-102.
  47. Dundar U, Solak O, Toktas H, Demirdal US, Subasi V, Kavuncu V, Evcik D. Effect of aquatic exercise on ankylosing spondylitis: A randomized controlled trial. *Rheumatol Int.* 2014; 34:1505-1511.
  48. Martey C, Sengupta R. Physical therapy in axial spondyloarthritis: Guidelines, evidence and clinical practice. *Curr Opin Rheumatol.* 2020; 32:365-370.
  49. Shi Z, Zhou H, Lu L, Pan B, Wei Z, Yao X, Kang Y, Liu L, Feng S. Aquatic exercises in the treatment of low back pain: A systematic review of the literature and meta-analysis of eight studies. *Am J Phys Med Rehabil.* 2018; 97:116-122.
  50. Angioni MM, Denotti A, Pinna S, Sanna C, Montisci F, Dessole G, Loi A, Cauli A. Spa therapy induces clinical improvement and protein changes in patients with chronic back pain. *Reumatismo.* 2019; 71:119-131.
  51. So BCL, Kwok SC, Lee PH. Effect of aquatic exercise on sleep efficiency of adults with chronic musculoskeletal pain. *J Phys Act Health.* 2021; 18:1037-1045.
  52. Galletti L, Ricci V, Andreoli E, Galletti S. Treatment of a calcific bursitis of the medial collateral ligament: A rare cause of painful knee. *J Ultrasound.* 2019; 22:471-476.
  53. McLaughlin P, Hurley M, Chowdary P, Khair K, Stephensen D. Physiotherapy interventions for pain management in haemophilia: A systematic review. *Haemophilia.* 2020; 26:667-684.
  54. Feldberg G, Ricciardi JBS, Zorzi AR, Colella MP, Ozelo MC. Aquatic exercise in patients with haemophilia: Electromyographic and functional results from a prospective cohort study. *Haemophilia.* 2021;

- 27:e221-e229.
55. Dimitrakopoulou A, English B, Kartsonaki C, Gledhill A, Schilders E. The effectiveness of hydrotherapy on return to play in sports following hip arthroscopic surgery: A comparative study. *Hip Int.* 2024; 34:115-121.
  56. Lee CH, Kim IH. Aquatic exercise and land exercise treatments after total knee replacement arthroplasty in elderly women: A comparative study. *Medicina (Kaunas).* 2021; 57.
  57. Li X, Xu Y, Li H, Jia L, Wang J, Liang S, Cai A, Tan X, Wang L, Wang X, Huang Y, Tao E, Ye H, Asakawa T. Verification of pain-related neuromodulation mechanisms of icariin in knee osteoarthritis. *Biomed Pharmacother.* 2021; 144:112259.
  58. Hong-Baik I, Ubeda-D'Ocasar E, Cimadevilla-Fernandez-Pola E, Jimenez-Diaz-Benito V, Hervas-Perez JP. The effects of non-pharmacological interventions in fibromyalgia: A systematic review and metanalysis of predominant outcomes. *Biomedicines.* 2023; 11.
  59. Pye C, Clark N, Bruniges N, Peffers M, Comerford E. Current evidence for non-pharmaceutical, non-surgical treatments of canine osteoarthritis. *J Small Anim Pract.* 2024; 65:3-23.
  60. Dong R, Wu Y, Xu S, Zhang L, Ying J, Jin H, Wang P, Xiao L, Tong P. Is aquatic exercise more effective than land-based exercise for knee osteoarthritis? *Medicine (Baltimore).* 2018; 97:e13823.
  61. Ma J, Chen X, Xin J, Niu X, Liu Z, Zhao Q. Overall treatment effects of aquatic physical therapy in knee osteoarthritis: A systematic review and meta-analysis. *J Orthop Surg Res.* 2022; 17:190.
  62. Wang J, Chen Z, Chen X, Yang Y, Gan W, Wang F. Impact of Bad Ragaz Ring in hot spring water on knee osteoarthritis: A prospective observational study. *Medicine (Baltimore).* 2023; 102:e34457.
  63. Duan X, Wei W, Zhou P, Liu X, Yu J, Xu Y, Huang L, Yang S. Effectiveness of aquatic exercise in lower limb osteoarthritis: A meta-analysis of randomized controlled trials. *Int J Rehabil Res.* 2022; 45:126-136.
  64. Munukka M, Waller B, Hakkinen A, Nieminen MT, Lammentausta E, Kujala UM, Paloneva J, Kautiainen H, Kiviranta I, Heinson A. Effects of progressive aquatic resistance training on symptoms and quality of life in women with knee osteoarthritis: A secondary analysis. *Scand J Med Sci Sports.* 2020; 30:1064-1072.
  65. Sarzi-Puttini P, Giorgi V, Atzeni F, *et al.* Fibromyalgia position paper. *Clin Exp Rheumatol.* 2021; 39 Suppl 130:186-193.
  66. Zamuner AR, Andrade CP, Arca EA, Avila MA. Impact of water therapy on pain management in patients with fibromyalgia: current perspectives. *J Pain Res.* 2019; 12:1971-2007.
  67. Calandre EP, Rodriguez-Claro ML, Rico-Villademoros F, Vilchez JS, Hidalgo J, Delgado-Rodriguez A. Effects of pool-based exercise in fibromyalgia symptomatology and sleep quality: A prospective randomised comparison between stretching and Ai Chi. *Clin Exp Rheumatol.* 2009; 27:S21-28.
  68. Galvao-Moreira LV, de Castro LO, Moura ECR, de Oliveira CMB, Nogueira Neto J, Gomes L, Leal PDC. Pool-based exercise for amelioration of pain in adults with fibromyalgia syndrome: A systematic review and meta-analysis. *Mod Rheumatol.* 2021; 31:904-911.
  69. Smith HS, Harris R, Clauw D. Fibromyalgia: an afferent processing disorder leading to a complex pain generalized syndrome. *Pain Physician.* 2011; 14:E217-245.
  70. Mas AJ, Carmona L, Valverde M, Ribas B, Group ES. Prevalence and impact of fibromyalgia on function and quality of life in individuals from the general population: Results from a nationwide study in Spain. *Clin Exp Rheumatol.* 2008; 26:519-526.
  71. Bidonde J, Busch AJ, Webber SC, Schachter CL, Danyliw A, Overend TJ, Richards RS, Rader T. Aquatic exercise training for fibromyalgia. *Cochrane Database Syst Rev.* 2014; 2014:CD011336.
  72. Acosta-Gallego A, Ruiz-Montero PJ, Castillo-Rodriguez A. Land- and pool-based intervention in female fibromyalgia patients: A randomized-controlled trial. *Turk J Phys Med Rehabil.* 2018; 64:337-343.
  73. Fernandes G, Jennings F, Nery Cabral MV, Pirozzi Buosi AL, Natour J. Swimming improves pain and functional capacity of patients with fibromyalgia: A randomized controlled trial. *Arch Phys Med Rehabil.* 2016; 97:1269-1275.
  74. de Medeiros SA, de Almeida Silva HJ, do Nascimento RM, da Silva Maia JB, de Almeida Lins CA, de Souza MC. Mat Pilates is as effective as aquatic aerobic exercise in treating women with fibromyalgia: A clinical, randomized and blind trial. *Adv Rheumatol.* 2020; 60:21.
  75. Fonseca ACS, Faria PC, Alcantara MA, Pinto WD, De Carvalho LG, Lopes FG, Pernambuco AP. Effects of aquatic physiotherapy or health education program in women with fibromyalgia: A randomized clinical trial. *Physiother Theory Pract.* 2021; 37:620-632.
  76. Kwok MMY, So BCL, Heywood S, Lai MCY, Ng SSM. Effectiveness of deep water running on improving cardiorespiratory fitness, physical function and quality of life: A systematic review. *Int J Environ Res Public Health.* 2022; 19.
  77. Lv X, Wang J, Bao Y, Tang Y, Xing W, Wu Q, Mao G, Wang G. The effectiveness of balneotherapy and aquatic exercise on bone metabolism: A systematic review and meta-analysis. *Complement Ther Clin Pract.* 2021; 44:101429.
  78. Li Y, Wang W. [Clinical study of BRRM hydrotherapy assisted functional rehabilitation after lower limb fracture surgery]. *J Med Res.* 2023; 52:94-97 (Arirical in Chinese).
  79. Schinzel E, Kast S, Kohl M, von Stengel S, Jakob F, Kersch-Schindl K, Kladny B, Lange U, Peters S, Thomasius F, Clausen J, Uder M, Kemmler W. The effect of aquatic exercise on bone mineral density in older adults. A systematic review and meta-analysis. *Front Physiol.* 2023; 14:1135663.
  80. Murtezani A, Nevzati A, Ibraimi Z, Sllamniku S, Meka VS, Abazi N. The effect of land versus aquatic exercise program on bone mineral density and physical function in postmenopausal women with osteoporosis: A randomized controlled trial. *Ortop Traumatol Rehabil.* 2014; 16:319-325.
  81. Singh SP, Borthwick KG, Qureshi FM. Commentary: Comparison of an innovative rehabilitation, combining reduced conventional rehabilitation with balneotherapy, and a conventional rehabilitation after anterior cruciate ligament reconstruction in athletes. *Front Surg.* 2021; 8:665748.
  82. Schneider KN, Weller JF, P KB, Ahlbaumer G. Arthroscopic anterior cruciate ligament re-repair using internal brace augmentation - A case report. *J Orthop Case Rep.* 2019; 10:11-15.
  83. Buckthorpe M, Pirotti E, Villa FD. Benefits and

- use of aquatic therapy during rehabilitation after acl reconstruction -A clinical commentary. *Int J Sports Phys Ther.* 2019; 14:978-993.
84. Garcia Carrasco D, Aboitiz Cantalapiedra J. Effectiveness of motor imagery or mental practice in functional recovery after stroke: A systematic review. *Neurologia.* 2016; 31:43-52.
  85. Peultier-Celli L, Mainard D, Wein F, Paris N, Boisseau P, Ferry A, Gueguen R, Chary-Valckenaere I, Paysant J, Perrin P. Comparison of an innovative rehabilitation, combining reduced conventional rehabilitation with balneotherapy, and a conventional rehabilitation after anterior cruciate ligament reconstruction in athletes. *Front Surg.* 2017; 4:61.
  86. Roi GS, Creta D, Nanni G, Marcacci M, Zaffagnini S, Snyder-Mackler L. Return to official Italian First Division soccer games within 90 days after anterior cruciate ligament reconstruction: A case report. *J Orthop Sports Phys Ther.* 2005; 35:52-61; discussion 61-56.
  87. Hajouj E, Hadian MR, Mir SM, Talebian S, Ghazi S. Effects of innovative aquatic proprioceptive training on knee proprioception in athletes with anterior cruciate ligament reconstruction: A randomized controlled trial. *Arch Bone Jt Surg.* 2021; 9:519-526.
  88. So BC, Kwok MY, Chan YL, Lam HK, Chang HH, Chan TK, Leung CK, Tse HT. Lower-limb muscle activity during aquatic treadmill running in individuals with anterior cruciate ligament reconstruction. *J Sport Rehabil.* 2022; 31:894-903.
  89. Bei N, Long D, Bei Z, Chen Y, Chen Z, Xing Z. Effect of water exercise therapy on lower limb function rehabilitation in hemiplegic patients with the first stroke. *Altern Ther Health Med.* 2023; 29:429-433.
  90. Li Y, Zheng G. The efficacy of aquatic therapy in stroke rehabilitation: A protocol for systematic review and meta-analysis. *Medicine (Baltimore).* 2021; 100:e27825.
  91. Gu X, Zeng M, Cui Y, Fu J, Li Y, Yao Y, Shen F, Sun Y, Wang Z, Deng D. Aquatic strength training improves postural stability and walking function in stroke patients. *Physiother Theory Pract.* 2023; 39:1626-1635.
  92. Ghayour Najafabadi M, Shariat A, Dommerholt J, Hakakzadeh A, Nakhostin-Ansari A, Selk-Ghaffari M, Ingle L, Cleland JA. Aquatic therapy for improving lower limbs function in post-stroke survivors: A systematic review with meta-analysis. *Top Stroke Rehabil.* 2022; 29:473-489.
  93. Chae CS, Jun JH, Im S, Jang Y, Park GY. Effectiveness of hydrotherapy on balance and paretic knee strength in patients with stroke: A systematic review and meta-analysis of randomized controlled trials. *Am J Phys Med Rehabil.* 2020; 99:409-419.
  94. Nayak P, Mahmood A, Natarajan M, Hombali A, Prashanth CG, Solomon JM. Effect of aquatic therapy on balance and gait in stroke survivors: A systematic review and meta-analysis. *Complement Ther Clin Pract.* 2020; 39:101110.
  95. Zughbor N, Alwahshi A, Abdelrahman R, Elnekiti Z, Elkareish H, Gabor MG, Ramakrishnan S. The effect of water-based therapy compared to land-based therapy on balance and gait parameters of patients with stroke: A systematic review. *Eur Neurol.* 2021; 84:409-417.
  96. Pereira JA, de Souza KK, Pereira SM, Ruschel C, Hubert M, Michaelsen SM. The kinematics of paretic lower limb in aquatic gait with equipment in people with post-stroke hemiparesis. *Clin Biomech (Bristol, Avon).* 2019; 70:16-22.
  97. Saquetteo MB, da Silva CM, Martinez BP, Sena CDC, Pontes SS, da Paixao MTC, Gomes Neto M. Water-based exercise on functioning and quality of life in poststroke persons: A systematic review and meta-analysis. *J Stroke Cerebrovasc Dis.* 2019; 28:104341.
  98. Carrasco AC, Silva MF, Dela Bela LF, Paixao L, Pelegrinelli ARM, Dias JM, Kawano MM, Facci LM, Cardoso JR. Evaluation of quality of life in individuals with chronic stroke who underwent aquatic exercises: A case series. *NeuroRehabilitation.* 2021; 48:563-570.
  99. Nascimento LR, Flores LC, de Menezes KKP, Teixeira-Salmela LF. Water-based exercises for improving walking speed, balance, and strength after stroke: A systematic review with meta-analyses of randomized trials. *Physiotherapy.* 2020; 107:100-110.
  100. Radder DLM, Ligia Silva de Lima A, Domingos J, Keus SHJ, van Nimwegen M, Bloem BR, de Vries NM. Physiotherapy in Parkinson's disease: A meta-analysis of present treatment modalities. *Neurorehabil Neural Repair.* 2020; 34:871-880.
  101. Sirbu CA, Thompson DC, Plesa FC, Vasile TM, Jianu DC, Mitrica M, Anghel D, Stefani C. Neurorehabilitation in multiple sclerosis-A review of present approaches and future considerations. *J Clin Med.* 2022; 11.
  102. Amedoro A, Berardi A, Conte A, Pelosin E, Valente D, Maggi G, Tofani M, Galeoto G. The effect of aquatic physical therapy on patients with multiple sclerosis: A systematic review and meta-analysis. *Mult Scler Relat Disord.* 2020; 41:102022.
  103. Warutkar V, Gulrandhe P, Morghade S, Krishna Kovala R, Qureshi MI. Physiotherapy for multiple sclerosis patients from early to transition phase: A scoping review. *Cureus.* 2022; 14:e30779.
  104. Onan D, Ekizoglu E, Arikan H, Tasdelen B, Ozge A, Martelletti P. The efficacy of physical therapy and rehabilitation approaches in chronic migraine: A systematic review and meta-analysis. *J Integr Neurosci.* 2023; 22:126.
  105. Kapel A, Kovacic T, Kos N, Velnar T. Impact of a 12-month multifaceted neurological physiotherapy intervention on gross motor function in women with Rett syndrome. *J Integr Neurosci.* 2022; 21:59.
  106. Moritz TA, Snowdon DA, Peiris CL. Combining aquatic physiotherapy with usual care physiotherapy for people with neurological conditions: A systematic review. *Physiother Res Int.* 2020; 25:e1813.
  107. Bejot Y, Daubail B, Giroud M. Epidemiology of stroke and transient ischemic attacks: Current knowledge and perspectives. *Rev Neurol (Paris).* 2016; 172:59-68.
  108. Asakawa T, Zong L, Wang L, Xia Y, Namba H. Unmet challenges for rehabilitation after stroke in China. *Lancet.* 2017; 390:121-122.
  109. Bocchio M, Nabavi S, Capogna M. Synaptic plasticity, engrams, and network oscillations in amygdala circuits for storage and retrieval of emotional memories. *Neuron.* 2017; 94:731-743.
  110. Cronin NJ, Valtonen AM, Waller B, Poyhonen T, Avela J. Effects of short term water immersion on peripheral reflex excitability in hemiplegic and healthy individuals: A preliminary study. *J Musculoskelet Neuronal Interact.* 2016; 16:58-62.
  111. Saleh MSM, Rehab NI, Aly SMA. Effect of aquatic versus land motor dual task training on balance and gait of patients with chronic stroke: A randomized controlled

- trial. *NeuroRehabilitation*. 2019; 44:485-492.
112. Lee SY, Im SH, Kim BR, Han EY. The effects of a motorized aquatic treadmill exercise program on muscle strength, cardiorespiratory fitness, and clinical function in subacute stroke patients: A randomized controlled pilot trial. *Am J Phys Med Rehabil*. 2018; 97:533-540.
  113. Parfitt R, Hensman MY, Lucas SJE. Cerebral blood flow responses to aquatic treadmill exercise. *Med Sci Sports Exerc*. 2017; 49:1305-1312.
  114. Perez-de la Cruz S. Influence of an aquatic therapy program on perceived pain, stress, and quality of life in chronic stroke patients: A randomized trial. *Int J Environ Res Public Health*. 2020; 17.
  115. Pérez-de la Cruz S. Comparison of aquatic therapy vs. dry land therapy to improve mobility of chronic stroke patients. *Int J Environ Res Public Health*. 2020; 17.
  116. Pérez-de la Cruz S. Comparison between three therapeutic options for the treatment of balance and gait in stroke: A randomized controlled trial. *Int J Environ Res Public Health*. 2021; 18.
  117. Rafsten L, Danielsson A, Sunnerhagen KS. Anxiety after stroke: A systematic review and meta-analysis. *J Rehabil Med*. 2018; 50:769-778.
  118. Zhang Y, Wang YZ, Huang LP, Bai B, Zhou S, Yin MM, Zhao H, Zhou XN, Wang HT. Aquatic therapy improves outcomes for subacute stroke patients by enhancing muscular strength of paretic lower limbs without increasing spasticity: A randomized controlled trial. *Am J Phys Med Rehabil*. 2016; 95:840-849.
  119. Asakawa T, Sugiyama K, Nozaki T, Sameshima T, Kobayashi S, Wang L, Hong Z, Chen S, Li C, Namba H. Can the latest computerized technologies revolutionize conventional assessment tools and therapies for a neurological disease? The example of Parkinson's disease. *Neurol Med Chir (Tokyo)*. 2019; 59:69-78.
  120. Asakawa T, Fang H, Sugiyama K, Nozaki T, Kobayashi S, Hong Z, Suzuki K, Mori N, Yang Y, Hua F, Ding G, Wen G, Namba H, Xia Y. Human behavioral assessments in current research of Parkinson's disease. *Neurosci Biobehav Rev*. 2016; 68:741-772.
  121. Asakawa T, Fang H, Sugiyama K, *et al*. Animal behavioral assessments in current research of Parkinson's disease. *Neurosci Biobehav Rev*. 2016; 65:63-94.
  122. Navarro-Zaragoza J, Cuenca-Bermejo L, Almela P, Laorden ML, Herrero MT. Could small heat shock protein HSP27 be a first-line target for preventing protein aggregation in Parkinson's disease? *Int J Mol Sci*. 2021; 22.
  123. Jung YJ, Choi H, Oh E. Melatonin attenuates MPP(+)-induced apoptosis *via* heat shock protein in a Parkinson's disease model. *Biochem Biophys Res Commun*. 2022; 621:59-66.
  124. Hunt AP, Minett GM, Gibson OR, Kerr GK, Stewart IB. Could heat therapy be an effective treatment for alzheimer's and parkinson's diseases? A narrative review. *Front Physiol*. 2019; 10:1556.
  125. Carroll LM, Morris ME, O'Connor WT, Clifford AM. Community aquatic therapy for Parkinson's disease: An international qualitative study. *Disabil Rehabil*. 2022; 44:4379-4388.
  126. Bloem BR, Henderson EJ, Dorsey ER, Okun MS, Okubadejo N, Chan P, Andrejack J, Darweesh SKL, Munneke M. Integrated and patient-centred management of Parkinson's disease: A network model for reshaping chronic neurological care. *Lancet Neurol*. 2020; 19:623-634.
  127. da Silva AZ, Israel VL. Effects of dual-task aquatic exercises on functional mobility, balance and gait of individuals with Parkinson's disease: A randomized clinical trial with a 3-month follow-up. *Complement Ther Med*. 2019; 42:119-124.
  128. Kurt EE, Buyukturan B, Buyukturan O, Erdem HR, Tuncay F. Effects of Ai Chi on balance, quality of life, functional mobility, and motor impairment in patients with Parkinson's disease. *Disabil Rehabil*. 2018; 40:791-797.
  129. Zhu Z, Yin M, Cui L, Zhang Y, Hou W, Li Y, Zhao H. Aquatic obstacle training improves freezing of gait in Parkinson's disease patients: A randomized controlled trial. *Clin Rehabil*. 2018; 32:29-36.
  130. Terrens AF, Soh SE, Morgan P. The safety and feasibility of a Halliwick style of aquatic physiotherapy for falls and balance dysfunction in people with Parkinson's disease: A single blind pilot trial. *PLoS One*. 2020; 15:e0236391.
  131. da Silva AZ, Iucksch DD, Israel VL. Aquatic dual-task training and its relation to motor functions, activities of daily living, and quality of life of individuals with Parkinson's disease: A randomized clinical trial. *Health Serv Insights*. 2023; 16:11786329231180768.
  132. Miller KJ, Suarez-Iglesias D, Seijo-Martinez M, Ayan C. Physiotherapy for freezing of gait in Parkinson's disease: A systematic review and meta-analysis. *Rev Neurol*. 2020; 70:161-170.
  133. Clerici I, Maestri R, Bonetti F, Ortelli P, Volpe D, Ferrazzoli D, Frazzitta G. Land Plus Aquatic therapy versus land-based rehabilitation alone for the treatment of freezing of gait in Parkinson disease: A randomized controlled trial. *Phys Ther*. 2019; 99:591-600.
  134. Iucksch DD, Siega J, Leveck GC, de Araujo LB, Melo TR, Israel VL. Improvement of balance, motor aspects, and activities of daily living in Parkinson's disease after a sequential multimodal aquatic- and land-based intervention program. *Rehabil Res Pract*. 2023; 2023:2762863.
  135. Sun W, Wang Q, Yang T, Feng C, Qu Y, Yang Y, Li C, Sun Z, Asakawa T. A meta-analysis evaluating effects of the rotigotine in Parkinson's disease, focusing on sleep disturbances and activities of daily living. *Neurol Sci*. 2022; 43:5821-5837.
  136. Loureiro APC, Burkot J, Oliveira J, Barbosa JM. WATSU therapy for individuals with Parkinson's disease to improve quality of sleep and quality of life: A randomized controlled study. *Complement Ther Clin Pract*. 2022; 46:101523.
  137. Bonzano L, Tacchino A, Bricchetto G, Roccatagliata L, Dessypris A, Feraco P, Lopes De Carvalho ML, Battaglia MA, Mancardi GL, Bove M. Upper limb motor rehabilitation impacts white matter microstructure in multiple sclerosis. *Neuroimage*. 2014; 90:107-116.
  138. Pareto D, Sastre-Garriga J, Alonso J, Galan I, Arevalo MJ, Renom M, Montalban X, Rovira A. Classic block design "pseudo"-resting-state fMRI changes after a neurorehabilitation program in patients with multiple sclerosis. *J Neuroimaging*. 2018; 28:313-319.
  139. Bahmani SD, Motl RW, Razazian N, Khazaie H, Brand S. Aquatic exercising may improve sexual function in females with multiple sclerosis - An exploratory study. *Mult Scler Relat Disord*. 2020; 43:102106.
  140. Shariat A, Ghayour Najafabadi M, Soroush Fard Z, Nakhostin-Ansari A, Shaw BS. A systematic review with meta-analysis on balance, fatigue, and motor function

- following aquatic therapy in patients with multiple sclerosis. *Mult Scler Relat Disord*. 2022; 68:104107.
141. Souza PS, Goncalves ED, Pedroso GS, Farias HR, Junqueira SC, Marcon R, Tuon T, Cola M, Silveira PCL, Santos AR, Calixto JB, Souza CT, de Pinho RA, Dutra RC. Physical exercise attenuates experimental autoimmune encephalomyelitis by inhibiting peripheral immune response and blood-brain barrier disruption. *Mol Neurobiol*. 2017; 54:4723-4737.
  142. Guo LY, Lozinski B, Yong VW. Exercise in multiple sclerosis and its models: Focus on the central nervous system outcomes. *J Neurosci Res*. 2020; 98:509-523.
  143. Barone M, Mendozzi L, D'Amico F, *et al*. Influence of a high-impact multidimensional rehabilitation program on the gut microbiota of patients with multiple sclerosis. *Int J Mol Sci*. 2021; 22.
  144. Kargarfard M, Etemadifar M, Baker P, Mehrabi M, Hayatbakhsh R. Effect of aquatic exercise training on fatigue and health-related quality of life in patients with multiple sclerosis. *Arch Phys Med Rehabil*. 2012; 93:1701-1708.
  145. Kargarfard M, Shariat A, Ingle L, Cleland JA, Kargarfard M. Randomized controlled trial to examine the impact of aquatic exercise training on functional capacity, balance, and perceptions of fatigue in female patients with multiple sclerosis. *Arch Phys Med Rehabil*. 2018; 99:234-241.
  146. Guthrie TC, Nelson DA. Influence of temperature changes on multiple sclerosis: Critical review of mechanisms and research potential. *J Neurol Sci*. 1995; 129:1-8.
  147. Scorcine C, Verissimo S, Couto A, Madureira F, Guedes D, Fragoso YD, Colantonio E. Effect of 12 weeks of aquatic strength training on individuals with multiple sclerosis. *Arq Neuropsiquiatr*. 2022; 80:505-509.
  148. Gurpinar B, Kara B, Idiman E. Effects of aquatic exercises on postural control and hand function in multiple sclerosis: Halliwick versus aquatic plyometric exercises: A randomised trial. *J Musculoskelet Neuronal Interact*. 2020; 20:249-255.
  149. Hao Z, Zhang X, Chen P. Effects of different exercise therapies on balance function and functional walking ability in multiple sclerosis disease patients-A network meta-analysis of randomized controlled trials. *Int J Environ Res Public Health*. 2022; 19.
  150. Asakawa T, Yang Y, Xiao Z, Shi Y, Qin W, Hong Z, Ding D. Stumbling blocks in the investigation of the relationship between age-related hearing loss and cognitive impairment. *Perspect Psychol Sci*. 2024; 19:137-150.
  151. Mathys H, Peng Z, Boix CA, *et al*. Single-cell atlas reveals correlates of high cognitive function, dementia, and resilience to Alzheimer's disease pathology. *Cell*. 2023; 186:4365-4385 e4327.
  152. Jia X, Chen Q, Yao C, Asakawa T, Zhang Y. alpha-synuclein regulates Cyclin D1 to promote abnormal initiation of the cell cycle and induce apoptosis in dopamine neurons. *Biomed Pharmacother*. 2024; 173:116444.
  153. Jia X, Chen Q, Zhang Y, Asakawa T. Multidirectional associations between the gut microbiota and Parkinson's disease, updated information from the perspectives of humoral pathway, cellular immune pathway and neuronal pathway. *Front Cell Infect Microbiol*. 2023; 13:1296713.
  154. Wilson RS, Segawa E, Boyle PA, Anagnos SE, Hibel LP, Bennett DA. The natural history of cognitive decline in Alzheimer's disease. *Psychol Aging*. 2012; 27:1008-1017.
  155. Peng Y, Song P, Karako T, Asakawa T. Blocking progression from intervenable mild cognitive impairment to irreversible dementia, what can we do? *Biosci Trends*. 2024.
  156. Gelfo F, Petrosini L, Mandolesi L, Landolfo E, Caruso G, Balsamo F, Bonarota S, Bozzali M, Caltagirone C, Serra L. Land/water aerobic activities: Two sides of the same coin. A comparative analysis on the effects in cognition of Alzheimer's disease. *J Alzheimers Dis*. 2024; 98:1181-1197.
  157. Serra L, Petrosini L, Mandolesi L, Bonarota S, Balsamo F, Bozzali M, Caltagirone C, Gelfo F. Walking, running, swimming: An analysis of the effects of land and water aerobic exercises on cognitive functions and neural substrates. *Int J Environ Res Public Health*. 2022; 19.
  158. Tortora C, Di Crosta A, La Malva P, Prete G, Ceccato I, Mammarella N, Di Domenico A, Palumbo R. Virtual reality and cognitive rehabilitation for older adults with mild cognitive impairment: A systematic review. *Ageing Res Rev*. 2024; 93:102146.
  159. Antonenko D, Fromm AE, Thams F, Kuzmina A, Backhaus M, Knochenhauer E, Li SC, Grittner U, Floel A. Cognitive training and brain stimulation in patients with cognitive impairment: A randomized controlled trial. *Alzheimers Res Ther*. 2024; 16:6.
  160. Ren Y, Wang Q, Liu H, Wang G, Lu A. Effects of immersive and non-immersive virtual reality-based rehabilitation training on cognition, motor function, and daily functioning in patients with mild cognitive impairment or dementia: A systematic review and meta-analysis. *Clin Rehabil*. 2024; 38:305-321.
  161. Kim JH, Jung YS, Kim JW, Ha MS, Ha SM, Kim DY. Effects of aquatic and land-based exercises on amyloid beta, heat shock protein 27, and pulse wave velocity in elderly women. *Exp Gerontol*. 2018; 108:62-68.
  162. Becker BE, Lynch S. Case report: Aquatic therapy and end-stage dementia. *PM R*. 2018; 10:437-441.
  163. Henwood T, Neville C, Baguley C, Beattie E. Aquatic exercise for residential aged care adults with dementia: Benefits and barriers to participation. *Int Psychogeriatr*. 2017; 29:1439-1449.
  164. Akinola BI, Gbiri CA, Odebiyi DO. Effect of a 10-week aquatic exercise training program on gross motor function in children with spastic cerebral palsy. *Glob Pediatr Health*. 2019; 6:2333794X19857378.
  165. Aisen ML, Kerkovich D, Mast J, Mulroy S, Wren TA, Kay RM, Rethlefsen SA. Cerebral palsy: Clinical care and neurological rehabilitation. *Lancet Neurol*. 2011; 10:844-852.
  166. Franki I, Desloovere K, De Cat J, Feys H, Molenaers G, Calders P, Vanderstraeten G, Himpens E, Van Broeck C. The evidence-base for basic physical therapy techniques targeting lower limb function in children with cerebral palsy: A systematic review using the International Classification of Functioning, Disability and Health as a conceptual framework. *J Rehabil Med*. 2012; 44:385-395.
  167. Munoz-Blanco E, Merino-Andres J, Aguilar-Soto B, Garcia YC, Puente-Villalba M, Perez-Corrales J, Gueita-Rodriguez J. Influence of aquatic therapy in children and youth with cerebral palsy: A qualitative case study in a special education school. *Int J Environ Res Public Health*. 2020; 17.
  168. Adar S, Dundar U, Demirdal US, Ulasli AM, Toktas H, Solak O. The effect of aquatic exercise on spasticity, quality of life, and motor function in cerebral palsy. *Turk J Phys Med Rehabil*. 2017; 63:239-248.

169. Ballington SJ, Naidoo R. The carry-over effect of an aquatic-based intervention in children with cerebral palsy. *Afr J Disabil.* 2018; 7:361.
170. Rohn S, Novak Pavlic M, Rosenbaum P. Exploring the use of Halliwick aquatic therapy in the rehabilitation of children with disabilities: A scoping review. *Child Care Health Dev.* 2021; 47:733-743.
171. Fatima Z, Rashaquat Y. Effect of hydrotherapy on spasticity and gross motor functions among spastic cerebral palsy children. *Pakistan J Rehab.* 2019; 8:13-18.
172. Nagle EF, Sanders ME, Franklin BA. Aquatic high intensity interval training for cardiometabolic health: Benefits and training design. *Am J Lifestyle Med.* 2017; 11:64-76.
173. Ayme K, Gavarry O, Rossi P, Desruelle AV, Regnard J, Boussuges A. Effect of head-out water immersion on vascular function in healthy subjects. *Appl Physiol Nutr Metab.* 2014; 39:425-431.
174. Depiazzi J, Smith N, Gibson N, Wilson A, Langdon K, Hill K. Aquatic high intensity interval training to improve aerobic capacity is feasible in adolescents with cerebral palsy: Pilot randomised controlled trial. *Clin Rehabil.* 2021; 35:222-231.
175. Clapham ED, Lamont LS, Shim M, Lateef S, Armitano CN. Effectiveness of surf therapy for children with disabilities. *Disabil Health J.* 2020; 13:100828.
176. Souza DM, Yamamoto MEP, Carvalho JA, Rocha VAD, Fogaca VD, Rossato LM. Practice of immersion in hot water to relieve pain in neonatology: An integrative review. *Rev Bras Enferm.* 2024; 77:e20230260.
177. Ostojic K, Paget S, Kyriagis M, Morrow A. Acute and chronic pain in children and adolescents with cerebral palsy: Prevalence, interference, and management. *Arch Phys Med Rehabil.* 2020; 101:213-219.
178. Caputo G, Ippolito G, Mazzotta M, Sentenza L, Muzio MR, Salzano S, Conson M. Effectiveness of a multisystem aquatic therapy for children with autism spectrum disorders. *J Autism Dev Disord.* 2018; 48:1945-1956.
179. Gueita-Rodriguez J, Ogonowska-Slodownik A, Morgulec-Adamowicz N, Martin-Prades ML, Cuenca-Zaldivar JN, Palacios-Cena D. Effects of aquatic therapy for children with autism spectrum disorder on social competence and quality of life: A mixed methods study. *Int J Environ Res Public Health.* 2021; 18.
180. Xu N, Li X, Zhong Y. Inflammatory cytokines: Potential biomarkers of immunologic dysfunction in autism spectrum disorders. *Mediators Inflamm.* 2015; 2015:531518.
181. Ansari S, AdibSaber F, Elmieh A, Gholamrezaei S. The effect of water-based intervention on sleep habits and two sleep-related cytokines in children with autism. *Sleep Med.* 2021; 82:78-83.
182. Sourvinos S, Mavropoulos A, Kasselimis DS, Korasidi A, Voukouni AL, Papadopoulos P, Vlaseros S, Damianos G, Potagas C, Damianos D. Brief Report: Speech and language therapy in children with ASD in an aquatic environment: The ASLT (aquatic speech and language therapy) program. *J Autism Dev Disord.* 2021; 51:1406-1416.
183. Mortimer R, Privopoulos M, Kumar S. The effectiveness of hydrotherapy in the treatment of social and behavioral aspects of children with autism spectrum disorders: A systematic review. *J Multidiscip Healthc.* 2014; 7:93-104.
184. Asakawa T. Focusing on development of novel sampling approaches and alternative therapies for COVID-19: Are they still useful in an era after the pandemic? *Biosci Trends.* 2022; 16:386-388.
185. Asakawa T, Cai Q, Shen J, *et al.* Sequelae of long COVID, known and unknown: A review of updated information. *Biosci Trends.* 2023; 17:85-116.
186. Bailly M, Evrard B, Coudeyre E, Rochette C, Meriade L, Blavignac C, Fournier AC, Bignon YJ, Dutheil F, Duclos M, Thivel D. Health management of patients with COVID-19: Is there a room for hydrotherapeutic approaches? *Int J Biometeorol.* 2022; 66:1031-1038.
187. Antonelli M, Donelli D. Respiratory rehabilitation for post-COVID19 patients in spa centers: First steps from theory to practice. *Int J Biometeorol.* 2020; 64:1811-1813.
188. Romano-Bertrand S, Aho Glele LS, Grandbastien B, Lepelletier D, French Society for Hospital H. Preventing SARS-CoV-2 transmission in rehabilitation pools and therapeutic water environments. *J Hosp Infect.* 2020; 105:625-627.
189. Ogonowska-Slodownik A, Labecka MK, Kaczmarczyk K, McNamara RJ, Starczewski M, Gajewski J, Maciejewska-Skrendo A, Morgulec-Adamowicz N. Water-based and land-based exercise for children with post-COVID-19 condition (postCOVIDkids)-protocol for a randomized controlled trial. *Int J Environ Res Public Health.* 2022; 19.
190. Lucas DF, de Souza SF, de Carvalho BK, Biernaski J, Borato M, Melo TR, Araujo LB, Israel EVL. Impacts of COVID-19 on neuropsychomotor development from the perspective of the International Classification of Functioning, Disability and Health in a case series of children aged 4 to 24 months assessed in land and aquatic settings. *Health Serv Insights.* 2023; 16:11786329221147270.
191. Grishechkina IA, Lobanov AA, Andronov SV, Rachin AP, Fesyun AD, Ivanova EP, Masiero S, Maccarone MC. Long-term outcomes of different rehabilitation programs in patients with long COVID syndrome: A cohort prospective study. *Eur J Transl Myol.* 2023; 33.
192. Ogonowska-Slodownik A, Labecka MK, Maciejewska-Skrendo A, McNamara RJ, Kaczmarczyk K, Starczewski M, Gajewski J, Morgulec-Adamowicz N. Effect of water-based vs. land-based exercise intervention (postcovidkids) on exercise capacity, fatigue, and quality of life in children with post COVID-19 condition: A randomized controlled trial. *J Clin Med.* 2023; 12.
193. Cantarero-Villanueva I, Fernandez-Lao C, Caro-Moran E, Morillas-Ruiz J, Galiano-Castillo N, Diaz-Rodriguez L, Arroyo-Morales M. Aquatic exercise in a chest-high pool for hormone therapy-induced arthralgia in breast cancer survivors: A pragmatic controlled trial. *Clin Rehabil.* 2013; 27:123-132.
194. Fujimoto S, Iwawaki Y, Takishita Y, Yamamoto Y, Murota M, Yoshioka S, Hayano A, Hosokawa T, Yamanaka R. Effects and safety of mechanical bathing as a complementary therapy for terminal stage cancer patients from the physiological and psychological perspective: A pilot study. *Jpn J Clin Oncol.* 2017; 47:1066-1072.
195. Park R, Park C. Comparison of foot bathing and foot massage in chemotherapy-induced peripheral neuropathy. *Cancer Nurs.* 2015; 38:239-247.
196. Fransen M, Nairn L, Winstanley J, Lam P, Edmonds J. Physical activity for osteoarthritis management: A randomized controlled clinical trial evaluating hydrotherapy or Tai Chi classes. *Arthritis Rheum.* 2007; 57:407-414.
197. Goldman V, Weiss PL, Weil Y, Eylon S. Hydrotherapy for

- patients with external fixation: Effect on infectious events. *J Pediatr Orthop.* 2023; 43:187-191.
198. Alikhajeh Y, Afroundeh R, Mohammad Rahimi GR, Bayani B. The effects of aquatic exercise training on functional and hemodynamic responses in patients with heart failure: A systematic review and meta-analysis. *Biol Res Nurs.* 2025; 27:127-141.
199. Meyer K, Bucking J. Exercise in heart failure: Should aqua therapy and swimming be allowed? *Med Sci Sports Exerc.* 2004; 36:2017-2023.
200. Meyer K. Left ventricular dysfunction and chronic heart failure: Should aqua therapy and swimming be allowed? *Br J Sports Med.* 2006; 40:817-818.
201. Guerrero D. [La cure thermale en dermatologie, mode d'emploi: Use of thermal cures in dermatology]. *Ann Dermatol Venereol.* 2020; 147:1S44-41S48. (in French w/ English abstract)
202. Chen XL, Yu LP, Zhu Y, Wang TY, Han J, Chen XY, Zhang JH, Huang JL, Qian XL, Wang B. Combined effect of hydrotherapy and transcranial direct-current stimulation on children with cerebral palsy: A protocol for a randomized controlled trial. *Medicine (Baltimore).* 2021; 100:e27962.
203. Miyoshi T, Hiramatsu K, Yamamoto S, Nakazawa K, Akai M. Robotic gait trainer in water: Development of an underwater gait-training orthosis. *Disabil Rehabil.* 2008; 30:81-87.

Received November 6, 2024; Revised December 18, 2024; Accepted December 24, 2024.

*\*Address correspondence to:*

Tetsuya Asakawa, Institute of Neurology, National Clinical Research Center for Infectious Diseases, the Third People's Hospital of Shenzhen, No. 29 Bulan Road, Shenzhen, Guangdong 518112, China.

E-mail: asakawat1971@gmail.com

Released online in J-STAGE as advance publication January 3, 2025.

# Post-stroke dysphagia: Neurological regulation and recovery strategies

Xinyue Li<sup>1</sup>, Minmin Wu<sup>1</sup>, Jiongliang Zhang<sup>1</sup>, Donghui Yu<sup>1</sup>, Yuting Wang<sup>1</sup>, Yumeng Su<sup>1</sup>, Xiangyu Wei<sup>1</sup>, Xun Luo<sup>2</sup>, Qing Mei Wang<sup>3,\*</sup>, Luwen Zhu<sup>4,\*</sup>

<sup>1</sup>Heilongjiang University of Chinese Medicine, Harbin, Heilongjiang, China;

<sup>2</sup>School of Psychiatry, Wenzhou Medical University, Wenzhou, China;

<sup>3</sup>Stroke Biological Recovery Laboratory, Spaulding Rehabilitation Hospital, the Teaching Affiliate of Harvard Medical School, Boston, MA, USA;

<sup>4</sup>The Second Affiliated Hospital of Heilongjiang University of Chinese Medicine, Harbin, Heilongjiang, China.

**SUMMARY:** Swallowing is a complex process requiring precise coordination of numerous muscles in the head and neck to smoothly guide ingested material from the mouth to the stomach. Animal and human studies have revealed a complex network of neurons in the brainstem, cortex, and cerebellum that coordinate normal swallowing. The interactions between these regions ensure smooth and efficient swallowing. However, the current understanding of the neurophysiological mechanisms involved in post-stroke dysphagia (PSD) is incomplete, and complete functional connectivity for swallowing recovery remains understudied and requires further exploration. In this review, we discussed the neuroanatomy of swallowing and the pathogenesis of PSD and summarized the factors affecting PSD recovery. We also described the plasticity of neural networks affecting PSD, including enhancing activation of neural pathways, cortical reorganization, regulation of extracellular matrix dynamics and its components, modulation of neurotransmitter delivery, and identification of potential therapeutic targets for functional recovery in PSD. Finally, we discussed the therapeutic strategies based on functional compensation and motor learning. This review aimed to provide a reference for clinicians and researchers to promote the optimization of PSD treatments and explore future research directions.

**Keywords:** stroke, dysphagia, neurological regulation, pathogenesis, recovery mechanisms

## 1. Introduction

Swallowing is the physiological process of transporting food, drinks, or saliva from the oral cavity through the pharynx and esophagus to the stomach, encompassing three phases: oral, pharyngeal, and esophageal. Dysphagia is the impaired ability to safely and effectively transport food from the mouth to the stomach, caused by structural or functional damage to the jaw, lips, tongue, soft palate, pharynx, esophagus, or other related organs. Symptoms may include choking on water, difficulty swallowing, sore throat, food getting stuck, reflux, or vomiting. Dysphagia can result from various causes, including neurological conditions such as stroke and Parkinson's disease (PD), muscle disorders like amyotrophic lateral sclerosis (ALS), and structural issues including esophageal strictures, tumors, or esophageal tears.

Central nervous system (CNS) disorders are the most common causes of dysphagia, with post-stroke dysphagia (PSD) being the most prevalent. Studies have shown

that the incidence of PSD is as high as 80% (1), making it one of the most common complications in post-stroke patients, while 13%-18% of patients have persistent dysphagia within 6 months after the onset of the disease (2). PSD increases the risk of aspiration pneumonia, respiratory infections, and malnutrition, which in turn leads to prolonged hospital stays, higher post-discharge mortality rates, and significant impacts on patients' physical and mental health, potentially endangering their lives (3).

Despite the gradual increase in the understanding and research on PSD, there is still a need to strengthen our knowledge of the influencing factors, recovery mechanisms, and therapeutic approaches, as well as to enhance interdisciplinary cooperation. Currently, the complexity of factors influencing PSD, along with a lack of systematic research and insufficient interdisciplinary cooperation, makes it difficult to establish comprehensive management standards and unified treatment guidelines. This, in turn, affects patients' recovery outcomes and quality of life. Therefore, this review aimed to explore

the pathogenesis of PSD in depth, the factors and mechanisms that affect recovery, and its treatment. We also sought to integrate the concept of interdisciplinary cooperation and propose a future vision for exploring the application of novel technological tools for the assessment and intervention of dysphagia. This review seeks to provide new perspectives and reference points for the management and clinical practice of PSD.

## 2. About swallowing

### 2.1. Anatomy and physiological mechanism of swallowing

Swallowing is a complex physiological process that involves the coordinated action of multiple organs, such as the oral cavity, pharynx, and esophagus, to ensure the smooth passage of food and liquid from the oral cavity to the stomach. The swallowing process is divided into three phases: the oral, pharyngeal, and esophageal phases, in which food is first chewed and mixed with saliva to form a bolus in the mouth, while enzymes in the saliva begin to digest the carbohydrates. The tongue then pushes the food bolus from the oral cavity to the pharynx, with the movement of its back helping propel the food mass toward the pharynx. The soft palate rises during this stage, preventing food from entering the nasal cavity. During the pharyngeal phase, the cricopharyngeal muscles of the pharynx, including the superior, middle, and inferior pharyngeal constrictor muscles, begin to contract, pushing the food bolus towards the esophagus. At this point, the epiglottis drops, covering the larynx, and preventing food from entering the trachea. The vocal cords protect the airways and ensure the smooth passage of food. In the esophageal phase, food is propelled toward the stomach by peristaltic movements of the esophagus. The upper esophageal sphincter (UES) relaxes to allow food to enter the esophagus, while the lower esophageal sphincter (LES) opens as the food reaches the stomach, ensuring smooth passage into the stomach (4). The coordinated action of these structures and mechanisms allows the swallowing process to proceed smoothly, ensuring the efficient transport of food from the mouth to the stomach, while protecting the respiratory tract from food and fluids.

The swallowing activity is closely associated with the medulla oblongata of the brainstem. The dorsal swallow group (DSG) and ventral swallow group (VSG) of the medulla oblongata constitute the central pattern generator (CPG) of the brainstem. The dorsolateral region includes the nucleus tractus solitarius (NTS) and the rhombencephalic parvicellular reticular formation (RFpc), while the ventrolateral region consists of the nucleus ambiguus (NA) and its surrounding reticular formation. Transsynaptic transmission of both anterograde and retrograde tracer experiments have shown that during swallowing, motor neurons controlled

by the NA in the VSG (motor neurons of cranial nerves V, VII, IX, X, and XII) are activated sequentially by the DSG to ensure the completion of physiological swallowing (5). The initiation of swallowing is usually triggered by the stimulation of receptors in the oral cavity (e.g. taste buds and tactile receptors). When these receptors detect the presence of food or liquid, signals are transmitted to the swallowing centers in the brainstem to initiate the swallowing process (Figure 1) (6).

Through electrophysiological and neuroanatomical studies, researchers have found two structures in the brainstem called hemi-CPGs, which are located on both sides of the medulla oblongata and show a symmetrical distribution. When stimulating a peripheral nerve (usually the superior laryngeal nerve) on one side, the ipsilateral hemi-CPG is activated first, and the activation signal is then transmitted to the contralateral hemi-CPG through direct synaptic connections of interneurons to achieve synchronous activation of both sides (5). Lang *et al.* (7) further demonstrated that the NTS plays a key role in the synchronization of two hemi-CPGs, while injury to the peripheral nerve fibers does not affect this synchronization process. If unilateral damage occurs in the brainstem, or if the NTS on one side is completely damaged, the initiation of swallowing and rhythmic control are consequently lost. However, in this case, stimulation of the superior laryngeal nerve on the other side still triggers a complete swallowing action, suggesting that the regulation of swallowing function may depend on the unilateral control mechanism of the CPG and synchronization between the two halves of the CPG.

The muscles responsible for bolus preparation and formation during the oral phase are controlled by the trigeminal (V), facial (VII), and hypoglossal (XII) nerves (5). The trigeminal nerve performs both sensory and motor functions. Its three branches (ophthalmic, maxillary, and mandibular) transmit tactile, temperature, and nociceptive information from the oral cavity and pharynx to the brainstem. This allows the CNS to monitor the location and state of food, ensuring the timely initiation of swallowing reflex. The mandibular branch of the trigeminal nerve also controls the movement of the masticatory muscles, which are crucial for chewing and mixing food into an easy-to-swallow bolus, the effectiveness of which is vital for subsequent swallowing. The facial nerve is primarily responsible for the movement of the facial muscles, aiding in efficiently pushing food onto the tongue and preventing it from being retained in the cheeks. It regulates secretion from the salivary glands, particularly the sublingual and submandibular glands, which are important for lubricating food and facilitating swallowing. Furthermore, the facial nerve is responsible for taste sensation in the anterior two-thirds of the tongue, contributing to the perception of food and the pleasure associated with swallowing. The hypoglossal nerve

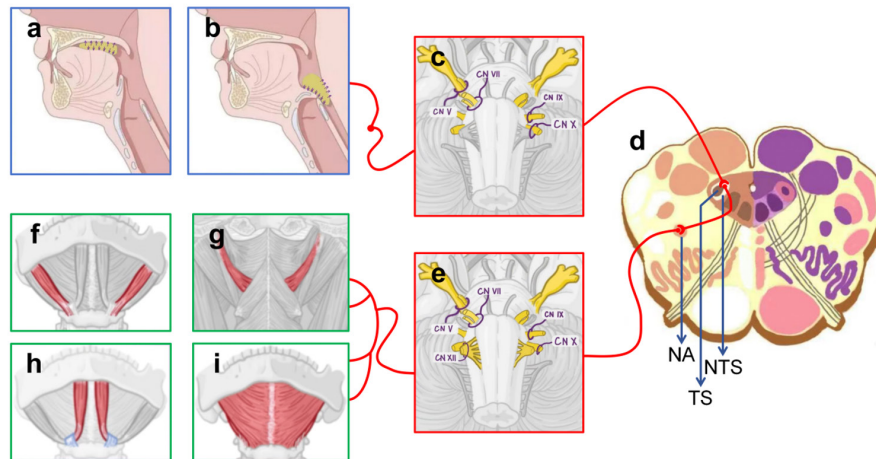


**Figure 1. Mechanisms of swallowing.** (a) Oral phase; (b) Pharyngeal phase; (c) Afferent nerves (V, VII, IX, X); (d) Medulla oblongata horizontal section; (e) Efferent nerves (V, VII, IX, X, XII); (f) Stylohyoid muscle; (g) Stylopharyngeus muscle; (h) Anterior belly of digastric muscle; (i) Mylohyoid muscle. When a food bolus stimulates the receptors in the oral and pharyngeal regions, the signal transmission is conveyed by the afferent nerves (cranial nerves V, VII, IX, and X) to the swallowing center in the brainstem, specifically the medulla oblongata. Within the medulla, the signal is transmitted from the NTS and TS in the dorsolateral region to the NA in the ventrolateral region. Activation of the motor neurons (cranial nerves V, VII, IX, X, and XII) controlled by the NA ensues, thereby innervating the muscles associated with swallowing and ensuring the completion of physiological swallowing. NTS: nucleus tractus solitarius; NA: nucleus ambiguus; TS: tractus solitaries.

innervates all movements of the tongue, including the intralingual and extralingual muscles. By controlling the precise movement of the tongue, it processes the chewed food into a bolus and propels it to the pharynx. During the pharyngeal phase, the recurrent laryngeal nerve controls laryngeal elevation and vocal fold closure, while the vagus nerve (X) regulates the downward movement of the epiglottis to cover the larynx. Together, they prevent food from entering the trachea and respiratory tract (8). The glossopharyngeal nerve (IX) is primarily responsible for transmitting sensory information from the pharynx to the CNS, initiating the swallowing reflex and ensuring the smooth passage of food into the esophagus. Additionally, at the esophageal stage, the vagus nerve regulates smooth muscle movement in the esophagus and coordinates peristalsis and sphincter activity. Overall, the coordinated action of these nervous systems ensures a smooth and effective swallowing process, preventing food from accidentally entering the trachea and ensuring it reaches the stomach.

## 2.2. Factors affecting the function of swallowing

Many factors affect swallowing function, including diet, smoking, alcohol consumption, and neurological disorders. Broadly speaking, they can be categorized into physiological, pathological and psychological factors, which interfere with the swallowing function to varying degrees through different pathways (Figure 2).

### 2.2.1. Physiological factors

The influence of diet on the swallowing function is significant. It is well known that hard, dry, and rough foods (e.g. nuts, dried fruits, and whole grains) may cause

dysphagia, whereas soft and moist foods (e.g. cooked vegetables, soups, and purees) are easier to swallow. In addition, foods that are too hot or cold may cause throat discomfort and complicate swallowing. Moreover, foods high in fiber can lead to the accumulation of food debris, making swallowing difficult. Thin liquids (e.g. water) may be challenging for patients with dysphagia but thickeners can adjust the consistency of liquids, enhancing airway protection by promoting more timely laryngeal vestibular closure (9), which eases swallowing and reduces the risk of choking.

The effects of smoking and alcohol consumption on swallowing function are similar, and both threaten oral, pharyngeal, and esophageal health. Smoking was confirmed to be a significant predictor of dysphagia and aspiration pneumonia in a study of 189 older individuals with follow-up periods of up to 4 years (10). Acute systemic alcohol exposure has been shown to inhibit the pharyngeal-esophageal sphincter contraction reflex (PUCR) and reflex pharyngeal swallowing (RPS) (11). Specifically, chronic cigarette smoke, nicotine, and alcohol stimulation can cause oral dryness and reduced salivary secretion, leading to issues such as oral ulcers and gingivitis, which can impair masticatory function (12). Long-term smoking and alcohol consumption also lead to tissue and structural changes in the larynx and esophagus, such as mucosal degeneration, hyperplasia, and fibrosis of tissue structures, resulting in a delay in the function of swallowing-related structures and interference with normal swallowing process (13). Swallowing is a complex reflex that requires coordination by the CNS. Nicotine and alcohol slow the initiation and execution of the swallowing reflex by inhibiting the CNS, thereby making swallowing sluggish and impairing its coordination (11).

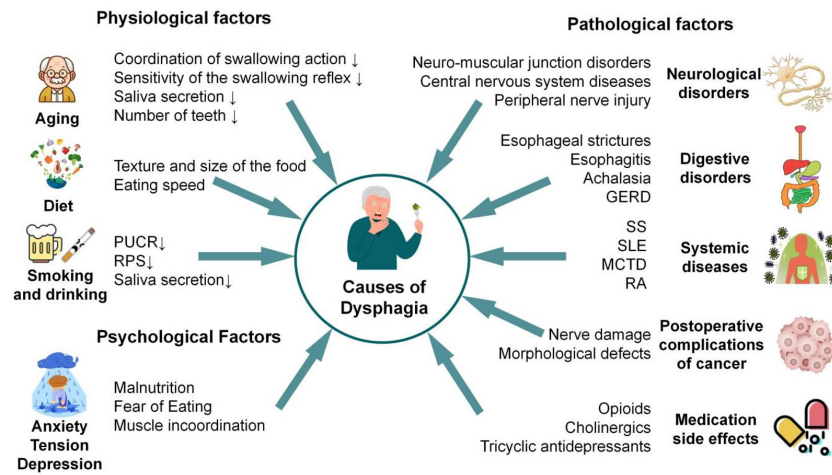


**Figure 2. Causes of dysphagia.** Factors affecting swallowing function can be categorized into physiological factors, including diet, smoking and alcohol consumption, and aging. And pathological factors, which can be categorized into neurological, digestive, and systemic disorders, as well as postoperative complications of cancer and medication side effects. In addition, psychological factors caused by anxiety, tension, and depression are also included. These factors interfere with swallowing function to varying degrees through different pathways. PUCR: pharyngeal-esophageal sphincter contraction reflex; RPS: reflex pharyngeal swallowing; GERD: gastroesophageal reflux disease; SS: sjögren's syndrome; SLE: systemic lupus erythematosus; MCTD: mixed connective tissue disease; RA: rheumatoid arthritis.

Aging affects the swallowing function both physiologically and structurally, increasing the risk of aspiration, choking, and malnutrition in older adults. The European Union Geriatrics Society White Paper showed that the prevalence of dysphagia in nursing homes exceeds 60%, and up to half of the older population over 60 years of age experience some type of swallowing disorder (14). Physiologically, the speed and sensitivity of the swallowing reflex diminish with age, indicating that the initiation of the swallowing maneuver becomes delayed, thereby increasing the risk of aspiration and choking. Simultaneously, aging leads to degeneration of the CNS and peripheral nervous system (PNS), slowing nerve conduction and impairing the coordination of nerves involved in swallowing, making the process more difficult. Additionally, the decline in salivary gland function and reduced salivary secretion in older individuals lead to dry mouth and insufficient lubrication of food, making it harder to form a food mass and increasing the risk of aspiration during swallowing (15). Structurally, the number of teeth affects the chewing ability. Multiple regression analysis found that the rates of swallowing problems in older adults with 0-24 and 25-32 remaining teeth were 2.04% and 1.31%, respectively, indicating that tooth loss is associated with reduced swallowing function in this demographic (16).

### 2.2.2. Pathological factors

A wide range of pathological factors affect the swallowing function in adults, including neurological disorders, digestive disorders, systemic diseases, and side effects of neurological medications, all of which may lead to dysphagia. Stroke is the most common neurological condition that causes dysphagia, and

damage to areas of the brain that control swallowing can result in a dull or uncoordinated swallowing reflex. Subdural lesions of the brainstem, including the pontine and medulla oblongata, are the most common causes of dysphagia (17). Flowers *et al.* (18) found that in a randomized sample of 250 patients with stroke, dysphagia prevalence was 37-45% *via* screening, 51-55% through clinical assessment, and 64-78% with instrumental techniques. PD causes the degeneration of motor neurons, affecting the coordination and strength of the swallowing muscles, resulting in stiffness of the muscles in the oral and pharyngeal regions. The basal ganglia are the primary sites of pathology in PD, and videofluoroscopy can reveal oropharyngeal involvement, as evidenced by dysphagia and impaired transit of the meal bolus between the pharynx and proximal esophagus (19). A meta-analysis by Kalf *et al.* (20) showed that dysphagia occurred in 35% of patients with PD in studies examining subjective outcomes; however, in studies using objective measures, the proportion was as high as 82%. Patients with Alzheimer's disease (AD) experience a progressive loss of swallowing function and cognitive decline (21). A scoping review conducted by Affoo *et al.* (22) showed that the prevalence of dysphagia in patients with AD ranges from 32% to 45% when assessed clinically and from 84% to 93% when assessed instrumentally. ALS affects motor neurons and leads to weakness, atrophy of the swallowing muscles, and a decrease in the saliva clearance rate (23).

Peripheral nerve injuries such as those affecting the trigeminal, facial, and hypoglossal nerves can impair the function of the muscles of the mouth and tongue, leading to difficulties in food processing and propulsion (24). Digestive disorders that can cause swallowing difficulties include esophagitis, esophageal stricture,

esophageal cancer, gastroesophageal reflux disease (GERD), and achalasia cardia (25). Patients with Sjögren's syndrome (SS), systemic lupus erythematosus (SLE), mixed connective tissue disease (MCTD), and rheumatoid arthritis (RA) experience various degrees of dysphagia (25). The anticholinergic and antidopaminergic effects of antipsychotics and tricyclic antidepressants should not be overlooked, as they cause dry mouth, interfering with the lubrication of the food bolus, and reduce the coordination and strength of peristalsis (26). Patients who have undergone radiation or chemotherapy for cancer experience prolonged chewing and swallowing owing to dry mouth compared to their condition before treatment (27).

### 2.2.3. Psychological Factors

It is important to note that psychological factors are closely linked to impaired swallowing function. Stressful emotions such as anxiety and tension can not only lead to incoordination of the muscles involved in swallowing but may also trigger spasms, thereby exacerbating symptoms of dysphagia. For instance, patients may experience difficulty swallowing or even choking during meals due to nervousness. The impact of these psychological factors on swallowing function extends beyond the physiological level and can affect social interactions as well. Studies have shown that among patients with dysphagia, 45% consider eating to be a negative experience, 41% feel anxious or panicked during meals, and 36% avoid dining with others due to fear of embarrassing situations (28). These emotional and psychological changes not only diminish the quality of life but may also lead to malnutrition, further exacerbating muscle atrophy and swallowing dysfunction, creating a vicious cycle.

Depression is another significant psychological factor contributing to dysphagia. Patients with depression often experience symptoms such as low mood, slowed thinking, and reduced cognitive function. These symptoms can impair the swallowing reflex and the coordination of swallowing actions, leading to prolonged food retention in the oral cavity and increasing the risk of aspiration (29). Additionally, persistent loss of appetite, reduced food intake, or even refusal to eat can result in physical weakness, further aggravating swallowing difficulties. Lin *et al.* (30) found in a survey of elderly individuals across 18 care facilities that those with depressive symptoms had a higher frequency of dysphagia compared to those without such symptoms. Furthermore, studies on PD (31), multiple sclerosis (32), and GERD (33) have identified a significant positive correlation between depressive symptoms and dysphagia. Moreover, patients with depression may develop a fear of eating, worrying about choking or aspiration during meals. This fear can inhibit swallowing function, worsening dysphagia.

## 3. Pathogenesis of PSD

The etiology of PSD encompasses a multitude of intricate physiological pathways, which can be categorized into several distinct yet interrelated components. These include impairments to the cortical swallowing center, disruptions to cortical descending fibers, lesions within the brainstem, alterations in the extrapyramidal system and cerebellum, and damage to the cerebral nerves. Dysfunction or injury to any of these neural substrates may precipitate dysregulation of the swallowing process, characterized by impaired coordination, delayed pharyngeal response, and an elevated risk of aspiration during deglutition (Figure 3).

### 3.1. Cortical swallowing center impairment

Empirical evidence derived from both human and animal studies has delineated the cortical regions primarily implicated in the orchestration of swallowing, which are predominantly localized within the primary motor cortex (M1), primary sensory cortex (S1), insula, cingulate gyrus, supplementary motor area (SMA), and premotor cortex, and other cortical domains. These areas are pivotal in the initiation of deglutition and the regulation of the oropharyngeal phase (34). Various cortical lesions result in distinct dysphagic phenotypes, predominantly manifesting as challenges in the initiation of swallowing and delays in pharyngeal reflexes. The primary motor and sensory cortices, collectively referred to as the primary sensorimotor cortex (SM1), are situated within the precentral gyrus of the frontal lobe and the postcentral gyrus of the parietal lobe. SM1 is a well-characterized cortical region that plays a significant role in swallowing, with dysfunction primarily contributing to the impaired control of swallowing movements. Daniels *et al.* (35) have demonstrated that lesions within M1 confer a higher risk of aspiration compared to those within S1. Advanced spatial delineation of SM1 *via* diffusion-weighted MRI has revealed that S1 lesions are correlated with impaired laryngeal vestibular closure and pharyngeal residue, while M1 lesions are associated with compromised laryngeal elevation (36). The insula, another cortical component, is integral to the initiation of swallowing by processing sensory inputs and interfacing with SM1 across both hemispheres to modulate the timing of swallowing onset following mastication or other oral activities (37). Research has indicated that the absence of insular activation is linked to pharyngeal dysphagia, which significantly elevates swallowing thresholds, impairs the patient's capacity to plan swallowing movements, and results in uncoordinated or abnormal swallow completion, thereby heightening the risk of aspiration (37). The cingulate gyrus is instrumental in the early stages of swallowing by generating swallowing commands through the retrieval of relevant memories. Consequently, disruptions

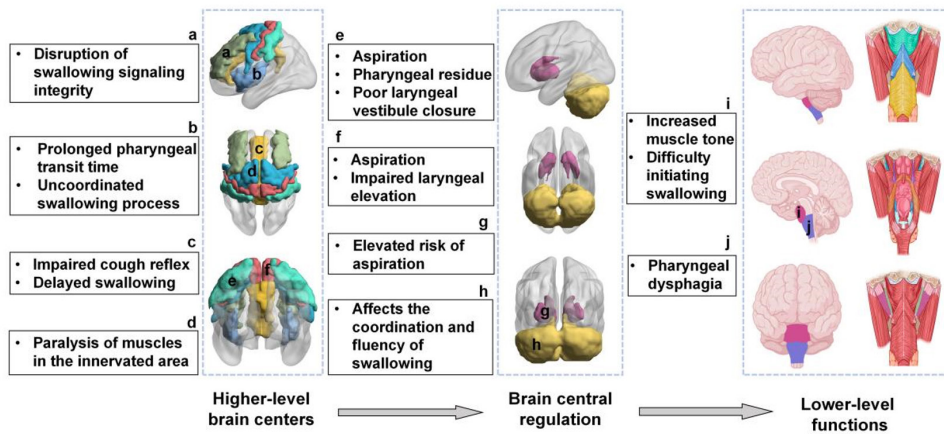


**Figure 3. Pathogenesis of PSD.** (a) Supplementary motor area (SMA); (b) Insula; (c) Cingulate gyrus; (d) Premotor cortex; (e) primary sensory cortex (S1); (f) primary motor cortex (M1); (g) Basal ganglia; (h) Cerebellum; (i) Pons; (j) Medulla oblongata. In the sections higher-level brain centers and brain central regulation, the lateral, upper and frontal views of the brain are presented from top to bottom. In the lower-level functions, from top to bottom, they are the lateral view, sagittal cut and frontal view of the brain. The swallowing signal can be conducted via the following pathways: M1, S1, insula, cingulate gyrus, SMA, and premotor cortex serve as higher-level central nervous system structures, transmitting swallowing signals to subcortical structures such as the basal ganglia and cerebellum. These subcortical structures, in turn, innervate brainstem nuclei and neural clusters, such as the pons and medulla oblongata, which control muscles associated with swallowing, including the stylohyoid, stylopharyngeus, and the posterior belly of the digastric muscle. Damage to different cortical areas can lead to varied manifestations of dysphagia.

in cingulate gyrus activation can impair the issuance of swallowing commands, leading to delays in swallowing and the potential development of dysphagia (38). The SMA, which shares substantial common information with M1 in the cingulate cortex, is crucial in the processing of swallowing motor functions, and damage to this area may result in compromised or delayed swallowing command signals, thereby disrupting the integrity of swallowing signaling and precipitating swallowing disorders (39). The premotor cortex projects to both pyramidal and extrapyramidal systems and is tasked with integrating afferents from the frontal cortex, basal ganglia, cerebellum, and other regions, with injuries to this area primarily presenting as muscle paralysis within the innervated region (34).

### 3.2. Cortical descending fiber impairment

Cortical descending fibers originate from the large pyramidal cells of the cerebral cortex and descend into the spinal cord, ending directly or indirectly at the anterior horn motor neurons of the spinal cord in what is known as the corticospinal fiber, and at the somatomotor nuclei and special visceral motor nuclei within the brainstem in what is known as the corticonuclear fibres. These fibers also synapse with the somatomotor nuclei and special visceral motor nuclei within the brainstem, facilitating the innervation of voluntary musculature involved in the act of swallowing. Disruption of the white matter within the corticospinal fibers can sever the connection between the swallowing center and cortical descending fibers, impairing bilateral cortical connectivity and precipitating dysphagia. The corticonuclear fibre is known to exert a facilitatory influence on the medullary swallowing center, participating in the active swallowing process

(40). Damage to the corticonuclear fibre can lead to prolongation of the pharyngeal phase of deglutition, while reflexive swallowing activity remains relatively preserved. Further damage affecting inhibitory neuronal loops can result in the loss of high-level inhibition at the medullary swallowing center, preventing the initiation of active swallowing (41).

### 3.3. Brainstem injury

In the context of brainstem injury, the medullary swallowing center is the second largest swallowing center after the cortex and subcortex. It includes the NA, NTS, and surrounding reticular structures, which control and regulate the swallowing reflex. Lesions to the medullary swallowing center can remove the inhibition of the pharyngeal phase, resulting in its prolongation (42). Daniels *et al.* (6) observed that infratentorial infarcts, particularly those involving the pontine bridges and medulla oblongata, are more likely to cause swallowing deficits compared to supratentorial infarcts, with the medulla oblongata being the most significantly affected. Unilateral damage to the medullary swallowing center can result in unilateral paralysis of the vocal cords, soft palate, and laryngeal muscles, with less severe impairment of swallowing function, whereas bilateral damage can lead to the loss of the pharyngeal reflex (43). However, Handy *et al.* (44) noted through clinical observation that patients with acute unilateral medullary stroke often exhibit bilateral pharyngeal muscle paralysis, sluggish pharyngeal reflex, and prolonged pharyngeal phase. The underlying mechanisms are not uniform. One possible cause is damage to the medulla oblongata nucleus. When the nucleus of the medulla oblongata is lesioned, the connection between the medulla oblongata

and the thalamus is disrupted, leading to a series of motor, sensory, and cognitive effects, including bilateral pharyngeal muscle paralysis (45). Another potential mechanism is that the medullary swallowing center functions as a unified entity. Damage to one side can interrupt the connection with the contralateral center and affect the innervation of contralateral nerve fibers, leading to dysfunction of the entire center. This manifests as uncoordinated muscle activities, prolonged pharyngeal phase, and swallowing dysfunction. However, with active treatment and the body's compensatory mechanisms, intact central neurons on the ipsilateral side can gradually establish contact with the contralateral swallowing center, thereby improving swallowing function.

### 3.4. Extrapyramidal and cerebellar system impairment

Extrapyramidal and cerebellar system impairments refer to damage to the neurological structures outside the pyramidal system that regulate muscle tone and coordinate muscle activity, enabling the execution of fine and random movements (46). Extrapyramidal injuries can lead to dystonia in swallowing muscles, characterized by muscle stiffness or tremor, resulting in inflexible and uncoordinated swallowing movements (42). Furthermore, the extrapyramidal system plays a crucial role in the coordination of swallowing movements by influencing and controlling all conduction pathways of somatic movements, including the cerebral cortex, cerebellum, and brainstem reticular formation. Damage to this system can compromise this coordination, leading to impaired food propulsion during swallowing and affecting the smoothness and accuracy of deglutition (47).

### 3.5. Cranial nerve injury

Normal deglutition is facilitated by the coordinated activity of several cranial nerves, predominantly the V, X, and XII nerves. Impairment of these nerves, which are integral to the swallowing process, can result in a spectrum of dysphagic symptoms, including pharyngeal muscle weakness, impaired bolus propulsion, discoordinated soft palate movements, and incomplete closure of the laryngeal orifice, thereby prolonging the pharyngeal phase (5). X nerve is particularly crucial, with its dorsal nucleus regulating the majority of the soft palate, pharyngeal, and cricopharyngeal muscles. It is responsible for innervating soft palate elevation, vocal fold closure, and epiglottic reflexion. Dysfunction of the X nerve can severely compromise swallowing function, leading to paralysis of the majority of its innervated muscles, insufficient laryngeal closure, hoarseness, choking, and dysphagia (48). Additionally, X nerve damage can diminish sensory feedback during swallowing, reducing sensation at the tongue base and epiglottis, and increasing the risk of aspiration (24).

The V nerve, governed by four major nuclei —

sensory, pontine, spinal tract, and motor nuclei — plays a pivotal role in swallowing. The trigeminal motor nucleus is the sole motor nucleus among these, receiving and processing afferent impulses from motor neurons in the brainstem and spinal cord. Its dorsal aspect is the reticular formation, which relays and transmits sensory information related to swallowing to the thalamic nuclei, including tactile and gustatory sensations in the pharynx, auditory sensations in the larynx, vocal cord vibrations, and laryngeal muscle tension. Its ventral aspect is part of the cortical-subcortical pathway that governs swallowing. Consequently, the trigeminal nucleus and its surrounding area serve as a relay station. Injury to the ventral aspect of the trigeminal motor nucleus can disrupt the swallowing conduction pathway, leading to paralysis of the oral muscles it innervates, such as the masticatory muscles, stylohyoid muscle, mylohyoid muscle, and the anterior belly of digastric muscle, and consequently prolonging the pharyngeal phase (49). The trigeminal spinal fiber nucleus also innervates facial sensation, and damage to this nucleus can reduce sensation in the oral cavity, tongue, and soft palate, potentially delaying swallow triggering and increasing the risk of aspiration (50).

The tongue, primarily functioning in the oral phase, also contributes to the pharyngeal phase through the propulsive force generated by its muscular movements. Therefore, damage to the XII nerve can lead to paralysis of the lingual muscles, resulting in poor propulsion of food in the oral cavity and prolonged retention of food, which may cause food to flow out of the oral cavity or prematurely into the pharynx, increasing the risk of aspiration and pharyngeal dysphagia (24).

## 4. Factors affecting recovery from PSD

A variety of factors influence recovery from PSD, including the type and site of stroke, the patient's functional status, the presence of comorbidities, sex differences, the kinematic characteristics of the hyoid bone and epiglottis, and the necessity of performing a tracheostomy. These factors work together to determine the patient's recovery and degree of improvement in the swallowing function (Figure 4).

In terms of the type and site of stroke, patients with hemorrhagic stroke are more likely to develop PSD than those having ischemic stroke (51). Hemorrhagic strokes usually involve larger areas of brain damage, and direct hemorrhage and secondary cerebral edema may directly affect the areas in the brainstem and cerebral cortex that control swallowing. In addition, increased intracranial pressure due to hemorrhage disrupts cerebrospinal fluid flow (52), which may further impair the neural network involved in swallowing. Swallowing kinematic analysis also demonstrates that the vertical laryngeal movements of patients with hemorrhagic stroke are significantly lower than those of patients with ischemic stroke,

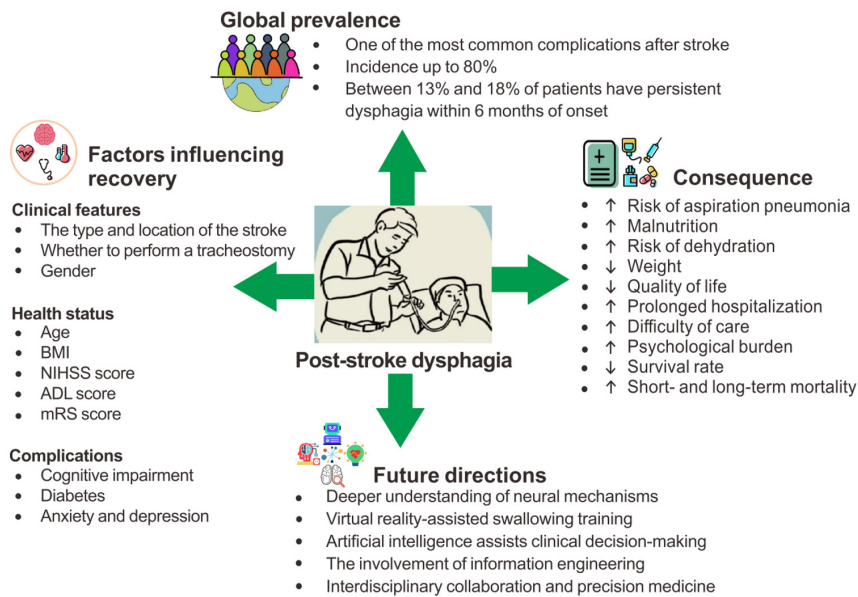


**Figure 4. Post-stroke dysphagia.** This figure presents a concise summary of PSD, highlighting its global prevalence, factors influencing recovery, consequences, and future research directions. BMI: body mass index; NIHSS: national institutes of health stroke scale; ADL: activity of daily living; mRS: modified Rankin scale.

suggesting that patients with hemorrhagic stroke have a more pronounced reduction in tongue movements and slower recovery during swallowing (53). Li *et al.* (54) showed that patients with left and right hemisphere stroke may exhibit different swallowing difficulties, with pharyngeal dyskinesia being more prominent in patients with right hemisphere stroke and reduced oral coordination being more prominent in patients with left hemisphere stroke. Additionally, comparative analysis of functional magnetic resonance imaging (fMRI) of brain activation in patients with left and right hemisphere stroke revealed that brain activation during a swallowing task is smaller in patients with left hemisphere damage than in those with right hemisphere damage. This suggests that the left cerebral hemisphere is more dominant in swallowing function and that patients with left hemisphere pathology may experience more severe dysphagia (54). The swallowing-related structures, the NA and the NTS, are located in the lateral medulla of the brainstem and control the coordination of the swallowing reflex and associated muscles; thus, brainstem stroke is also a poor prognostic factor for PSD (55). Dysphagia is a common clinical feature in patients with lateral medullary syndrome (LMS), with prevalence rates ranging from 51% to 94% (56). However, the severity and duration of dysphagia in patients with LMS are highly variable, ranging from very mild and transient to extremely severe and requiring months or even years of nasogastric feeding. Slow recovery is often associated with silent aspiration, which can lead to aspiration pneumonia. Swallowing control mechanisms in the brain require bilateral inputs to maintain normal function. When one side of the brain is injured, the other side can partially compensate for this injury, thus reducing dysphagia (57). Bilateral injuries lack this compensatory mechanism

and worsen dysphagia compared with unilateral injuries. Cerebellar stroke accounts for approximately 4% of all strokes, and a retrospective cohort study conducted in 2023 showed that 11.45% of patients with cerebellar infarction have dysphagia (58). Studies have shown that after an isolated cerebellar stroke, pharyngeal reflexes may disappear, along with tremors, incoordination, and imprecise movements related to swallowing (46). This is attributed to the cerebellum's ability to receive information indirectly through the complex spinal cord — medulla oblongata — reticular formation pathway, enabling it to make various motor adjustments with the help of these structures. A cerebellar stroke may result in the disruption of cerebellar function and its connecting structures, such as the reticular formation, leading to the loss of the inhibitory reflex, which, in turn, affects swallowing.

In terms of functional status, advanced age, low Body Mass Index (BMI), high National Institutes of Health Stroke Scale (NIHSS) scores, and low Activity of Daily Living (ADL) scores are negative predictors of PSD recovery, whereas a modified Rankin scale (mRS) score of 0 is a predictor of good prognosis (59). As age increases, the neuroplasticity of the brain and swallowing-related muscle tissues declines, requiring more rehabilitative support and a longer period to recover swallowing function. A low BMI indicates malnutrition or reduced muscle mass. The BMI of patients with PSD is positively correlated with swallowing ability at discharge, and those with a low BMI tend to have poorer swallowing rehabilitation. In addition, patients with malnutrition upon admission often exhibit more severe dysphagia (60). In recent years, the concept of sarcopenic dysphagia has been proposed, where the reduction in overall muscle mass in patients with stroke

is accompanied by changes in swallowing-related muscle groups. This results in weakened muscle strength, masticatory weakness, muscle contraction disorders, and loss of muscle function, all of which slow down stroke rehabilitation and the recovery of swallowing function (61). The NIHSS is a standardized scale used to assess the severity of stroke, evaluating levels of consciousness, speech, motor function, and sensory function. One study found that an NIHSS score > 9 is an early predictor of dysphagia (62). High NIHSS scores usually reflect more severe neurological damage, with multiple impaired functions of the brain regions, and dysphagia may coexist with other neurological dysfunctions, increasing the complexity of recovery. ADL and mRS scores assess an individual's independence in daily life. Low ADL and high mRS scores indicate greater dependence and individualized rehabilitation therapy to gradually restore overall function (17).

In the PSD recovery process, the presence of comorbidities significantly affects the effectiveness of rehabilitation, particularly in patients with cognitive impairment, diabetes, and psychiatric conditions such as anxiety and depression. Studies have found a correlation between cognitive impairment and dysphagia — the presence of cognitive impairment on admission is associated with a poor outcome of dysphagia at discharge (21). At this stage, cognitive problems in patients with PSD are still not adequately addressed, yet improvements in cognitive function are important for the recovery of swallowing ability. Cognitive deficits can affect dysphagia through various mechanisms, including attention, awareness, planning and organizational skills, memory, language skills, and behavioral and psychological states. The impairment of these cognitive functions makes swallowing recovery more difficult and increases the risk of aspiration and other complications. For example, when cognitive impairment affects behavioral control, patients may exhibit inappropriate behaviors such as impatient or unconscious rapid swallowing during the deglutition process, which can lead to dysphagia and aspiration (63). Therefore, improving the patients' cognitive function, especially by enhancing the cognitive control of swallowing maneuvers, can improve their control, coordination, and safety during swallowing, thereby reducing dysphagia and improving food intake. Several studies have demonstrated the negative effects of diabetes on PSD recovery (64,65), showing that diabetes is more strongly associated with ischemic stroke in women than in men, with a more pronounced difference in patients with type 1 diabetes (66). Neurological factors associated with diabetes contribute to the increased risk of PSD by elevating the incidence of stroke (64). The hyperglycemic state, accompanied by microvascular and macrovascular damage in patients with diabetes, is thought to affect neuroplasticity and impair the ability to recover from injury (65). Depression and anxiety have been associated with dysphagia. Studies have found that

anxiolytics, antidepressants, and sedative medications are used more frequently in older adults with dysphagia than in those without swallowing problems (67). Rudolph *et al.* (68) used a case-control study to explore the effects of psychotropic medications on swallowing function and found that swallowing function is diminished in patients using these medications and that higher dosages are associated with worse swallowing function. Drugs such as loxapine and phenazopyridine have also been shown to have deleterious effects on swallowing function in older individuals (69), with the anticholinergic effects of the drugs potentially leading to dry mouth and reduced salivation, thus affecting food lubrication. The effects of these drugs on the nigrostriatal pathway can lead to extrapyramidal symptoms and delayed dyskinesia, including dysphagia.

There is a link between PSD severity and sex; in general, women have more severe strokes and poorer swallowing functions (70). The International Stroke Trial showed a higher mortality rate in women, with 8003 women and 9367 men randomly assigned to the aspirin or heparin group, with a 14-day mortality rate of 11.0% in women versus 8.7% in men and a 6-month mortality rate of 24.5% in women versus 19.3% in men (71). In addition, women performed worse than men in stroke-related outcomes and measured dimensions such as disability, quality of life, anxiety, and depression (72). Some scholars have different perceptions regarding the association between PSD and sex. Renoux *et al.* (73) found no difference in stroke severity and degree of swallowing dysfunction between men and women after adjusting for age and premorbid mRS scores, suggesting that differences between men and women may be due to age and premorbid functional status rather than sex itself. We believe that the sex difference is justified owing to significant physiological differences in muscle strength, bone structure, and hormone levels, which may affect the recovery of swallowing muscle groups and the efficiency of neural repair after a stroke. This can lead to slower recovery of swallowing functions in women with stroke.

The kinematic parameters of the hyoid and epiglottis include movement trajectory, velocity, amplitude, and onset position, which are potentially useful in predicting PSD recovery. Lee *et al.* (74) analyzed a video fluoroscopic swallowing study (VFSS) and concluded that altered initial posterior movement of the hyoid and reduced horizontal forward movement during swallowing may be new kinematic indicators of poor prognosis for PSD. These changes in hyoid motion trajectory can lead to poor relaxation of the UES, accumulation of residue in the piriform sinus, and an increased risk of aspiration. In addition, movement of the epiglottis is recognized as an important mechanism for airway protection during swallowing. During normal swallowing, the epiglottis moves from a vertical resting position to a full downward tilt and then returns to the resting position. Frame-by-frame tracking of the hyoid position revealed that

when food reaches the pharynx, reduced and sluggish movement of the epiglottis leads to incomplete laryngeal protection, thereby causing aspiration and delaying the recovery process (9).

It is worth noting that most previous studies predicting the prognosis of swallowing function excluded patients who underwent tracheostomy, probably to improve the manageability of the study and the reliability of the results. Tracheal intubation or tracheotomy in the acute phase of stroke has more significant adverse effects on swallowing improvement (75), and invasive maneuvers may damage the muscles and nerves controlling the swallowing process, causing biomechanical alterations in the trachea, which can result in altered pharyngeal phases.

In conclusion, we described the multiple factors that influence recovery from PSD, and a comprehensive understanding of these factors may help develop a more individualized and precise rehabilitation intervention strategy, which can significantly improve the recovery of patients with dysphagia and their quality of life.

## 5. Mechanisms of recovery from PSD

Recovery from PSD is mainly based on neural remodeling and redistribution mechanisms. Neural remodeling refers to the nervous system's adaptation to new functional demands after an injury by altering synaptic connections and neural circuits. Synaptic plasticity is one of the mechanisms underlying neural remodeling. Damaged neural circuits can facilitate learning, memory, and recovery by strengthening synaptic connections that allow neural networks to adjust to experiences and environmental changes. Simultaneously, other regions of the brain and spinal cord can take over the functions of the damaged regions, and this functional redistribution often relies on the reorganization of neural networks. For example, in patients with PSD, the lateral brain regions may compensate for the damaged prefrontal regions, partially restoring impaired swallowing through the synergistic and compensatory effects of different brain regions to enhance the control and regulation of the swallowing process.

Neuroplastic mechanisms ensure the coordination and smoothness of swallowing process by enhancing neural pathway activation and cortical reorganization. These processes promote repair and support functional recovery by mediating the interrelated effects of the extracellular matrix (ECM) and peripheral neuronal network (PNN), while improving signaling efficiency through modulation of neurotransmitter levels, all of which significantly enhance swallowing recovery in post-stroke patients.

### 5.1. Activation of neural pathways and cortical reorganization of the brain

Swallowing involves the coordination of multiple

neural pathways, including the cortical, brainstem, vagus, trigeminal, and hypoglossal nerves. When an individual performs a specific swallowing function, the relevant neural networks in the brain are activated and coordinated to ensure a smooth and effective swallowing process. After a stroke, damage to brain areas responsible for swallowing can reduce the signaling efficiency of neural pathways, impair swallowing sensation, and hinder muscle control, resulting in weakened swallowing function that compromises both the safety and effectiveness of swallowing. According to the principles of neuroplasticity, swallowing-related neural networks can be activated through constant practice or external stimulation, which promotes the frequent activity of undamaged neurons, enhancing the connections between neurons and the efficiency of information transmission. In a study using blood oxygen level-dependent fMRI to examine brain activity during different swallowing maneuvers before and after treatment in patients with dysphagia caused by medullary infarction revealed that in the acute phase of stroke, only partial activation of the bilateral precentral gyrus and left lingual gyrus occurred during saliva swallowing. Forceful swallowing of saliva increased the activation of the bilateral auxiliary motor area, posterior central gyrus, and right insular cortex and increased thalamic activation after swallowing rehabilitation training (37). In addition, repetitive transcranial magnetic stimulation (rTMS) (76) and motor-evoked potentials (MEP) (54), as observed in MRI studies, have shown hyperactivation of the contralateral hemisphere in patients with PSD during functional recovery. This suggests that the improvement of dysphagia in patients with stroke may be related to compensatory brain mechanisms and the activation of regions bilaterally involved in the cortical representation of swallowing.

Simultaneously, cortical areas of the brain reorganize, with undamaged regions redistributing functions to compensate for the damaged areas. Patients with higher stroke severity have increased levels of default mode network (DMN) connectivity, reflecting a compensatory strategy for the function of the damaged part of the brain. Additionally, higher functional connectivity between brain networks decreases as patients with stroke recover (77). Prolonged compensatory brain activity is thought to reflect maladaptive brain plasticity, which can lead to poorer functioning in patients with stroke. Similarly, Huang *et al.* (78) proposed that improved swallowing function in these patients after swallowing training, as observed in MRI studies, is associated with reduced brain functional network connectivity. This suggests that the brain becomes less reliant on internal thought and more focused on the swallowing process during automated swallowing tasks. A cross-sectional study showed that enhanced resting-state functional connectivity between the precuneus, left and right anterior central gyri, and right para-motor area is negatively associated

with the Rosenbek penetration aspiration scale (PAS) and positively correlated with UES opening duration (UOD), suggesting that patients with stronger functional connectivity between the anterior central gyrus and medulla oblongata have a lower risk of penetration and aspiration and a longer UOD (79). Further studies have found that brain fMRI in patients with hemispheric and brainstem stroke showed different neurological changes. In patients with hemispheric stroke, improvement in the Functional Oral Intake Scale (FOIS) is associated with reduced functional brain connectivity in the ventral DMN of the precuneus, as observed on fMRI. Conversely, in patients with brainstem stroke, improvement in FOIS is linked to reduced functional brain connectivity in the left sensorimotor network of the posterior central region, as characterized by brain fMRI (78).

In summary, recovery from PSD is a complex process involving neural reorganization and functional connectivity changes at multiple levels. Modulation of cortical–medulla functional connectivity and changes in swallowing-related brain networks can serve as biomarkers for characterizing the recovery of swallowing function. By combining advanced neuroimaging techniques with behavioral assessments, we can further precisely assess the dynamic changes in these connections during swallowing and their clinical relevance, providing important clues for understanding the mechanisms of activation and cortical reorganization of neural pathways in the brain after PSD. However, given the limited published literature on the subject and the small number of included patients, the available data are insufficient for predictive modeling of swallowing function measures. In future studies, the predictive value of cortical–medulla connectivity for swallowing function and recovery should be further investigated, with the aim of revealing its mechanism of action in neural remodeling.

## 5.2. Regulatory role of the ECM and its members

The ECM is a structural scaffold embedded in brain cells and the vascular system, consisting of a variety of proteins (*e.g.* collagen, fibronectin, and glycosaminoglycans) and cytokines, which provide the support and signals required for cell growth, migration, and differentiation. The ECM in the CNS exhibits diverse morphologies, including diffuse, homogeneous, amorphous, and nearly ubiquitous substrates, as well as highly organized structures. Highly reticulated extracellular matrices known as PNNs typically encase neurons and serve supportive, protective, and regulatory functions during neuronal activity (80). A study of PNNs in the M1 of male PSD mice showed that electroacupuncture (EA)-induced increased c-Fos expression, enhanced spike firing, and potentiated excitatory postsynaptic currents (sEPSCs) in excitatory neurons, which improved swallowing function. However,

after the removal of PNNs in the contralateral M1, stroke-induced swallowing dysfunction occurred, and the effect of EA disappeared, suggesting that PNNs may be involved in stroke pathogenesis and EA-mediated improvement in swallowing function (81). Meanwhile, the structure of PNNs changes rapidly after stroke onset, facilitating more efficient  $\gamma$ -aminobutyric acid (GABA) signaling and enhancing the dynamic reorganization of interneurons. The remodeling of PNNs and their associated synapses occurs earlier than the recovery of function, suggesting that remodeling of PNNs is an early and critical step in the recovery of function (82). This may indicate that dynamic changes in the PNN affect the survival and regeneration of neurons associated with swallowing, modulate inhibitory signaling between neurons, and promote the recovery of swallowing function.

In the ECM, proteases and protease inhibitors aid in post-stroke recovery by regulating their own activities to maintain basement membrane integrity. This remodeling and regulation of the ECM is experience-dependent (83). Enhanced activity of ECM proteases, such as tissue plasminogen activator (tPA) and matrix metalloproteinase-9 (MMP-9), has been observed in the brain tissues of both mice and patients after stroke in response to enriched environmental interventions. Meanwhile, the expression of a disintegrin and metalloproteinase with thrombospondin motifs 4 (ADAMTS4) and its inhibitor, tissue inhibitor of matrix metalloproteinase-1 (TIMP1), tends to remain balanced (84). This suggests that swallowing-related skill training and physical therapy may promote neuroplasticity by modulating the activity of proteases and protease inhibitors and enhancing the ability of the nervous system to self-adjust and adapt to the environment and experiences, which in turn may influence the recovery of swallowing function.

After stroke, ECM members regulate the migration and activation of inflammation-related factors, thereby affecting the healing and repair processes of the injured area (83). It is hypothesized that the PSD recovery process is also related to the inflammatory regulatory effects of the ECM. In preclinical studies of ischemic stroke, tenascin-C in the ECM, which is mainly expressed during embryonic CNS development and at lower levels in adults, reappears after brain injury. Tenascin-C mitigates astrogliosis following ischemic stroke in mice and modulates the interaction between microglia and astrocytes, thereby promoting the proliferation of the microvasculature and neural stem cells in the penumbra, reconstruction of the neurovascular unit, and neural repair (85). Fibronectin is highly expressed in animal models of ischemic stroke, with its expression level peaks in the infarct region 7 days after middle cerebral artery occlusion (MCAO) (86). Fibronectin enhances the local immune response by promoting the migration of immune cells to the site of inflammation, and its

upregulation contributes to neuronal cell adhesion and migration in the injured region, thereby supporting neural regeneration (83). In clinical studies of ischemic stroke, polymerase-associated factor 1 (PAF1) supports regeneration by enhancing the activity of regulatory T cells and inhibiting the synthesis of pro-inflammatory cytokines. Elevated levels of PAF1 are associated with a better prognosis after ischemic stroke (87).

In ischemic stroke, there is limited data on changes in the ECM and its components in human subjects from clinical studies, compared to the more extensive findings in preclinical research. Further studies are necessary to elucidate the changes and functions of other ECM members in the brain and circulation of patients. Furthermore, in the context of hemorrhagic stroke, there is a scarcity of experimental and clinical data regarding changes in the ECM and its components within the interstitial matrix, basement membrane, and perineuronal nets. Consequently, further comprehensive research is necessary to assess alterations in the ECM and its constituents in hemorrhagic stroke.

### 5.3. Role of neurotransmitters

Neurotransmitters are chemicals that transmit signals between neurons and play important roles in the recovery of the swallowing function after stroke.

Substance P (SP), a neuropeptide widely found in the CNS and PNS, promotes nerve repair, enhances neuroplasticity, and regulates neuroinflammation by binding to its receptor neurokinin-1 (NK1), which positively contributes to PSD recovery. After a stroke, cerebral damage often leads to diminished swallowing reflexes. Capsaicin, by stimulating unmyelinated C-fibers and releasing tachykinins such as SP, promotes the reconstruction of neural pathways and enhances the swallowing reflex through activation of the NK1 receptor on the glossopharyngeal nerve (88). The SP can also facilitate the neural circuit of swallowing control. The release of transient receptor potential vanilloid subtype 1 (TRPV1) agonists can enhance the sensitivity of the brainstem and cortical regions to sensory inputs from the oral cavity and pharynx, enhancing the brain's perception of these signals and promoting the initiation of the swallowing reflex. This facilitates the initiation and execution of the swallowing reflex (89). Neuroinflammation often accompanies stroke, exacerbates neurological damage, and delays functional recovery. SP regulates the neuro-immune system feedback mechanism by interacting with the NK1 receptor, which helps to balance the local inflammatory response, promotes neuroprotection, attenuates neurological damage, and facilitates the neural repair process to some extent (90). Clinical and animal experimental studies have shown that the level of SP can be used as a potential biomarker for predicting swallowing recovery, as higher concentrations of SP

suggest better recovery of the swallowing reflex and more pronounced improvement in swallowing function (91,92). Pharmacological modulation of the action of SP or modulation of NK1 receptor activation may help accelerate the recovery of the gag reflex and reduce dysphagia, providing a new target for the clinical treatment of PSD.

Glutamate, the main excitatory neurotransmitter, promotes communication between neurons. It can enhance the activity of swallowing-related neural circuits and help re-establish swallowing function in both the oropharyngeal and complete swallowing phases (5). Studies have shown that swallowing behavior can be effectively induced by microinjections of glutamate at the NTS site in the brain, and that the process is similar to electrical or mechanical stimulation, suggesting that excitatory amino acid (EAA) receptors play an important role in inducing swallowing during the oropharyngeal phase (93). The key role of EAA in the complete swallowing phase was further confirmed by their ability to initiate specific esophageal peristaltic contractions by injecting glutamate and EAA agonists into the subcentral nuclear region of rats (94). It is worth emphasizing that specific neurons in the NTS are responsible for initiating and patterning the processes of swallowing and esophageal peristalsis. Therefore, the response produced by glutamate injection results in coordinated muscle activity, rather than haphazard movement (5). In addition, experimental results with agonists and antagonists of EAA receptors have revealed that activation of either N-methyl-D-aspartate (NMDA) receptors or non-NMDA receptors triggers swallowing and esophageal contractions; however, activation of NMDA receptors is more effective than that of non-NMDA receptors, which is related to the high-density distribution of NMDA receptors in the NTS region (5).

Inhibitory phenomena also play important roles in swallowing. The neurotransmitter GABA is a major mediator of synaptic inhibition. It helps to regulate homeostasis in the body, prevents neuronal overexcitation, and protects the stability of the swallowing center. During the swallowing process, GABA controls the different phases of swallowing by inhibiting the transmission of nerve signals. The swallowing preparation phase prevents non-target activities from interfering with the initiation of the swallowing reflex. During swallowing, it coordinates the actions of different muscle groups to ensure smooth passage of food through the esophagus. In the recovery phase, it helps the neural network restore baseline activity and prevents overexcitation from triggering secondary muscle spasms or overreactivity (5). Similarly, Wang and Bieger (95) showed that the local injection of GABA or a GABA agonist such as muscimol inhibits motor events associated with swallowing and esophageal peristalsis. When swallowing involves only the oropharyngeal phase, it can proceed normally with the local administration of

a subthreshold dose of the GABA receptor antagonist bicuculline. This allows the oropharyngeal phase to follow primary peristalsis (95). In contrast, during rapid rhythmic swallowing, the administration of bicuculline can release inhibition, preventing the initiation of the esophageal phase, and thus the completing rhythmic swallowing process (95). This suggests that GABA plays a key role in coordinating swallowing by regulating its rhythm and phases, inhibiting neural activity to ensure efficient coupling between the oropharyngeal phase and esophageal peristalsis.

Acetylcholine is responsible for transmitting neural signals from the brain to the pharynx and esophagus. Thus, the release of acetylcholine and the enhancement of its receptor activity during swallowing recovery can promote the contraction of the pharyngeal and esophageal muscles, helping the swallowing process proceed smoothly. During swallowing, striated muscles actively push food through the mouth and into the pharynx, while smooth muscles push food from the esophagus to the stomach. Acetylcholine responds heterogeneously to different muscle types by acting on striated muscles through motor neuron activation of nicotinic acetylcholine receptors (nAChRs) to accomplish the swallowing maneuver and on smooth muscles through parasympathetic activation of muscarinic acetylcholine receptors (mAChRs) to propel food to the stomach (5). Additionally, the involvement of acetylcholine receptors in the coupling process between the oropharynx and esophagus may vary among species; systemic injections of the anticholinergic drug atropine have been found to block the esophageal phase of swallowing in sheep (96), whereas in cats and humans, atropine injections do not block esophageal peristalsis (97). Based on the heterogeneity of the response to acetylcholine in different muscle types, the clinical treatment of dysphagia should be based on an in-depth understanding of the specific pathomechanisms and the development of drugs with a high degree of selectivity to avoid unnecessary interference with healthy swallowing muscle groups. Furthermore, in cross-species drug development and clinical trials, differences in the responses of different species to acetylcholine and its receptors need to be fully considered. Even within the same species, differences in the response to acetylcholine may exist between individuals owing to genetic variation, receptor subtype distribution, drug metabolism, and other factors, requiring adjustment of the drug dosage or selection of different therapeutic strategies based on individual patient characteristics.

Stimulation of GABA receptors in the vagal nucleus can modulate the excitatory effects of glutamate and acetylcholine (98), suggesting a dynamic balance between these neurotransmitters. This balance ensures an appropriate ratio of excitability to inhibition, facilitating the fine regulation of neural activity and promoting orderly neural function. A lack of such a

regulatory mechanism can lead to dysregulation of the balance between excitability and inhibition in the nervous system, thus affecting the coordination of swallowing. Over-excitability may lead to aspiration and choking, while under-excitability can cause delayed or incomplete swallowing responses. Therefore, the activity of glutamate, GABA, and acetylcholine and the balanced relationship among the three may be important biomarkers for assessing the recovery of swallowing function. Drugs and neuromodulation techniques targeting EAA, GABA, and acetylcholine receptors may be an effective means of treating PSD. In the future, brain imaging techniques, such as electroencephalography (EEG) or fMRI, can be used to observe the activity patterns of different neurotransmitters and changes in related neural circuits in animal models or patients with stroke. The extent of recovery of the swallowing function can be predicted by assessing the relationship between neurotransmitter receptor activity and swallowing behavior.

## 6. Treatment strategies based on functional compensation and motor learning

Functional compensation refers to adapting environments, tools, or strategies to help patients overcome dysphagia and ensure that they can safely ingest food and fluids. Motor learning involves the improvement of the coordination and efficiency of swallowing movements through practice and training. In patients with PSD, a combination of compensatory and motor learning approaches can effectively promote recovery of swallowing function. This can be achieved through proper food selection; control of dose and viscosity; the use of various swallowing techniques, movements, and exercises to strengthen the swallowing muscles and improve sputum production; and the application of various neural stimuli to swallowing-related muscles to increase prehyoid bone movement. In 2024, Bendix *et al.* published an article in *The Lancet* illustrating intervention strategies and treatment methods for dysphagia (99). Herein, we discuss several additional treatment methods, including noninvasive approaches like vacuum swallowing and acupuncture, as well as invasive treatments such as botulinum toxin A (BTX-A) injections, balloon catheter dilatation, cricopharyngeal muscle myotomy (CPM), and cricopharyngeal peroral endoscopic myotomy (CP-POEM) (Table 1).

### 6.1. Non-invasive methods

Non-invasive Brain Stimulation (NIBS) is a sophisticated and multi-dimensional strategy for modulating brain activity, holding broad potential in the therapeutic management of PSD. NIBS facilitates the initiation of neuroplastic changes by modulating the excitability of cerebral hemispheres, specifically reducing excitability

in the compromised hemisphere while enhancing that of the contralateral, unaffected hemisphere, through the application of electric or magnetic fields. The principal modalities of NIBS employed in PSD treatment are tDCS and rTMS. These two methodologies differ subtly in their approach to eliciting excitatory or inhibitory effects. The tDCS modulates neuronal activity by altering electrode positions, whereas rTMS achieves this by adjusting stimulation frequency. Specifically, tDCS enhances brain plasticity through the application of a mild electrical stimulation *via* a constant, low-intensity direct current. The anodal stimulation results in the depolarization of the resting membrane potential, thereby augmenting neuronal excitability, while cathodal stimulation induces hyperpolarization, diminishing neuronal excitability. While rTMS influences cerebral metabolism and neural activity by generating induced currents through magnetic fields that act upon the cerebral cortex, with high frequencies employed to augment cortical excitability and stimulate localized neuronal activity, and low frequencies used to reduce cortical excitability and inhibit neuronal cell function. A network meta-analysis has demonstrated that rTMS outperforms tDCS in enhancing swallowing function and diminishing aspiration risk in PSD patients (100). This superiority may stem from rTMS's enhanced capacity to penetrate the skull and access the cerebral cortex through magnetic field action, coupled with its precise localization. Furthermore, tDCS induces only local neuronal currents, which are incapable of spontaneous neuronal firing, and thus cannot elicit movements by activating the motor cortex of the intact efferent pathway, as rTMS can (101). It is noteworthy that, in terms of adverse effects, rTMS carries a risk of inducing epilepsy (101), dizziness (102), headaches (102), or epistaxis (103), while tDCS predominantly results in transient dizziness and mild headaches (104). Consequently, in clinical practice, physicians must balance the therapeutic benefits against the potential adverse effects, evaluate the efficacy and safety profiles of rTMS and tDCS for PSD, and choose the most appropriate treatment plan for patients.

Vacuum swallowing is a novel, noninvasive approach for compensatory swallowing. A case report suggests that patients with LMS, who have weak pharyngeal contractions and impaired UES function, involuntarily achieve vacuum swallowing through diaphragm contraction during swallowing. This approach also creates negative pressure in the esophagus and increases pressure in the LES, improving the pharyngeal passage of food through compensatory swallowing operations (105). Furthermore, patients can modulate the intensity of the negative pressure within the esophagus by voluntarily controlling the contraction of the primary and accessory respiratory muscles during the swallowing process (56). Velopharyngeal contractile integral (VPCI) measures pharyngeal contractility, or "vigor", including contraction

pressure, duration, and frequency. An increase in VPCI can be observed during vacuum swallowing, which results in an involuntary prolongation of swallowing time and enhanced contraction. This is similar to the effects of the Mendelsohn maneuver, where the larynx is elevated for a few seconds by forcefully pushing against the palate during swallowing, and the Shaker exercise, where the head is lifted through repetitive head-lifting movements in the supine position (105). Vacuum swallowing provides an effective compensatory strategy for the recovery of swallowing function in patients with dysphagia by promoting changes in physiological mechanisms and increasing pharyngeal contractility.

Acupuncture, a traditional treatment, has shown potential effectiveness in the rehabilitation of PSD and has been recommended by the World Health Organization as an alternative and complementary therapy for the treatment of stroke and the improving its sequelae (106). Acupuncture can reduce dysphagia by stimulating specific acupoints, modulating nervous system function, and improving nerve signaling during swallowing. In addition, acupuncture helps relax the pharynx and related muscles, reducing tension and spasms, thus facilitating smoother swallowing and playing a compensatory role. Excitatory neurons in layer 5 (L5) of the M1 control swallowing activity. EA stimulation of the CV23 acupoint (EA-CV23), as a peripheral stimulation strategy, has been demonstrated to improve swallowing function in PSD model mice by activating motor cortical inputs to the NTS *via* the parabrachial nuclei (PBN) (107). These findings highlight the crucial role of the M1-PBN-NTS neural pathway in mediating the protective effects of EA-CV23 against swallowing disorders, thereby suggesting a promising therapeutic approach for the treatment of dysphagia. However, there is a lack of high-quality RCTs that comprehensively assess the efficacy of acupuncture for PSD. Wu *et al.* identified the core acupoints most strongly correlated with PSD — GB20, CV23, EX-HN14, Gongxue, MS6, SJ17, EX-HN12, and EX-HN13 — utilizing data mining techniques. Through complex network, correlation, and cluster analyses, they identified GB20, CV23, and MS6 as the most evidence-supported acupoints for PSD (108). These results provide scientific evidence and clinical support for the use of acupuncture to improve PSD by modulating neural networks and stimulating specific acupoints. As part of a comprehensive treatment program, acupuncture is expected to help patients regain their swallowing ability more effectively in the future.

## 6.2. Invasive methods

BTX-A is a neurotoxin that inhibits the release of acetylcholine from presynaptic cholinergic nerve endings, blocks neuromuscular transmission, reduces overactive muscle tone, and aids in the relaxation of the UES and other swallowing-related muscles (109).

**Table 1. Treatment of PSD**

| Category                    | Intervention Method               | Specific Practices   | Advantages  | Disadvantages   | Results   |
|-----------------------------|-----------------------------------|--|---|---|---|
| Protective Intervention     | Dietary adjustment                | Using concentrated liquid, soft food, pureed food, etc.  | Oral food residue↓                                  | Palatability and appetite↓                                      | Aspiration↓   |
|                             | Oral hygiene                      | Gargle method, negative pressure brushing, hot and cold oral brushing, etc.  | Oral comfort↑                                       | Difficult to implement in patients with impaired consciousness. | Oral pathogens↓, Aspiration pneumonia↓                              |
|                             | Nutritional supplementation       | Nasogastric tube or gastrostomy tube (PEG) if necessary  | Suitable for long-term use                          | Risk of blockage  | BMI↑, total protein↑, albumin↑, hemoglobin↑                         |
| Rehabilitative Intervention | Behavioral strategies             | 1. Maintaining a sitting or semi-reclining position while eating 2. Using specialized feeding tools to enable self-feeding | Eating autonomy and sensation↑                      | Nursing complexity↑   | Aspiration pneumonia↓, nutrition↑, quality of life↑                 |
|                             | Sensory training                  | Including vibration stimulation, ice acid stimulation, K point stimulation, etc.   | Personalized treatment and high safety              | Long training duration, significant individual variability      | Swallowing reflex↑, initiation time of pharyngeal swallowing↓       |
|                             | Swallowing training               | Including oral motor exercises, tongue retraction exercises, swallowing reflex training, etc.                              |   |   | Coordination of swallowing muscles↑, muscle strength↑               |
| Pharmacological Treatment   | TRPV-1 receptor agonists          | Such as capsaicin, piperine, resiniferatoxin   | Multimodal stimulation with a wide range of options | Possible adverse effects: oral pain, discomfort                 | Pharyngeal sensation↑   |
|                             | GABA medications                  | Such as baclofen   | Muscle spasms↓                                      | Possible adverse effects: cognitive impairment                  | Regulation of excitatory amino acids and acetylcholine excitability |
|                             | ACE inhibitors                    | Such as captopril, enalapril, benazepril   |   | Possible adverse effects: dry cough, angioedema                 | Substance P↑, cough reflex↑   |
|                             | Anticholinergic drugs             | Such as clonazepam, tiotropium   |   | Saliva secretion↓, relaxation of smooth muscles                 | Aspiration and cough↓   |
|                             | Dopaminergic drugs                | Such as levodopa, dopamine receptor agonists, benserazide  |   | Latency of swallowing response↓                                 | Swallowing safety↑  |
|                             | Gastrointestinal prokinetic drugs | Such as domperidone, mosapride, itopride   |   | Gastrointestinal motility↑                                      | Nutrient absorption↑  |

TRPV1: transient receptor potential vanilloid subtype 1; GABA:  $\gamma$ -aminobutyric acid; ACE: angiotensin Converting Enzyme; tDCS: transcranial direct current stimulation; rTMS: repetitive transcranial magnetic stimulation; PES: pharyngeal electrical stimulation; NMES: neuromuscular electrical stimulation; UES: upper esophageal sphincter; CPA: cricopharyngeal achalasia; BTX-A: botulinum toxin A; CPM: cricopharyngeal muscle myotomy; CP-POEM: cricopharyngeal peroral endoscopic myotomy.

**Table 1. Treatment of PSD (continued)**

| Category   | Intervention Method         | Specific Practices  | Advantages  | Disadvantages  | Results   |
|--|-----------------------------|---|---|--|---|
| Neurostimulation Techniques                                    | tDCS                        | Anodal stimulation increases the excitability of the affected side, while cathodal stimulation decreases the excitability of the healthy side           | Non-invasive, high safety, flexible regulation, sustained effects | Device dependency, stimulation discomfort, significant individual variability, requires continuous treatment | Cortical excitability↑                                    |
|  | rTMS                        | High frequency stimulation enhances the excitability of the affected side, while low frequency stimulation reduces the excitability of the healthy side |   |  | Neural plasticity↑  |
|  | PES                         | High frequency (5.0 Hz) stimulation can extend swallowing response time, low frequency (0.2 Hz) stimulation can increase cortical excitability          |   |  | Motor cortex reorganization↑                              |
|  | NMES                        | Low frequency stimulation of the healthy side, high frequency stimulation of the affected side  |   |  | Strength↑, endurance↑ and activity↑ of swallowing muscles |
| Traditional Chinese Medicine Treatment                         | Acupuncture                 | The strongest evidence for acupoints is GB20, CV23, and MS6   | High safety, individualized treatment protocols                   | Requires continuous treatment  | Swallowing nerve signal transmission↑                     |
|  | BTX-A injection             | Injection site is the cricopharyngeus muscle, dosage range varies and is individual   | Multiple localization techniques, significant efficacy            | Significant individual variation in dosage, limited duration of efficacy                                     | Tension of UES and other swallowing-related muscles↓      |
| Invasive Methods (mainly for treating UES dysfunction and CPA) | Balloon catheter dilatation | Start with a small volume balloon and gradually increase  | Simple procedure, significant therapeutic outcomes                | Strict indications, repeated treatments may be required  | Rhythmicity and timing of swallowing↑                     |
|  | CPM and CP-POEM             | Direct action on the cricopharyngeus muscle or lower esophageal sphincter through surgery   | Good long-term effects  | Surgical risk↑, postoperative care requirements↑   | Muscle tension↓, esophageal diameter↑                     |

TRPV1: transient receptor potential vanilloid subtype 1; GABA:  $\gamma$ -aminobutyric acid; ACE: angiotensin Converting Enzyme; tDCS: transcranial direct current stimulation; rTMS: repetitive transcranial magnetic stimulation; PES: pharyngeal electrical stimulation; NMES: neuromuscular electrical stimulation; UES: upper esophageal sphincter; CPA: cricopharyngeal achalasia; BTX-A: botulinum toxin A; CPM: cricopharyngeal muscle myotomy; CP-POEM: cricopharyngeal peroral endoscopic myotomy.

BTX-A is minimally invasive, safe, and reproducible and is often used in clinical practice to treat UES dysfunction and cricopharyngeal achalasia (CPA). Schneider *et al.* first reported the use of BTX-A to treat swallowing dysfunction in 1994 (110). After BTX-A injection, the nervous system adapts to a new swallowing mechanism, enabling patients to learn new swallowing patterns and strategies through repetitive practice, thereby performing swallowing maneuvers more smoothly. However, current clinical studies are limited by small sample sizes, lack of standardized injection protocols, and inconsistent therapeutic outcomes. Therefore, larger studies with clear injection methods, subject criteria, and outcome definitions are needed to further investigate the therapeutic value of BTX-A in dysphagia.

The basic principle of balloon catheter dilatation is to insert a controllable inflatable balloon catheter into the patient's oral cavity under endoscopic guidance, confirm that the balloon catheter is located at the exact position of the stricture through endoscopic observation, and utilize its dilatation to gradually increase the esophageal lumen and promote smooth passage of food. Sensory input from balloon-guided active repetitive swallowing can influence the swallowing CPG and motor responses, enhancing plasticity in the swallowing centers of the brainstem, associated cortical areas, and subcortical structures, thereby improving or restoring the swallowing rhythm (111). However, current clinical applications have found that the presence of an endoscope during dilatation may reduce the efficacy of dilatation therapy and that the discomfort and trauma caused by the endoscope may increase the risk of perforation, bleeding, and aspiration. Compared to traditional balloon dilation, videofluoroscopy-guided balloon dilation is an innovative technique that allows esophageal dilation under visualization, offering enhanced visual control and reducing the risk of perforation and other complications. Both active and passive modes of balloon catheter dilatation have been shown to be effective; however, active balloon dilatation allows flexibility in adjusting the dilatation regimen and pressure settings according to the patient's actual situation, and data at the FOIS level has shown that active dilatation is more effective (112). Despite published guidelines (113), balloon catheter dilatation protocols have not been standardized across institutions. Balloon diameters and pressures, as well as the duration of each dilation, vary significantly depending on the operator's personal preference and experience. Currently, the universal standard recommends a maximum balloon diameter of 20 mm for symptomatic relief in adults and 10 mm in children. Therefore, future studies should focus on determining the optimal balloon diameter, dilation pressure, and duration, as well as establishing standardized operating practices to improve treatment outcomes and minimize the risk of complications.

When conservative therapies such as medication

and swallowing training are ineffective, CPM can be performed to improve the patient's ability to swallow by relieving the excessive tension of the cricopharyngeal muscles. In 2016, Nair *et al.* (114) reported on a patient with dysphagia lasting more than 1.5 years who showed no improvement after BTX-A injection. After undergoing CPM, the patient was able to eat orally, had the original PEG tube removed, and experienced significant improvements in nutritional status and mood. CP-POEM is an emerging minimally invasive endoscopic procedure for patients with UES dysfunction and CPA. The first retrospective study of CP-POEM for the treatment of oropharyngeal dysphagia demonstrated clinical and technical success in all 27 patients who underwent the procedure, showing improvement in dysphagia scores. During a median follow-up of 42.3 months, only one patient experienced reflux recurrence without dysphagia (115). This suggests that CP-POEM is a safe and effective alternative treatment option with low recurrence rates and favorable long-term outcomes. However, due to the limited number of current studies, the long-term outcomes of CP-POEM should be further evaluated through prospective studies.

Aging, functional decline, and comorbid conditions are common in older adults, and age-related changes in swallowing function may precede dysphagia. In patients with PSD and comorbid sarcopenia, addressing muscle loss and reduced swallowing muscle mass can help accelerate the recovery of swallowing function. In addition to regular swallowing rehabilitation training and physical therapy, it is necessary to ensure adequate protein and energy intake. This underscores the importance of an interdisciplinary team in managing and treating PSD. Effective collaboration among neurologists, speech therapists, physical therapists, dietitians, and caregivers, along with multifaceted interventions such as speech therapy, nutrition support, and physical therapy, helps manage PSD more systematically and effectively, ultimately improving the function and quality of life of older adults.

These integrative treatment strategies offer diverse pathways for the recovery of patients with PSD, emphasizing the importance of personalized medicine and the need for multidisciplinary collaboration. However, we must recognize the existing problems. First, because the site, directionality, and hemispheric coordination of the swallowing network are not fully understood, the lack of knowledge limits the optimization of neuromodulatory procedures, and the current study design and methodology lack uniform standards and norms, making it difficult to compare and generalize the results. Therefore, future studies should aim to establish standardized study designs and assessment indices to improve the reproducibility of the studies and the validity of the results, which, in turn, will provide a more solid scientific basis for clinical practice. Second, many studies have focused on the short-term efficacy of

PSD, while less attention has been paid to the long-term effects of treatment and its impact on the quality of life; thus, long-term follow-up studies are needed. Finally, different treatments may operate through various neural mechanisms; however, the current understanding of the neurobiological mechanisms of dysphagia remains limited. Systematic basic research is needed to clarify the mechanisms of action of these treatments.

## 7. Future directions

Owing to the bilateral innervation characteristics and neuroplasticity of the swallowing function, there is a certain potential for recovery of the swallowing function in post-stroke patients. Promoting the plasticity of neural networks by enhancing neural pathway activation, cortical reorganization, mediating ECM dynamics and its components, and modulating neurotransmitter transmission are key therapeutic targets for recovering swallowing function in patients with PSD. However, studies on the specific neural mechanisms and brain regions involved in swallowing recovery are limited. Although the cerebral cortex, brainstem, and cerebellum play important roles in the swallowing process, researchers have yet to identify the specific brain regions crucial for swallowing recovery and how these regions contribute to functional recovery through neural connections and network reorganization. In addition, existing studies tend to focus on specific regions of the cerebral cortex such as the motor and perceptual cortices, whereas relatively little research has been conducted on the brainstem and its downstream structures. Due to this lack of in-depth understanding of these neural mechanisms, clinical interventions often lack relevance and effectiveness.

In future management and treatment of PSD, information engineering will drive technological innovation and facilitate diagnostic advances, enabling the management of individual-based dysfunction patterns and their susceptibility risk factors through digital means. For example, wearable devices can monitor the swallowing process of patients in real time; collect physiological data such as heart rate, swallowing frequency, and hyoid trajectory; and analyze changes in swallowing function using intelligent algorithms, thus enabling personalized swallowing assessment and prediction. Meanwhile, virtual reality technology can simulate the swallowing environment to help patients perform swallowing training in a safe environment and provide real-time feedback to guide patients in improving their swallowing skills and dietary choices, thereby improving their swallowing ability and confidence. Additionally, AI-based assessment systems have been developed to analyze large amounts of patient swallowing video or audio data through machine learning to identify patterns of swallowing disorders, thereby providing accurate support for clinical

decision-making. Interdisciplinary collaboration not only promotes technological innovation but also better meets the individualized needs of patients and promotes the development of precision medicine. The combination of medicine and engineering has become an important driving force for medical innovation.

## 8. Conclusion

This review thoroughly explored the neurophysiological mechanisms, influencing factors, recovery mechanisms, and therapeutic strategies of PSD and proposed a series of integrated therapeutic approaches based on functional compensation and motor learning. Neural remodeling and functional redistribution mechanisms are central to PSD recovery and involve a wide range of brain regions and neural networks. Activation of damaged neural pathways, enhanced cortical reorganization of the brain, and modulation of the ECM and neurotransmitters are critical steps in the recovery process. Research suggests that effective PSD management requires a multidisciplinary approach incorporating physical therapy, speech therapy, acupuncture, and other emerging medical and industrial techniques. Future research should focus on precise neurobiological mechanisms to develop more effective therapeutic strategies, especially by applying modern technologies such as artificial intelligence and virtual reality to personalized medicine to provide optimal rehabilitation for patients with PSD.

*Funding:* This work was supported by a grant from the National Natural Science Foundation of China (No.82174477) and the Heilongjiang Key R&D Program (2022ZX06C24).

*Conflict of Interest:* The authors have no conflicts of interest to disclose.

## References

1. Takizawa C, Gemmell E, Kenworthy J, Speyer R. A systematic review of the prevalence of oropharyngeal dysphagia in stroke, Parkinson's disease, Alzheimer's disease, head injury, and pneumonia. *Dysphagia*. 2016; 31:434-441.
2. Mann G, Hankey GJ, Cameron D. Swallowing function after stroke: Prognosis and prognostic factors at 6 months. *Stroke*. 1999; 30:744-748.
3. Martin SS, Aday AW, Almarzooq ZI, *et al.* 2024 heart disease and stroke statistics: A report of US and global data from the American Heart Association. *Circulation*. 2024; 149:e347-e913.
4. Sasegbon A, Cheng I, Hamdy S. The neurorehabilitation of post-stroke dysphagia: Physiology and pathophysiology. *The Journal of physiology*. *J Physiol*. 2025; 603:617-634.
5. Jean A. Brain stem control of swallowing: Neuronal network and cellular mechanisms. *Physiol Rev*. 2001; 81:929-969.
6. Daniels SK, Pathak S, Mukhi SV, Stach CB, Morgan RO,

- Anderson JA. The relationship between lesion localization and dysphagia in acute stroke. *Dysphagia*. 2017; 32:777-784.
7. Lang IM. Brain stem control of the phases of swallowing. *Dysphagia*. 2009; 24:333-348.
  8. McCarty EB, Chao TN. Dysphagia and swallowing disorders. *Med Clin North Am*. 2021; 105:939-954.
  9. Nagy A, Molfenter SM, Péladeau-Pigeon M, Stokely S, Steele CM. The effect of bolus consistency on hyoid velocity in healthy swallowing. *Dysphagia*. 2015; 30:445-451.
  10. Langmore SE, Terpenning MS, Schork A, Chen Y, Murray JT, Lopatin D, Loesche WJ. Predictors of aspiration pneumonia: How important is dysphagia? *Dysphagia*. 1998; 13:69-81.
  11. Dua KS, Surapaneni SN, Santharam R, Knuff D, Hofmann C, Shaker R. Effect of systemic alcohol and nicotine on airway protective reflexes. *Am J Gastroenterol*. 2009; 104:2431-2438.
  12. Ebihara S, Izukura H, Miyagi M, Okuni I, Sekiya H, Ebihara T. Chemical senses affecting cough and swallowing. *Curr Pharm Des*. 2016; 22:2285-2289.
  13. Chebib N, Cuvelier C, Malézieux-Picard A, Parent T, Roux X, Fassier T, Müller F, Prendki V. Pneumonia prevention in the elderly patients: The other sides. *Aging Clin Exp Res*. 2021; 33:1091-1100.
  14. Bajjens LW, Clavé P, Cras P, Ekberg O, Forster A, Kolb GF, Leners JC, Masiero S, Mateos-Nozal J, Ortega O, Smithard DG, Speyer R, Walshe M. European Society for Swallowing Disorders - European Union Geriatric Medicine Society white paper: Oropharyngeal dysphagia as a geriatric syndrome. *Clin Interv Aging*. 2016; 11:1403-1428.
  15. Peyron MA, Woda A, Bourdiol P, Hennequin M. Age-related changes in mastication. *J Oral Rehabil*. 2017; 44:299-312.
  16. Shimazaki Y, Saito M, Nonoyama T, Tadokoro Y. Oral factors associated with swallowing function in independent elders. *Oral Health Prev Dent*. 2020; 18:683-691.
  17. Ko N, Lee HH, Sohn MK, *et al*. Status of dysphagia after ischemic stroke: A Korean nationwide study. *Arch Phys Med Rehabil*. 2021; 102:2343-2352.e3.
  18. Flowers HL, Silver FL, Fang J, Rochon E, Martino R. The incidence, co-occurrence, and predictors of dysphagia, dysarthria, and aphasia after first-ever acute ischemic stroke. *J Commun Disord*. 2013; 46:238-248.
  19. Perry L, Love CP. Screening for dysphagia and aspiration in acute stroke: A systematic review. *Dysphagia*. 2001; 16:7-18.
  20. Kalf JG, de Swart BJ, Bloem BR, Munneke M. Prevalence of oropharyngeal dysphagia in Parkinson's disease: A meta-analysis. *Parkinsonism Relat Disord*. 2012; 18:311-315.
  21. Castagna A, Ferrara L, Asnaghi E, Rega V, Fiorini G. Functional limitations and cognitive impairment predict the outcome of dysphagia in older patients after an acute neurologic event. *NeuroRehabilitation*. 2019; 44:413-418.
  22. Affoo RH, Foley N, Rosenbek J, Kevin Shoemaker J, Martin RE. Swallowing dysfunction and autonomic nervous system dysfunction in Alzheimer's disease: A scoping review of the evidence. *J Am Geriatr Soc*. 2013; 61:2203-2213.
  23. James E, Ellis C, Brassington R, Sathasivam S, Young CA. Treatment for sialorrhea (excessive saliva) in people with motor neuron disease/amyotrophic lateral sclerosis. *Cochrane Database Syst Rev*. 2022; 5:Cd006981.
  24. Tsujimura T, Suzuki T, Yoshihara M, Sakai S, Koshi N, Ashiga H, Shiraishi N, Tsuji K, Magara J, Inoue M. Involvement of hypoglossal and recurrent laryngeal nerves on swallowing pressure. *J Appl Physiol* (1985). 2018; 124:1148-1154.
  25. Philpott H, Garg M, Tomic D, Balasubramanian S, Sweis R. Dysphagia: Thinking outside the box. *World J Gastroenterol*. 2017; 23:6942-6951.
  26. Aldridge KJ, Taylor NF. Dysphagia is a common and serious problem for adults with mental illness: A systematic review. *Dysphagia*. 2012; 27:124-137.
  27. Nakajima Y, Tsujimura T, Tsutsui Y, Chotirungsan T, Kawada S, Dewa N, Magara J, Inoue M. Atropine facilitates water-evoked swallows *via* central muscarinic receptors in anesthetized rats. *Am J Physiol Gastrointest Liver Physiol*. 2023; 325:G109-G121.
  28. Ekberg O, Hamdy S, Woisard V, Wuttge-Hannig A, Ortega P. Social and psychological burden of dysphagia: Its impact on diagnosis and treatment. *Dysphagia*. 2002; 17:139-146.
  29. Zeng H, Zeng X, Xiong N, Wang L, Yang Y, Wang L, Li H, Zhao W. How stroke-related dysphagia relates to quality of life: The mediating role of nutritional status and psychological disorders, and the moderating effect of enteral nutrition mode. *Front Nutr*. 2024; 11:1339694.
  30. Lin LC, Wang TG, Chen MY, Wu SC, Portwood MJ. Depressive symptoms in long-term care residents in Taiwan. *J Adv Nurs*. 2005; 51:30-37.
  31. Miller N, Allcock L, Hildreth AJ, Jones D, Noble E, Burn DJ. Swallowing problems in Parkinson disease: Frequency and clinical correlates. *J Neurol Neurosurg Psychiatry*. 2009; 80:1047-1049.
  32. Ranucci D, Falco F, Nicoletta V, Di Monaco C, Migliaccio L, Lamagna F, Caracciolo F, Eliano M, Petracca M, Moccia M, Brescia Morra V, Carotenuto A, Lanzillo R. Dysphagia assessment in patients with multiple sclerosis - an additional piece to disability burden. *Ann Clin Transl Neurol*. 2024; 11:2958-2966.
  33. Zamani M, Alizadeh-Tabari S, Chan WW, Talley NJ. Association between anxiety/depression and gastroesophageal reflux: A systematic review and meta-analysis. *Am J Gastroenterol*. 2023; 118:2133-2143.
  34. Cheng I, Takahashi K, Miller A, Hamdy S. Cerebral control of swallowing: An update on neurobehavioral evidence. *J Neurol Sci*. 2022; 442:120434.
  35. Daniels SK, Foundas AL. Lesion localization in acute stroke patients with risk of aspiration. *J Neuroimaging*. 1999; 9:91-98.
  36. Wilmskoetter J, Bonilha L, Martin-Harris B, Elm JJ, Horn J, Bonilha HS. Mapping acute lesion locations to physiological swallow impairments after stroke. *Neuroimage Clin*. 2019; 22:101685.
  37. Gu F, Han J, Zhang Q, Li X, Wang Y, Wu J. Cortical compensation mechanism for swallowing recovery in patients with medullary infarction-induced dysphagia. *Front Neurol*. 2024; 15:1346522.
  38. Qin Y, Tang Y, Liu X, Qiu S. Neural basis of dysphagia in stroke: A systematic review and meta-analysis. *Front Hum Neurosci*. 2023; 17:1077234.
  39. Choi S, Pyun SB. Repetitive transcranial magnetic stimulation on the supplementary motor area changes brain connectivity in functional dysphagia. *Brain Connect*. 2021; 11:368-379.

40. Jang SH, Lee J, Kim MS. Dysphagia prognosis prediction *via* corticobulbar tract assessment in lateral medullary infarction: A diffusion tensor tractography study. *Dysphagia*. 2021; 36:680-688.
41. Im S, Han YJ, Kim SH, Yoon MJ, Oh J, Kim Y. Role of bilateral corticobulbar tracts in dysphagia after middle cerebral artery stroke. *Eur J Neurol*. 2020; 27:2158-2167.
42. Ertekin C, Aydogdu I, Tarlaci S, Turman AB, Kiylioglu N. Mechanisms of dysphagia in suprabulbar palsy with lacunar infarct. *Stroke*. 2000; 31:1370-1376.
43. Cho YJ, Ryu WS, Lee H, Kim DE, Park JW. Which factors affect the severity of dysphagia in lateral medullary infarction? *Dysphagia*. 2020; 35:414-418.
44. Singh S, Hamdy S. Dysphagia in stroke patients. *Postgrad Med J*. 2006; 82:383-391.
45. Numasawa Y, Hattori T, Ishiai S, Kobayashi Z, Kamata T, Kotera M, Ishibashi S, Sanjo N, Mizusawa H, Yokota T. Depressive disorder may be associated with raphe nuclei lesions in patients with brainstem infarction. *J Affect Disord*. 2017; 213:191-198.
46. Hajipour M, Sobhani-Rad D, Zainae S, Farzadfar MT, Khaniki SH. Dysphagia following cerebellar stroke: Analyzing the contribution of the cerebellum to swallowing function. *Front Neurol*. 2023; 14:1276243.
47. Rangarathnam B, Kamarunas E, McCullough GH. Role of cerebellum in deglutition and deglutition disorders. *Cerebellum*. 2014; 13:767-776.
48. Prescott SL, Liberles SD. Internal senses of the vagus nerve. *Neuron*. 2022; 110:579-599.
49. Kecskes S, Matesz C, Birinyi A. Termination of trigeminal primary afferents on glossopharyngeal-vagal motoneurons: Possible neural networks underlying the swallowing phase and visceromotor responses of prey-catching behavior. *Brain Res Bull*. 2013; 99:109-116.
50. Capra NF. Mechanisms of oral sensation. *Dysphagia*. 1995; 10:235-247.
51. Krekeler BN, Schieve HJP, Khoury J, *et al*. Health factors associated with development and severity of poststroke dysphagia: An epidemiological investigation. *J Am Heart Assoc*. 2024; 13:e033922.
52. Wilmskoetter J, Martin-Harris B, Pearson WG Jr, Bonilha L, Elm JJ, Horn J, Bonilha HS. Differences in swallow physiology in patients with left and right hemispheric strokes. *Physiol Behav*. 2018; 194:144-152.
53. Seo HG, Oh BM, Han TR. Swallowing kinematics and factors associated with laryngeal penetration and aspiration in stroke survivors with dysphagia. *Dysphagia*. 2016; 31:160-168.
54. Li S, Luo C, Yu B, Yan B, Gong Q, He C, He L, Huang X, Yao D, Lui S, Tang H, Chen Q, Zeng Y, Zhou D. Functional magnetic resonance imaging study on dysphagia after unilateral hemispheric stroke: A preliminary study. *J Neurol Neurosurg Psychiatry*. 2009; 80:1320-1329.
55. Lee WH, Lim MH, Seo HG, Seong MY, Oh BM, Kim S. Development of a novel prognostic model to predict 6-month swallowing recovery after ischemic stroke. *Stroke*. 2020; 51:440-448.
56. Jang SH, Kim MS. Dysphagia in lateral medullary syndrome: A narrative review. *Dysphagia*. 2021; 36:329-338.
57. Beharry A, Michel P, Faouzi M, Kuntzer T, Schweizer V, Diserens K. Predictive factors of swallowing disorders and bronchopneumonia in acute ischemic stroke. *J Stroke Cerebrovasc Dis*. 2019; 28:2148-2154.
58. Huang L, Wang Y, Sun J, Zhu L, Liu J, Wu Y, Shan C, Yan J, Wan P. Incidence and risk factors for dysphagia following cerebellar stroke: A retrospective cohort study. *Cerebellum*. 2024; 23:1293-1303.
59. Wang L, Qiao J, Sun F, Wei X, Dou Z. Demographic and clinical factors associated with recovery of poststroke dysphagia: A meta-analysis. *Brain Behav*. 2023; 13:e30333.
60. Shimizu A, Maeda K, Koyanagi Y, Kayashita J, Fujishima I, Mori N. The global leadership initiative on malnutrition-defined malnutrition predicts prognosis in persons with stroke-related dysphagia. *J Am Med Dir Assoc*. 2019; 20:1628-1633.
61. Fujishima I, Fujiu-Kurachi M, Arai H, *et al*. Sarcopenia and dysphagia: Position paper by four professional organizations. *Geriatr Gerontol Int*. 2019; 19:91-97.
62. Jeyaseelan RD, Vargo MM, Chae J. National Institutes of Health Stroke Scale (NIHSS) as an early predictor of poststroke dysphagia. *PM R*. 2015; 7:593-598.
63. Qiao J, Wu ZM, Ye QP, Dai Y, Dou ZL. Relationship between post-stroke cognitive impairment and severe dysphagia: A retrospective cohort study. *Brain Sci*. 2022; 12:803.
64. Yang C, Pan Y. Risk factors of dysphagia in patients with ischemic stroke: A meta-analysis and systematic review. *PloS One*. 2022; 17:e0270096.
65. Banda KJ, Chu H, Kang XL, Liu D, Pien LC, Jen HJ, Hsiao SS, Chou KR. Prevalence of dysphagia and risk of pneumonia and mortality in acute stroke patients: A meta-analysis. *BMC Geriatr*. 2022; 22:420.
66. Rexrode KM, Madsen TE, Yu AYX, Carcel C, Lichtman JH, Miller EC. The impact of sex and gender on stroke. *Circ Res*. 2022; 130:512-528.
67. Karisik A, Dejakum B, Moelgg K, *et al*. Association between dysphagia and symptoms of depression and anxiety after ischemic stroke. *Eur J Neurol*. 2024; 31:e16224.
68. Rudolph JL, Gardner KF, Gramigna GD, McGlinchey RE. Antipsychotics and oropharyngeal dysphagia in hospitalized older patients. *J Clin Psychopharmacol*. 2008; 28:532-535.
69. Miarons Font M, Rofes Salsench L. Antipsychotic medication and oropharyngeal dysphagia: Systematic review. *Eur J Gastroenterol Hepatol*. 2017; 29:1332-1339.
70. Phan HT, Reeves MJ, Blizzard CL, *et al*. Sex differences in severity of stroke in the INSTRUCT study: A meta-analysis of individual participant data. *J Am Heart Assoc*. 2019; 8:e010235.
71. Niewada M, Kobayashi A, Sandercock PA, Kamiński B, Członkowska A; International Stroke Trial Collaborative Group. Influence of gender on baseline features and clinical outcomes among 17,370 patients with confirmed ischaemic stroke in the international stroke trial. *Neuroepidemiology*. 2005; 24:123-128.
72. Reeves MJ, Bushnell CD, Howard G, Gargano JW, Duncan PW, Lynch G, Khatiwoda A, Lisabeth L. Sex differences in stroke: Epidemiology, clinical presentation, medical care, and outcomes. *Lancet Neurol*. 2008; 7:915-926.
73. Renoux C, Coulombe J, Li L, Ganesh A, Silver L, Rothwell PM. Confounding by pre-morbid functional status in studies of apparent sex differences in severity and outcome of stroke. *Stroke*. 2017; 48:2731-2738.
74. Lee WH, Lim MH, Seo HG, Oh BM, Kim S. Hyoid kinematic features for poor swallowing prognosis in patients with post-stroke dysphagia. *Sci Rep*. 2021;

- 11:1471.
75. Tsuzuki K, Mori N, Hayami Y, Oshima O, Sugawara H, Tsuji T. Predictors of complete oral intake in patients with stroke after tracheostomy. *J Am Heart Assoc.* 2024; 13:e000180.
  76. Hamdy S, Aziz Q, Rothwell JC, Power M, Singh KD, Nicholson DA, Tallis RC, Thompson DG. Recovery of swallowing after dysphagic stroke relates to functional reorganization in the intact motor cortex. *Gastroenterology.* 1998; 115:1104-1112.
  77. Wang Y, Lu M, Liu R, Wang L, Wang Y, Xu L, Wu K, Chen C, Chen T, Shi X, Li K, Zou Y. Acupuncture alters brain's dynamic functional network connectivity in stroke patients with motor dysfunction: A randomised controlled neuroimaging trial. *Neural Plast.* 2023; 2023:8510213.
  78. Huang YC, Hsu TW, Leong CP, Hsieh HC, Lin WC. Clinical Effects and Differences in Neural Function Connectivity Revealed by MRI in Subacute Hemispheric and Brainstem Infarction Patients With Dysphagia After Swallowing Therapy. *Frontiers in neuroscience.* 2018; 12:488.
  79. Dai M, Qiao J, Wei X, Chen H, Shi Z, Dou Z. Increased cortical-medulla functional connectivity is correlated with swallowing in dysphagia patients with subacute infratentorial stroke. *Neuroimage Clin.* 2022; 35:103104.
  80. Dong Y, Zhao K, Qin X, Du G, Gao L. The mechanisms of perineuronal net abnormalities in contributing aging and neurological diseases. *Ageing Res Rev.* 2023; 92:102092.
  81. Yuan S, Shi J, Tang X, Deng B, Wu Z, Qiu B, Lin S, Ji C, Wang L, Cui S, Xu N, Yao L. The role of perineuronal nets in the contralateral hemisphere in the electroacupuncture-mediated rehabilitation of poststroke dysphagia mice. *eNeuro.* 2023; 10:ENEURO.0234-23.2023.
  82. Dzyubenko E, Willig KI, Yin D, Sardari M, Tokmak E, Labus P, Schmermund B, Hermann DM. Structural changes in perineuronal nets and their perforating GABAergic synapses precede motor coordination recovery post stroke. *J Biomed Sci.* 2023; 30:76.
  83. Li H, Ghorbani S, Ling CC, Yong VW, Xue M. The extracellular matrix as modifier of neuroinflammation and recovery in ischemic stroke and intracerebral hemorrhage. *Neurobiol Dis.* 2023; 186:106282.
  84. Quattromani MJ, Pruvost M, Guerreiro C, Backlund F, Englund E, Asperg A, Jaworski T, Hakon J, Ruscher K, Kaczmarek L, Vivien D, Wieloch T. Extracellular matrix modulation is driven by experience-dependent plasticity during stroke recovery. *Mol Neurobiol.* 2018; 55:2196-2213.
  85. Dzyubenko E, Manrique-Castano D, Pillath-Eilers M, Vasileiadou P, Reinhard J, Faissner A, Hermann DM. Tenascin-C restricts reactive astrogliosis in the ischemic brain. *Matrix Biol.* 2022; 110:1-15.
  86. Wu CT, Chen MC, Liu SH, Yang TH, Long LH, Guan SS, Chen CM. Bioactive flavonoids icaritin and icariin protect against cerebral ischemia-reperfusion-associated apoptosis and extracellular matrix accumulation in an ischemic stroke mouse model. *Biomedicines.* 2021; 9:1719.
  87. Al Qawasmeh M, Alhusban A, Alfwaress F. An evaluation of the ability of thrombospondin-1 to predict stroke outcomes and mortality after ischemic stroke. *Int J Neurosci.* 2020; 1-4.
  88. Jin Y, Sekizawa K, Fukushima T, Morikawa M, Nakazawa H, Sasaki H. Capsaicin desensitization inhibits swallowing reflex in guinea pigs. *Am J Respir Crit Care Med.* 1994; 149:261-263.
  89. Suntrup-Krueger S, Muhle P, Kampe I, Egidi P, Ruck T, Lenze F, Jungheim M, Gminski R, Labeit B, Claus I, Warnecke T, Gross J, Dziewas R. Effect of capsaicinoids on neurophysiological, biochemical, and mechanical parameters of swallowing function. *Neurotherapeutics.* 2021; 18:1360-1370.
  90. Safwat A, Helmy A, Gupta A. The role of substance P within traumatic brain injury and implications for therapy. *J Neurotrauma.* 2023; 40:1567-1583.
  91. Ikeda J, Kojima N, Saeki K, Ishihara M, Takayama M. Perindopril increases the swallowing reflex by inhibiting substance P degradation and tyrosine hydroxylase activation in a rat model of dysphagia. *Eur J Pharmacol.* 2015; 746:126-131.
  92. Niimi M, Hashimoto G, Hara T, Yamada N, Abo M, Fujigasaki H, Ide T. Relationship between frequency of spontaneous swallowing and salivary substance P level in patients with acute stroke. *Dysphagia.* 2018; 33:414-418.
  93. Kessler JP, Jean A. Evidence that activation of N-methyl-D-aspartate (NMDA) and non-NMDA receptors within the nucleus tractus solitarius triggers swallowing. *Eur J Pharmacol.* 1991; 201:59-67.
  94. Hashim MA, Bieger D. Excitatory amino acid receptor-mediated activation of solitary deglutitive loci. *Neuropharmacology.* 1989; 28:913-921.
  95. Wang YT, Bieger D. Role of solitary GABAergic mechanisms in control of swallowing. *Am J Physiol.* 1991; 261:R639-R646.
  96. Car A, Roman C, Zougrana OR. Effects of atropine on the central mechanism of deglutition in anesthetized sheep. *Exp Brain Res.* 2002; 142:496-503.
  97. Greenwood B, Blank E, Dodds WJ. Nicotine stimulates esophageal peristaltic contractions in cats by a central mechanism. *Am J Physiol.* 1992; 262:G567-G571.
  98. Bieger D. Neuropharmacologic correlates of deglutition: Lessons from fictive swallowing. *Dysphagia.* 1991; 6:147-164.
  99. Labeit B, Michou E, Trapl-Grundschober M, Suntrup-Krueger S, Muhle P, Bath PM, Dziewas R. Dysphagia after stroke: Research advances in treatment interventions. *Lancet Neurol.* 2024; 23:418-428.
  100. Li L, Huang H, Jia Y, Yu Y, Liu Z, Shi X, Wang F. Systematic review and network meta-analysis of noninvasive brain stimulation on dysphagia after stroke. *Neural Plast.* 2021; 2021:3831472.
  101. Nyffeler T, Müri R. Comment on: Safety, ethical considerations, and application guidelines for the use of transcranial magnetic stimulation in clinical practice and research, by Rossi *et al.* (2009). *Clin Neurophysiol.* 2010; 121:980.
  102. Zhong L, Rao J, Wang J, Li F, Peng Y, Liu H, Zhang Y, Wang P. Repetitive transcranial magnetic stimulation at different sites for dysphagia after stroke: A randomized, observer-blind clinical trial. *Front Neurol.* 2021; 12:625683.
  103. Ünlüer NÖ, Temuçin ÇM, Demir N, Serel Arslan S, Karaduman AA. Effects of low-frequency repetitive transcranial magnetic stimulation on swallowing function and quality of life of post-stroke patients. *Dysphagia.* 2019; 34:360-371.
  104. Nitsche MA, Liebetanz D, Antal A, Lang N, Tergau F, Paulus W. Modulation of cortical excitability by weak direct current stimulation--technical, safety and functional aspects. *Suppl Clin Neurophysiol.* 2003; 56:255-276.
  105. Kunieda K, Sugiyama J, Nomoto A, Ohno T, Shigematsu

- T, Fujishima I. Compensatory swallowing methods in a patient with dysphagia due to lateral medullary syndrome-vacuum and prolonged swallowing: A case report. *Medicine (Baltimore)*. 2022; 101:e28524.
106. World Health Organization. Acupuncture: Review and analysis of reports on controlled clinical trials. World Health Organization. 2003; pp.1-81.
107. Yao L, Ye Q, Liu Y, *et al.* Electroacupuncture improves swallowing function in a post-stroke dysphagia mouse model by activating the motor cortex inputs to the nucleus tractus solitarius through the parabrachial nuclei. *Nat Commun*. 2023; 14:810.
108. Wu M, Song W, Wang X, Tang Q, Gao W, Zhu L. Exploring the rules of related parameters in acupuncture for post-stroke dysphagia based on data mining. *Front Neurol*. 2024; 15:1394348.
109. Terré R, Panadés A, Mearin F. Botulinum toxin treatment for oropharyngeal dysphagia in patients with stroke. *Neurogastroenterol Motil*. 2013; 25:896-e702.
110. Schneider I, Thumfart WF, Pototschnig C, Eckel HE. Treatment of dysfunction of the cricopharyngeal muscle with botulinum A toxin: introduction of a new, noninvasive method. *Ann Otol Rhinol Laryngol*. 1994; 103:31-35.
111. Dodds WJ. The physiology of swallowing. *Dysphagia*. 1989; 3:171-178.
112. Dou Z, Zu Y, Wen H, Wan G, Jiang L, Hu Y. The effect of different catheter balloon dilatation modes on cricopharyngeal dysfunction in patients with dysphagia. *Dysphagia*. 2012; 27:514-520.
113. Standards of Practice Committee; Egan JV, Baron TH, *et al.* Esophageal dilation. *Gastrointest Endosc*. 2006; 63:755-760.
114. Nair SS, Surendaran AJ, Menon JR, Sreedharan SE, Sylaja PN. Persistent post-stroke dysphagia treated with cricopharyngeal myotomy. *Ann Indian Acad Neurol*. 2016; 19:249-251.
115. Al Ghamdi SS, Bejjani M, Hernández Mondragón OV, Parsa N, Yousaf MN, Aghaie Meybodi M, Ghandour B, Krustri C, Phalanusitthepha C, Ngamruengphong S, Nieto JM, Khashab MA. Peroral endoscopic myotomy for management of cricopharyngeal bars (CP-POEM): A retrospective evaluation. *Endoscopy*. 2022; 54:498-502.

Received January 24, 2025; Revised February 10, 2025; Accepted February 17, 2025.

*\*Address correspondence to:*

Luwen Zhu, The Second Affiliated Hospital of Heilongjiang University of Chinese Medicine, 411 Guogeli Street, Nangang District, Heilongjiang Harbin, China.  
E-mail: zhuluwen1983@126.com

Qing Mei Wang, Stroke Biological Recovery Laboratory, Spaulding Rehabilitation Hospital, the Teaching Affiliate of Harvard Medical School, Boston, MA, USA.  
E-mail: Wang.Qingmei@mgh.harvard.edu

Released online in J-STAGE as advance publication February 22, 2025.

# From light to insight: Functional near-infrared spectroscopy for unravelling cognitive impairment during task performance

Na Liu<sup>1,§</sup>, Lingling Yang<sup>1,§</sup>, Xiuqing Yao<sup>1,2,3,\*</sup>, Yaxi Luo<sup>1,\*</sup>

<sup>1</sup>Department of Rehabilitation, The Second Affiliated Hospital of Chongqing Medical University, Chongqing, China;

<sup>2</sup>Chongqing Municipality Clinical Research Center for Geriatric Medicine, Chongqing, China;

<sup>3</sup>Department of Rehabilitation Therapy, Chongqing Medical University, Chongqing, China.

**SUMMARY:** Cognitive impairment refers to the impairment of higher brain functions such as perception, thinking or memory that affects the individual's ability to perform daily or social activities. Studies have found that changes in neuronal activity during tasks in patients with cognitive impairment are closely related to changes in cerebral cortical hemodynamics. Functional near-infrared spectroscopy is an indirect method to measure neural activity based on changes in blood oxygen concentration in the cerebral cortex. Due to its strong anti-motion interference, high compatibility, and almost no restriction on participants and environment, it has shown great potential in the research field of cognitive impairment. Recognizing these benefits, this comprehensive review systematically elucidates the rationale, historical development, advantages and disadvantages of functional near-infrared spectroscopy, and also discusses the applications of combining functional near-infrared spectroscopy with other detection techniques. Additionally, this review summarized how functional near-infrared spectroscopy can be applied to cognitive impairment caused by different diseases, ultimately aiding the study of neural mechanisms of cognitive activities, which is crucial for the diagnosis, differentiation and treatment of cognitive impairment.

**Keywords:** functional near-infrared spectroscopy, cognitive impairment, neurological diseases, psychiatric diseases, rehabilitation of cognitive impairment

## 1. Introduction

The growing prevalence of cognitive impairment is predominantly attributed to an aging population, further compounded by rising psychological stress. This escalating challenge profoundly undermines individual quality of life and imposes substantial economic strains on families and society. Dementia, a leading cause of cognitive impairment, represents a critical global health challenge, with the number of affected individuals projected to reach 139 million by 2050 (1). Another major category of mental disorders associated with cognitive impairment is currently among the most economically burdensome diseases worldwide (2).

Cognition encompasses a wide range of intricate and advanced brain functions, such as perception, attention, memory, and thinking. It represents the human brain's capacity to extract, process, and retain information through thought, experience, and emotion. Any factor that disrupts the normal structure and function of the brain can lead to cognitive impairment. Common causes of cognitive impairment include chronic neurodegenerative diseases, stroke, traumatic brain injury (TBI), and mental

disorders (3,4).

Neurodegenerative diseases affecting memory mainly include Alzheimer's disease (AD), Parkinson's disease (PD) and so on. AD is the leading cause of dementia (5). The fifth edition of the Diagnostic and Statistical Manual of Mental Disorders of the American Psychiatric Association (DSM-5) classifies mild cognitive impairment (MCI) and dementia as "neurocognitive disorders", which are prevalent degenerative conditions affecting the central nervous system, primarily in older individuals but also in younger populations, particularly those with genetic predispositions. MCI represents an intermediate stage between normal cognition and dementia, characterized by largely preserved functional ability (6,7). Dementia is typically diagnosed when cognitive impairment significantly impairs social or occupational functioning. Mental disorders such as schizophrenia (SCZ), depression, and autism spectrum disorder (ASD), often influenced by genetic factors, are also among the major contributors to cognitive impairment.

However, the diagnosis of cognitive impairment is highly complex. In clinical practice, the diagnosis of

various subtypes of cognitive impairment relies primarily on clinical manifestations and auxiliary examinations. Auxiliary examinations encompass imaging studies, laboratory tests, and other assessments. The clinical manifestations mainly depend on the judgment of the doctor. During cognitive function assessments, clinicians initially conduct a subjective evaluation and closely monitor changes in patients' daily lives. Patients or their family members may report symptoms such as memory loss and cognitive decline. If patients neglect or withhold relevant information, doctors should actively inquire and observe for signs of cognitive decline during communication, such as forgetting important items like keys, appointments, or medication. Patients may also report changes in mood and behavior, including anxiety, depression, or apathy. However, it is crucial to note that a certain degree of cognitive slowing is a typical feature of normal aging (8). Distinguishing whether a patient's cognitive decline holds diagnostic significance poses a challenge for general clinicians.

Objective assessment is a crucial component in diagnosing cognitive impairment. Two commonly used screening scales in clinical practice are the Mini-Mental State Examination (MMSE) and the Montreal Cognitive Assessment (MoCA). While these evaluation methods are simple to administer, they can be influenced by subjective factors such as region, language proficiency, and education level of the subjects. Accurate interpretation often requires experienced clinicians. To overcome these limitations, additional auxiliary examinations are frequently employed in the diagnostic process, including functional magnetic resonance imaging (fMRI), electroencephalograms (EEG), and positron emission tomography (PET). But there are still dilemmas in the use of these research tools. EEG has low spatial resolution and poses challenges in source tracing analysis (9). The equipment for fMRI is expensive and bulky (10), requiring participants to be completely immobilized in a closed and noisy environment during the scanning process which hinders the examination of brain function during task performance (11). PET is invasive as it requires the use of radioisotopes and involves ionizing radiation exposure effects (11,12). Therefore, the development of new assessment tools for cognitive impairment research is crucial.

Functional near-infrared spectroscopy (fNIRS), is an emerging optical imaging technology that has gained attention in recent years. The myriad advantages it offers in monitoring brain function have piqued the interest of researchers, despite its current nascent stage of development (13). fNIRS provides valuable information with high temporal and spatial resolution for localizing brain function during cognitive task performance. This capability enables stereotyping and localization diagnosis of brain function, introducing a new dimension to brain function detection. Furthermore, fNIRS is highly compatible with other techniques, making it a

valuable complement to existing detection methods. The integration of multi-dimensional cognitive function evaluation holds the potential to enhance the accuracy and sensitivity of cognitive impairment.

Based on the aforementioned reasons, this review provides a comprehensive summary of the principles, applications, and historical evolution of fNIRS technology. It focuses on the extensive use of fNIRS in the domain of cognitive impairment related to neurological and psychiatric diseases. The objective is to offer a comprehensive overview of the current application status and future prospects of fNIRS in the field of cognitive impairment.

A systematic search of the PubMed database was conducted using the terms "(functional near-infrared spectroscopy OR fNIRS) AND (Cognitive impairment OR Cognitive disorder OR Cognitive decline OR Cognitive dysfunction)", initially identifying 826 articles. To refine the selection, filters were applied for article type, publication period, and language, narrowing the pool to 126 studies. The retrieved records were then imported into a citation management software for further screening and removal of duplicates. Inclusion criteria: Eligible studies encompassed Clinical Studies, Clinical Trials, Comparative Studies, Evaluation Studies, Observational Studies, Randomized Controlled Trials, and Validation Studies. Articles published between 2005 and 2024 were considered, ensuring coverage of nearly two decades of research in the field. Exclusion criteria: Studies were excluded if they were written in non-English languages or if fNIRS was not employed to measure brain activation during cognitive tasks.

## 2. The rationale for fNIRS

Spectroscopy theory serves as one of fNIRS' fundamental theoretical foundations. The two major chromophores in biological tissues are oxyhemoglobin (HbO<sub>2</sub>) and deoxyhemoglobin (HbR). These proteins exhibit different light absorption characteristics for near-infrared light, with absorption varying according to wavelength (Figure 1A). HbR absorbs more strongly below 790 nm, while HbO<sub>2</sub> absorbs more strongly above 790 nm (14). During fNIRS measurements, near-infrared light of different wavelengths is emitted by the light source and passes through the layers of cranial structures to reach the neuronal tissue. Within the tissue, light undergoes absorption and scattering. The absorption and scattering processes adhere to the Beer-Lambert law, enabling the noninvasive quantification of cortical HbO<sub>2</sub> and HbR concentrations through a modified Beer-Lambert law (15). These concentration changes can be used as surrogate markers of cerebral blood flow (CBF), thus providing a new means to study brain function (12).

Another crucial principle underlying fNIRS stems from neurovascular coupling (NC) (Figure 1B). It

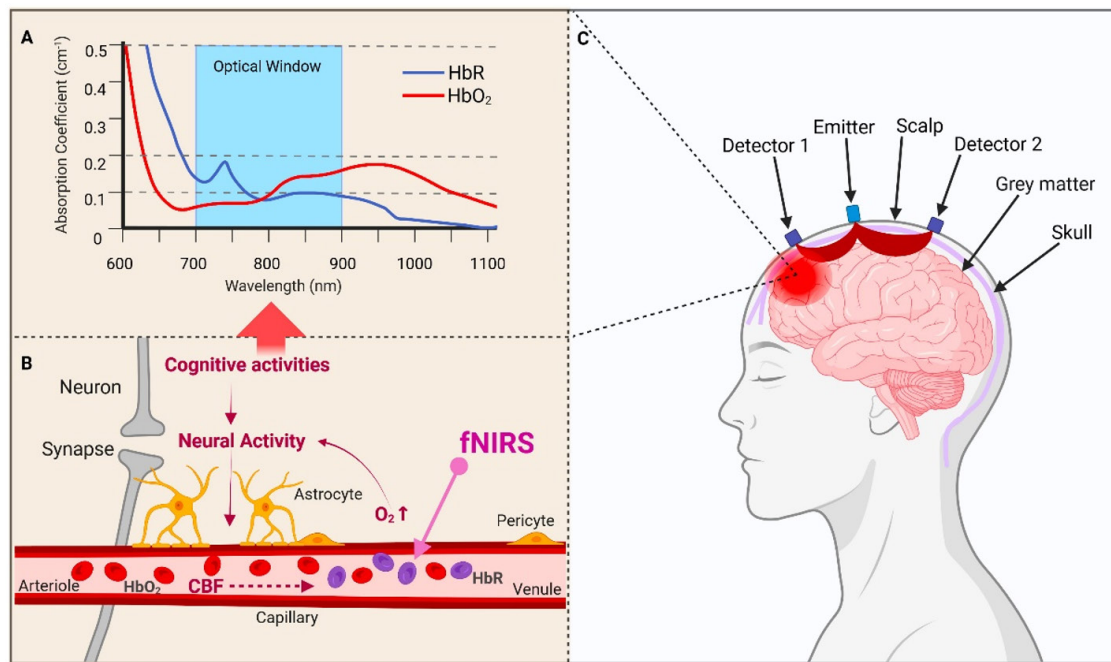


**Figure 1. The basic principles of fNIRS.** The basic principles of fNIRS including the absorption coefficient of oxygenated and deoxygenated hemoglobin at different wavelengths (A), the mechanism of neurovascular coupling (B), and the propagation path of near-infrared light (C). (A): it shows that oxygenated hemoglobin (HbO<sub>2</sub>) and deoxygenated hemoglobin (HbR) can be absorbed simultaneously in the near infrared wavelength range of 700-900 nm. (B): when cognitive activity occurs, cerebral blood flow (CBF) flows from arterioles to venules, local CBF increases, HbR decreases (shown in purple blood cells), HbO<sub>2</sub> increases (shown in red blood cells), and more O<sub>2</sub> is produced to supply neuronal activity. Thus, fNIRS can indirectly reflect the neuronal activity by measuring the changes of HbO<sub>2</sub> and HbR. (C): illustration of the path (shown in red banana shape) followed by the near-infrared photons from the light source through the different layers of the head to the detector.

involves the intricate connections between neural activity, CBF, and blood oxygen levels. These connections involve neurons, glial cells, neurotransmitters, and chemical molecules within the brain microenvironment. Increased neuronal activity leads to an elevation in regional CBF, meeting the higher metabolic demands of the brain while simultaneously triggering an increase in oxygen delivery (16). Furthermore, NC involves a process wherein heightened brain activity during affective or cognitive tasks corresponds with increased blood flow and oxygen consumption (17). Neuronal activity relies on oxygen supplied through blood metabolism to sustain its functionality. Consequently, local changes in cerebral hemodynamics occur during cognitive processes, leading to enhanced blood flow towards activated brain regions, which is reflected by an increase in HbO<sub>2</sub> concentration and a decrease in HbR concentration (15).

Based on the aforementioned theory, fNIRS is a non-invasive and safe technique that utilizes near-infrared light to target specific brain regions on the surface of the subject's head. This light, with a wavelength range of 700-900 nm, can penetrate the skull and reach the cerebral cortex, which is approximately 20-30 mm deep in the brain, after undergoing reflection, scattering, and absorption by the tissue. The emitted light then exits the scalp in a "banana-shaped" path and is captured by a nearby detector (Figure 1C) (11). fNIRS enables the assessment of relative concentration variations of two

hemoglobin species within the cerebral cortex through the detection of light absorption at distinct wavelengths. This approach provides insights into CBF alterations, facilitating the monitoring of local brain tissue metabolism. Consequently, it allows for an understanding of neural activity in the brain during cognitive tasks.

### 3. History of fNIRS development and application in the field of cognition

The development and application of fNIRS in the field of cognition can be traced back to the late 1970s when Jobsis first reported the use of near-infrared light to noninvasively monitor changes in cortical tissue oxygenation in cats (18). In 1993, Hoshi and colleagues used fNIRS to study cognitive function and found that HbO<sub>2</sub> concentration increased and HbR concentration decreased in the prefrontal cortex (PFC) of subjects during task performance (19). And they first recorded PET and fNIRS data simultaneously in 1994 (20).

The ability of fNIRS to monitor oxygenation levels led to its rapid application in various diseases, including mental disorders (21), stroke (22), PD (23), multiple sclerosis (MS) (24), and so on. In 1996, Kleinschmidt performed the first simultaneous fMRI and fNIRS to record human brain activation (25). In 1997, Fallgatter published the first article in his series of fNIRS studies, demonstrating a loss of hemispheric functional asymmetry in Alzheimer's

dementia (26). In 1998, the first commercial single-channel continuous wave imaging system was used in neonates, and an increase in HbO<sub>2</sub> was found in the visual cortex of awake infants induced by visual stimuli (27). Sakatani *et al.* used fNIRS to measure changes in HbO<sub>2</sub> and HbR in the frontal lobes of Parkinson's patients during electrical stimulation. They found that these changes resembled those observed during cognitive tasks, indicating the involvement of a complex neuronal circuit in the frontal lobe (23). In 2004, Macket *et al.* recorded the first simultaneous magnetoencephalogram (MEG) and fNIRS data (28). fNIRS has been increasingly utilized to investigate a wide range of cognitive domains, including executive function, attention, memory, language, cognition, and decision-making. Numerous studies have employed fNIRS to elucidate the neural mechanisms underlying infant brain development and cognitive maturation (29-31). With its high ecological validity, fNIRS enables the observation of brain activity during naturalistic settings and realistic social interactions. Moreover, fNIRS has been applied to studying cognitive processes in diverse real-world scenarios (32,33). Looking ahead, this technique holds promise for applications in everyday life, providing insights into the brain activity patterns of healthy adults during dynamic, real-world tasks and contributing to a deeper understanding of human behavior.

With the deepening of research, the equipment for fNIRS is being gradually upgraded. In 1989, the first commercial single-channel fNIRS system was introduced (34). In 1998, the first 10-channel fNIRS system was first used in the clinic (35). Initially, before 2010, the focus was primarily on increasing the number of channels, transitioning from single-channel or multiple measurements to multi-channel systems for a single measurement. Presently, more advanced high-density systems have been developed to accurately measure the blood flow in the cerebral cortex over a wider range. To enhance the applicability of fNIRS in various experimental environments and fields, efforts have been made to free the equipment from complex fiber optic cables. In 2009, a battery-powered wireless 22-channel system for adult PFC measurement appeared (36). Nowadays, multi-channel, wireless portable wearable devices have been used in many fNIRS studies, and fNIRS has made important progress in understanding brain activity, which is one of the potential advantages of fNIRS over other neuroimaging modalities. Advancements in hardware have led to the development of new high-density fNIRS systems, enabling comprehensive whole-brain measurements. Future efforts in fNIRS design are likely to focus on further enhancing the temporal and spatial resolution of the technology, as well as improving its overall accuracy. (Figure 2).

#### 4. Application of fNIRS in the cognitive domain

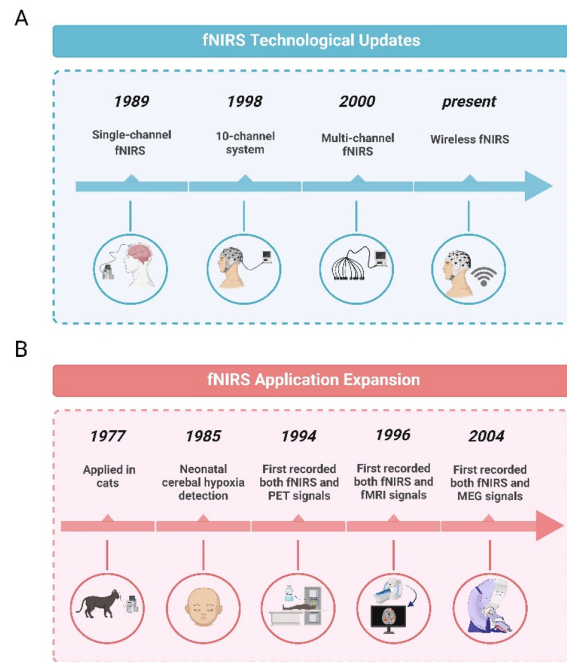


**Figure 2. The historical development of fNIRS.** Illustration of technology updates (A) and application expansion (B) of fNIRS at different points in time.

In recent years, brain cognitive function has remained a focal point of research in neuroimaging and electrophysiology. The diagnosis of cognitive impairment necessitates a combination of subjective assessment and objective evidence. Commonly utilized imaging modalities in clinical practice include fMRI, EEG, and PET. Meanwhile, fNIRS has undergone significant advancements, evolving from single-channel to multi-channel systems and from single-region to whole-brain imaging. This progress has overcome previous limitations in studying brain regions associated with cognitive function, paving the way for broader clinical applications. fNIRS offers several advantages over other imaging techniques when applied in the cognitive domain.

Firstly, fNIRS is currently the only hemodynamic neuroimaging technology capable of directly monitoring changes in the concentration of both HbO<sub>2</sub> and HbR (37). In contrast, the blood oxygen level dependent (BOLD) responses measured by fMRI are based on the proportion of HbR and do not provide information on hemoglobin concentration alone (14). The richer information provided by fNIRS allows for a more intuitive reflection of cortical activity and facilitates the use of differential analysis techniques, making it well-suited for real-time monitoring of temporal and spatial changes in cerebral blood oxygenation during cognitive tasks. Some researchers have even suggested that HbO<sub>2</sub> may be a more reliable indicator of cortical activation than HbR (38).

Secondly, fNIRS is able to detect changes in the cerebral hemodynamics of participants during task

execution and is applicable to all possible participant populations, from newborns to the elderly, with fewer restrictions on participant behavior. Additionally, fNIRS is portable and easy to wear, allowing for studies involving freely moving subjects without being constrained by the experimental environment. This makes fNIRS particularly suitable for research on cognitive tasks performed in naturalistic settings by individuals of different age groups (39).

Thirdly, compared with EEG, fNIRS offers a higher spatial resolution, which can locate the brain response to specific cortical areas (12). Compared with fMRI, fNIRS provides a higher temporal resolution, enabling better differentiation of signal contamination caused by physiological system signals and motion artifacts. Moreover, fNIRS is a non-ionizing technique, making it safer for human use compared to PET (9).

Finally, fNIRS demonstrates compatibility with other electrical and magnetic devices (40). fNIRS can be used simultaneously with fMRI, EEG, PET (41) to complement each other achieve optimized imaging analysis. Studies have reported that combining fNIRS with another neuroimaging technique, such as EEG or fMRI, yields more efficient detection results than using either method alone (42). Additionally, fNIRS can be used to further investigate the mechanisms of neural stimulation techniques, including transcranial direct current stimulation (43). Apart from these unique advantages, fNIRS also possesses universal benefits such as non-invasiveness, cost-effectiveness, portability, and noise-free operation. Table 1 provides a

comparison between fNIRS and commonly used imaging examinations in the cognitive field (15,44,45).

### 5. Combined application of fNIRS and other imaging techniques in the cognitive domain

At present, numerous studies highlight the potential benefits of integrating fNIRS and other imaging techniques, allowing researchers to investigate brain function from multiple perspectives and obtain a more comprehensive understanding of neural processes.

The combination of EEG and fNIRS offers advantages in terms of temporal and spatial resolution. EEG provides high temporal resolution, capturing the fast dynamics of neuronal electrical activity, while fNIRS provides better spatial resolution, allowing for the localization of cortical activation. Moreover, EEG and fNIRS measure different aspects of brain activity, with EEG reflecting neuronal electrical activity and fNIRS capturing metabolic responses. This built-in validation of identified brain activity enhances the reliability of the results obtained from these two modalities (46). The complementary nature of the measurements obtained from EEG and fNIRS can provide a more comprehensive understanding of brain activity and function, offering a unique neural monitoring platform to investigate the NC mechanism (47).

A study conducted by Cicalese *et al.* (48) examined the classification of subjects based on the degree of dementia using an EEG-fNIRS hybrid model. The results showed that when EEG and fNIRS were used

**Table 1. The comparison of fNIRS with other neuroimaging techniques**

| Technology | Advantages  | Disadvantages  | Indications  | Contraindications  |
|------------|---|--|--|--|
| fNIRS      | <ol style="list-style-type: none"> <li>1. Good temporal resolution</li> <li>2. Good spatial resolution</li> <li>3. Insensitive to motion artifacts</li> <li>4. Good compatibility</li> <li>5. Non-invasive</li> <li>6. Portable and cost-effective</li> </ol> | <ol style="list-style-type: none"> <li>1. Restricted to cortical measurements</li> </ol>   | <ol style="list-style-type: none"> <li>1. Safe for all age groups</li> <li>2. Cognitive and behavioral studies</li> <li>3. Real-time brain monitoring</li> </ol> | <ol style="list-style-type: none"> <li>1. Care with severe scalp injuries</li> </ol>   |
| fMRI       | <ol style="list-style-type: none"> <li>1. Excellent spatial resolution</li> <li>2. Whole-brain imaging</li> <li>3. Non-invasive</li> </ol>  | <ol style="list-style-type: none"> <li>1. Limited temporal resolution</li> <li>2. Sensitive to movement artifacts</li> <li>3. Expensive and non-portable</li> <li>4. Limited compatibility</li> <li>5. Relatively noisy</li> </ol> | <ol style="list-style-type: none"> <li>1. Functional brain mapping</li> <li>2. Neurovascular coupling studies</li> </ol>   | <ol style="list-style-type: none"> <li>1. Claustrophobia</li> <li>2. Metal implants or devices</li> <li>3. Severe kidney dysfunction (due to contrast agents)</li> </ol> |
| EEG        | <ol style="list-style-type: none"> <li>1. Excellent temporal resolution</li> <li>2. Non-invasive</li> <li>3. Portable and cost-effective</li> </ol>   | <ol style="list-style-type: none"> <li>1. Limited spatial resolution</li> <li>2. Prone to noise from muscle activity</li> <li>3. Limited compatibility</li> <li>4. Requires conductive scalp gel</li> </ol>                        | <ol style="list-style-type: none"> <li>1. Rapid detection of brain activity</li> </ol>   | <ol style="list-style-type: none"> <li>1. Severe scalp injuries</li> <li>2. Hypersensitivity to conductive gel</li> </ol>  |
| PET        | <ol style="list-style-type: none"> <li>1. Good spatial resolution</li> <li>2. High sensitivity for metabolic activity</li> <li>3. Target specific molecules with tracers</li> </ol>   | <ol style="list-style-type: none"> <li>1. Limited temporal resolution</li> <li>2. Invasive</li> <li>3. Limited compatibility</li> <li>4. Expensive and non-portable</li> </ol>   | <ol style="list-style-type: none"> <li>1. Metabolic brain function studies</li> </ol>  | <ol style="list-style-type: none"> <li>1. Pregnancy and children</li> <li>2. Severe kidney dysfunction</li> <li>3. Allergies to radiotracers</li> </ol>                  |

*Abbreviation:* fNIRS: functional near-infrared spectroscopy. fMRI: functional magnetic resonance imaging. EEG: electroencephalograms. PET: positron emission tomography.

independently, the accuracy was 65.52% and 58.62%, respectively. However, when the EEG-fNIRS hybrid model was employed, the accuracy increased to 79.31%, demonstrating the enhanced performance achieved by integrating the complementary characteristics of EEG and fNIRS. These findings suggest that the hybrid EEG-fNIRS system holds promise as a tool to enhance the diagnostic and evaluation processes for diseases such as AD. Cognitive deficits in AD have been linked to the disruption of brain networks (49). Li (50) used the fNIRS-EEG method to investigate the dynamic and local changes in AD-related brain networks, demonstrating the feasibility of this technique. This approach allows for the examination of both hemodynamic and electrical aspects of brain activity, providing valuable insights into the pathophysiology of AD.

The combination of fMRI and fNIRS is one of the most commonly used multimodal imaging approaches. This is because fMRI equipment is generally not suitable for conducting experiments with participants in sitting or standing positions (51). On the other hand, fNIRS is applicable to a wide range of experimental conditions and can accommodate participants in various positions. Additionally, while fNIRS provides limited whole-brain coverage, the high spatial resolution of fMRI compensates for this limitation, resulting in a complementary combination of the two techniques.

Some researchers have used fMRI and fNIRS to verify the feasibility of combining multiple techniques. Pereira (52) employed the fMRI-fNIRS multimodal approach to examine the possibility of converting spatial neuronal information from fMRI motion patterns into fNIRS settings of HbO<sub>2</sub> and HbR concentrations. This innovative technique aimed to enhance the understanding of motor function by revealing detailed information about neural activity using fNIRS measurements.

## 6. Application of fNIRS in the cognitive impairment related to neurological and psychiatric diseases

### 6.1. Cognitive impairment associated with neurological diseases

#### 6.1.1. Alzheimer's disease

AD is the most prevalent neurodegenerative disease globally and currently lacks a cure. Early pharmacological intervention and regular physical exercise can decelerate disease progression and enhance patients' quality of life (53). MCI acts as a transitional stage between normal aging and AD. It is important to note that not all individuals with MCI will progress to AD (54). MCI can serve as an early indicator of AD, and early diagnosis is crucial for timely intervention to delay the onset of dementia (55).

fNIRS has shown promise in this area and provided insights into the functional alterations in the brain section

associated with cognitive impairment. Ates suggests that the neural network behind emotion enhanced memory may involve interactions between frontal and subcortical regions. So, Ates and his colleagues used fNIRS to measure cortical activity during an emotional n-back task in 20 AD patients and 20 healthy older adults of similar age and sex. They found that only in positive emotional words, AD patients have higher HbO<sub>2</sub> concentrations than healthy controls, and the cortical activity of AD patients with positive emotion words was hemispheric and left side activity was higher (56). Katzorke *et al.* selected 110 subjects from a cohort of 604 participants, half each with MCI patients and half each with healthy controls. Using fNIRS to measure hemodynamic responses during a verbal fluency task (VFT), the investigators found decreased hemodynamic responses in the inferior frontotemporal cortex in the MCI group. The hemodynamic response pattern during VFT can be used as one of the bases for early detection of AD (57). These studies show that AD or MCI patients with cognitive decline have reduced cortical oxygenation during cognitive tasks, which is consistent with the previous argument (Figure 3).

Studies have shown that visuospatial deficits are one of the first symptoms of AD and are associated with lower activation of the parietal epithelial cortex as assessed by functional imaging (58). Zeller *et al.* (59) utilized fNIRS to investigate the activation of parietal regions in patients with AD and healthy subjects during visuospatial tasks. Interestingly, they found that although healthy subjects exhibited significant parietal activation, there was no difference in visuospatial performance between the two groups. In a study by Haberstumpf *et al.* long-term participation in the Vogel Study was analyzed in healthy older adults performing a clock-hand-angle discrimination task (ADT) during visuospatial processing. Using fNIRS, significant activation in the parietal cortex was observed during visuospatial tasks, and this activation showed a significant increase in neuronal brain activity with increasing task difficulty (60). Building upon these findings, Haberstumpf *et al.* conducted a similar study on individuals with MCI (61) the activation of the parietal cortex, observed in healthy subjects, was significantly reduced in MCI patients. These results suggest that deficits in visuospatial processing in the parietal cortex may serve as a risk factor for the progression of MCI or AD. Therefore, measuring parietal cortex activation using fNIRS could potentially be employed as a reliable marker for the early detection and diagnosis of AD.

Cognitive function requires a high level of functional interaction between network region. Functional connectivity, which refers to the synchronized activity between different brain regions, is thought to play a crucial role in cognitive processes. Research suggests that changes in functional connectivity may precede alterations in the activation of specific brain regions

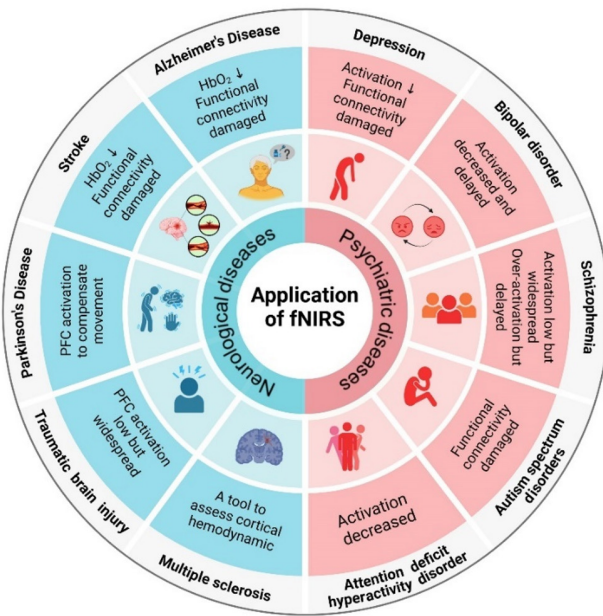


**Figure 3. Application of fNIRS in cognitive impairment associated with central nervous system diseases.** Illustration of application of fNIRS in the cognitive impairment related to neurological and psychiatric diseases. Left: neurological diseases (shown in blue), including Alzheimer's disease (AD), stroke, Parkinson's disease (PD), traumatic brain injury (TBI) and multiple sclerosis (MS). Using fNIRS, decreased HbO<sub>2</sub> and impaired brain functional connectivity can be detected in some regions of the cerebral cortex in AD and stroke patients, activation of the non-motor prefrontal cortex (PFC) can be observed in PD patients to compensate for motor function, and lower but more extensive activation of the PFC can be detected in TBI patients. In patients with MS, fNIRS can be used as a tool to assess cortical hemodynamics. Right: psychiatric diseases (shown in pink), including depression, bipolar disorder (BD), schizophrenia (SCZ), autism spectrum disorders (ASD) and attention deficit hyperactivity disorder (ADHD). Using fNIRS, decreased cortical activation and impaired brain functional connectivity can be detected in patients with depression, decreased and delayed cortical activation can be observed in BD patients, reduced but more widespread cortical activation in SCZ patients, or delayed over-activation, can be detected, damaged brain functional connectivity can be observed in ASD patients, and decreased cortical activation can be detected in ADHD patients.

(62). Tang and Chan (54) used fNIRS to analyze the functional connectivity of mild AD, MCI, and normal aging and found that the brain network of normal aging individuals exhibited higher regularity compared to AD patients, indicating that fNIRS can be a feasible tool for distinguishing AD from normal aging based on functional connectivity patterns. Nguyen *et al.* (63) used fNIRS to detect brain functional connectivity in cognitively normal older adults and patients with MCI, and found that in the VFT task, the inter-hemispheric connectivity in the healthy control group was significantly higher than the intra-hemispheric connectivity. It can be used as an effective indicator to distinguish cognitively normal elderly from MCI patients. In addition, left hemisphere connectivity was significantly reduced in MCI patients during the VFT task, and these findings demonstrate the potential of fNIRS to study brain functional connectivity in neurodegenerative diseases. Chan *et al.* (64) also

proposed that brain functional connectivity analysis based on fNIRS can be used as an effective set of features for the diagnosis of AD, and AD patients have loss of brain functional connectivity and non-significant laterality. Moreover, connectivity disruption and frontal lobe oxygenation changes are more severe in AD patients than in patients with mild cognitive impairment (Figure 3) (11).

### 6.1.2. Stroke

Cognitive impairment is a common consequence of stroke, and fNIRS has emerged as a valuable tool for assessing brain activity and monitoring changes during cognitive tasks in patients with post-stroke cognitive impairment (PSCI) (65,66). Kong *et al.* (65) specifically focused on evaluating the functional connectivity of relevant cortex during memory tasks using fNIRS. They found that a decreased level of functional connectivity may serve as a marker of PSCI (Figure 3). Zou *et al.* employed fNIRS to study the differences in functional connectivity of brain networks between patients with PSCI and healthy controls. They discovered that the functional connectivity of brain networks in PSCI patients was significantly lower compared to healthy controls. However, there was no significant difference in functional connectivity between PSCI patients and stroke patients without PSCI (67).

fNIRS is frequently used to assess the effectiveness of cognitive rehabilitation in stroke patients. Monitoring changes in brain activity during rehabilitation training using fNIRS is crucial for understanding the compensatory changes that underlie functional recovery after brain injury, ultimately improving the outcomes of rehabilitation interventions (68). Yang *et al.* (69) used fNIRS to evaluate the effect of transcranial direct current stimulation (tDCS) on the rehabilitation of cognitive impairment in stroke patients. After tDCS treatment, fNIRS measured increased activation of the left superior temporal cortex and improved functional connectivity between the cerebral hemispheres in stroke patients. Huo *et al.* (70) used fNIRS to evaluate the changes in effective connectivity within the cortical network induced by median nerve electrical stimulation (MNES) in stroke patients, and found that the effective connectivity between bilateral prefrontal PFC and left occipital lobe (LOL) in stroke patients in the MNES state was significantly higher than that in the resting state. Zhang *et al.* (71) used fNIRS as one of the indicators to evaluate the effect of intermittent theta burst stimulation (iTBS) combined with cognitive training on the treatment of PSCI. The left dorsolateral prefrontal cortex (DLPFC), prefrontal polar cortex, and left Broca's region were activated. These studies collectively suggest that fNIRS can serve as an effective tool for monitoring and evaluating brain activity in stroke patients undergoing cognitive rehabilitation. By providing objective measures of brain function, fNIRS can assist clinicians in

formulating and optimizing individualized rehabilitation treatment programs, as well as accurately assessing rehabilitation efficacy and prognosis.

### 6.1.3. Parkinson's Disease

PD is a neurodegenerative disorder characterized by motor symptoms and various non-motor symptoms, including cognitive decline, particularly in executive function (72). Stuart *et al.* used fNIRS to measure PFC activity during tasks to distinguish between PD patients and healthy individuals (73). It has been shown that executive dysfunction leads to freezing of gait (FOG), which is a common episodic disorder in PD patients (74). Previous studies have shown that PD patients often compensate for impaired motor function by activating the PFC (75). Currently, in PD, fNIRS is mainly used to investigate changes in cortical activity during gait and postural stability tasks (76). Maidan *et al.* (77) used fNIRS to measure HbO<sub>2</sub> levels in Brodmann area 10 before and during FOG revealing a direct association between FOG and dysfunction in the frontal lobe. However, there are exceptions to the compensatory activation pattern. Bonilauri *et al.* (78) used fNIRS to evaluate PD at different stages. They divided 39 PD patients into early PD and middle PD groups based on the Hoehn-Yahr (HY) scale and employed a whole-head fNIRS system with 102 measurement channels to monitor brain activity. The group-level activation map indicated that the middle PD group exhibited higher activation in the frontal regions compared to the early PD group, while the opposite pattern was observed in the motor and occipital regions. This suggests that the PFC in non-motor regions may provide a compensatory mechanism for PD-related movement disorders (Figure 3).

### 6.1.4. Traumatic brain injury

TBI can result in long-term neurobehavioral and cognitive impairment (79). Executive function deficits, which involve the PFC, are commonly observed in patients with neurocognitive impairment following TBI (80). Chang *et al.* recruited 37 patients with neurocognitive impairment after TBI and 60 healthy controls to measure HbO<sub>2</sub> in the PFC region during the Stroop and n-back tasks using a 22-channel fNIRS device. The results revealed that TBI patients exhibited lower but more widespread brain activation during the 2-back and Stroop color word congruency tasks compared to healthy controls (Figure 3) (81). Plenger *et al.* used fNIRS to evaluate neural changes in TBI patients during the Stroop task. Compared with the healthy group, the patient group had a significant increase in HbO<sub>2</sub> in the bilateral frontal lobe and greater neural activity in the frontal lobe (82). These findings indicate the potential of fNIRS in identifying frontal inefficiency in TBI patients.

### 6.1.5. Multiple sclerosis

MS is a degenerative disease that affects the central nervous system, characterized by inflammation, demyelination, and axonal damage (83), and cognitive impairment and motor impairment are common in patients with MS (84). Stojanovic-Radic *et al.* (85) used fNIRS to examine differences in neural activation in the orbitofrontal brain regions during a working memory (WM) task between individuals with MS and healthy controls. The results demonstrated that the MS group exhibited elevated HbO<sub>2</sub> concentrations and increased brain activation in the left superior frontal gyrus at lower levels of task difficulty (1-back), but decreased activation at higher levels of task difficulty (2-back and 3-back) compared to healthy controls (Figure 3). This study was the first to utilize fNIRS to investigate brain activation during a cognitive task in individuals with MS.

The application of fNIRS in cognitive impairment in neurological diseases are reported in Table 2.

## 6.2. Cognitive impairment associated with Psychiatric diseases

Cognitive impairment is a common characteristic of various mental disorders, including depression. fNIRS has emerged as a valuable tool in psychiatric research, allowing for the measurement of cortical dysfunction during cognitive tasks. It has been utilized in several mental disorders such as SCZ, Major depressive disorder (MDD), and bipolar disorder (BD) The application of fNIRS in cognitive impairment in psychiatric diseases are summarized in Table 3.

### 6.2.1. Depression

Depression is often associated with cognitive impairment (86), and executive function, which relies on the PFC, is one aspect of cognition that is affected. The PFC is involved in various high-level cognitive functions, including executive function, WM, and language processing (87).

Kondo *et al.* (88) used fNIRS to assess changes in prefrontal and temporal lobe HbO<sub>2</sub> concentrations during pleasant and unpleasant image recall tasks in patients with MDD and healthy controls. It was found that HbO<sub>2</sub> in the bilateral frontal region of MDD group was significantly lower than that of the control group during the unpleasant state. Downey *et al.* (89) used fNIRS to measure frontal lobe hemodynamic responses during category VFT and WM n-back tasks in depressed patients and found that bilateral frontal lobe hemoglobin responses were lower. Liu (90) used fNIRS to monitor the concentration of HbO<sub>2</sub> in the brain of adolescents with depression and healthy controls. The study revealed that depressed adolescents exhibited significantly lower cortical activation of hemodynamic responses in the PFC

compared to healthy controls. The mean inter-channel connectivity strength was also found to be higher in the healthy control group than in the depression group. These findings suggest that adolescents with depression exhibit abnormal brain activation patterns and reduced task-related functional connectivity compared to their healthy counterparts. In Ishii's study, MDD patients showed significantly lower activation in PFC areas and inferior parietal areas, especially in the left, when performing a word-making task than controls (91). These studies suggest that the brains of depressed patients exhibit abnormal activation patterns compared to healthy controls, and fNIRS may be a useful tool for assessing psychophysiological indicators of depressed patients and distinguishing depressed patients from normal individuals (Figure 3).

### 6.2.2. Bipolar disorder

BD, characterized by the presence of both manic and depressive episodes, with depressive episodes being a typical symptom. Similar to depression, the PFC plays a significant role in the pathophysiology of BD. Kameyama (92) used fNIRS to compare changes in HbO<sub>2</sub> concentration in the frontal lobe during cognitive and motor tasks in BD, MDD, and healthy controls. The study found that individuals with BD exhibited delayed onset activation in the frontal lobe (Figure 3), while those with MDD showed reduced activation in the frontal lobe. These differences in frontal activation patterns suggest that fNIRS may be a reliable tool for differentiating between BD and MDD. Nishimura (93) compared prefrontal hemodynamic responses during cognitive tasks between the hypomanic and depressive states in individuals with BD. They used fNIRS to assess prefrontal function during VFT in hypomanic, depressed, and healthy control groups. The study revealed that VFT performance did not differ significantly between the hypomanic, depressive, and healthy control groups. However, the activation rate in the PFC was significantly lower in individuals with BD compared to the healthy control group (Figure 3). The left DLPFC exhibits significantly greater hemodynamic changes in individuals with BD during hypomanic episodes compared to those with depression. Furthermore, the severity of hypomanic symptoms was positively correlated with activation in the left DLPFC and frontopolar cortex in BD patients. Follow-up measurements in hypomanic patients showed decreased prefrontal activation after the resolution of hypomanic symptoms. These findings suggest that there are distinct differences in prefrontal hemodynamics corresponding to manic and depressive states in individuals with BD, and fNIRS may serve as a valuable tool for objectively assessing the state-dependent characteristics of prefrontal hemodynamics in BD.

### 6.2.3. Schizophrenia

Cognitive impairment is a core feature of SCZ and is often observed years before the onset of overt psychotic symptoms (94). Koike (95) used multi-channel fNIRS to measure hemodynamic changes during n-back WM tasks with different cognitive loads in patients with SCZ and healthy controls and found that the activation of prefrontal activity was reduced but more extensive in SCZ patients (Figure 3). Noda (96) used fNIRS to focus on the changes in HbO<sub>2</sub> levels in the prefrontal and temporal lobes in the late stage of the task and found an abnormal re-increase of HbO<sub>2</sub> levels. Kumar (97) used fNIRS to examine hemodynamic activity during WM tasks in SCZ. The results found delayed but compensatory hyperactivation in the right frontopolar cortex of the SCZ (Figure 3), which, the authors speculate, may underlie the WM deficit in the SCZ. According to the above studies, Hemodynamic changes in WM of patients with chronic SCZ detected using fNIRS may be a potential biomarker.

As a novel neurophysiological approach, fNIRS is increasingly being used in the study of SCZ and frontal lobe dysfunction. To date, several studies have employed fNIRS to assess hemodynamic changes in the frontal lobe in various contexts, demonstrating that distinct hemodynamic response patterns may serve as potential imaging biomarkers in individuals with SCZ and fNIRS may become an effective clinical tool for evaluating this population.

### 6.2.4. Autism spectrum disorder/ attention deficit hyperactivity disorder

ASD is characterized by impaired social communication accompanied by stereotyped behaviors and limited interests (DSM-5). Executive dysfunction is partly responsible for these symptoms (98). A special feature of fNIRS for this population is the ability to study neural development from an early age (99), leading to a better understanding of the neural mechanisms of ASD. Unlike fMRI, which requires a closed environment with loud noise and patient immobilization, fNIRS is quiet and portable, making it more suitable for individuals with ASD who may have difficulty tolerating the fMRI environment (100). However, some individuals with ASD may also resist wearing near-infrared caps, limiting the feasibility of traditional fNIRS approaches (101). Therefore, the development of remote and non-contact near-infrared systems is a future direction in this field. Chan *et al.* (102) used fNIRS to measure prefrontal hemodynamic data in individuals with ASD and typically developing (TD) individuals. The study revealed significantly lower functional connectivity in the PFC of individuals with ASD compared to TD individuals. Han *et al.* (103) used fNIRS to investigate the impact of WM load on functional connectivity in the PFC of individuals with ASD. The findings revealed that individuals with high-functioning ASD exhibited WM impairment that was accompanied by load-dependent changes in intra-

**Table 2. Summary of fNIRS applications on neurological diseases**

| Reference        | Research object   | Activation Task  | Brain Region                                    | Results  | Evidence   |
|------------------|---|--|---|--|--|
| Zeller (59)      | Mild AD: <i>n</i> = 13<br>HC: <i>n</i> = 13                       | Modified version of the BLOT (line orientation versus color naming)              | Parietal  | AD especially low increases in [oxy-Hb] during line orientation were found in the upper half of the probe set covering the superior-parietal cortex.                                 | AD showed significantly less increase in [oxy-Hb] in the superior-parietal cortex in the line orientation task than controls, but there was no difference in color naming. |
| Ateş (56)        | AD: <i>n</i> = 20<br>HC: <i>n</i> = 20                            | The n-back task (0-back, and 1-back WM task)                                     | Bilateral prefrontal                            | In the PEW condition, activity in Ch8 and Ch11 (left ventral PFC) was significantly higher in the AD compared to HC after FDR correction.  | AD had the higher [oxy-Hb] than the HC only in the PEW condition.  |
| Katzorke (57)    | MCI: <i>n</i> = 55<br>HC: <i>n</i> = 55                           | The letter VFT; the category VFT   | Bilateral frontotemporal                        | Both hemispheres of MCI showed decreased hemodynamic responses in the inferior frontotemporal region in category VFT compared to HC (HC: $-2.53 \pm 0.39$ ; MCI: $-1.08 \pm 0.39$ ). | MCI had a decreased hemodynamic response in the inferior frontotemporal cortex.  |
| Tang & Chan (54) | Mild AD: <i>n</i> = 18<br>MCI: <i>n</i> = 12<br>HC: <i>n</i> = 31 | The category VFT   | Prefrontal                                      | FC edge count decreased across groups (T2a: HC=307, MCI=193, AD=170; T2b: HC=49, MCI=30, AD=25). In AD, FC distribution became evenly spread across the left and right PFC.          | AD had loss of FC and insignificant laterality between left and right PFC.   |
| Nguyen (63)      | MCI: <i>n</i> = 42<br>HC: <i>n</i> = 42                           | 4 different paradigms: a resting state, an oddball task, a 1-back task and a VFT | Prefrontal                                      | During VFT, MCI inter1-4 hemispheric connectivity ([oxy-Hb]) was significantly lower than HC ( $p = 0.002$ , $0.003$ , $6E-5$ , $7E-4$ ).  | MCI reduced significantly left hemisphere connectivity on the VFT.   |
| Y. L. Chan (64)  | Mild AD: <i>n</i> = 16<br>HC: <i>n</i> = 26                       | The category VFT   | Prefrontal                                      | Mild AD showed significantly lower connectivity than HC using the proposed method ( $p < 0.05$ ), with no significant laterality detected ( $p > 0.05$ ).                            | AD had loss of connectivity and insignificant laterality.  |
| Haberstumpf (61) | MCI: <i>n</i> = 59<br>HC: <i>n</i> = 59                           | The clock-hand-angle discrimination task   | Parietal  | MCI showed reduced brain activity in the ROI compared to HC (MCI: Mean = $0.03$ , SD = $0.04$ ; HC: Mean = $0.05$ , SD = $0.05$ ).   | MCI showed significantly less increase in cortical activation and reduced brain activity and laterality compared to HC.  |
| Huo (70)         | Stroke: <i>n</i> = 23   | The resting state; the MNES state  | Bilateral PFC, motor cortex, and occipital lobe | Effective connectivity increased significantly (left PFC→LOL: $P = 0.048$ ; right PFC→LOL: $P = 0.002$ ).  | Stroke in the MNES state had significantly higher effective connectivity from left PFC and right PFC to LOL compared with the resting state.                               |
| C. Yang (69)     | Stroke: <i>n</i> = 22<br>HC: <i>n</i> = 14                        | The letter VFT   | Prefrontal                                      | Stroke had lower $\beta$ values than HC. FC between bilateral hemispheres in stroke increased after 14 tDCS sessions, notably between the 7th and 14th sessions.                     | The FC between the cerebral hemispheres and the cortical activation of stroke patients was lower than that of HC but increased after tDCS.                                 |

*Abbreviation:* AD: Alzheimer's disease. HC: healthy control. BLOT: Benton Line Orientation Task. [oxy-Hb]: oxygenated hemoglobin. WM: working memory. PEW: positive emotional words. FDR: false discovery rate. MCI: mild cognitive impairment. VFT: verbal fluency task. FC: functional connectivity. PFC: prefrontal cortex. ROI: region of interest. SD: standard deviation. MNES: Mini-Mental State Examination. LOL: left occipital lobe. tDCS: transcranial Direct Current Stimulation. PSCI: Post-stroke cognitive impairment. STR: patients without cognitive impairment after stroke. CDT: Clock drawing test. DST: Digit span test. CBT: Corsi Block-tapping test. RHD: patients with PSCI who have right hemisphere damage. CPT: continuous performance test. NPSCI: Non-PSCI. YA: young adults. OA: older adults. PD: Parkinson's Disease. CSRT: choice stepping reaction time task. iCSRT: inhibitory choice stepping reaction time. SST: a Stroop stepping test. SMA: supplementary motor areas. MD: mean difference. CI: confidence interval. TBI: traumatic brain injury. DLPFC: dorsolateral prefrontal cortex. VLPFC: ventrolateral prefrontal cortex. MS: multiple sclerosis.

**Table 2. Summary of fNIRS applications on neurological diseases (continued)**

| Reference      | Research object   | Activation Task   | Brain Region  | Results   | Evidence   |
|----------------|---|---|---|---|--|
| Kong (65)      | PSCI (Stroke):<br>n = 19<br>STR: n = 27<br>HC: n = 26   | The CDT, DST, and CBT   | Bilateral motor sense cortex and prefrontal lobe          | FC between motor sense and frontal lobe was the lowest in PSCI ( $P < 0.05$ ).  | PSCI showed decreased FC between bilateral motor sense cortex and between motor sense cortex and frontal lobe during CDT and CBT.  |
| X. Li (66)     | RHD (Stroke):<br>n = 16<br>HC: n = 32                   | The X version of CPT  | Prefrontal  | No significant [Oxy-Hb] activation in HC after ~35 s, while RHD showed multiple reactivations in bilateral PFCs with greater activation than HC, exceeding the first peak.            | RHD had neural compensation in both prefrontal lobes; but the rate of compensation was slower on the affected side.  |
| Zou (67)       | PSCI (Stroke):<br>n = 16<br>NPSCI: n = 16<br>HC: n = 16 | The resting-state   | Prefrontal, somatosensory, and motor cortices             | Interhemispheric FC: $p = 0.005$ , $p = 0.013$ , Bonferroni corrected.<br>Right hemisphere FC: $p = 0.008$ , Bonferroni corrected.  | PSCI exhibited significantly decreased interhemispheric FC and intra-right hemispheric FC compared with the HC.  |
| Stuart (73)    | PD: n = 24<br>YA: n = 25<br>OA: n = 19                  | 2 different motor tasks: a 2-min 360° turning-in-place task, a 2-min walking task | Prefrontal  | Significant differences during walking: overall PFC ( $p = 0.025$ ), left PFC ( $p = 0.012$ ), and early walking period (first 40s, $p = 0.007$ ).                                    | PD had higher PFC activation than YA and OA during walking and turning, with significant group differences for bilateral PFC activation, left PFC activation, and the early period (first 40s) of walking. |
| Sharon (75)    | PD: n = 34<br>OA: n = 26                                | Obstacle negotiation task   | Prefrontal  | PD exhibited a greater increase in PFC activation than OA across phases (interaction: group x PFC activation, $p < 0.001$ , Cohen's $d = 0.63$ ).                                     | PD showed greater increases in PFC activation during and after obstacle crossing compared to the OA.   |
| Pelicioni (76) | PD: n = 52<br>HC: n = 95                                | Three stepping tests (CSRT, iCSRT, and SST)                                       | Dorsolateral PFC, Broca's area, SMA, and premotor cortex  | DLPFC: [MD: -2.44, 95% CI: -4.32 to -0.55], $p = 0.012$ ; SMA: [MD: -2.25, 95% CI: -4.35 to -0.16], $p = 0.035$ ; Premotor cortex: [MD: -1.96, 95% CI: -3.85 to -0.07], $p = 0.042$ . | PD exhibited reduced DLPFC activity in the iCSRT and reduced SMA and premotor cortex activity in the SST.  |
| Plenger (82)   | TBI: n = 14<br>HC: n = 13                               | 2 Stroop task: dot color naming task, incongruent task                            | Bilateral frontal, temporal, and mid to inferior parietal | TBI demonstrated greater [oxy-Hb] increases from resting baseline in bilateral DLPFC and VLPFC compared to the HC.  | TBI had a significant increase in [oxy-Hb] in bilateral frontal regions during the color naming task.  |
| Chang (81)     | TBI: n = 30<br>HC: n = 55                               | The Stroop tasks; the n-back tasks  | Prefrontal  | Significant differences in [oxy-Hb] levels were observed. the Stroop task: Ch 3, 4, 8, 9, 11, 12, 14, 15, 21; the 2-back task: Ch 2, 3, 7, 9, 10, 11, 14, 15, 18, 21, 22.             | TBI exhibited lower but more widespread activation during the 2-back and Stroop color word consistency tasks.  |

*Abbreviation:* AD: Alzheimer's disease. HC: healthy control. BLOT: Benton Line Orientation Task. [oxy-Hb]: oxygenated hemoglobin. WM: working memory. PEW: positive emotional words. FDR: false discovery rate. MCI: mild cognitive impairment. VFT: verbal fluency task. FC: functional connectivity. PFC: prefrontal cortex. ROI: region of interest. SD: standard deviation. MNES: Mini-Mental State Examination. LOL: left occipital lobe. iDCS: transcranial Direct Current Stimulation. PSCI: Post-stroke cognitive impairment. STR: patients without cognitive impairment after stroke. CDT: Clock drawing test. DST: Digit span test. CBT: Corsi Block-tapping test. RHD: patients with PSCI who have right hemisphere damage. CPT: continuous performance test. NPSCI: Non-PSCI. YA: young adults. OA: older adults. PD: Parkinson's Disease. CSRT: choice stepping reaction time task. iCSRT: inhibitory choice stepping reaction time. SST: a Stroop stepping test. SMA: supplementary motor areas. MD: mean difference. CI: confidence interval. TBI: traumatic brain injury. DLPFC: dorsolateral prefrontal cortex. VLPFC: ventrolateral prefrontal cortex. MS: multiple sclerosis.

**Table 2. Summary of fNIRS applications on neurological diseases (continued)**

| Reference      | Research object          | Activation Task    | Brain Region | Results  | Evidence  |
|----------------|--------------------------|--------------------|--------------|--|---|
| Stojanovi (85) | MS: n = 13<br>HC: n = 12 | The n-back WM task | Prefrontal   | MS showed increased [oxy-Hb] in the left superior frontal gyrus from 0-back to 1-back, followed by a decrease from 1-back to higher loads. | MS showed increased brain activation during the lower difficulty task and decreased brain activation during the higher difficulty tasks compared with the HC. |

*Abbreviation:* AD: Alzheimer's disease. HC: healthy control. BLOT: Benton Line Orientation Task. [oxy-Hb]: oxygenated hemoglobin. WM: working memory. PEW: positive emotional words. FDR: false discovery rate. MCI: mild cognitive impairment. VFT: verbal fluency task. FC: functional connectivity. PFC: prefrontal cortex. ROI: region of interest. SD: standard deviation. MNES: Mini-Mental State Examination. LOL: left occipital lobe. tDCS: transcranial Direct Current Stimulation. PSCI: Post-stroke cognitive impairment. STR: patients without cognitive impairment after stroke. CDT: Clock drawing test. DST: Digit span test. CBT: Corsi Block-tapping test. RHD: patients with PSCI who have right hemisphere damage. CPT: continuous performance test. NPSCI: Non-PSCI. YA: young adults. OA: older adults. PD: Parkinson's Disease. CSRT: choice stepping reaction time task. iCSRT: inhibitory choice stepping reaction time. SST: a Stroop stepping test. SMA: supplementary motor areas. MD: mean difference. CI: confidence interval. TBI: traumatic brain injury. DLPFC: dorsolateral prefrontal cortex. VLPFC: ventrolateral prefrontal cortex. MS: multiple sclerosis.

right hemisphere connectivity. These results suggest that disruptions in functional neural connectivity during different cognitive processes may contribute to the poor performance on WM tasks observed in individuals with ASD (Figure 3).

Attention deficit hyperactivity disorder (ADHD) is one of the most common developmental disorders. ADHD is characterized by persistent inattention and hyperactive impulsive symptoms (104). Some researchers (105) have explored the method of distinguishing between children with ADHD and TD children based on fNIRS. Insufficient activation of the right prefrontal lobe as assessed by fNIRS was found to serve as a potentially valid biomarker for classifying children with ADHD at the individual level (Figure 3).

### 7. Application of fNIRS in the rehabilitation of cognitive impairment

The frequent occurrence of neurological and psychiatric diseases is often accompanied by a high incidence of cognitive impairment, which is one of the most significant functional disabilities affecting patients, alongside motor disorders, thereby impacting daily life. Consequently, early diagnosis and rehabilitation evaluation of cognitive impairment have become increasingly important. fNIRS, a robust tool for assessing brain self-regulation, plays a pivotal role in the early diagnosis and evaluation of cognitive impairment. Yoo *et al.* demonstrated the utility of fNIRS in distinguishing patients with MCI from healthy controls, successfully identifying differences in 15 individuals with MCI and 15 age-matched healthy participants. This study highlights the potential of fNIRS as a novel approach for the early diagnosis of AD (106). In clinical practice, symptom assessment for patients with depression and SCZ primarily relies on standardized scales. In a study by Vural Keleş and colleagues, participants were stratified into high-score and low-score groups based on their Beck Depression Inventory scores. The authors compared WM performance and hemodynamic changes between the groups. While no significant differences in WM performance were observed, fNIRS analysis revealed significantly greater activation in the right frontal lobe of the high-score group compared to the low-score group, providing novel insights into the neurophysiological underpinnings of depression (107). The diagnosis of ADHD is predominantly based on clinical observation and behavioral assessment scales, which can be subjective (108). To address this limitation, researchers have explored the use of fNIRS for ADHD diagnosis. Crippa *et al.* demonstrated significant differences in brain activation levels between children with ADHD and healthy controls, achieving a diagnostic accuracy exceeding 80% (109). Furthermore, the capacity of fNIRS to provide real-time monitoring of cerebral hemodynamics offers a valuable complement

**Table 3. Summary of fNIRS applications on Psychiatric diseases**

| Reference      | Research object                                | Activation Task  | Brain Region               | Results   | Evidence   |
|----------------|--|--|----------------------------|---|--|
| Kondo (88)     | MDD: $n = 25$<br>HC: $n = 25$                  | The image recall task with pleasant and unpleasant image | Forehead and temporal      | During the unpleasant image task, [Oxy-Hb] increased significantly in the bilateral frontal-temporal region of HC ( $q = 0.05$ , $\alpha\text{FDR} > 0.025$ ) but not in MDD.                               | MDD had a significantly lower [Oxy-Hb] than HC in the bilateral frontal region during the unpleasant condition.  |
| Downey (89)    | <b>Depression:</b><br>$n = 18$<br>HC: $n = 51$ | The category VFT; WM n-back task                         | Frontal                    | In the n-Back task, patients exhibited a significant [Oxy-Hb] decrease over time ( $F_{(6,85)} = 5.310$ , $p = 0.008$ ).  | Depressed patients had bilaterally lower frontal [Oxy-Hb] responses to the cognitive tasks compared with HC.   |
| Ishii (91)     | MDD: $n = 29$<br>HC: $n = 29$                  | The word production task                                 | Frontal to temporoparietal | Significantly smaller [Oxy-Hb] increase at 12 channels, especially in the left PFC (Ch 4, 6, 9).  | MDD showed significantly smaller activation than the controls in the PFC area and inferior parietal area during the word production task, especially in the left area.                             |
| Liu (90)       | MDD: $n = 72$<br>HC: $n = 74$                  | The letter VFT   | Prefrontal                 | Mean connectivity: MDD = 0.303, HC = 0.400; $t = -15.586$ , $p < 0.001$ .   | MDD had significantly less cortical activation in the hemodynamic responses of [Oxy-Hb] and lower mean channel-to-channel connectivity strength than HC.   |
| Kameyama (92)  | BD: $n = 17$<br>MDD: $n = 11$<br>HC: $n = 17$  | The letter VFT; The right-finger-tapping task            | Frontal and temporal       | BD and MDD exhibited reduced early task activation, but BD demonstrated significant late-task increases in four frontal channels.   | BD and MDD showed by preserved but delayed and reduced frontal lobe activation, respectively.  |
| Nishimura (93) | DBD: $n = 16$<br>HBD: $n = 11$<br>HC: $n = 12$ | The letter VFT   | Prefrontal                 | Significant group differences in 12 channels across bilateral DLPFC, VLPFC, and right anterior temporal cortex (FDR-corrected $p < 0.05$ ). HBD had larger [Oxy-Hb] changes than DBD in Ch 49 (left DLPFC). | BD exhibited significantly lower activation during the VFT than HC in the broader bilateral PFC. Hemodynamic changes in the left DLPFC in the HBD were significantly larger than those in the DBD. |
| Koike (95)     | SCZ: $n = 26$<br>HC: $n = 26$                  | The n-back task  | Prefrontal                 | SCZ showed significant activation during the 1-back task at 19 channels and during the 2-back task at 24 channels.  | SCZ showed reduced activation in the PFC but more extensive activation areas.  |
| Noda (96)      | SCZ: $n = 30$<br>HC: $n = 30$                  | The letter VFT   | Prefrontal/temporal        | In SCZ, [oxy-Hb] aberrant re-increase was observed immediately after the VFT period following a rapid decrease (visual inspection).   | SCZ in the VFT period after the end of [oxy - Hb] abnormal immediately after falling rapidly rise again.   |
| Kumar (97)     | SCZ: $n = 15$<br>HC: $n = 22$                  | The n-back task  | Frontal                    | The right PFC showed a trend of inverted U-shaped activation with higher levels during 1-back > 0-back ( $p = 0.09$ ) and 1-back > 2-back ( $p = 0.07$ ).   | A delayed but compensatory hyperactivation of right frontopolar cortex noted in SCZ may underlie the WM deficit.   |

*Abbreviation:* MDD: major depressive disorder. HC: healthy control. [oxy-Hb]: oxygenated hemoglobin. FDR: false discovery rate. VFT: verbal fluency task. PFC: prefrontal cortex. BD: bipolar disorder. DBD: depressed bipolar disorder. HBD: hypomanic bipolar disorder. DLPFC: dorsolateral prefrontal cortex. VLPFC: ventrolateral prefrontal cortex. SCZ: schizophrenia. WM: working memory. ADHD: attention deficit hyperactivity disorder. ASD: autism spectrum disorder. WCST: Wisconsin Card Sorting Task. FC: functional connectivity.

**Table 3. Summary of fNIRS applications on Psychiatric diseases (continued)**

| Reference           | Research object                          | Activation Task | Brain Region | Results   | Evidence  |
|---------------------|--|-----------------|--------------|---|---|
| Monden (105)        | ADHD: <i>n</i> = 30<br>HC: <i>n</i> = 30 | A go/no-go task | Prefrontal   | HC showed significant [oxy-Hb] increases at Ch 5 ( <i>d</i> = 0.741), Ch 6 ( <i>d</i> = 0.755), and Ch 10 ( <i>d</i> = 1.046), while ADHD showed no significant activation in these channels. | The right prefrontal hypoactivation assessed by fNIRS would serve as a potentially effective biomarker for classifying ADHD children at the individual level. |
| M. M. Y. Chan (102) | ASD: <i>n</i> = 29<br>HC: <i>n</i> = 26  | The WCST        | Prefrontal   | In ASD, FC was lower in the right lateral PFC during acquisition ( <i>p</i> = 0.005) and in the bilateral PFC during application (right: <i>p</i> = 0.006; left: <i>p</i> = 0.006).           | ASD individuals showed significantly lower prefrontal FC than typical developing individuals during WCST.   |
| Han (103)           | ASD: <i>n</i> = 22<br>HC: <i>n</i> = 24  | The n-back task | Prefrontal   | In ASD, a trend toward significance in right medial PFC connectivity was observed between 0-back and 1-back ( <i>p</i> = 0.030, uncorrected), with no significant effects on the left.        | A disruption of functional neural connections that support different cognitive processes may underlie poor performance in WM tasks in ASD.                    |

*Abbreviation:* MDD: major depressive disorder. HC: healthy control. [oxy-Hb]: oxygenated hemoglobin. FDR: false discovery rate. VFT: verbal fluency task. PFC: prefrontal cortex. BD: bipolar disorder. DBD: depressed bipolar disorder. HBD: hypomanic bipolar disorder. DLPFC: dorsolateral prefrontal cortex. VLPFC: ventrolateral prefrontal cortex. SCZ: schizophrenia. WM: working memory. ADHD: attention deficit hyperactivity disorder. ASD: autism spectrum disorder. WCST: Wisconsin Card Sorting Task. FC: functional connectivity.

to traditional scale-based assessments in rehabilitation contexts.

Beyond its diagnostic applications, fNIRS is also widely used in evaluating the efficacy of treatments for cognitive impairment, often in combination with various neural modulation techniques such as tDCS (69) and MNES (70). By enabling real-time and repeated dynamic monitoring of brain function, fNIRS allows for the observation of individual cortical responses, thereby facilitating the determination of optimal stimulation parameters, including intensity, frequency, and duration. This approach is crucial for evaluating rehabilitation outcomes and optimizing intervention strategies.

### 8. Conclusions

Cognition fundamentally relies on the normal functioning of the cerebral cortex. Any factors that disrupt the structure or function of the cerebral cortex can lead to cognitive impairment, with common causes including neurodegenerative and psychiatric diseases. Different forms of cognitive impairment are often interconnected, such that deficits in one domain may give rise to abnormalities in others, making the diagnosis and treatment of cognitive impairment particularly challenging (110). fNIRS, as a non-invasive and portable neuroimaging modality, is particularly well-suited for studying hemodynamic responses in the cortex during cognitive tasks in populations such as children, older adults, and individuals with unique needs. Additionally, fNIRS holds significant promise for advancing cognitive neuroscience in real-world contexts. Recent advancements in fNIRS research have begun to elucidate the complex relationships between cognitive processes—such as learning, memory, and language—and regional CBF and metabolism. Beyond its applications in cognitive research, fNIRS has shown potential in investigating brain functional changes induced by physical activity. The application of fNIRS in rehabilitation is particularly noteworthy for its ability to provide precise imaging-based evidence to guide intervention planning. A key to improving rehabilitation outcomes lies in the development of targeted clinical interventions based on brain function remodeling. In future clinical practice, the development of comprehensive brain function assessment frameworks based on fNIRS may allow real-time monitoring of cortical responses induced by rehabilitation, thereby providing insights into neural plasticity. Advanced analysis of fNIRS data could not only deepen our understanding of the mechanisms underlying this technology but also inform the design of personalized rehabilitation plans, offering valuable perspectives on treatment efficacy and prognosis.

However, its current limitation in penetrating deep brain structures, restricts its full potential. fNIRS relies on light penetration and reflection, typically reaching

a depth of 1.5 to 2cm. Consequently, it is unable to capture comprehensive structural images or anatomical information (12). Its primary utility lies in studying metabolic activities in superficial areas, rather than deep structures like the hippocampus or amygdala (11). To unlock the full capabilities of fNIRS, it is crucial to overcome this limitation and extend its application to explore deep brain function. Consequently, the integration of fNIRS with other imaging modalities is an inevitable trend in its development. Multimodal imaging approaches offer a more comprehensive and systematic assessment of brain function. Motion artifacts affect most imaging techniques, including fNIRS. However, fNIRS exhibits relatively higher tolerance to motion artifacts compared to other neuroimaging methods, making it suitable for use during physical activities (37). To address motion artifacts in fNIRS studies, researchers have devised various methods to minimize signals originating from non-brain tissue activities. Among these methods, short-channel subtraction has demonstrated notable efficacy in reducing extracerebral responses and is often regarded as the "gold standard" (67). Despite its application across multiple research domains, the absence of standardized protocols for data processing and analysis in fNIRS studies significantly hinders cross-study comparisons (15,42).

A considerable body of research on fNIRS has primarily focused on the blood flow and metabolism within brain regions associated with various types of cognitive impairment. However, the understanding of the brain network mechanisms underlying fNIRS remains limited, with divergent theoretical perspectives, particularly regarding brain network connectivity and the synergistic interactions between brain regions. Consequently, there is substantial potential for further exploration and refinement of fNIRS in this context. This review provides an overview of the application of fNIRS in cognitive impairment associated with various diseases and highlights its potential in the early detection and diagnosis of AD and MCI. By measuring oxygenation levels in the frontal, temporal, and parietal lobes during cognitive tasks and comprehensively analyzing the brain functional connectivity, fNIRS can provide valuable insights into the study of cognitive impairment related to central nervous system diseases. This review aims to stimulate further research in the field of fNIRS, facilitating the exploration of neural mechanisms underlying cognitive activity. It is anticipated that with ongoing technological advancements, fNIRS will evolve into a more user-friendly research tool with expanded clinical applications.

### Acknowledgements

The figures were created with Bio-Render.com.

*Funding:* This work was funded by the National Natural

Science Foundation of China (Grant No.82371427, Grant No.82401656), Natural Science Foundation of Chongqing, China (CSTB2023NSCQBHX0018, CSTB2023NSCQ-MSX0323) and Kuanren Talents Program of the Second Affiliated Hospital of Chongqing Medical University (Grant No. kryc-lj-2105) and Postgraduate Research and Project of Chongqing Province (Grant No. CYB240199).

*Conflict of Interest:* The authors have no conflicts of interest to disclose.

### References

1. World Alzheimer Report 2022 – Life after diagnosis: Navigating treatment, care and support. <https://www.alzint.org/u/World-Alzheimer-Report-2022.pdf> (accessed January 11, 2025).
2. Koshiyama D, Fukunaga M, Okada N, *et al.* White matter microstructural alterations across four major psychiatric disorders: mega-analysis study in 2937 individuals. *Mol Psychiatry*. 2020; 25:883-895.
3. Hottman DA, Chernick D, Cheng S, Wang Z, Li L. HDL and cognition in neurodegenerative disorders. *Neurobiol Dis*. 2014; 72:22-36.
4. Sun MK. Roles of neural regeneration in memory pharmacology. *Neural Regen Res*. 2018; 13:406.
5. Scheltens P, De Strooper B, Kivipelto M, Holstege H, Chételat G, Teunissen CE, Cummings J, van der Flier WM. Alzheimer's disease. *Lancet*. 2021; 397:1577-1590.
6. Hill NTM, Mowszowski L, Naismith SL, Chadwick VL, Valenzuela M, Lampit A. Computerized Cognitive Training in Older Adults With Mild Cognitive Impairment or Dementia: A Systematic Review and Meta-Analysis. *Am J Psychiatry*. 2017; 174(3):29-340.
7. Hugo J, Ganguli M. Dementia and Cognitive Impairment. *Clin Geriatr Med*. 2014; 30:421-442.
8. Grady C. The cognitive neuroscience of ageing. *Nat Rev Neurosci*. 2012; 13:491-505.
9. Perrey S. Non-invasive NIR spectroscopy of human brain function during exercise. *Methods*. 2008; 45:289-299.
10. Cutini S, Brigadoi S. Unleashing the future potential of functional near-infrared spectroscopy in brain sciences. *J Neurosci Methods*. 2014; 232:152156.
11. Yeung MK, Chan AS. Functional near-infrared spectroscopy reveals decreased resting oxygenation levels and task-related oxygenation changes in mild cognitive impairment and dementia: A systematic review. *J Psychiatr Res*. 2020; 124:58-76.
12. Lloyd-Fox S, Blasi A, Elwell CE. Illuminating the developing brain: the past, present and future of functional near infrared spectroscopy. *Neurosci Biobehav Rev*. 2010; 34:269–284.
13. Kinder KT, Heim HLR, Parker J, Lowery K, McCraw A, Eddings RN, Defenderfer J, Sullivan J, Buss AT. Systematic review of fNIRS studies reveals inconsistent chromophore data reporting practices. *Neurophotonics*. 2022; 9:040601.
14. Chen WL, Wagner J, Heugel N, Sugar J, Lee YW, Conant L, Malloy M, Heffernan J, Quirk B, Zinos A, Beardsley SA, Prost R, Whelan HT. Functional Near-Infrared Spectroscopy and Its Clinical Application in the Field of Neuroscience: Advances and Future Directions. *Front Neurosci*. 2020; 14:724.

15. Herold F, Wiegel P, Scholkmann F, Müller NG. Applications of Functional Near-Infrared Spectroscopy (fNIRS) Neuroimaging in Exercise-Cognition Science: A Systematic, Methodology-Focused Review. *J Clin Med*. 2018; 7:466.
16. Fabiani M, Gordon BA, Maclin EL, Pearson MA, Brumback-Peltz CR, Low KA, McAuley E, Sutton BP, Kramer AF, Gratton G. Neurovascular coupling in normal aging: a combined optical, ERP and fMRI study. *Neuroimage*. 2014; 85:592-607.
17. Jean-Pierre P. Integrating functional near-infrared spectroscopy in the characterization, assessment, and monitoring of cancer and treatment-related neurocognitive dysfunction. *Neuroimage*. 2014; 85:408-414.
18. Jöbsis FF. Noninvasive, Infrared Monitoring of Cerebral and Myocardial Oxygen Sufficiency and Circulatory Parameters. *Science*. 1977; 198:1264-1267.
19. Hoshi Y, Tamura M. Detection of dynamic changes in cerebral oxygenation coupled to neuronal function during mental work in man. *Neurosci Lett*. 1993; 150:5-8.
20. Hoshi Y, Onoe H, Watanabe Y, Andersson J, Bergström M, Lilja A, Långström B, Tamura M. Non-synchronous behavior of neuronal activity, oxidative metabolism and blood supply during mental tasks in man. *Neurosci Lett*. 1994; 172:129-133.
21. Okada F, Tokumitsu Y, Hoshi Y, Tamura M. Impaired interhemispheric integration in brain oxygenation and hemodynamics in schizophrenia. *Eur Arch Psychiatry Clin Neurosci*. 1994; 244:17-25.
22. Sakatani K, Xie Y, Lichty W, Li S, Zuo H. Language-activated cerebral blood oxygenation and hemodynamic changes of the left prefrontal cortex in poststroke aphasic patients: a near-infrared spectroscopy study. *Stroke*. 1998; 29:1299-1304.
23. Sakatani K, Katayama Y, Yamamoto T, Suzuki S. Changes in cerebral blood oxygenation of the frontal lobe induced by direct electrical stimulation of thalamus and globus pallidus: a near infrared spectroscopy study. *J Neurol Neurosurg Psychiatry*. 1999; 67:769-773.
24. Malagoni AM, Felisatti M, Lamberti N, Basaglia N, Manfredini R, Salvi F, Zamboni P, Manfredini F. Muscle oxygen consumption by NIRS and mobility in multiple sclerosis patients. *BMC Neurol*. 2013; 13:52.
25. Kleinschmidt A, Obrig H, Requardt M, Merboldt KD, Dirnagl U, Villringer A, Frahm J. Simultaneous recording of cerebral blood oxygenation changes during human brain activation by magnetic resonance imaging and near-infrared spectroscopy. *J Cereb Blood Flow Metab*. 1996; 16:817-826.
26. Fallgatter AJ, Roesler M, Sitzmann L, Heidrich A, Mueller TJ, Strik WK. Loss of functional hemispheric asymmetry in Alzheimer's dementia assessed with near-infrared spectroscopy. *Cogn Brain Res*. 1997; 6:67-72.
27. Meek JH, Firbank M, Elwell CE, Atkinson J, Braddick O, Wyatt JS. Regional hemodynamic responses to visual stimulation in awake infants. *Pediatr Res*. 1998; 43:840-843.
28. Mackert BM, Wübbeler G, Leistner S, Uludag K, Obrig H, Villringer A, Trahms L, Curio G. Neurovascular coupling analyzed non-invasively in the human brain. *Neuroreport*. 2004; 15:63-66.
29. Kelsey CM, Farris K, Grossmann T. Variability in Infants' Functional Brain Network Connectivity Is Associated With Differences in Affect and Behavior. *Front Psychiatry*. 2021; 12:685754.
30. Hoyniak CP, Quiñones-Camacho LE, Camacho MC, Chin JH, Williams EM, Wakschlag LS, Perlman SB. Adversity is Linked with Decreased Parent-Child Behavioral and Neural Synchrony. *Dev Cogn Neurosci*. 2021; 48:100937.
31. Lee OW, Mao D, Wunderlich J, Balasubramanian G, Haneman M, Korneev M, McKay CM. Two Independent Response Mechanisms to Auditory Stimuli Measured with Functional Near-Infrared Spectroscopy in Sleeping Infants. *Trends Hear*. 2024; 28:23312165241258056.
32. Pinti P, Aichelburg C, Gilbert S, Hamilton A, Hirsch J, Burgess P, Tachtsidis I. A Review on the Use of Wearable Functional Near-Infrared Spectroscopy in Naturalistic Environments. *Jpn Psychol Res*. 2018; 60:347-373.
33. Hirsch J, Tiede M, Zhang X, Noah JA, Salama-Manteau A, Biriotti M. Interpersonal Agreement and Disagreement During Face-to-Face Dialogue: An fNIRS Investigation. *Front Hum Neurosci*. 2020; 14:606397.
34. Cope M, Delpy DT. System for long-term measurement of cerebral blood and tissue oxygenation on newborn infants by near infra-red transillumination. *Med Biol Eng Comput*. 1988; 26:289-294.
35. Watanabe E, Maki A, Kawaguchi F, Takashiro K, Yamashita Y, Koizumi H, Mayanagi Y. Non-invasive assessment of language dominance with near-infrared spectroscopic mapping. *Neurosci Lett*. 1998; 256:49-52.
36. Atsumori H, Kiguchi M, Obata A, Sato H, Katura T, Funane T, Maki A. Development of wearable optical topography system for mapping the prefrontal cortex activation. *Rev Sci Instrum*. 2009; 80:043704.
37. Agbangla NF, Audiffren M, Albinet CT. Use of near-infrared spectroscopy in the investigation of brain activation during cognitive aging: A systematic review of an emerging area of research. *Ageing Res Rev*. 2017; 38:52-66.
38. Cui X, Bray S, Bryant DM, Glover GH, Reiss AL. A quantitative comparison of NIRS and fMRI across multiple cognitive tasks. *NeuroImage*. 2011; 54:2808-2821.
39. Pinti P, Tachtsidis I, Hamilton A, Hirsch J, Aichelburg C, Gilbert S, Burgess PW. The present and future use of functional near-infrared spectroscopy (fNIRS) for cognitive neuroscience. *Ann N Y Acad Sci*. 2020; 1464:5-29.
40. Quaresima V, Ferrari M. Functional Near-Infrared Spectroscopy (fNIRS) for Assessing Cerebral Cortex Function During Human Behavior in Natural/Social Situations: A Concise Review. *Organ Res Methods*. 2019; 22:46-68.
41. Moosmann M, Ritter P, Krastel I, Brink A, Thees S, Blankenburg F, Taskin B, Obrig H, Villringer A. Correlates of alpha rhythm in functional magnetic resonance imaging and near infrared spectroscopy. *Neuroimage*. 2003; 20:145-158.
42. Doherty EJ, Spencer CA, Burnison J, Čeko M, Chin J, Eloy L, Haring K, Kim P, Pittman D, Powers S, Pugh SL, Roumis D, Stephens JA, Yeh T, Hirshfield L. Interdisciplinary views of fNIRS: Current advancements, equity challenges, and an agenda for future needs of a diverse fNIRS research community. *Front Integr Neurosci*. 2023; 17:1059679.
43. McKendrick R, Parasuraman R, Ayaz H. Wearable functional near infrared spectroscopy (fNIRS) and transcranial direct current stimulation (tDCS): expanding vistas for neurocognitive augmentation. *Front Syst Neurosci*. 2015; 9:27.

44. Cohen MX. Where Does EEG Come From and What Does It Mean? *Trends Neurosci.* 2017; 40:208-218.
45. Yang D, Hong KS, Yoo SH, Kim CS. Evaluation of Neural Degeneration Biomarkers in the Prefrontal Cortex for Early Identification of Patients With Mild Cognitive Impairment: An fNIRS Study. *Front Hum Neurosci.* 2019; 13:317.
46. Li R, Yang D, Fang F, Hong KS, Reiss AL, Zhang Y. Concurrent fNIRS and EEG for Brain Function Investigation: A Systematic, Methodology-Focused Review. *Sensors (Basel).* 2022; 22:5865.
47. Pinti P, Siddiqui MF, Levy AD, Jones EJH, Tachtsidis I. An analysis framework for the integration of broadband NIRS and EEG to assess neurovascular and neurometabolic coupling. *Sci Rep.* 2021; 11:3977.
48. Cicalese PA, Li R, Ahmadi MB, Wang C, Francis JT, Selvaraj S, Schulz PE, Zhang Y. An EEG-fNIRS hybridization technique in the four-class classification of alzheimer's disease. *J Neurosci Methods.* 2020; 336:108618.
49. Pini L, de Lange SC, Pizzini FB, Boscolo Galazzo I, Manenti R, Cotelli M, Galluzzi S, Cotelli MS, Corbetta M, van den Heuvel MP, Pievani M. A low-dimensional cognitive-network space in Alzheimer's disease and frontotemporal dementia. *Alzheimers Res Ther.* 2022; 14:199.
50. Li R, Nguyen T, Potter T, Zhang Y. Dynamic cortical connectivity alterations associated with Alzheimer's disease: An EEG and fNIRS integration study. *NeuroImage Clin.* 2019; 21:101622.
51. Buccino AP, Keles HO, Omurtag A. Hybrid EEG-fNIRS Asynchronous Brain-Computer Interface for Multiple Motor Tasks. *PloS One.* 2016; 11:e0146610.
52. Pereira J, Direito B, Lührs M, Castelo-Branco M, Sousa T. Multimodal assessment of the spatial correspondence between fNIRS and fMRI hemodynamic responses in motor tasks. *Sci Rep.* 2023; 13:2244.
53. Folch J, Petrov D, Ettcheto M, Abad S, Sánchez-López E, García ML, Olloquequi J, Beas-Zarate C, Auladell C, Camins A. Current Research Therapeutic Strategies for Alzheimer's Disease Treatment. *Neural Plast.* 2016; 2016:8501693.
54. Tang TB, Chan YL. Functional Connectivity Analysis on Mild Alzheimer's Disease, Mild Cognitive Impairment and Normal Aging using fNIRS. *Annu Int Conf IEEE Eng Med Biol Soc.* 2018; 2018:17-20.
55. Paraskevaidi M, Morais CLM, Freitas DLD, Lima KMG, Mann DMA, Allsop D, Martin-Hirsch PL, Martin FL. Blood-based near-infrared spectroscopy for the rapid low-cost detection of Alzheimer's disease. *Analyst.* 2018; 143:5959-64.
56. Ateş FE, Cangöz B, Özel Kızıl ET, Baskak B, Baran Z, Özgüven HD. Frontal activity during a verbal emotional working memory task in patients with Alzheimer's disease: A functional near-infrared spectroscopy study. *Psychiatry Res Neuroimaging.* 2017; 261:29-34.
57. Katzorke A, Zeller JBM, Müller LD, Lauer M, Polak T, Deckert J, Herrmann MJ. Decreased hemodynamic response in inferior frontotemporal regions in elderly with mild cognitive impairment. *Psychiatry Res Neuroimaging.* 2018; 274:11-18.
58. Thiyagesh SN, Farrow TF, Parks RW, Accosta-Mesa H, Young C, Wilkinson ID, Hunter MD, Woodruff PW. The neural basis of visuospatial perception in Alzheimer's disease and healthy elderly comparison subjects: An fMRI study. *Psychiatry Res.* 2009; 172:109-116.
59. Zeller JBM, Herrmann MJ, Ehlis AC, Polak T, Fallgatter AJ. Altered Parietal Brain Oxygenation in Alzheimer's Disease as Assessed With Near-Infrared Spectroscopy. *Am J Geriatr Psychiatry.* 2010; 18:433-441.
60. Haberstumpf S, Seidel A, Lauer M, Polak T, Deckert J, Herrmann MJ. Neuronal correlates of the visual-spatial processing measured with functional near-infrared spectroscopy in healthy elderly individuals. *Neuropsychologia.* 2020; 148:107650.
61. Haberstumpf S, Seidel A, Lauer M, Polak T, Deckert J, Herrmann MJ. Reduced parietal activation in participants with mild cognitive impairments during visual-spatial processing measured with functional near-infrared spectroscopy. *J Psychiatr Res.* 2022; 146:31-42.
62. Bokde AL, Lopez-Bayo P, Meindl T, Pechler S, Born C, Faltraco F, Teipel SJ, Möller HJ, Hampel H. Functional connectivity of the fusiform gyrus during a face-matching task in subjects with mild cognitive impairment. *Brain.* 2006; 129:1113-1124.
63. Nguyen T, Kim M, Gwak J, Lee JJ, Choi KY, Lee KH, Kim JG. Investigation of brain functional connectivity in patients with mild cognitive impairment: A functional near-infrared spectroscopy (fNIRS) study. *J Biophotonics.* 2019; 12:e201800298.
64. Chan YL, Ung WC, Lim LG, Lu CK, Kiguchi M, Tang TB. Automated Thresholding Method for fNIRS-Based Functional Connectivity Analysis: Validation With a Case Study on Alzheimer's Disease. *IEEE Trans Neural Syst Rehabil Eng.* 2020; 28:1691-1701.
65. Kong Y, Peng W, Li J, Zhu C, Zhang C, Fan Y. Alteration in brain functional connectivity in patients with post-stroke cognitive impairment during memory task: A fNIRS study. *J Stroke Cerebrovasc Dis.* 2023; 32:107280.
66. Li X, Huang F, Guo T, Feng M, Li S. The continuous performance test aids the diagnosis of post-stroke cognitive impairment in patients with right hemisphere damage. *Front Neurol.* 2023; 14:1173004.
67. Zou J, Yin Y, Lin Z, Gong Y. The analysis of brain functional connectivity of post-stroke cognitive impairment patients: an fNIRS study. *Front Neurosci.* 2023; 17:1168773.
68. Kato J, Yamada T, Kawaguchi H, Matsuda K, Higo N. Functional near-infrared-spectroscopy-based measurement of changes in cortical activity in macaques during post-infarct recovery of manual dexterity. *Sci Rep.* 2020; 10:6458.
69. Yang C, Zhang T, Huang K, Xiong M, Liu H, Wang P, Zhang Y. Increased both cortical activation and functional connectivity after transcranial direct current stimulation in patients with post-stroke: A functional near-infrared spectroscopy study. *Front Psychiatry.* 2022; 13:1046849.
70. Huo C, Li X, Jing J, Ma Y, Li W, Wang Y, Liu W, Fan Y, Yue S, Wang Y, Li Z. Median Nerve Electrical Stimulation-Induced Changes in Effective Connectivity in Patients With Stroke as Assessed With Functional Near-Infrared Spectroscopy. *Neurorehabil Neural Repair.* 2019; 33:1008-1017.
71. Zhang Y, Chu M, Zheng Y, Zhang F, Yu H, Ye X, Xie H, Chen J, Qian Z, Zeng C, Chen W, Pei Z, Zhang Y, Chen J. Effects of Combined Use of Intermittent Theta Burst Stimulation and Cognitive Training on Poststroke Cognitive Impairment: A Single-Blind Randomized Controlled Trial. *Am J Phys Med Rehabil.* 2024; 103:318-

- 324.
72. Hofmann A, Rosenbaum D, Int-Veen I, Ehlis AC, Brockmann K, Dehnen K, von Thaler AK, Berg D, Fallgatter AJ, Metzger FG; TREND Study Consortium. Abnormally reduced frontal cortex activity during Trail-Making-Test in prodromal parkinson's disease-a fNIRS study. *Neurobiol Aging*. 2021; 105:148-158.
  73. Stuart S, Belluscio V, Quinn JF, Mancini M. Pre-frontal Cortical Activity During Walking and Turning Is Reliable and Differentiates Across Young, Older Adults and People With Parkinson's Disease. *Front Neurol*. 2019; 10:536.
  74. Kostic VS, Agosta F, Pievani M, Stefanova E, Jecmenica-Lukic M, Scarale A, Spica V, Filippi M. Pattern of brain tissue loss associated with freezing of gait in Parkinson disease. *Neurology*. 2012; 78:409-416.
  75. Sharon T, Kurz I, Bernad-Elazari H, Shustak S, Galperin I, Giladi N, Mirelman A, Hausdorff JM, Maidan I. Which obstacle attributes place additional demands on higher-level cognitive function in patients with Parkinson's disease? *Parkinsonism Relat Disord*. 2020; 78:178-183.
  76. Pelicioni PHS, Lord SR, Okubo Y, Sturnieks DL, Menant JC. People With Parkinson's Disease Exhibit Reduced Cognitive and Motor Cortical Activity When Undertaking Complex Stepping Tasks Requiring Inhibitory Control. *Neurorehabil Neural Repair*. 2020; 34:1088-1098.
  77. Maidan I, Bernad-Elazari H, Gazit E, Giladi N, Hausdorff JM, Mirelman A. Changes in oxygenated hemoglobin link freezing of gait to frontal activation in patients with Parkinson disease: an fNIRS study of transient motor-cognitive failures. *J Neurol*. 2015; 262:899-908.
  78. Bonilauri A, Sangiuliano Intra F, Rossetto F, Borgnis F, Baselli G, Baglio F. Whole-Head Functional Near-Infrared Spectroscopy as an Ecological Monitoring Tool for Assessing Cortical Activity in Parkinson's Disease Patients at Different Stages. *Int J Mol Sci*. 2022; 23:14897.
  79. Vacchiano C, Silva S. Characterization of bilateral frontal lobe cerebral oxygen saturation in patients with mild traumatic brain injury. *Nurs Outlook*. 2017; 65:S36-43.
  80. Panwar N, Purohit D, Deo Sinha V, Joshi M. Evaluation of extent and pattern of neurocognitive functions in mild and moderate traumatic brain injury patients by using Montreal Cognitive Assessment (MoCA) score as a screening tool: An observational study from India. *Asian J Psychiatry*. 2019; 41:60-65.
  81. Chang F, Li H, Li N, Zhang S, Liu C, Zhang Q, Cai W. Functional near-infrared spectroscopy as a potential objective evaluation technique in neurocognitive disorders after traumatic brain injury. *Front Psychiatry*. 2022; 13:903756.
  82. Plenger P, Krishnan K, Cloud M, Bosworth C, Qualls D, Marquez De La Plata C. fNIRS-based investigation of the Stroop task after TBI. *Brain Imaging Behav*. 2016; 10:357-366.
  83. Adingupu DD, Evans T, Soroush A, Hansen A, Jarvis S, Brown L, Dunn JF. Temporal Pattern of Cortical Hypoxia in Multiple Sclerosis and Its Significance on Neuropsychological and Clinical Measures of Disability. *Ann Neurol*. 2023; 94:1067-1079.;
  84. Hernandez ME, Holtzer R, Chaparro G, Jean K, Balto JM, Sandroff BM, Izzetoglu M, Motl RW. Brain activation changes during locomotion in middle-aged to older adults with multiple sclerosis. *J Neurol Sci*. 2016; 370:277-283.
  85. Stojanovic-Radic J, Wylie G, Voelbel G, Chiaravalloti N, DeLuca J. Neuroimaging and cognition using functional near infrared spectroscopy (fNIRS) in multiple sclerosis. *Brain Imaging Behav*. 2015; 9:302-311.
  86. Knight MJ, Baune BT. Cognitive dysfunction in major depressive disorder. *Curr Opin Psychiatry*. 2018; 31:26-31.
  87. Pu S, Matsumura H, Yamada T, Ikezawa S, Mitani H, Adachi A, Nakagome K. Reduced frontopolar activation during verbal fluency task associated with poor social functioning in late-onset major depression: Multi-channel near-infrared spectroscopy study. *Psychiatry Clin Neurosci*. 2008; 62:728-37.
  88. Kondo A, Shoji Y, Morita K, Sato M, Ishii Y, Yanagimoto H, Nakano S, Uchimura N. Characteristics of oxygenated hemoglobin concentration change during pleasant and unpleasant image-recall tasks in patients with depression: Comparison with healthy subjects. *Psychiatry Clin Neurosci*. 2018; 72:611-622.
  89. Downey D, Brigadoi S, Trevithick L, Elliott R, Elwell C, McAllister-Williams RH, Anderson IM. Frontal haemodynamic responses in depression and the effect of electroconvulsive therapy. *J Psychopharmacol*. 2019; 33:1003-1014.
  90. Liu X, Cheng F, Hu S, Wang B, Hu C, Zhu Z, Zhuang W, Mei X, Li X, Zhou Q, Zhang W, Tang Y, Zhou D. Cortical activation and functional connectivity during the verbal fluency task for adolescent-onset depression: A multi-channel NIRS study. *J Psychiatr Res*. 2022; 147:254-261.
  91. Ishii Y, Shoji Y, Sato M, Nakano S, Kondo A, Kodama H, Morita K. The Changes in Concentration of Cerebral Oxygenated Hemoglobin During Single Event-Related Japanese Shiritori Task in Patients With Major Depression Disorder: Comparison With Healthy Subjects. *Front Psychiatry*. 2021; 12:709771.
  92. Kameyama M, Fukuda M, Yamagishi Y, Sato T, Uehara T, Ito M, Suto T, Mikuni M. Frontal lobe function in bipolar disorder: a multichannel near-infrared spectroscopy study. *Neuroimage*. 2006; 29:172-184.
  93. Nishimura Y, Takahashi K, Ohtani T, Ikeda-Sugita R, Kasai K, Okazaki Y. Dorsolateral prefrontal hemodynamic responses during a verbal fluency task in hypomanic bipolar disorder. *Bipolar Disord*. 2015; 17:172-183.
  94. Owen MJ, Sawa A, Mortensen PB. Schizophrenia. *Lancet Lond Engl*. 2016; 388:86-97.
  95. Koike S, Takizawa R, Nishimura Y, Kinou M, Kawasaki S, Kasai K. Reduced but broader prefrontal activity in patients with schizophrenia during n-back working memory tasks: A multi-channel near-infrared spectroscopy study. *J Psychiatr Res*. 2013; 47:12401246.
  96. Noda T, Nakagome K, Setoyama S, Matsushima E. Working memory and prefrontal/temporal hemodynamic responses during post-task period in patients with schizophrenia: A multi-channel near-infrared spectroscopy study. *J Psychiatr Res*. 2017; 95:288-298.
  97. Kumar V, Nichenmetla S, Chhabra H, Sreeraj VS, Rao NP, Kesavan M, Varambally S, Venkatasubramanian G, Gangadhar BN. Prefrontal cortex activation during working memory task in schizophrenia: A fNIRS study. *Asian J Psychiatr*. 2021; 56:102507.
  98. Ikeda T, Hirai M, Sakurada T, Monden Y, Tokuda T, Nagashima M, Shimoizumi H, Dan I, Yamagata T. Atypical neural modulation in the right prefrontal cortex during an inhibitory task with eye gaze in autism spectrum disorder as revealed by functional near-infrared spectroscopy. *Neurophotonics*. 2018; 5:035008.
  99. Conti E, Scaife E, Bosetti C, Marchi V, Costanzo V, Dell'Oste V, Mazziotti R, Dell'Osso L, Carmassi C,

- Muratori F, Baroncelli L, Calderoni S, Battini R. Looking for "fNIRS Signature" in Autism Spectrum: A Systematic Review Starting From Preschoolers. *Front Neurosci.* 2022; 16:785993.
100. Zhang F, Roeyers H. Exploring brain functions in autism spectrum disorder: A systematic review on functional near-infrared spectroscopy (fNIRS) studies. *Int J Psychophysiol Off J Int Organ Psychophysiol.* 2019; 137:41-53.
  101. Su WC, Culotta M, Tsuzuki D, Bhat A. Movement kinematics and cortical activation in children with and without autism spectrum disorder during sway synchrony tasks: an fNIRS study. *Sci Rep.* 2021; 11:15035.
  102. Chan MMY, Chan MC, Lai OLH, Krishnamurthy K, Han YMY. Abnormal Prefrontal Functional Connectivity Is Associated with Inflexible Information Processing in Patients with Autism Spectrum Disorder (ASD): An fNIRS Study. *Biomedicines.* 2022; 10:1132.
  103. Han YMY, Chan MC, Chan MMY, Yeung MK, Chan AS. Effects of working memory load on frontal connectivity in children with autism spectrum disorder: a fNIRS study. *Sci Rep.* 2022 ;12:1522.
  104. Gallagher A, Wallois F, Obrig H. Functional near-infrared spectroscopy in pediatric clinical research: Different pathophysiologicals and promising clinical applications. *Neurophotronics.* 2023; 10:023517.
  105. Monden Y, Dan I, Nagashima M, Dan H, Uga M, Ikeda T, Tsuzuki D, Kyutoku Y, Gunji Y, Hirano D, Taniguchi T, Shimoizumi H, Watanabe E, Yamagata T. Individual classification of ADHD children by right prefrontal hemodynamic responses during a go/no-go task as assessed by fNIRS. *Neuroimage Clin.* 2015; 9:1-12.
  106. Yoo SH, Woo SW, Shin MJ, Yoon JA, Shin YI, Hong KS. Diagnosis of Mild Cognitive Impairment Using Cognitive Tasks: A Functional Near-Infrared Spectroscopy Study. *Curr Alzheimer Res.* 2020; 17:1145-1160.
  107. Vural Keleş Ö, Yıldırım E. Depression affects working memory performance: A Functional Near Infrared Spectroscopy (fNIRS) Study. *Psychiatry Res Neuroimaging.* 2023; 329:111581.
  108. Thapar A, Cooper M. Attention deficit hyperactivity disorder. *Lancet Lond Engl.* 2016; 387:1240-1250.
  109. Crippa A, Salvatore C, Molteni E, Mauri M, Salandi A, Trabattoni S, Agostoni C, Molteni M, Nobile M, Castiglioni I. The Utility of a Computerized Algorithm Based on a Multi-Domain Profile of Measures for the Diagnosis of Attention Deficit/Hyperactivity Disorder. *Front Psychiatry.* 2017; 8:189.
  110. Birlé C, Slavoaca D, Balea M, Livint Popa L, Muresanu I, Stefanescu E, Vacaras V, Dina C, Strilciuc S, Popescu BO, Muresanu DF. Cognitive function: holarchy or holacracy? *Neurol Sci.* 2021; 42:89-99.
  111. Vanderwert RE, Nelson CA. The use of near-infrared spectroscopy in the study of typical and atypical development. *NeuroImage.* 2014; 85:264-271.
- Received November 12, 2024; Revised January 13, 2025; Accepted January 22, 2025.
- §These authors contributed equally to this work.
- \*Address correspondence to:  
Xiuqing Yao and Yaxi Luo, Department of Rehabilitation, The Second Affiliated Hospital of Chongqing Medical University, Chongqing, China.  
E-mail: dryaoxq@cqmu.edu.cn (XY); luoyaxi@hospital.cqmu.edu.cn (YL)
- Released online in J-STAGE as advance publication January 25, 2025.

# Growth and differentiation factor 15: An emerging therapeutic target for brain diseases

Yingying Zhou<sup>1,§</sup>, Lei Dou<sup>1,§</sup>, Luyao Wang<sup>1</sup>, Jiajie Chen<sup>1</sup>, Ruxue Mao<sup>1</sup>, Lingqiang Zhu<sup>2</sup>, Dan Liu<sup>3</sup>, Kai Zheng<sup>1,\*</sup>

<sup>1</sup>Department of Geriatrics, Tongji Hospital, Tongji Medical College, Huazhong University of Science and Technology, Wuhan, Hubei, China;

<sup>2</sup>Department of Pathophysiology, School of Basic Medicine, Tongji Medical College, Huazhong University of Science and Technology, Wuhan, Hubei, China;

<sup>3</sup>Department of Medical Genetics, School of Basic Medicine, Tongji Medical College, Huazhong University of Science and Technology, Wuhan, Hubei, China.

**SUMMARY:** Growth and differentiation factor 15 (GDF15), a member of the transforming growth factor- $\beta$  superfamily, is considered a stress response factor and has garnered increasing attention in recent years due to its roles in neurological diseases. Although many studies have suggested that GDF15 expression is elevated in patients with neurodegenerative diseases (NDDs), glioma, and ischemic stroke, the effects of increased GDF15 expression and the potential underlying mechanisms remain unclear. Notably, many experimental studies have shown the multidimensional beneficial effects of GDF15 on NDDs, and GDF15 overexpression is able to rescue NDD-associated pathological changes and phenotypes. In glioma, GDF15 exerts opposite effects, it is both protumorigenic and antitumorigenic. The causes of these conflicting findings are not comprehensively clear, but inhibiting GDF15 is helpful for suppressing tumor progression. GDF15 is also regarded as a biomarker of poor clinical outcomes in ischemic stroke patients, and targeting GDF15 may help prevent this disease. Thus, we systematically reviewed the synthesis, transcriptional regulation, and biological functions of GDF15 and its related signaling pathways within the brain. Furthermore, we explored the potential of GDF15 as a therapeutic target and assessed its clinical applicability in interventions for brain diseases. By integrating the latest research findings, this study provides new insights into the future treatment of neurological diseases.

**Keywords:** GDF15, Alzheimer's disease, Parkinson's disease, glioma, ischemic stroke

## 1. Introduction

The number of patients with brain disease in European populations almost doubled from 2010 (179 million) to 2017 (324 million) (1,2). The diseases with the top five medical costs per patient are multiple sclerosis (MS), brain tumors, stroke, dementia, and Parkinson's disease (PD) (1). In 2017, brain diseases caused 1.2 million deaths in European populations, the primary causes of which were dementia and stroke (2). Brain diseases are undoubtedly urgent and major challenges for neuroscientists. Therefore, a detailed understanding of the mechanism of brain diseases is crucial for the development of effective therapeutic strategies.

Growth and differentiation factor 15 (GDF15), a key cellular stress responsive factor, is a member of the transforming growth factor- $\beta$  (TGF- $\beta$ ) superfamily of proteins and is widely distributed throughout peripheral tissues and the brain. The basal expression of GDF15

is low; however, its expression can be strongly induced in response to cellular stress following tissue injury (3). GDF15 expression is significantly increased in individuals with various neurological diseases (4,5), including Alzheimer's disease (AD), PD, amyotrophic lateral sclerosis (ALS), MS, glioma and acute ischemic stroke (6,7). Notably, identifying whether the overall physiological functions of upregulated GDF15 play protective or harmful roles in brain diseases is important. A body of evidence has indicated that GDF15 helps suppress the inflammatory response, regulates energy homeostasis and body weight, protects endothelial cell function, and inhibits the growth of early cancers but facilitates the proliferation and invasion of advanced cancers (8-10). However, the functions of GDF15 and the associated signaling pathways in nerve cells and brain diseases are poorly understood.

Additionally, several epidemiological studies have revealed the relationships between high levels of GDF15

and the risks of dementia and AD (11), PD (12), and the severity of MS (13). In contrast, based on current experimental studies, upregulated GDF15 has beneficial effects on the pathogenesis of neurodegenerative diseases (NDDs), such as AD (14,15), PD (16,17), and Huntington's disease (HD), through many pathways (18). Similarly, contradictory findings concerning the effects of GDF15 on glioma have been reported. On the one hand, GDF15 promotes the proliferation and invasion of cancer cells and is involved in immune escape (19-21). On the other hand, GDF15 can be transcriptionally activated by the tumor suppressor gene p53 (22). Given these contrasting discoveries, the physiological roles of GDF15 in brain diseases appear to be much more complicated than expected.

Importantly, previous studies have reported that exogenous GDF15 promotes the clearance of amyloid- $\beta$  (A $\beta$ ), inhibits neuroinflammation and apoptosis, and increases synaptic activity in an AD model (14,15,23,24). GDF15 is also essential for maintaining the survival of midbrain dopaminergic neurons and contributes to alleviating PD-like motor symptoms (16,17). In addition, decreasing the level of GDF15 derived from glioma inhibits tumor growth (19,20). GDF15 expression in tumors is associated with the regulation of the immune microenvironment (25). Neutralizing antibodies against GDF15 and the GDF15 receptor, glial cell-derived neurotrophic factor family receptor  $\alpha$ -like (GFRAL), are useful for relieving cachexia in patients with advanced cancer through increased food intake (26). GDF15 deficiency also has beneficial effects on atherosclerotic plaque stabilization and the inhibition of plaque progression (27,28), which provides a theoretical foundation for the clinical application of GDF15 in preventing cerebrovascular diseases. A series of robust studies have suggested that GDF15 is a promising potential therapeutic target for the treatment of brain diseases. Therefore, in this review, we systematically summarize the effects of GDF15 and the potential mechanisms involved in brain diseases. Moreover, we comprehensively evaluated the clinical applicability of GDF15 as a new therapeutic target for treatment of brain diseases.

## 2. GDF15-related mechanisms

### 2.1. Synthesis and secretion of GDF15

GDF15 is also known as macrophage inhibitory cytokine 1 (MIC-1) and nonsteroidal anti-inflammatory drug-activated gene-1 (NAG-1). The human GDF15 locus is located on chromosome 19p12-13.1, as shown by fluorescence *in situ* hybridization, and comprises only two exons of 309 bp and 891 bp separated by a 2.9-kb intron (29). The GDF15 mRNA contains a long open reading frame encoding a protein of 308 amino acids, including a signal peptide of 29 amino acids, a

propeptide of 165 amino acids and a mature peptide of 114 amino acids (30). GDF15, a member of the TGF- $\beta$  superfamily, presents high sequence homology and a conserved nine-cysteine region (31). The crystal structure of GDF15 reveals an unexpected disulfide bonding configuration that contains a novel (1 $\rightarrow$ 2, 3 $\rightarrow$ 7) disulfide arrangement not previously identified for the other nine cysteine family members (1 $\rightarrow$ 3, 2 $\rightarrow$ 7) (32). The 6th cysteine forms a disulfide bond with a free 6th cysteine from another pro-GDF15 monomer to form a pro-GDF15 homodimer (33). Through proteolytic cleavage of the dimeric pro-GDF15 precursor at a furin-like site, mature GDF15 is secreted as a 25 kDa disulfide-linked homodimer in the endoplasmic reticulum (33,34). Mature GDF15 is subsequently secreted into the extracellular matrix and can be detected in the blood and cerebrospinal fluid (CSF). In addition, matrix metalloproteinase-26 (MMP-26) and paired basic amino acid-cleaving enzyme 4 (PACE4) mediate the maturation of pro-GDF15 (35). Unlike other TGF- $\beta$  superfamily proteins, the propeptide is not required for proper GDF15 folding and secretion (33). We knew very little about the function of pro-GDF15 before Min KW *et al.* reported that pro-GDF15 is also expressed in the nucleus and plays a role in transcriptional regulation by interrupting the DNA-binding activity of the small mother against decapentaplegic (Smad) complex, as shown in Figure 1 (36). They reported that nuclear pro-GDF15 attenuates TGF- $\beta$  signaling through the interruption of DNA binding to the Smad complex upon TGF- $\beta$  stimulation

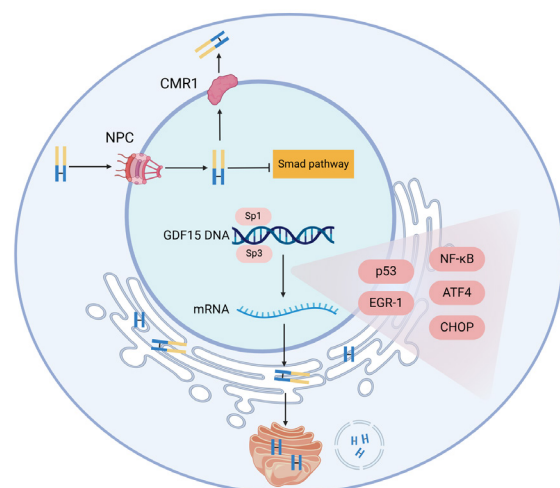


**Figure 1. Synthesis and transcriptional regulation of GDF15.** The basal physiological transcriptional regulation of GDF15 is mediated by Sp1 and Sp3. Pro-GDF15 monomer consists of a propeptide (yellow short-lines) and a mature peptide (blue lines). Two pro-GDF15 monomers form a homodimer linker by disulfide bond (black lines). The maturation of pro-GDF15 occurs in endoplasmic reticulum, through proteolytic cleavage of the pro-GDF15 dimeric at a conserved furin-like site. Pro-GDF15 can translocate from cytoplasm to nucleus by nuclear pore complex (NPC), followed by its exportation by chromosome region maintenance 1 (CMR1). In addition, nuclear pro-GDF15 interrupts the DNA-binding activity of Smad complex.

(36). Moreover, the antitumorigenic activity of GDF15 is increased by blocking the translocation of GDF15 from the cytoplasm to the nucleus (37). Whether this regulation of GDF15 translocation is beneficial for alleviating neurological pathological changes is worthy of further in-depth study.

## 2.2. Transcriptional regulation of GDF15 expression

A promoter analysis revealed a TATA-like motif (TATAAA) upstream of the ATG start codon in the *GDF15* gene, which is conserved among the human, rat and mouse genes (31,38). Numerous transcription factors, including p53, early growth response-1 (EGR-1), nuclear factor kappa-light-chain-enhancer of activated B cells (NF- $\kappa$ B), Sp1 (specificity protein 1), Sp3 (specificity protein 3), and activator proteins 1 and 2, have been identified as transcriptional regulators of GDF15 expression (22,38-40).

Under healthy conditions, the basal physiological transcriptional regulation of GDF15 is mediated by Sp1 and Sp3, and the level of *GDF15* gene expression depends on the availability of specific proteins and cofactors (40). Researchers cloned the GDF15 promoter region and revealed that the region between -133 and +41 base pairs contains three Sp1 binding sites, which confer basal transcription-specific activity of GDF15 expression (40).

p53, a tumor suppressor gene, can transactivate the GDF15 promoter in a p53 dose-dependent and p53 binding site-dependent manner (22). At least two p53 binding sites are present in the GDF15 promoter, both of which can transactivate the GDF15 promoter (22). In glioma cell lines, GDF15 mRNA and protein expression is decreased in cell lines with p53 mutations or deletions (41). GDF15 is an important intercellular mediator of p53-mediated suppression of tumor function. Overexpression or pharmacological induction of p53 strongly upregulates GDF15 expression in lung, osteosarcoma, and prostate cancer cells and in breast cancer cell lines (42-44). However, p53-induced expression of GDF15 also confers resistance to cisplatin in ovarian tumors (45). The biological functions of GDF15 induced by p53 in different tumors may be complex and inconsistent. The phenotypes likely depend on the specific type of cancer cell and stage.

EGR-1, which regulates differentiation, growth, and apoptosis and is significantly upregulated in patients with AD and glioma (46,47), is another transcriptional regulator of GDF15 expression that contains three zinc finger domains. EGR-1 increases GDF15 promoter activity and expression in a dose-dependent manner and thereby contributes to silibinin-induced apoptosis in HT29 colon carcinoma cells (48). Another study reported that troglitazone induces GDF15 expression and correlates with EGR-1 levels; cotransfection and gel shift assays suggested that EGR-1-binding sites are located

within the -73 to -51 region of the GDF15 promoter (39). Furthermore, methylation of the GDF15 promoter at the -53 site blocks EGR-1 binding and thereby suppresses GDF15 induction (49).

Furthermore, NF- $\kappa$ B has been validated as a direct transcriptional regulator of GDF15 that suppresses macrophage-mediated immune surveillance during the early stages of tumorigenesis (50). GDF15 is also regulated by circular RNAs, long noncoding RNAs, microRNAs, hormones and drugs (24,51). In primary mouse hepatocytes, metformin stimulates the secretion of GDF15 by increasing the expression of activating transcription factor 4 (ATF4) and C/EBP homologous protein (CHOP) (52). ATF4 binds to the GDF15 promoter and positively regulates GDF15 expression, which suppresses lipopolysaccharide-induced inflammation in human nasal epithelial cells (53). Importantly, ATF4 levels are increased in both the AD-affected brain and an AD mouse model (54). Under glucose deprivation, ATF4-dependent fructolysis is required to maintain glioblastoma multiforme cell growth (55). These results indicate that the ATF4/GDF15 pathway possibly contributes to the pathogenesis of AD and glioblastoma.

## 2.3. The receptor of GDF15

GFRAL has been identified as the high-affinity receptor of GDF15, which requires the coreceptor rearranged during transfection (RET) to elicit intracellular signaling in response to GDF15 stimulation (56). GFRAL is encoded by the *GFRAL* gene, which is located on the short arm of chromosome 6 in humans; it consists of 9 exons and encodes a 394 amino acid protein (31). GFRAL is a distant member of the TGF- $\beta$  family of receptors, and GDF15 binds to this receptor with high affinity but has no interaction with other members of the TGF- $\beta$  family of receptors (57). *In vivo*, GDF15 induces the activation of neurons in the area postrema (AP) and nucleus tractus solitarius (NTS), which coexpress GFRAL and RET; then, the activated GFRAL-RET heterodimer induces stimulatory phosphorylation of extracellular signal-regulated kinase (ERK) (32). *In vitro*, in a cell line with stable overexpression of human GFRAL and RET, the phosphorylation level of protein kinase B (AKT) was also increased (56).

Current findings concerning tissues expressing GFRAL are inconsistent. Several previous groups reported that the GFRAL transcript is only detected in the brain and is not detected in peripheral tissues. In terms of the temporal and spatial characteristics of mRNA, the GFRAL mRNA level in the cerebral cortex and hippocampus peaks at birth and then decreases, whereas in adult mice, GFRAL transcripts are relatively abundant in the substantia nigra, hippocampus and spinal cord (58). However, a series of subsequent studies provided convincing evidence that GFRAL protein expression occurs only in neurons in the AP and NTS

(32,56,57,59). This expression distribution is conserved in rodents, monkeys and humans(59). These studies also showed that GDF15-mediated reductions in food intake and body weight in obese mice are abolished in GFRAL knockout mice (56,57,59). Emmerson *et al.* reported that increased membrane-type I matrix metalloproteinase (MT1-MMP) activation induced by obesity is an endogenous negative regulator of GFRAL in the context of obesity (60). In addition, treatment with a neutralizing monoclonal antibody against GFRAL prevented the cisplatin-induced decrease in wheel running and accelerated recovery, indicating that the GDF15/GFRAL axis mediates cisplatin-induced fatigue in mice (61). Importantly, recent study not only confirmed the results for GFRAL expression in the brainstem but also revealed that the GFRAL protein is detectable in the prefrontal cortex, hippocampal CA1 region, arcuate nucleus and peripheral tissues (including the liver, small intestine, fat, kidney and muscle tissues) (62). In addition, GFRAL is an endothelial cell receptor for GDF15 because GDF15 signaling events in endothelial cells are blocked by small interfering RNA-mediated knockdown of GFRAL (63).

GDF15, with various biological functions, is widely expressed in the periphery and brain; thus, the widespread expression of its receptor is plausible. The current understanding of the physiological function of the GDF15/GFRAL axis focuses solely on its metabolic effects. We urgently need to determine the distribution of GFRAL expression and the mechanism of action of the GDF15/GFRAL axis under physiological and pathological conditions. In addition, whether other signaling pathways, rather than associations with the GFRAL-RET heterodimer, are involved is another interesting issue.

#### 2.4. Biological functions of GDF15 in brain diseases

GDF15 is expressed at relatively low levels in healthy individuals. However, GDF15 expression can be strongly induced in response to cellular stress during tissue

injury (3). As shown in Figure 2, GDF15 is upregulated in patients with various brain diseases, which is likely associated with the activation of the transcription factors EGR-1, p53, NF-κB, ATF4, and CHOP, resulting in increased survival of neurons and neurogenesis, a reduced inflammatory reaction, increased repair ability after injury, the regulation of energy metabolism, and the promotion or inhibition of tumor growth. In Table 1, we provide a detailed summary of the effects of GDF15 and the associated potential mechanisms in brain diseases.

In humans, the physiological concentration of GDF15 in the serum ranges from 200 to 1200 pg/mL (64), with a positive correlation with age (65). The CSF GDF15 level is positively correlated with the serum GDF15 level in the same subject (66). The author also reported that mature GDF15 protein expression (predominantly localized in neurons) in the hippocampus of older individuals is greater than that in adults, but no differences were observed in the cortex or cerebellum (66). GDF15 may be involved in the regulation of hippocampus-related learning and memory deficits during aging and dementia.

Healthy neonatal and adult rat brain synthesizes GDF15 at the site of choroid plexus epithelial cells, where the GDF15 mRNA can be detected *via in situ* hybridization, after which the protein is secreted into the CSF to nourish the brain and spinal cord neurons (3,17,67). In addition, the GDF15 protein can be visualized in ependymal cells and the subventricular zone (SVZ) (3). The SVZ is one of the major regions involved in adult neurogenesis (68). GDF15 is involved in neurogenesis in the developing brain (69); notably, exogenous GDF15 has also been shown to promote hippocampal adult neural stem cell (NSC) proliferation and neuronal differentiation in an AD model (23).

Following a cryogenic lesion of the cortex, the GDF15 mRNA and protein are highly upregulated in regions adjacent to the lesion site and the dorsal thalamus (3). Colocalization analysis suggested that the upregulated GDF15 protein is predominantly

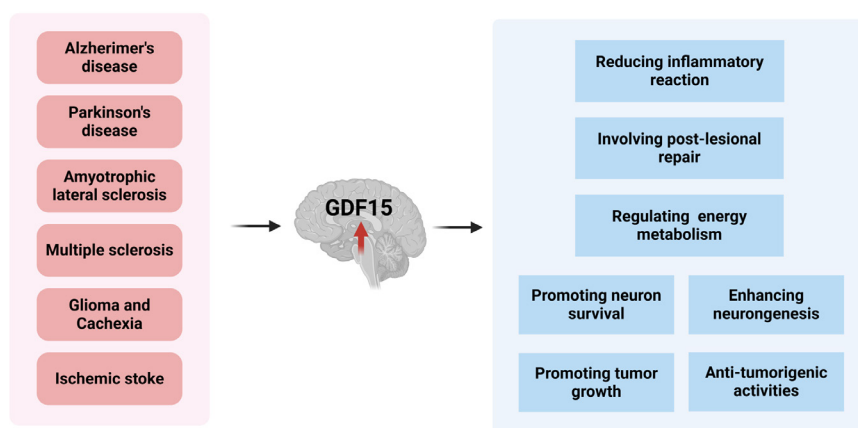


Figure 2. The biological functions of GDF15 in brain diseases.

**Table 1. The effects of GDF15 and associated potential mechanisms on brain diseases**

| Diseases                                   | Effects  | Mechanisms   | References   |
|--|--|--|--|
| AD   | Aβ clearance↑                                      | Increasing the expression of IDE in microglia through TGFβRII; Upregulating IDE and NEP through activation of AKT/GSK-3β/β-catenin pathway   | (14,15)  |
|  | Synaptic activity↑                                 | Unknown  | (23)   |
|  | Hippocampal NSC proliferation and differentiation↑ | Promoting EGFR signaling   | (23,69)  |
|  | Neuronal apoptosis and neuroinflammation↓          | Activating the AKT/GSK-3β/β-catenin pathway; Upregulating SIRT1 expression to inhibit the Nrf2/HO-1 axis   | (15,24)  |
|  | Oxidative stress↓<br>Mitochondria function↑        | Upregulating SIRT1 expression to inhibit the Nrf2/HO-1 axis<br>Unknown   | (24)<br>(66)   |
| PD   | Dopaminergic neurons survival↑                     | Probably acts directly on neurons but not glial cells  | (16,17)  |
|  | Microglial response↑                               | Unknown  | (16)   |
|  | Neuronal apoptosis↓                                | Upregulating PGC1α via p53, dependent on Akt/mTOR phosphorylation  | (84)   |
|  | Mitochondria function↑                             | Upregulating PGC1α via p53; regulating the PI3K/Akt signaling pathway  | (83,84)  |
| MS   | Neuroinflammation↓                                 | Unknown  | (13)   |
| HD   | ER stress-induced apoptosis↓                       | Glucocorticoids inhibit the transcription of GDF15   | (18)   |
| Protumorigenic activity of GDF15 in glioma | Migration and invasion↑                            | Decreasing GDF15 expression inhibits the NF-κB pathway; The invasive capacity is coordinately regulated by RSU-1 and GDF15   | (20,21);<br>(50,92);<br>(94)   |
|  | Proliferation↑<br>Immune escape↑                   | Unknown<br>Inhibiting maturation and function of DCs; Suppressing infiltration and cytotoxicity of T cells, B cells, and NK cells; Interfering with LFA-1/β2-integrin-mediated T cells adhesion to activated endothelial cells | (20,21)<br>(19),20);<br>(25,100)   |
|  | Radioresistance↑                                   | Regulated by the transcription factor WWTR1/TAZ; activating the ERK1/2 pathway   | (93,98)  |
|  | Cancer cachexia                                    | Food intake↓   | Activating hypothalamic neurons through the formation of the GDF15-GFRAL-RET complex |
| Ischemic stroke                            | Atherosclerotic plaque stability↓                  | GDF15 deficiency inhibits CCR2-mediated macrophage chemotaxis  | (28)   |
|  | Atherosclerotic plaque progression↑                | GDF15 deficiency suppresses the IL-6-dependent inflammatory response and decreases cell apoptosis  | (27)   |
|  | Platelet aggregation↓                              | In DVT, GDF15 reduces platelet aggregation induced by ADP in concentration-dependent manner  | (114)  |
|  | Angiogenesis↑                                      | In acute MI, the activation of GDF15-TRPV4 axis can promote angiogenesis   | (115)  |

Abbreviations: ↑ (enhancement); ↓ (inhibition); Alzheimer's disease (AD); Amyloid-β (Aβ); Neural stem cell (NSC); Insulin-degrading enzyme (IDE); Transforming growth factor-β receptor II (TGFβRII); Neprilysin (NEP); Epidermal growth factor receptor (EGFR); Silent information regulator sirtuin 1 (SIRT1); Nuclear respiratory factor (Nrf2); Heme oxygenase 1 (HO-1); Peroxisome proliferator-activated receptor γ co-activator-1 alpha (PGC1α); Parkinson's disease (PD); Phosphoinositide 3-kinase (PI3K); Protein kinase B (AKT); Nuclear factor kappa-light-chain-enhancer of activated B cells (NF-κB); Ras suppressor 1 (RSU-1); Glycogen synthase kinase 3β (GSK-3β); Multiple sclerosis (MS); Huntington's disease (HD); Endoplasmic reticulum (ER); Dendritic cells (DCs); Natural killer cells (NK); Lymphocyte function-associated antigen 1 (LFA-1); WW Domain containing transcription regulator 1 (WWTR1); extracellular signal-regulated kinase (ERK); glial cell-derived neurotrophic factor family receptor α-like (GFRAL); rearranged during transfection (RET); C-C chemokine receptor type 2 (CCR2); Interleukin-6 (IL-6); Deep venous thrombosis (DVT); Adenosine diphosphate (ADP); Myocardial infarction (MI); Transient receptor potential vanilloid 4 (TRPV4)

expressed in lesioned neurons but is expressed in only a few microglia (approximately 15%), not astroglia (3). However, Maikl *et al.* found that GDF15 is an astrocyte-derived trigger of astrocyte remodeling associated with tight junction strengthening at the blood-brain barrier (70). Additionally, treatment with kainic acid increased GDF15 expression in activated astrocytes throughout the hippocampal region, and lipopolysaccharide (100 ng/mL) dramatically increased GDF15 expression in primary astrocytes in a time-dependent manner (71). GDF15 mRNA expression is strongly upregulated in the hippocampus and parietal cortex after an ischemic lesion

caused by occlusion of the middle cerebral artery (72). A similar pattern of GDF15 induction was observed in a cell model of AD, in which GDF15 mRNA and protein levels were specifically increased in cells cocultured with Aβ-treated microglia (14). Thus, extensive evidence suggests that GDF15, a pivotal stress response cytokine, probably exerts positive effects on the repair of brain lesions.

Importantly, GDF15-deficient mice exhibit progressive postnatal losses of spinal cord motor and dorsal root ganglionic neurons, reaching an approximately 20% maximum at 6 months (73). Sensory

neurons in the dorsal root ganglia are also involved, whereas sympathetic neurons are not affected (73). This evidence suggests that GDF15 is an important trophic factor for motor and sensory neurons. Using GDF15 knockout mice, Day *et al.* observed that GDF15 is required for the reductions in food intake, body mass, fasting insulin and glucose intolerance caused by metformin in high-fat diet-fed mice (52). In addition, GDF15 deficiency exacerbates dopaminergic neuron death and reduces the microglial response in a 6-hydroxydopamine (6-OHDA) mouse model of PD (16). The effects of GDF15 on cancers are different and complex, partially depending on the specific type of cancer cell. However, in glioma, high GDF15 expression is an independent risk factor for the overall survival of patients with lower-grade gliomas (21), indicating that GDF15 predicts tumor progression (19). Moreover, many experimental studies support the protumorigenic functions of GDF15 in glioma.

### 3. The roles of GDF15 in neurological diseases

#### 3.1. AD

AD is the most common NDD and is characterized by decreased learning and memory, the deposition and aggregation of A $\beta$ , tau neurofibrillary tangles and neuronal loss. The potential pathogenic mechanisms of AD are not entirely clear. Accumulating evidence indicates that GDF15 is related to cognitive decline, all-cause dementia and the AD risk (11,74-78). GDF15 is also regarded as a biomarker of aging, and the circulating level of GDF15 is positively correlated with age (65). A relationship between serum GDF15 levels and cognitive performance and decline has been reported by Fuchs.

T *et al.*, who investigated a large community-dwelling elder cohort and first reported the association of higher serum GDF15 levels with poorer global cognitive function; their results indicated that the serum GDF15 level is a biomarker of cognitive decline, and an analysis of receiver operating characteristic (ROC) curve revealed that a GDF15 level exceeding 2764 pg/ml was associated with a 20% chance of decline from normal cognition to mild cognitive impairment (MCI) or dementia (11). In addition, two recent studies involving plasma proteomics analysis of healthy adults revealed that GDF15 is one of the genes most strongly associated with the risk of AD and dementia (74,78). In general, GDF15 can be considered a biomarker of age-related cognitive dysfunction. However, the specific potential molecular mechanisms of this regulation are less well known. Conclusive evidence on whether elevated levels of GDF15 are helpful or harmful for cognitive performance is still unavailable.

The expression of mature GDF15 protein is upregulated in the frontal cortex and hippocampus of AD patients (66). Although this study did not discuss the effects and mechanisms of increased levels of endogenous GDF15 in the brains of AD patients, this protein is definitely not detrimental. Exogenous recombinant GDF15 leads to a decrease in A $\beta$  plaque deposition in *in vitro* and *in vivo* models of AD, and this effect is abolished by treatment with a GDF15-specific siRNA(14). Increased GDF15 levels in individuals AD, which potentially indicate neural injury, do not likely represent a cause of the disease but rather a compensatory response to stresses. Increased GDF15 levels are likely a beneficial adaptive reaction to AD-related pathology.

Previous studies have elucidated the potential signaling pathways mediated by GDF15 in the

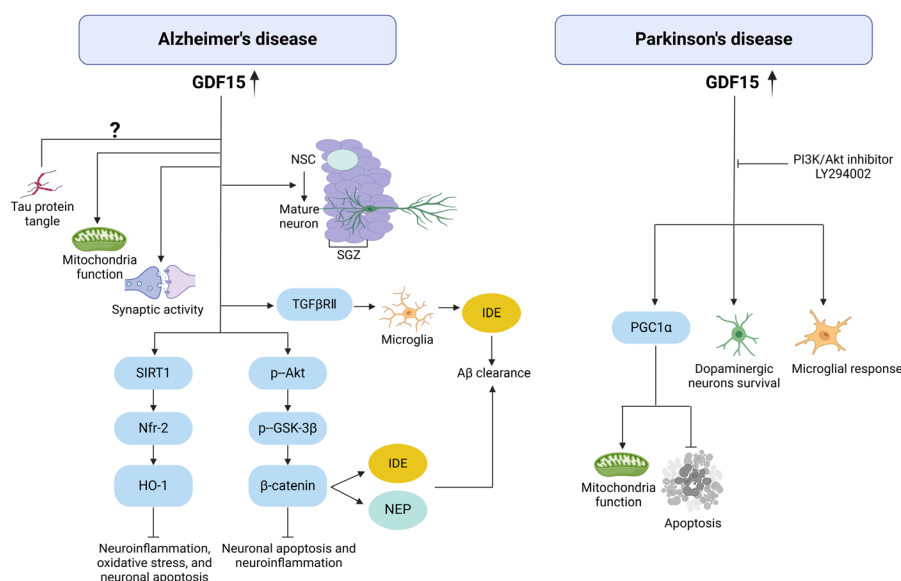


Figure 3. The effects and potential associated pathways of increased GDF15 in Alzheimer's disease and Parkinson's diseases. Neural stem cell (NSC); Subgranular zone (SGZ); Insulin-degrading enzyme (IDE); Transforming growth factor- $\beta$  receptor II (TGF $\beta$ RII); Neprilysin (NEP).

pathogenesis of AD (as shown in Figure 3). In APP/PS1 mice, human umbilical cord blood-derived mesenchymal stem cells (hUCB-MSCs) promoted endogenous adult hippocampal neurogenesis and synaptic activity through the secretion of the paracrine factor GDF15 (23). Notably, in the developing hippocampus, GDF15 promotes epidermal growth factor receptor (EGFR) expression in hippocampal precursors through the activation of active CXCR4 chemokine receptor (CXCR) 4 and the regulation of the proliferation and migration of precursors (69). The inhibition of GDF15 expression in hUCB-MSCs *via* a GDF15 siRNA reduced the proliferation of NSCs, and this effect was restored by the addition of recombinant GDF15 (23). Another study revealed that hUCB-MSCs promote the ability of microglia to clear A $\beta$  through the regulation of GDF15 secretion (14). Moreover, exogenous recombinant GDF15 injection in the hippocampus of 5XFAD mice led to an increase in A $\beta$  degradation through increased insulin-degrading enzyme (IDE) expression in microglia (14). These researchers also reported that this process was mediated by TGF- $\beta$  receptor type II, whereas Mullican *et al.* reported no interaction between the TGF- $\beta$  family receptor and GDF15, except for GFRAL (57). More convincing studies are needed to support these findings. In A $\beta$ 42-treated SH-SY5Y cells, GDF15 derived from mesenchymal stem cells (MSCs) promoted the degradation of the A $\beta$ 42 protein, thereby increasing cell viability and suppressing apoptosis and inflammation through the activation of the AKT/ glycogen synthase kinase 3 $\beta$ (GSK-3 $\beta$ )/ $\beta$ -catenin pathway to upregulate neprilysin (NEP) and IDE (15). In addition, mitochondrial dysfunction has been implicated in the pathophysiology of AD(26), and GDF15 is likely involved in counteracting mitochondrial dysfunction and neuroinflammation in the AD-affected brain (66).

However, the abovementioned studies did not include behavioral experiments to validate improvements in learning and memory abilities. Although exogenous recombinant GDF15 promotes A $\beta$  clearance in both cell and mouse models of AD, the function of endogenously unregulated GDF15 in the AD environment is still unclear. Pathological tau accumulation is another prominent characteristic of AD and is driven by A $\beta$  plaque deposition (79). However, to date, no related studies on how GDF15 affects tau pathology in individuals with AD have been reported.

In contrast, Conte *et al.* reported that plasm GDF15 levels in AD patients are similar to those in controls without dementia (80). One study reported that GDF15 levels are decreased in both APP/PS1 mouse brains and A $\beta$ -treated SH-SY5Y cells (24). We believe that these results should be interpreted with caution because the specific brain areas of APP/PS1 mice analyzed by Western blotting were not noted. The experimental materials and methods used for A $\beta$ -treated cells were inconsistent with those used in previous studies (14). However, these studies also demonstrated the protective

effects of GDF15 on AD, and overexpression of the GDF15 plasmid protected SHSY5Y cells from A $\beta$ -induced inflammation, oxidative stress, and neuronal apoptosis through the silent information regulator sirtuin 1 (SIRT1)/ nuclear respiratory factor (Nrf2)/ heme oxygenase 1(HO-1) axis (24).

We believe that GDF15 expression in the brain likely increases in a compensatory manner under AD conditions to protect neurons from injury caused by AD-related pathology. The stresses that can lead to chronically elevated GDF15 expression may be the same as those that cause the pathogenesis of AD. However, under pathophysiological conditions, the compensatory effect is not sufficient to counteract such severe injury. In centenarians who do not present with cognitive impairment or neuropathological features of AD, functionally mature GDF15 is even more highly secreted than it is in AD patients (66). In these centenarian individuals, the higher expression of GDF15 than in AD patients may delay the onset of age-related diseases such as AD by decades (66). Thus, given the strong association between higher levels of GDF15 and poorer cognitive performance, the upregulation of GDF15 in patients with AD seems to be an unsuccessful attempt to address this issue. Therefore, GDF15 and its involved signaling pathways are potential new therapeutic targets for AD. Recently, GFRAL expression has been detected in the hippocampal CA1 region, but the function of the GDF15/GFRAL axis in the hippocampus of individuals with AD has not been fully elucidated. Whether targeting GFRAL can alleviate AD-related pathology is worthy of further investigation.

### 3.2. PD

PD is an age-related neurodegenerative disorder of unknown origin that ranks second only to AD in prevalence (81). PD neuropathology is characterized by the selective loss of dopaminergic neurons in the substantia nigra pars compacta. The serum GDF15 level is significantly higher in PD patients than in healthy controls (12,82) and is an independent risk factor for the severity of motor symptoms (12). GDF15 is considered a trophic factor for midbrain dopaminergic neurons (as shown in Figure 3). *In vivo*, exogenous application of GDF15 significantly prevents 6-OHDA-mediated pathological rotational behavior and reduces the loss of dopaminergic neurons in the substantia nigra (17). GDF15 may also increase the mitochondrial function and proliferation of neuronal HT22 cells by regulating the phosphoinositide 3-kinase (PI3K)/protein kinase B (Akt) signaling pathway (83). Importantly, endogenous GDF15 can ameliorate the deleterious consequences of 6-OHDA-mediated lesions (16). Compared with that in GDF15<sup>+/+</sup> mice, the reduction in the number of dopaminergic neurons caused by 6-OHDA is aggravated in GDF15-deficient mice, as are the numbers of total

and activated microglia (16). A recent study revealed that overexpression of GDF15 by plasmid transfection protects mitochondrial function and inhibits apoptosis in SH-SY5Y cells treated with rotenone, a broadly used inducer of PD (84). Mechanistically, the neuroprotective effect of GDF15 is mediated by the upregulation of peroxisome proliferator-activated receptor  $\gamma$  coactivator-1 alpha (PGC1 $\alpha$ ) through the regulation of p53, and this effect is eliminated by treatment with the PI3K/Akt-specific inhibitor LY294002 (84).

However, in another 1-methyl-4-phenyl-1,2,3,6-tetrahydropyridine (MPTP)-intoxicated mouse model of PD, the absence of GDF15 did not affect the susceptibility and recovery capacity of dopaminergic neurons in the substantia nigra (85). The authors suggested that this result was caused by the intrinsic difference between the two mouse models (85). In both AD and PD, GDF15 presents a similar pattern of phenotypes and advantages; GDF15 is upregulated and exerts neuroprotective effects. In summary, GDF15 is indispensable for the intrinsic physiological function of dopaminergic neurons. When dopaminergic neurons are lesioned by 6-OHDA and rotenone, GDF15 expression increases, which is mediated by the upregulation of PGC1 $\alpha$  through the regulation of p53. Blocking the PI3K/Akt signaling pathway can eliminate the neuroprotective effects of GDF15.

### 3.3. Other NDDs

ALS is one of the most devastating NDDs and involves the selective loss of upper and lower motor neurons, leading to progressive paralysis. Research on the association between GDF15 and ALS is still in the initial stage. Mutations in the *CHCHD10* gene, which encodes a mitochondrial intermembrane space protein that is upregulated under stress conditions, are rare genetic causes with autosomal dominant inheritance (86). Subsequent research revealed that GDF15 transcripts and proteins are upregulated in the fibroblasts of ALS patients with *CHCHD10* mutations (87). Moreover, Younes *et al.* reported that the transcripts of the GDF15 low-affinity receptors TGF- $\beta$ R1 and TGF- $\beta$ R2, but not the cognate high-affinity receptor GFRAL, are detected in the spinal cord of a mouse model of ALS (88). However, no evidence of interactions between GDF15 and other TGF- $\beta$  family receptors, except for GFRAL, has been reported. In a cell-based PathHunter dimerization assay, GDF15 failed to induce a response in any of the cell lines tested, including those expressing more than twenty TGF- $\beta$  family receptors (57). The role of the GDF15/TGF- $\beta$ R axis in ALS should be carefully examined.

MS is a chronic, immune-mediated NDD. MS patients, especially patients with primary progressive MS, have higher CSF and serum levels of GDF15 than healthy controls do (89,90). Moreover, GDF15 is a

potential biomarker for stable MS, and a longitudinal study (mean observation time of 4.6–5.9 years) revealed that the serum level of GDF15 is significantly higher in patients with stable MS than in those with active MS (13). Increased GDF15 level may reflect an endogenous anti-inflammatory mechanism in patients with stable MS, but this mechanism is disrupted by unknown causes in patients with active MS (13).

In addition, GDF15 can antagonize endoplasmic reticulum stress-induced apoptosis and prevent HD-mediated neurodegeneration in flies through the antiapoptotic functions of glucocorticoids (18).

### 3.4. Glioma

GDF15 is one of the most important molecules in cancers. The effects of GDF15 on cancer development and progression are complicated and different, likely depending on the specific cancer type and stage (91).

In primary brain glioma, the most common type of brain cancer, extensive evidence suggests that GDF15 possesses protumorigenic activity, contributing to proliferation, invasion, metastasis, immune escape and radioresistance (19-21,92-94). Consistent with these findings, the mRNA and protein levels of GDF15 are elevated in glioma patients and are associated with poor clinical outcomes (19,20,95-97). Specifically, in patients with lower-grade gliomas, higher GDF15 expression is significantly associated with a higher histological grade and poorer histology and is an independent risk factor for shorter survival (19,21).

The protumorigenic activities of GDF15 have been documented in many studies. Silencing of GDF15 reduces the proliferation of malignant glioma cells, and the depletion of tumor-secreted GDF15 increases immune surveillance and delays the growth of glioma (20). Exogenous GDF15 stimulates the migration and invasion of glioma cells (94). Moreover, the invasive capacity is coordinately regulated by the relative expression of Ras suppressor 1 (RSU-1) and GDF15 in specific glioma cell lines (H4, SW1088 and A172)(92). Glioma stem cells (GSCs) are characterized by high radioresistance and are highly challenging to treat. High levels of GDF15, regulated by irradiation and WW domain-containing transcription factor 1 (WWTR1/TAZ), promote the intrinsic radioresistance of GSCs, while targeting GDF15 expression and blocking WWTR1/TAZ *via* the specific siRNAs in GSCs sensitizes the cells to irradiation (93). In addition, Zhu *et al.* reported that GDF15 promotes a GSC-like phenotype *via* activation of the ERK1/2 signaling pathway (98).

However, the molecular mechanisms underlying this GDF15 upregulation are less well known. NF- $\kappa$ B directly participates in the production of GDF15, as the colocalization of activated NF- $\kappa$ B and GDF15 was observed in the epithelial ducts of human patients with pancreatic adenocarcinoma (50). Decreasing

GDF15 expression inhibits the invasion and migration of glioma cell lines by regulating the NF- $\kappa$ B pathway (50). Therefore, targeting the expression of tumor-derived GDF15 is a promising therapeutic approach for brain glioma. Notably, GDF15 is also involved in modulating the tumor microenvironment and plays a detrimental immunoinhibitory role; tumor-secreted GDF15 suppresses the activity of macrophages, natural killer (NK) cells and dendritic cells (DCs) and reduces the infiltration of lymphocytes and T cells (25). DCs are antigen-presenting cells that play indispensable roles in antigen-specific immune responses. Tumor-derived GDF15 can suppress the maturation and function of DCs and contribute to tumor immune escape (99). GDF15 inhibits the infiltration and cytotoxicity of immune cells, including T cells, B cells, and NK cells (19,20). GDF15 also interferes with lymphocyte function-associated antigen 1 (LFA-1)/ $\beta$ 2-integrin-mediated T-cell adhesion to activated endothelial cells, while neutralizing antibodies against tumor-induced GDF15 improve both T-cell trafficking and therapeutic efficacy in murine tumor models (100). Thus, neutralizing antibodies against GDF15 may be potential immunotherapeutic strategies for glioma

Conversely, some studies have suggested that GDF15 is a tumor suppressor gene in glioblastoma (49,101). As discussed above, the tumor suppressor gene p53 can transactivate the GDF15 promoter and inhibit tumor cell growth (22). In addition, Kadowaki *et al.* reported that the basal expression of GDF15 in glioblastoma cell lines is low and that GDF15 overexpression significantly increases cell apoptosis. These researchers reported that hypermethylation of specific promoter sequences (-53 and +55 CpG sites) causes the transcriptional silencing of GDF15 (49). The proteasome inhibitor MG132 exerts antiglioblastoma effects by increasing the phosphorylation of protein in the p38 mitogen-activated protein kinase (MAPK) pathway followed by the induction of GDF15 expression (101).

Definite explanations for these conflicting conclusions are still lacking. In fact, in addition to its roles in glioma, GDF15 has dual roles in prostate cancer, breast cancer, gastric cancer and colorectal cancer (25). The effects of GDF15 (tumor-promoting or tumor-inhibiting) may depend on the cancer type and stage. In the early stages of cancer or in lower-grade malignancies, GDF15 seems to inhibit cancer cell growth, while it promotes cancer cell invasion and migration in the late stages or in higher-grade malignancies. Glioblastoma is the most malignant form of glioma, and the degree of malignancy likely results in this discrepancy. Additionally, the source of GDF15 may be another potential reason; compared with tumor-derived GDF15, drug/stress-induced GDF15 likely has opposite effects. Similar to pregnancy, fetal and placenta-derived GDF15, the major sources of GDF15 in maternal blood confirmed by mass spectrometry, are associated with an increased

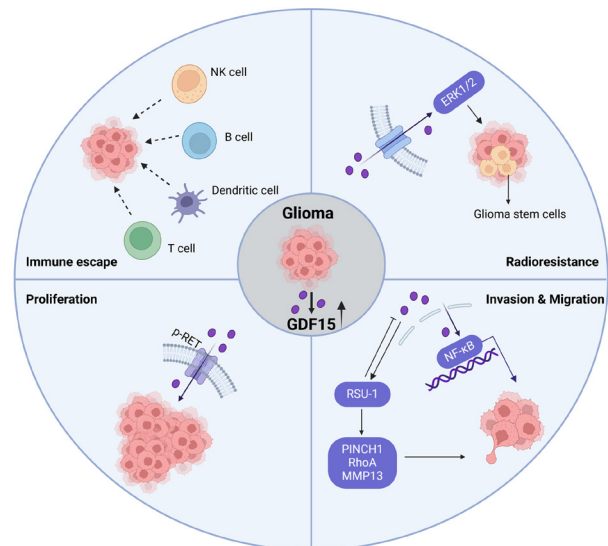


**Figure 4. The protumorigenic activities of tumor-derived GDF15 in glioma.** Including promoting invasion and migration, proliferation, immune escape and radioresistance of tumor cell.

risk of nausea and vomiting during human pregnancy (102). Blocking GDF15 activity in pregnant mothers may be an effective therapy for women suffering from hyperemesis gravidarum. Both tumor and feto-placental unit-derived GDF15 are foreign objects, that differ from individual stress-induced GDF15. Different sources may result in different variants and activities. Further studies can consider the use of mass spectrometry for detection. Notably, validating this supposition using primary neurons cocultured with GDF15 derived from cancer cell lines would be interesting. Most studies have suggested that GDF15 promotes the development of cancers; therefore, we focused on the protumorigenic activity of GDF15 in glioma (as shown in Figure 4), and decreasing tumor-derived GDF15 expression may contribute to suppressing tumor growth and improving patient prognosis. However, high-grade malignant glioma is likely to be an exception.

In the terminal stage of cancer, severe loss of appetite and weight loss are common symptoms that deteriorate the patient's condition and are associated with poor outcomes. Tumor-derived GDF15 was reported to be responsible for cancer cachexia through the activation of hypothalamic neurons, resulting in decreased food intake, which was reversed by antibodies against GDF15 (103). Importantly, Suriben R *et al.* reported a therapeutic antagonistic monoclonal antibody, 3P10, that targets GFRAL and blocks RET signaling by preventing RET recruitment to the GDF15-GFRAL complex (26). In tumor-bearing mice, treatment with 3P10 reversed excessive lipid oxidation and prevented cancer cachexia independently of food intake (26). Nevertheless, detailed studies on the pharmacokinetics of neutralizing antibodies against GDF15 and GFRAL are needed to better understand this therapeutic target.

### 3.5. Ischemic stroke

Ischemic stroke is one of the most prevalent neurological disorders and is characterized by recurrence and high disability and mortality rates. Atrial fibrillation (AF) is a risk factor for ischemic stroke. Importantly, in a cohort of 14,798 AF patients, those with high GDF15 levels were more vulnerable to stroke or systemic embolism events (0.9% vs. 2.03%) (104). In addition to the serum GDF15 level, the genotype and allele frequencies of the GDF15 rs1804826G/T polymorphism are related to ischemic stroke in the Chinese population (105). In addition, several studies have consistently shown that GDF15 is a prognostic biomarker for mortality and unfavorable outcomes after ischemic stroke (106-108). A high baseline serum GDF15 concentration (> 1,800 ng/L) can predict poor clinical outcomes in acute ischemic stroke patients (107). The baseline serum GDF15 concentration is independently associated with 3-month mortality in ischemic stroke patients after acute revascularization therapy (109). The relationships between increased GDF15 levels and depression and cognitive impairment after ischemic stroke have been identified recently (110,111). In contrast, in a prospective study with more than 20 years of follow-up, after controlling for competing events, Bao *et al.* reported that GDF15 is a strong biomarker for all-cause mortality but is less reliable for ischemic stroke (112). Thus, the baseline serum GDF15 concentration can provide additional information for screening ischemic stroke patients at high risk of an unfavorable prognosis.

In an ischemic stroke mouse model generated the occlusion of the middle cerebral artery, the expression of the GDF15 mRNA in the hippocampus and parietal cortex was dramatically upregulated at 3 h and 24 h after lesion induction (72). However, the size of the infarct area in the brain did not differ between GDF15 wild-type and knockout mice, suggesting that upregulated GDF15 may be involved in integrating postlesional responses (72). Although increased GDF15 expression may be associated with the development and progression of ischemic stroke, this increase does not indicate that GDF15 promotes ischemic stroke. A more plausible explanation is that GDF15 acts as a stress response factor involved in the repair of ischemic lesions.

In contrast, patients with carotid artery and cerebral atherosclerosis are more susceptible to ischemic stroke. The vital question is not how to stop the formation of atherosclerosis but rather how to inhibit the progression of unstable plaques complicated with luminal thrombosis. GDF15 deficiency has a beneficial effect on plaque stabilization by inhibiting C-C chemokine receptor type 2 (CCR2)-mediated macrophage chemotaxis and regulating cell death (28). In addition, GDF15 deletion inhibits atherosclerotic progression by regulating cell apoptosis and interleukin-6 (IL-6)-dependent inflammatory responses to vascular injury (27). GDF15

inhibition may be a therapeutic strategy for preventing atherosclerotic plaque progression and ischemic stroke. However, in the late stage of atherosclerosis, GDF15 may exert beneficial effects on atherosclerosis by inhibiting monocyte recruitment and macrophage activation (113).

In patients with deep venous thrombosis (DVT), increased GDF15 levels are associated with an increased thrombus severity and can inhibit platelet aggregation induced by adenosine diphosphate (ADP) *in vitro* in a concentration-dependent manner (114). Moreover, the activation of GDF15/transient receptor potential vanilloid 4 (TRPV4) signaling promotes angiogenesis in individuals with acute myocardial infarction (MI) (115). The antiplatelet aggregation and proangiogenic effects of GDF15 need to be identified in individual with ischemic stroke.

### 4. Concluding remarks and future prospects

In clinical trials, therapies targeting GDF15 show potential in patients with cancer and cachexia. Ponegromab is a humanized monoclonal antibody that is a highly selective and potent inhibitor of GDF-15 (116). In an open-label clinical trial ( $n = 10$ ), participants with cancer and cachexia received 200 mg of ponegromab, which was administered subcutaneously every 3 weeks for 12 weeks (five doses total). Ponegromab is generally safe and well tolerated (117). Ponegromab prominently reduce serum GDF-15 concentrations (117). Recently, researchers published findings from a randomized, double-blind, 12-week phase 2 clinical trial, and reported that ponegromab results in increased weight gain and appetite, along with ameliorated cachexia symptoms and improved physical activity (118). Visugromab (CTL-002) is a GDF-15 neutralizing IgG4 monoclonal antibody, that can suppress the growth of tumors and displays promising clinical activities when used as neoadjuvant immunotherapy for advanced/metastatic relapsed/refractory tumors (119). In addition, a therapeutic antagonistic monoclonal antibody against GFRAL, 3P10, inhibits GDF15-driven GFRAL-RET signaling by preventing RET recruitment to the GDF15-GFRAL complex on the cell surface (26). In HT1080 mice, 3P10 reversed metabolic changes and weight loss induced by tumors, independent of food intake (26). However, several limitations of GDF15/GFRAL neutralizing antibodies in practical clinical applications should be acknowledged. First, the safety and efficacy of these treatments must be validated in a larger cohort of patients with cancer. Second, all three of these monoclonal antibodies produce a marked effect by blocking the interaction of GDF15 with GFRAL, which is likely applicable only to patients with elevated serum GDF15 levels. In glioblastoma cell lines and primary oligodendroglioma tumors, the basal expression of GDF15 is low, through DNA methylation-mediated transcriptional silencing (49). In these patients,

the abovementioned monoclonal antibodies may be ineffective. Third, whether these drugs can pass through the blood-brain barrier is another worthwhile problem to solve. Finally, we believe that upregulated GDF15 may be a double-edged sword; on the one hand, it exerts neuroprotective effects on NDDs and ischemic stroke; on the other hand, it is detrimental to tumor inhibition. We suppose that these effects likely depend in part on the source of GDF15; the former, which is induced by intrinsic stress responses, plays protective roles, whereas the latter, which is derived from deleterious tumors, plays harmful roles. Thus, the actual clinical value of GDF15 is likely to depend on the specific type of disease. In NDDs, additional exogenous recombinant GDF15 seems to be protective. Notably, close monitoring of the onset of tumors is essential when exogenous GDF15 is administered to treat neurological diseases.

In summary, although most of the available preclinical evidence initially showed that targeting GDF15 and related pathways has promising clinical application prospects in the treatment of brain diseases, especially AD, PD, glioma and cancer cachexia, several key problems remain to be solved. To date, we understand only the metabolic effects of the GDF15/GFRAL axis; thus, identifying further physiological functions is the top priority. In addition to the GDF15/GFRAL axis, the other potential signaling pathways affected by GDF15 need to be clarified. In addition, the efficacy and safety of these targets in humans need to be thoroughly studied in the future. Further studies should review and correct the controversial findings concerning GDF15 in glioma.

**Funding:** This work was supported by the Fundamental Research Funds for the Central Universities (item number: 2019kfyXKJC055), the National Key Research and Development Program of China (Project No. 2020YFC2004803), the Tongji Hospital Scientific Research Fund (2022A19) and the National Natural Science Foundation of China (Project No. 82371442).

**Conflict of Interest:** The authors have no conflicts of interest to disclose.

## References

- DiLuca M, Olesen J. The cost of brain diseases: a burden or a challenge? *Neuron*. 2014; 82:1205-1208.
- Raggi A, Leonardi M. Burden of brain disorders in Europe in 2017 and comparison with other non-communicable disease groups. *J Neurol Neurosurg Psychiatry*. 2020; 91:104-105.
- Schober A, Böttner M, Strelau J, Kinscherf R, Bonaterra GA, Barth M, Schilling L, Fairlie WD, Breit SN, Unsicker K. Expression of growth differentiation factor-15/macrophage inhibitory cytokine-1 (GDF-15/MIC-1) in the perinatal, adult, and injured rat brain. *J Comp Neurol*. 2001; 439:32-45.
- Conte M, Giuliani C, Chiariello A, Iannuzzi V, Franceschi C, Salvioli S. GDF15, an emerging key player in human aging. *Ageing Res Rev*. 2022; 75:101569.
- Burtscher J, Soltany A, Visavadiya NP, Burtscher M, Millet GP, Khoramipour K, Khamoui AV. Mitochondrial stress and mitokines in aging. *Aging cell*. 2023; 22:e13770.
- Xue XH, Tao LL, Su DQ, Guo CJ, Liu H. Diagnostic utility of GDF15 in neurodegenerative diseases: A systematic review and meta-analysis. *Brain Behav*. 2022; 12:e2502.
- Giudici KV, de Souto Barreto P, Guyonnet S, Morley JE, Nguyen AD, Aggarwal G, Parini A, Li Y, Bateman RJ, Vellas B. TNFR-1 and GDF-15 Are Associated With Plasma Neurofilament Light Chain and Progranulin Among Community-Dwelling Older Adults: A Secondary Analysis of the MAPT Study. *J Gerontol A Biol Sci Med Sci*. 2023; 78:569-578.
- Tsai VWW, Husaini Y, Sainsbury A, Brown DA, Breit SN. The MIC-1/GDF15-GFRAL Pathway in Energy Homeostasis: Implications for Obesity, Cachexia, and Other Associated Diseases. *Cell Metab*. 2018; 28:353-368.
- Baek SJ, Eling T. Growth differentiation factor 15 (GDF15): A survival protein with therapeutic potential in metabolic diseases. *Pharmacol Ther*. 2019; 198:46-58.
- Eddy AC, Trask AJ. Growth differentiation factor-15 and its role in diabetes and cardiovascular disease. *Cytokine Growth Factor Rev*. 2021; 57:11-18.
- Fuchs T, Trollor JN, Crawford J, Brown DA, Baune BT, Samaras K, Campbell L, Breit SN, Brodaty H, Sachdev P, Smith E. Macrophage inhibitory cytokine-1 is associated with cognitive impairment and predicts cognitive decline - the Sydney Memory and Aging Study. *Aging cell*. 2013; 12:882-889.
- Yao X, Wang D, Zhang L, Wang L, Zhao Z, Chen S, Wang X, Yue T, Liu Y. Serum Growth Differentiation Factor 15 in Parkinson Disease. *Neurodegener Dis*. 2017; 17:251-260.
- Amstad A, Coray M, Frick C, Barro C, Oechtering J, Amann M, Wischhusen J, Kappos L, Naegelin Y, Kuhle J, Mehling M. Growth differentiation factor 15 is increased in stable MS. *Neurol Neuroimmunol Neuroinflamm*. 2020; 7:e675.
- Kim DH, Lee D, Lim H, Choi SJ, Oh W, Yang YS, Chang JH, Jeon HB. Effect of growth differentiation factor-15 secreted by human umbilical cord blood-derived mesenchymal stem cells on amyloid beta levels in *in vitro* and *in vivo* models of Alzheimer's disease. *Biochem Biophys Res Commun*. 2018; 504:933-940.
- Xiong WP, Yao WQ, Wang B, Liu K. BMSCs-exosomes containing GDF-15 alleviated SH-SY5Y cell injury model of Alzheimer's disease via AKT/GSK-3 $\beta$ / $\beta$ -catenin. *Brain Res Bull*. 2021; 177:92-102.
- Machado V, Haas SJ, von Bohlen Und Halbach O, Wree A, Krieglstein K, Unsicker K, Spittau B. Growth/differentiation factor-15 deficiency compromises dopaminergic neuron survival and microglial response in the 6-hydroxydopamine mouse model of Parkinson's disease. *Neurobiol Dis*. 2016; 88:1-15.
- Strelau J, Sullivan A, Böttner M, Lingor P, Falkenstein E, Suter-Crazzolara C, Galter D, Jaszai J, Krieglstein K, Unsicker K. Growth/differentiation factor-15/macrophage inhibitory cytokine-1 is a novel trophic factor for midbrain dopaminergic neurons *in vivo*. *J Neurosci*. 2000; 20:8597-8603.
- Varadarajan S, Breda C, Smalley JL, Butterworth M,

- Farrow SN, Giorgini F, Cohen GM. The transrepression arm of glucocorticoid receptor signaling is protective in mutant huntingtin-mediated neurodegeneration. *Cell Death Differ.* 2015; 22:1388-1396.
19. Guo L, Chen Y, Hu S, Gao L, Tang N, Liu R, Qin Y, Ren C, Du S. GDF15 expression in glioma is associated with malignant progression, immune microenvironment, and serves as a prognostic factor. *CNS Neurosci Ther.* 2022; 28:158-171.
  20. Roth P, Junker M, Tritschler I, Mittelbronn M, Dombrowski Y, Breit SN, Tabatabai G, Wick W, Weller M, Wischhusen J. GDF-15 contributes to proliferation and immune escape of malignant gliomas. *Clin Cancer Res.* 2010; 16:3851-3859.
  21. Wang Y, Chen J, Chen C, Peng H, Lin X, Zhao Q, Chen S, Wang X. Growth differentiation factor-15 overexpression promotes cell proliferation and predicts poor prognosis in cerebral lower-grade gliomas correlated with hypoxia and glycolysis signature. *Life Sci.* 2022; 302:120645.
  22. Tan M, Wang Y, Guan K, Sun Y. PTGF-beta, a type beta transforming growth factor (TGF-beta) superfamily member, is a p53 target gene that inhibits tumor cell growth *via* TGF-beta signaling pathway. *Proc Natl Acad Sci U S A.* 2000; 97:109-114.
  23. Kim DH, Lee D, Chang EH, Kim JH, Hwang JW, Kim JY, Kyung JW, Kim SH, Oh JS, Shim SM, Na DL, Oh W, Chang JW. GDF-15 secreted from human umbilical cord blood mesenchymal stem cells delivered through the cerebrospinal fluid promotes hippocampal neurogenesis and synaptic activity in an Alzheimer's disease model. *Stem Cells Dev.* 2015; 24:2378-2390.
  24. Xiong W, Li D, Feng Y, Jia C, Zhang X, Liu Z. CircLPAR1 Promotes Neuroinflammation and Oxidative Stress in APP/PS1 Mice by Inhibiting SIRT1/Nrf-2/HO-1 Axis Through Destabilizing GDF-15 mRNA. *Mol Neurobiol.* 2023; 60:2236-2251.
  25. Siddiqui JA, Pothuraju R, Khan P, Sharma G, Muniyan S, Seshacharyulu P, Jain M, Nasser MW, Batra SK. Pathophysiological role of growth differentiation factor 15 (GDF15) in obesity, cancer, and cachexia. *Cytokine & growth factor reviews.* 2022; 64:71-83.
  26. Suriben R, Chen M, Higbee J, *et al.* Antibody-mediated inhibition of GDF15-GFRAL activity reverses cancer cachexia in mice. *Nat Med.* 2020; 26:1264-1270.
  27. Bonaterra GA, Zügel S, Thogersen J, Walter SA, Haberkorn U, Strelau J, Kinscherf R. Growth differentiation factor-15 deficiency inhibits atherosclerosis progression by regulating interleukin-6-dependent inflammatory response to vascular injury. *J Am Heart Assoc.* 2012; 1:e002550.
  28. de Jager SC, Bermúdez B, Bot I, *et al.* Growth differentiation factor 15 deficiency protects against atherosclerosis by attenuating CCR2-mediated macrophage chemotaxis. *J Exp Med.* 2011; 208:217-225.
  29. Lawton LN, Bonaldo MF, Jelenc PC, Qiu L, Baumes SA, Marcelino RA, de Jesus GM, Wellington S, Knowles JA, Warburton D, Brown S, Soares MB. Identification of a novel member of the TGF-beta superfamily highly expressed in human placenta. *Gene.* 1997; 203:17-26.
  30. Bootcov MR, Bauskin AR, Valenzuela SM, *et al.* MIC-1, a novel macrophage inhibitory cytokine, is a divergent member of the TGF-beta superfamily. *Proc Natl Acad Sci U S A.* 1997; 94:11514-11519.
  31. Lockhart SM, Saudek V, O'Rahilly S. GDF15: A Hormone Conveying Somatic Distress to the Brain. *Endocr Rev.* 2020; 41.
  32. Hsu JY, Crawley S, Chen M, *et al.* Non-homeostatic body weight regulation through a brainstem-restricted receptor for GDF15. *Nature.* 2017; 550:255-259.
  33. Bauskin AR, Zhang HP, Fairlie WD, He XY, Russell PK, Moore AG, Brown DA, Stanley KK, Breit SN. The propeptide of macrophage inhibitory cytokine (MIC-1), a TGF-beta superfamily member, acts as a quality control determinant for correctly folded MIC-1. *EMBOJ.* 2000; 19:2212-2220.
  34. Fairlie WD, Moore AG, Bauskin AR, Russell PK, Zhang HP, Breit SN. MIC-1 is a novel TGF-beta superfamily cytokine associated with macrophage activation. *J Leukoc Biol.* 1999; 65:2-5.
  35. Couture F, Sabbagh R, Kwiatkowska A, Desjardins R, Guay SP, Bouchard L, Day R. PACE4 Undergoes an Oncogenic Alternative Splicing Switch in Cancer. *Cancer Res.* 2017; 77:6863-6879.
  36. Min KW, Liggett JL, Silva G, Wu WW, Wang R, Shen RF, Eling TE, Baek SJ. NAG-1/GDF15 accumulates in the nucleus and modulates transcriptional regulation of the Smad pathway. *Oncogene.* 2016; 35:377-388.
  37. Lee J, Kim I, Yoo E, Baek SJ. Competitive inhibition by NAG-1/GDF-15 NLS peptide enhances its anti-cancer activity. *Biochem Biophys Res Commun.* 2019; 519:29-34.
  38. Böttner M, Laaff M, Schechinger B, Rappold G, Unsicker K, Suter-Crazzolara C. Characterization of the rat, mouse, and human genes of growth/differentiation factor-15/ macrophage inhibiting cytokine-1 (GDF-15/MIC-1). *Gene.* 1999; 237:105-111.
  39. Baek SJ, Kim JS, Nixon JB, DiAugustine RP, Eling TE. Expression of NAG-1, a transforming growth factor-beta superfamily member, by troglitazone requires the early growth response gene EGR-1. *J Biol Chem.* 2004; 279:6883-6892.
  40. Baek SJ, Horowitz JM, Eling TE. Molecular cloning and characterization of human nonsteroidal anti-inflammatory drug-activated gene promoter. Basal transcription is mediated by Sp1 and Sp3. *J Biol Chem.* 2001; 276:33384-33392.
  41. Strelau J, Schmeer C, Peterziel H, Sackmann T, Herold-Mende C, Steiner H, Weller M, Unsicker K. Expression and putative functions of GDF-15, a member of the TGF-beta superfamily, in human glioma and glioblastoma cell lines. *Cancer Lett.* 2008; 270:30-39.
  42. Li PX, Wong J, Ayed A, Ngo D, Brade AM, Arrowsmith C, Austin RC, Klamut HJ. Placental transforming growth factor-beta is a downstream mediator of the growth arrest and apoptotic response of tumor cells to DNA damage and p53 overexpression. *J Biol Chem.* 2000; 275:20127-20135.
  43. Kannan K, Amariglio N, Rechavi G, Givol D. Profile of gene expression regulated by induced p53: connection to the TGF-beta family. *FEBS Lett.* 2000; 470:77-82.
  44. Cheng JC, Chang HM, Leung PC. Wild-type p53 attenuates cancer cell motility by inducing growth differentiation factor-15 expression. *Endocrinology.* 2011; 152:2987-2995.
  45. Izaguirre DI, Ng CW, Kwan SY, Kun EH, Tsang YTM, Gershenson DM, Wong KK. The Role of GDF15 in Regulating the Canonical Pathways of the Tumor Microenvironment in Wild-Type p53 Ovarian Tumor and Its Response to Chemotherapy. *Cancers.* 2020; 12:3043.
  46. Gómez Ravetti M, Rosso OA, Berretta R, Moscato P.

- Uncovering molecular biomarkers that correlate cognitive decline with the changes of hippocampus' gene expression profiles in Alzheimer's disease. *PLoS One*. 2010; 5:e10153.
47. Choi BH, Kim CG, Bae YS, Lim Y, Lee YH, Shin SY. p21 Waf1/Cip1 expression by curcumin in U-87MG human glioma cells: role of early growth response-1 expression. *Cancer Res*. 2008; 68:1369-1377.
  48. Woo SM, Min KJ, Kim S, Park JW, Kim DE, Chun KS, Kim YH, Lee TJ, Kim SH, Choi YH, Chang JS, Kwon TK. Silibinin induces apoptosis of HT29 colon carcinoma cells through early growth response-1 (EGR-1)-mediated non-steroidal anti-inflammatory drug-activated gene-1 (NAG-1) up-regulation. *Chem Biol Interact*. 2014; 211:36-43.
  49. Kadowaki M, Yoshioka H, Kamitani H, Watanabe T, Wade PA, Eling TE. DNA methylation-mediated silencing of nonsteroidal anti-inflammatory drug-activated gene (NAG-1/GDF15) in glioma cell lines. *Int J Cancer*. 2012; 130:267-277.
  50. Ratnam NM, Peterson JM, Talbert EE, Ladner KJ, Rajasekera PV, Schmidt CR, Dillhoff ME, Swanson BJ, Haverick E, Kladney RD, Williams TM, Leone GW, Wang DJ, Guttridge DC. NF- $\kappa$ B regulates GDF-15 to suppress macrophage surveillance during early tumor development. *J Clin Invest*. 2017; 127:3796-3809.
  51. Jiang WW, Zhang ZZ, He PP, Jiang LP, Chen JZ, Zhang XT, Hu M, Zhang YK, Ouyang XP. Emerging roles of growth differentiation factor-15 in brain disorders (Review). *Exp Ther Med*. 2021; 22:1270.
  52. Day EA, Ford RJ, Smith BK, *et al*. Metformin-induced increases in GDF15 are important for suppressing appetite and promoting weight loss. *Nat Metab*. 2019; 1:1202-1208.
  53. Li A, Zhao F, Zhao Y, Liu H, Wang Z. ATF4-mediated GDF15 suppresses LPS-induced inflammation and MUC5AC in human nasal epithelial cells through the PI3K/Akt pathway. *Life Sci*. 2021; 275:119356.
  54. Wei N, Zhu LQ, Liu D. ATF4: A Novel Potential Therapeutic Target for Alzheimer's Disease. *Mol Neurobiol*. 2015; 52:1765-1770.
  55. Chen C, Zhang Z, Liu C, Wang B, Liu P, Fang S, Yang F, You Y, Li X. ATF4-dependent fructolysis fuels growth of glioblastoma multiforme. *Nat Commun*. 2022; 13:6108.
  56. Yang L, Chang CC, Sun Z, *et al*. GFRAL is the receptor for GDF15 and is required for the anti-obesity effects of the ligand. *Nat Med*. 2017; 23:1158-1166.
  57. Mullican SE, Lin-Schmidt X, Chin CN, *et al*. GFRAL is the receptor for GDF15 and the ligand promotes weight loss in mice and nonhuman primates. *Nat Med*. 2017; 23:1150-1157.
  58. Li Z, Wang B, Wu X, Cheng SY, Paraoan L, Zhou J. Identification, expression and functional characterization of the GRAL gene. *J Neurochem*. 2005; 95:361-376.
  59. Emmerson PJ, Wang F, Du Y, *et al*. The metabolic effects of GDF15 are mediated by the orphan receptor GFRAL. *Nat Med*. 2017; 23:1215-1219.
  60. Chow CFW, Guo X, Asthana P, *et al*. Body weight regulation *via* MT1-MMP-mediated cleavage of GFRAL. *Nat Metab*. 2022; 4:203-212.
  61. Chelette B, Chidomere CL, Dantzer R. The GDF15-GFRAL axis mediates chemotherapy-induced fatigue in mice. *Brain Behav Immun*. 2023; 108:45-54.
  62. Fichtner K, Kalwa H, Lin MM, Gong Y, Müglitz A, Kluge M, Krügel U. GFRAL Is Widely Distributed in the Brain and Peripheral Tissues of Mice. *Nutrients*. 2024; 16.
  63. Lee J, Jin YJ, Lee MS, Kim YM, Lee H. Macrophage inhibitory cytokine-1 promotes angiogenesis by eliciting the GFRAL-mediated endothelial cell signaling. *J Cell Physiol*. 2021; 236:4008-4023.
  64. Wiklund FE, Bennet AM, Magnusson PK, Eriksson UK, Lindmark F, Wu L, Yaghoutifam N, Marquis CP, Stattin P, Pedersen NL, Adami HO, Grönberg H, Breit SN, Brown DA. Macrophage inhibitory cytokine-1 (MIC-1/GDF15): a new marker of all-cause mortality. *Aging cell*. 2010; 9:1057-1064.
  65. Cimino I, Kim H, Tung YCL, *et al*. Activation of the hypothalamic-pituitary-adrenal axis by exogenous and endogenous GDF15. *Proc Natl Acad Sci U S A*. 2021; 118:e2106868118.
  66. Chiariello A, Valente S, Pasquinelli G, *et al*. The expression pattern of GDF15 in human brain changes during aging and in Alzheimer's disease. *Front Aging Neurosci*. 2022; 14:1058665.
  67. Böttner M, Suter-Crazzolara C, Schober A, Unsicker K. Expression of a novel member of the TGF- $\beta$  superfamily, growth/differentiation factor-15/macrophage-inhibiting cytokine-1 (GDF-15/MIC-1) in adult rat tissues. *Cell Tissue Res*. 1999; 297:103-110.
  68. Tong CK, Alvarez-Buylla A. SnapShot: adult neurogenesis in the V-SVZ. *Neuron*. 2014; 81:220-220.e221.
  69. Carrillo-García C, Prochnow S, Simeonova IK, Strelau J, Hölzl-Wenig G, Mandl C, Unsicker K, von Bohlen Und Halbach O, Ciccolini F. Growth/differentiation factor 15 promotes EGFR signalling, and regulates proliferation and migration in the hippocampus of neonatal and young adult mice. *Development*. 2014; 141:773-783.
  70. Malik VA, Zajicek F, Mittmann LA, Klaus J, Unterseer S, Rajkumar S, Pütz B, Deussing JM, Neumann ID, Rupperecht R, Di Benedetto B. GDF15 promotes simultaneous astrocyte remodeling and tight junction strengthening at the blood-brain barrier. *J Neurosci Res*. 2020; 98:1433-1456.
  71. Yi MH, Zhang E, Baek H, Kim S, Shin N, Kang JW, Lee S, Oh SH, Kim DW. Growth Differentiation Factor 15 Expression in Astrocytes After Excitotoxic Lesion in the Mouse Hippocampus. *Exp Neurobiol*. 2015; 24:133-138.
  72. Schindowski K, von Bohlen und Halbach O, Strelau J, Ridder DA, Herrmann O, Schober A, Schwaninger M, Unsicker K. Regulation of GDF-15, a distant TGF- $\beta$  superfamily member, in a mouse model of cerebral ischemia. *Cell Tissue Res*. 2011; 343:399-409.
  73. Strelau J, Strzelczyk A, Rusu P, Bendner G, Wiese S, Diella F, Altick AL, von Bartheld CS, Klein R, Sendtner M, Unsicker K. Progressive postnatal motoneuron loss in mice lacking GDF-15. *J Neurosci*. 2009; 29:13640-13648.
  74. Guo Y, You J, Zhang Y, Liu WS, Huang YY, Zhang YR, Zhang W, Dong Q, Feng JF, Cheng W, Yu JT. Plasma proteomic profiles predict future dementia in healthy adults. *Nat Aging*. 2024; 4:247-260.
  75. Wu PF, Zhang XH, Zhou P, Yin R, Zhou XT, Zhang W. Growth Differentiation Factor 15 Is Associated With Alzheimer's Disease Risk. *Front Genet*. 2021; 12:700371.
  76. McGrath ER, Himali JJ, Levy D, Conner SC, DeCarli C, Pase MP, Ninomiya T, Ohara T, Courchesne P, Satizabal CL, Vasani RS, Beiser AS, Seshadri S. Growth Differentiation Factor 15 and NT-proBNP as Blood-Based Markers of Vascular Brain Injury and Dementia. *J Am Heart Assoc*. 2020; 9:e014659.
  77. Lu WH, Gonzalez-Bautista E, Guyonnet S, Lucas A, Parini A, Walston JD, Vellas B, de Souto Barreto P. Plasma inflammation-related biomarkers are associated

- with intrinsic capacity in community-dwelling older adults. *J Cachexia Sarcopenia Muscle*. 2023; 14:930-939.
78. Walker KA, Chen J, Shi L, *et al*. Proteomics analysis of plasma from middle-aged adults identifies protein markers of dementia risk in later life. *Sci Transl Med*. 2023; 15:eadf5681.
  79. Hardy J, Allsop D. Amyloid deposition as the central event in the aetiology of Alzheimer's disease. *Trends Pharmacol Sci*. 1991; 12:383-388.
  80. Conte M, Sabbatinelli J, Chiariello A, Martucci M, Santoro A, Monti D, Arcaro M, Galimberti D, Scarpini E, Bonfigli AR, Giuliani A, Olivieri F, Franceschi C, Salvioli S. Disease-specific plasma levels of mitokines FGF21, GDF15, and Humanin in type II diabetes and Alzheimer's disease in comparison with healthy aging. *Geroscience*. 2021; 43:985-1001.
  81. Miller DB, O'Callaghan JP. Biomarkers of Parkinson's disease: Present and future. *Metabolism*. 2015; 64:S40-46.
  82. Miyaue N, Yabe H, Nagai M. Serum growth differentiation factor 15, but not lactate, is elevated in patients with Parkinson's disease. *J Neurol Sci*. 2020; 409:116616.
  83. Liu H, Liu J, Si L, Guo C, Liu W, Liu Y. GDF-15 promotes mitochondrial function and proliferation in neuronal HT22 cells. *J Cell Biochem*. 2019; 120:10530-10547.
  84. Li P, Lv H, Zhang B, Duan R, Zhang X, Lin P, Song C, Liu Y. Growth Differentiation Factor 15 Protects SH-SY5Y Cells From Rotenone-Induced Toxicity by Suppressing Mitochondrial Apoptosis. *Front Aging Neurosci*. 2022; 14:869558.
  85. Machado V, Gilsbach R, Das R, Schober A, Bogatyreva L, Hauschke D, Kriegelstein K, Unsicker K, Spittau B. Gdf-15 deficiency does not alter vulnerability of nigrostriatal dopaminergic system in MPTP-intoxicated mice. *Cell Tissue Res*. 2016; 365:209-223.
  86. Müller K, Andersen PM, Hübers A, Marroquin N, Volk AE, Danzer KM, Meitinger T, Ludolph AC, Strom TM, Weishaupt JH. Two novel mutations in conserved codons indicate that CHCHD10 is a gene associated with motor neuron disease. *Brain*. 2014; 137:e309.
  87. Straub IR, Weraarpachai W, Shoubridge EA. Multi-OMICs study of a CHCHD10 variant causing ALS demonstrates metabolic rewiring and activation of endoplasmic reticulum and mitochondrial unfolded protein responses. *Hum Mol Genet*. 2021; 30:687-705.
  88. Younes R, Issa Y, Jdaa N, Chouaib B, Brugiotti V, Challuau D, Raoul C, Scamps F, Cuisinier F, Hilaire C. The Secretome of Human Dental Pulp Stem Cells and Its Components GDF15 and HB-EGF Protect Amyotrophic Lateral Sclerosis Motoneurons against Death. *Biomedicines*. 2023; 11:2152.
  89. Kosa P, Wu T, Phillips J, Leinonen M, Masvekar R, Komori M, Wichman A, Sandford M, Bielekova B. Idebenone does not inhibit disability progression in primary progressive MS. *Mult Scler Relat Disord*. 2020; 45:102434.
  90. Baeva ME, Tottenham I, Koch M, Camara-Lemarroy C. Biomarkers of disability worsening in inactive primary progressive multiple sclerosis. *J Neuroimmunol*. 2024; 387:578268.
  91. Hasanpour Segherlou Z, Nouri-Vaskeh M, Noroozi Guilandehi S, Baghbanzadeh A, Zand R, Baradaran B, Zarei M. GDF-15: Diagnostic, prognostic, and therapeutic significance in glioblastoma multiforme. *J Cell Physiol*. 2021; 236:5564-5581.
  92. Louca M, Gkretsi V, Stylianopoulos T. Coordinated Expression of Ras Suppressor 1 (RSU-1) and Growth Differentiation Factor 15 (GDF15) Affects Glioma Cell Invasion. *Cancers*. 2019; 11:1159
  93. Bentaberry-Rosa A, Nicaise Y, Delmas C, Gouazé-Andersson V, Cohen-Jonathan-Moyal E, Seva C. Overexpression of Growth Differentiation Factor 15 in Glioblastoma Stem Cells Promotes Their Radioresistance. *Cancers*. 2023; 16:27.
  94. Codó P, Weller M, Kaulich K, Schraivogel D, Silginer M, Reifenberger G, Meister G, Roth P. Control of glioma cell migration and invasiveness by GDF-15. *Oncotarget*. 2016; 7:7732-7746.
  95. Scrideli CA, Carlotti CG, Jr., Okamoto OK, Andrade VS, Cortez MA, Motta FJ, Lucio-Eterovic AK, Neder L, Rosemberg S, Oba-Shinjo SM, Marie SK, Tone LG. Gene expression profile analysis of primary glioblastomas and non-neoplastic brain tissue: identification of potential target genes by oligonucleotide microarray and real-time quantitative PCR. *J Neurooncol*. 2008; 88:281-291.
  96. Shnaper S, Desbaillets I, Brown DA, Murat A, Migliavacca E, Schlupe M, Ostermann S, Hamou MF, Stupp R, Breit SN, de Tribolet N, Hegi ME. Elevated levels of MIC-1/GDF15 in the cerebrospinal fluid of patients are associated with glioblastoma and worse outcome. *Int J Cancer*. 2009; 125:2624-2630.
  97. Tsai SF, Tao M, Ho LI, Chiou TW, Lin SZ, Su HL, Harn HJ. Isochahulactone-induced DDIT3 causes ER stress-PERK independent apoptosis in glioblastoma multiforme cells. *Oncotarget*. 2017; 8:4051-4061.
  98. Zhu S, Yang N, Guan Y, Wang X, Zang G, Lv X, Deng S, Wang W, Li T, Chen J. GDF15 promotes glioma stem cell-like phenotype *via* regulation of ERK1/2-c-Fos-LIF signaling. *Cell Death Discov*. 2021; 7:3.
  99. Zhou Z, Li W, Song Y, Wang L, Zhang K, Yang J, Zhang W, Su H, Zhang Y. Growth differentiation factor-15 suppresses maturation and function of dendritic cells and inhibits tumor-specific immune response. *PloS One*. 2013; 8:e78618.
  100. Haake M, Haack B, Schäfer T, *et al*. Tumor-derived GDF-15 blocks LFA-1 dependent T cell recruitment and suppresses responses to anti-PD-1 treatment. *Nat Commun*. 2023; 14:4253.
  101. Shimizu S, Kadowaki M, Yoshioka H, Kambe A, Watanabe T, Kinyamu HK, Eling TE. Proteasome inhibitor MG132 induces NAG-1/GDF15 expression through the p38 MAPK pathway in glioblastoma cells. *Biochem Biophys Res Commun*. 2013; 430:1277-1282.
  102. Fejzo M, Rocha N, Cimino I, *et al*. GDF15 linked to maternal risk of nausea and vomiting during pregnancy. *Nature*. 2024; 625:760-767.
  103. Johnen H, Lin S, Kuffner T, *et al*. Tumor-induced anorexia and weight loss are mediated by the TGF-beta superfamily cytokine MIC-1. *Nat Med*. 2007; 13:1333-1340.
  104. Wallentin L, Hijazi Z, Andersson U, Alexander JH, De Caterina R, Hanna M, Horowitz JD, Hylek EM, Lopes RD, Asberg S, Granger CB, Siegbahn A. Growth differentiation factor 15, a marker of oxidative stress and inflammation, for risk assessment in patients with atrial fibrillation: insights from the Apixaban for Reduction in Stroke and Other Thromboembolic Events in Atrial Fibrillation (ARISTOTLE) trial. *Circulation*. 2014; 130:1847-1858.
  105. Xiang Y, Zhang T, Guo J, Peng YF, Wei YS. The

- Association of Growth Differentiation Factor-15 Gene Polymorphisms with Growth Differentiation Factor-15 Serum Levels and Risk of Ischemic Stroke. *J Stroke Cerebrovasc Dis.* 2017; 26:2111-2119.
106. Guo D, Zhu Z, Zhong C, *et al.* Prognostic Metrics Associated with Inflammation and Atherosclerosis Signaling Evaluate the Burden of Adverse Clinical Outcomes in Ischemic Stroke Patients. *Clin Chem.* 2020; 66:1434-1443.
  107. Yin J, Zhu Z, Guo D, Wang A, Zeng N, Zheng X, Peng Y, Zhong C, Wang G, Zhou Y, Chen CS, Chen J, Zhang Y, He J. Increased Growth Differentiation Factor 15 Is Associated with Unfavorable Clinical Outcomes of Acute Ischemic Stroke. *Clin Chem.* 2019; 65:569-578.
  108. Gröschel K, Schnaudigel S, Edelmann F, Niehaus CF, Weber-Krüger M, Haase B, Lahno R, Seegers J, Wasser K, Wohlfahrt J, Vollmann D, Stahrenberg R, Wachter R. Growth-differentiation factor-15 and functional outcome after acute ischemic stroke. *J Neurol.* 2012; 259:1574-1579.
  109. Brenière C, Méloux A, Pédard M, Marie C, Thouant P, Vergely C, Béjot Y. Growth Differentiation Factor-15 (GDF-15) Is Associated With Mortality in Ischemic Stroke Patients Treated With Acute Revascularization Therapy. *Front Neurol.* 2019; 10:611.
  110. Yang P, Wang S, Zhong C, Yin J, Yang J, Wang A, Xu T, Zhang Y. Association of Cardiac Biomarkers in Combination With Cognitive Impairment After Acute Ischemic Stroke. *J Am Heart Assoc.* 2024; 13:e031010.
  111. Zang Y, Zhu Z, Xie Y, Liu Z, Yin J, Yang P, Zhang K, Bu X, Wang A, Chen J, Zhang Y, He J. Serum Growth Differentiation Factor 15 Levels Are Associated With Depression After Ischemic Stroke. *J Am Heart Assoc.* 2022; 11:e022607.
  112. Bao X, Borné Y, Xu B, Orho-Melander M, Nilsson J, Melander O, Engström G. Growth differentiation factor-15 is a biomarker for all-cause mortality but less evident for cardiovascular outcomes: A prospective study. *Am HeartJ.* 2021; 234:81-89.
  113. Wang D, Day EA, Townsend LK, Djordjevic D, Jørgensen SB, Steinberg GR. GDF15: emerging biology and therapeutic applications for obesity and cardiometabolic disease. *Nat Rev Endocrinol.* 2021; 17:592-607.
  114. Liang W, Wei F, Yang C, Xie F, Shuai XX, Wang M, Yu M. GDF-15 is associated with thrombus burden in patients with deep venous thrombosis. *Thromb Res.* 2020; 187:148-153.
  115. Wei BY, Hou JN, Yan CP, Wen SY, Shang XS, Guo YC, Feng T, Liu TF, Chen ZY, Chen XP. Shexiang Baoxin Pill treats acute myocardial infarction by promoting angiogenesis *via* GDF15-TRPV4 signaling. *Biomed Pharmacother.* 2023; 165:115186.
  116. Breen DM, Kim H, Bennett D, *et al.* GDF-15 Neutralization Alleviates Platinum-Based Chemotherapy-Induced Emesis, Anorexia, and Weight Loss in Mice and Nonhuman Primates. *Cell Metab.* 2020; 32:938-950. e936.
  117. Crawford J, Calle RA, Collins SM, Weng Y, Lubaczewski SL, Buckeridge C, Wang EQ, Harrington MA, Tarachandani A, Rossulek MI, Revkin JH. A Phase Ib First-In-Patient Study Assessing the Safety, Tolerability, Pharmacokinetics, and Pharmacodynamics of Ponegromab in Participants with Cancer and Cachexia. *Clin Cancer Res.* 2024; 30:489-497.
  118. Groarke JD, Crawford J, Collins SM, *et al.* Ponegromab for the Treatment of Cancer Cachexia. *N Engl J Med.* 2024; 391:2291-2303.
  119. Bermejo IM, Miguel MJd, Alonso G, *et al.* Initial results from the phase 2A trial of visugromab (CTL-002) + nivolumab in advanced/metastatic anti-PD1/-L1 relapsed/refractory solid tumors (The GDFATHER-TRIAL). *J Clin Oncol.* 2023; 41:2501-2501. [https://doi.org/10.1200/JCO.2023.41.16\\_suppl.2501](https://doi.org/10.1200/JCO.2023.41.16_suppl.2501)
- Received September 30, 2024; Revised November 23, 2024; Accepted January 22, 2025.
- §These authors contributed equally to this work.  
\*Address correspondence to:  
Kai Zheng, Department of Geriatrics, Tongji Hospital, Tongji Medical College, Huazhong University of Science and Technology, 1095 Jiefang Rd. Wuhan 430030, Hubei, China.  
E-mail: diazna2002@sina.com
- Released online in J-STAGE as advance publication January 25, 2025.

# Intestinal microbiota distribution and changes in different stages of Parkinson's disease: A meta-analysis, bioinformatics analysis and *in vivo* simulation

Tingyue Jiang, Yu Wang, Wenxin Fan, Yifan Lu, Ge Zhang, Jiayuan Li, Renzhi Ma, Mengmeng Liu, Jinli Shi\*

School of Chinese Materia Medica, Beijing University of Chinese Medicine, Beijing, China.

**SUMMARY:** Parkinson's disease (PD) is a progressive disease that requires effective staging management. The role of intestinal microbiota in PD has been studied, but its changes at different stages are not clear. In this study, meta-analysis, bioinformatics analysis and *in vivo* simulation were used to explore the intestinal microbiota distribution of PD patients and models at different stages. Two PD models at different stages were established in rotenone-treated rats and MPTP-induced mice. The differences in the intestinal microbiota among the different stages of PD patients or models were compared and analyzed. There were significant differences between PD patients and controls, including *Actinobacteriota*, *Deltaproteobacteria*, *Clostridiales*, *Lachnospiraceae*, *Parabacteroides*, etc. Through bioinformatics analysis, we revealed significant differences between PD patients at different stages and controls, including *Actinobacteriota*, *Methanobacteria*, *Erysipelotrichales*, *Prevotellaceae*, *Parabacteroides*, *Parabacteroides gordonii*, etc. Through meta-analysis, we found that *Actinobacteriota* and *Erysipelotrichaceae* had significantly increased in the chronic MPTP model, while *Prevotellaceae* had significantly decreased. PD rats and mice presented significant damage to motor function, coordination, autonomous activity ability and gastrointestinal function, and the damage in the late group was greater than that in the early group. There were significant differences in intestinal microbiota between PD patients or models at different stages and the control groups. In the early stage, the dominant microbiota are *Akkermansia*, *Alistipes*, *Anaerotruncus*, *Bilophila*, *Rikenellaceae*, *Verrucomicrobia* and *Verrucomicrobiae*, whereas in the late stage, the dominant microbiota are *Actinobacteriota* and *Erysipelotrichaceae*. These differences can lay a foundation for subsequent research on the treatment and mechanism of PD at different stages.

**Keywords:** Parkinson's disease (PD), intestinal microbiota, meta-analysis, bioinformatics analysis, different stages, Staging simulation of PD

## 1. Introduction

Parkinson's disease (PD) is a common neurodegenerative disease. The symptoms and disease burden of PD patients gradually increase, which requires timely and effective stage management. Margaret Hoehn and Melvin Yahr developed the first PD scale, called the Hoehn-Yahr (HY) scale, which divides PD into five stages (1). Researchers have proposed a modified HY scale based on this, adding 0.5 grades to the original scale (2). Clinically, PD patients with HY scores between 1.0-2.5 are in the early stage, while PD patients with HY scores between 3-5 are in the middle to late stages of PD (3). However, the motor function scale is generally used for the diagnosis of PD in different stages, and more objective biomarkers are lacking. The identification of biomarkers for PD patients

and models at different stages has positive significance for the staging treatment and diagnosis of PD.

In recent years, many studies have clarified the role of the gut microbiome in communication between the gut and the brain, called the microbiota-gut-brain axis (4). Changes in the balance of gut microbes are closely associated with the progression of neurodegenerative diseases such as PD (5,6). As longitudinal studies have increased, some studies on gut microbiota distribution in PD patients or models have reported conflicting results (7). There is no consensus on which intestinal microbiota is closely related to PD patients or models, and there is a lack of systematic studies on the distribution of intestinal microbiota in different stages of PD patients or models. Clarifying these has positive significance for the treatment of different stages of PD based on

intestinal microbiota (8). In this study, meta-analysis, bioinformatics analysis and *in vivo* simulation were combined to explore the distribution of intestinal microbiota in different stages of PD patients or models, providing a basis for subsequent studies on the staging treatment and diagnosis of PD based on intestinal microbiota.

## 2. Materials and Methods

### 2.1. Search strategy and data extraction

We searched 7 databases including PubMed, Web of Science, the Cochrane Library, Embase, CNKI, Wanfang and VIP, from the establishment of the database to April 8, 2023. Subject words combined with free words were used for retrieval. The subject words were Parkinson Disease and Gastrointestinal Microbiome. The free word consists of their synonyms. First, we removed duplicate studies and then preliminarily screened the literature according to the title and abstract. Secondary screening was performed according to the inclusion and exclusion criteria. Basic information and the relative abundance of gut microbiota at different taxonomic levels were extracted from the included studies. The included studies with PD patients were assessed by two researchers using the Newcastle-Ottawa Scale (NOS), and studies with PD models were assessed by two researchers using the Systematic Review Centre for Laboratory Animal Experimentation (SYRCLE), with the average of the two researchers' scores calculated as NOS or SYRCLE scores. As for the staging definition of PD model, the 1-methyl-4-phenyl-1, 2, 3, 6-tetrahydropyridine (MPTP) model with staging was selected. The acute model was intraperitoneal injection of MPTP 4 times a day, the subchronic model was intraperitoneal injection of MPTP for 5 consecutive days, and the chronic model was intraperitoneal injection of MPTP for 5 weeks, twice a week (9). The rest of the search strategies and evaluation scales can be found in Supplemental data 1 (<https://www.biosciencetrends.com/action/getSupplementalData.php?ID=234>).

### 2.2. Inclusion and exclusion criteria

We used the following inclusion criteria: Relevant results were published in Chinese or English. For the study of PD patients, case-control trials were selected, and the study objects were PD patients with definite diagnosis or healthy controls. For PD models, the research objects were models with different stages and controls. There was no statistical significance in the general data between the PD patient group or model group and the control group, which was comparable. The study focused on the distribution of the intestinal microbiota, which describes the relative abundance of at least one intestinal microbe. Sufficient data can be obtained for meta-analysis.

We used the following exclusion criteria: The subjects were PD models without staging; The study was a review, meta-analysis or comment; The research data were incomplete or too few to be applied (the number of articles including gut microbes was at least  $\geq 3$ ); It was not clear whether products such as probiotics that affect the distribution of the intestinal microbiota were taken within three months; The results could not be converted into data, using the form of results such as images, fan charts that could not be converted into data.

### 2.3. Meta-analysis

Stata 17.0 was used for meta-analysis. A combination of a random effects model and fixed effects model was used to test the data. The standard mean difference (SMD) was used as the effect index, and the 95% confidence interval (CI) was calculated. We generated forest and funnel plots and performed sensitivity analysis and Egger bias analysis.

### 2.4. Bioinformatic analysis

We identified two studies in the National Center for Biotechnology Information (NCBI, <https://www.ncbi.nlm.nih.gov/>) database, study numbers PRJEB30615 and PRJNA588035. These were the only two studies that identified each patient's HY score and uploaded the original sequence of the gut microbiota. Quantitative Insights Into Microbial Ecology version 2 (QIIME2) software (Version QiiME2-202202) was used to analyze the raw data of intestinal microbiota. The feature table and representative table of the intestinal microbiota were obtained. These were used to construct evolutionary trees for species composition analysis and differential abundance analysis.

### 2.5. Animals and Study Design

Specific Pathogen Free (SPF) C57BL/6 male mice and SPF male Sprague Dawley (SD) rats were purchased from Beijing Vital River Laboratory Animal Technology Co., Ltd. The experimental animal license number is SCXK (Beijing) 2021-0006. All the animals were kept at the SPF Animal Laboratory Center of Beijing University of Chinese Medicine at ambient temperature ( $22 \pm 2$ ), relative humidity ( $50 \pm 10$  %), and a light and dark cycle of 12 h. All procedures conformed to the requirements of international ethics for laboratory animals, and the Animal Ethics Review Committee of Beijing University of Chinese Medicine approved these experiments (BUCM-2023090604-3121).

After 1 week of adaptation, the rats were randomly divided into control group, early PD group and late PD group ( $n = 10$ ) according to random number table classification. All rats in the PD group were injected subcutaneously with rotenone sunflower oil solvent

(1.5 mg/kg) once a day in the neck or back of the early group for 7 days (10,11), and in the late group for 28 days (12). The rats in the control group were injected subcutaneously with 1 mL/kg sunflower oil in the neck or back for 28 days. After 5 days of adaptation, the mice were randomly divided into control group, early PD group and late PD group ( $n=10$ ) according to random number table classification. Mice in all PD groups were intraperitoneally injected with MPTP[25 mg/(kg·3.5 d)], and the modeling duration was 7 days in the early group and 35 days in the late group. Mice in the control group were intraperitoneally injected with 10 mL/(kg·3.5 d) normal saline for 35 days (13). The participants were equipped with protective clothing, gas mask and goggles to prepare MPTP hydrochloride saline solution in the fume hood. After each experiment, the related equipment and liquid were treated to be harmless with 1% disinfectant 84.

## 2.6. Behavioral and gastrointestinal function tests

We used the pole test, inclined plate test and open field to investigate the behavioral function of rats and mice, and fecal water content to test the gastrointestinal function of rats and mice (14-18). The rat or mouse was placed on the top of a pole, and the time from placement to landing of the hind legs was recorded three times a week. The rat or mouse was placed vertically on the rubber pad of the inclined board. If the rat could stay on the inclined plate for 5 s and the mouse could stay on the inclined plate for 15 s, the angle of the inclined plate was increased until the stay time was less than 5 s or 15 s. The rats or mice were placed in an open field of their respective sizes. The bottom of the open field was divided into 16 (4×4) squares, the middle 4 (2×2) squares constituted the center area of the open field, and the remaining squares constituted the edge area. Video tracking technology was used to record the moving distance, moving speed and resting time of the rats in different areas of the open field within 10 min, and the above indices were recorded within 5 min for mice. Fresh feces were collected from each group every week, and the weight at the time of collection was measured as the wet weight of the feces. After drying at 65°C in a vacuum oven for 2 days, the weight was measured again as the dry weight of the feces. Fecal water content = (fecal wet weight - fecal dry weight)/fecal wet weight × 100%.

## 2.7. Sample collection and tissue pretreatment

After all the behavioral tests, the fresh feces of each group were collected, frozen in liquid nitrogen, and stored at -80 °C for future use. Rats were anesthetized intraperitoneally with 20% urethane and underwent cardiac perfusion. After fixation, the whole brain was quickly separated on ice. The obtained tissues were soaked in paraformaldehyde solution and then used for

immunohistochemistry.

## 2.8. 16S rRNA sequencing analysis

Total genomic DNA was extracted *via* the Cetyltrimethylammonium Bromide (CTAB) method. The diluted genomic DNA was amplified *via* Polymerase Chain Reaction (PCR) in the 16S V3-V4 region (primer sequences CCTAYGGGRBGCASCAG, GGACTACNNGGGTATCTAAT). Quantitative libraries were collected on the Illumina platform for sequencing. Paired-end reads were assigned according to the unique barcode of the sample and were truncated by cutting the barcode and primer sequence. QIIME2 software was used for species annotation and fast multiple sequence alignment, and the Silva 138.1 database was used for species annotation. The data of each sample were homogenized, and a phylogenetic tree was constructed. On this basis, alpha diversity indices were calculated, and beta diversity indices were compared. Linear discriminant analysis Effect Size (LEfSe) was used to reveal the differentiation of community structure, and Phylogenetic Investigation of Communities by Reconstruction of Unobserved States (PICRUSt2, V2.3.0) was used to predict the functional composition and metabolic potential of the microbiome.

## 2.9. Immunohistochemistry

Tissue sections were embedded in paraffin wax and dewaxed to water. Tissue sections were placed in citric acid antigen repair buffer for antigen repair in the microwave oven. Slices were placed in 3% hydrogen peroxide solution and incubated for 25 min in the dark. Samples were incubated with 3% Bovine Serum Albumin (BSA) for 30 min. Overnight incubation with anti-tyrosine hydroxylase (TH) was then performed at 4°C. Tissue was then incubated with the corresponding secondary antibodies for 50 min in the dark. Diaminobenzidine (DAB) chromogenic agent was added, and the nucleus was counterstained with hematoxylin. The images were observed using a fluorescence microscope (Nikon Eclipse C1, Tokyo, Japan). Image-pro plus 6.0 (Media Cybernetics, Inc., Rockville, MD, USA) was used for mean density analysis. Mean density was obtained from the cumulative optical density value/pixel area of the tissue.

## 2.10. Statistical analysis

SPSS 25.0 software was used for statistical analysis. Shapiro-Wilk was used for normality test before statistical analysis. Results matching normal distribution were compared between groups using the LSD test of one-way ANOVA. The Kruskal-Wallis test was used to compare species abundance differences and predict their functions. GraphPad Prism 8.0.2 software was used to

draw the correlation histogram and other results.

### 3. Results

#### 3.1. Study selection

2540 studies were retrieved. We removed 1063 duplicate and retracted articles and included 32 studies (19-50) in PD patients and 17 studies (51-67) in PD models for meta-analysis. The screening process is shown in Figure 1. Chinese and English studies in 9 different countries were included. 3356 samples were included, including 1718 PD patients, 1352 healthy controls, 145 PD models, and 141 control groups. All studies were matched for baseline data such as age and sex. NOS and SYRCLE scores of the included studies were all higher than 6.5. The basic information of the research subjects included in the studies is shown in Table 1 and Table 2.

#### 3.2. Intestinal microbiota with differential abundance between PD patients and healthy controls

Through meta-analysis, we found that there were generally significant differences between PD patients and healthy controls in 8 phyla of bacteria (*Actinobacteriota*, *Bacteroidetes*, *Verrucomicrobia*, etc.), 5 classes of bacteria (*Deltaproteobacteria*, *Methanobacteria*, *Verrucomicrobiae*, etc.), 4 orders of bacteria (*Clostridiales*, *Methanobacteriales*, *Verrucomicrobiales*,

etc.), 25 families of bacteria (*Fusobacteriaceae*, *Lachnospiraceae*, *Lactobacillaceae*, etc.), 32 genera of bacteria (*Lachnospira*, *Parabacteroides*, *Prevotella*, etc.) and 19 species of bacteria (*Akkermansia muciniphila*, *Faecalibacterium prausnitzii*, *Parabacteroides merdae*, etc.). These microbiomes and the trends of the differences are shown in Table 3. Forest plots and funnel plots of all the microbiota are shown in Supplemental data 2 (<https://www.biosciencetrends.com/action/getSupplementalData.php?ID=234>). The funnel plots of the vast majority of bacteria were symmetrical, and Egger bias was not present. However, owing to the literature limitations, the specific microbiome distribution and HY score of each patient could not be obtained.

#### 3.3. Intestinal microbiota with differential abundance between PD patients at different stages and healthy controls

Through bioinformatics analysis, we explored the microbiota with differential abundance between PD patients at different stages and healthy controls in PRJEB30615 (68) and PRJNA588035 (33). The two studies involved 47 patients with early PD, 26 patients with middle to late PD, and 64 healthy controls. There were significant differences in the relative abundance of 4 phyla of bacteria (*Actinobacteriota*, *Proteobacteria*, *Verrucomicrobia*, etc.), 7 classes of bacteria (*Actinobacteriota*, *Erysipelotrichia*, *Verrucomicrobiae*,

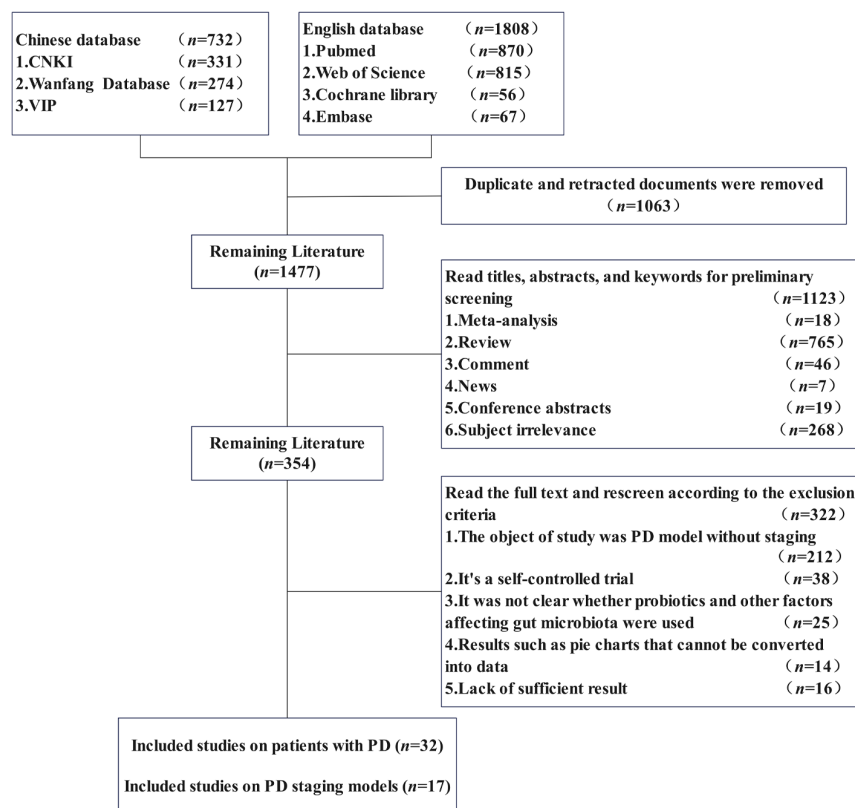


Figure 1. Literature selection process for the meta-analysis.

**Table 1. Basic information of the research subjects included in the literature**

| Included study           | Country and region |               | Sample size       |                   | Ages                   |                   | Detection method | Average HY score of PD patients | NOS score |
|--------------------------|--------------------|---------------|-------------------|-------------------|------------------------|-------------------|------------------|---------------------------------|-----------|
|                          | PD group           | Control group | PD group          | Control group     | Ages                   |                   |                  |                                 |           |
|                          |                    |               |                   |                   | PD group               | Control group     |                  |                                 |           |
| Aho VTE, 2019 (19)       | 64                 | 64            | 65.2 ± 5.52       | 64.45 ± 6.9       | 16S rRNA               | 2.5 (2-3)         | 6.5              |                                 |           |
| Babacan Y G, 2023 (20)   | 42                 | 42            | 60.62 ± 9.31      | 58.33 ± 9.61      | 16S rRNA               | 2 (1-3)           | 8                |                                 |           |
| Barchella M, 2018 (21)   | 193                | 113           | 67.6 ± 9.7        | 65.9 ± 9.9        | 16S rRNA               | 2.0 ± 0.8         | 7.5              |                                 |           |
| Bi ZA, 2018 (22)         | 14                 | 15            | 65.14 ± 9.11      | 60.80 ± 7.33      | 16S rRNA               | 2.32 ± 0.70       | 8                |                                 |           |
| Bolliri C, 2022 (23)     | 20                 | 20            | 67.8 ± 9.6        | 67.8 ± 9.6        | Metagenomic sequencing | 2.0 ± 1.0         | 8                |                                 |           |
| Cerroni R, 2022 (24)     | 18                 | 13            | 63.5 ± 8.1        | 62.8 ± 7.8        | 16S rRNA               | 2.15 ± 0.5        | 7.5              |                                 |           |
| Chen H, 2017 (25)        | 20                 | 20            | 63.60 ± 11.75     | 65.00 ± 11.09     | 16S rDNA               | 2.35 ± 0.95       | 7.5              |                                 |           |
| Cirstea MS, 2020 (26)    | 75                 | 50            | 66 (57.5, 69)     | 64.5 (57, 70)     | 16S rDNA               | /                 | 7.5              |                                 |           |
| Hill-Burns EM, 2017 (27) | 197                | 130           | 68.4 ± 9.2        | 70.3 ± 8.6        | 16S rRNA               | /                 | 6.5              |                                 |           |
| Li F, 2019 (28)          | 10                 | 10            | 79.5 ± 8.0        | 76.5 ± 7.5        | 16S rRNA               | 2.4 ± 1.1         | 7.5              |                                 |           |
| Li KS, 2020 (29)         | 26                 | 26            | 67.00 ± 3.89      | 69.08 ± 4.70      | 16S rRNA               | 2.50 (1.50, 2.50) | 8                |                                 |           |
|                          |                    |               | 69.08 ± 4.70      | 69.08 ± 4.70      | 16S rRNA               | 1.75 (1.00, 2.50) |                  |                                 |           |
| Li T, 2020 (30)          | 25                 | 25            | 68.89 ± 7.79      | 69.17 ± 7.17      | 16S rRNA               | /                 | 8                |                                 |           |
| Li Y, 2020 (31)          | 30                 | 30            | 67.0 ± 6.0        | 65.0 ± 8.0        | 16S rRNA               | 2                 | 8                |                                 |           |
| Lin AQ, 2018 (32)        | 75                 | 45            | 60.48 ± 10.72     | 63.20 ± 6.00      | 16S rRNA               | /                 | 7                |                                 |           |
| MAO LW, 2021 (33)        | 39                 | 39            | 63.95 ± 6.92      | 64.82 ± 6.86      | Metagenomic sequencing | 1.94 ± 0.91       | 8                |                                 |           |
| Nakahara K, 2023 (34)    | 5                  | 5             | 70.0 (67.0, 71.0) | 69.0 (59.0, 71.5) | 16S rRNA               | 2.0 (1.5, 2.5)    | 7                |                                 |           |
| Pietrucci D, 2019 (35)   | 80                 | 72            | 66.2 ± 8.7        | 62.6 ± 8.7        | 16S rRNA               | 2.5 ± 0.7         | 7.5              |                                 |           |
| Qian YW, 2020 (36)       | 40                 | 40            | 66.6 ± 7.1        | 66.3 ± 8.1        | Metagenomic sequencing | 2.3 ± 0.8         | 7.5              |                                 |           |
| Ren T, 2020 (37)         | 13                 | 14            | 60.00 ± 9.20      | 63.00 ± 8.76      | 16S rRNA               | 1.89 ± 0.49       | 7.5              |                                 |           |
| Scheperjans F, 2015 (38) | 72                 | 72            | 65.3 ± 5.5        | 64.5 ± 6.9        | 16S rRNA               | /                 | 7                |                                 |           |
| Tan AH, 2021 (39)        | 104                | 96            | 65.4 ± 8.4        | 62.4 ± 9.0        | 16S rRNA               | 2.2 ± 0.5         | 7                |                                 |           |
| Tetz G, 2018 (40)        | 31                 | 28            | 64.8 ± 9.5        | 65.6 ± 10.4       | Metagenomic sequencing | /                 | 7                |                                 |           |
| Tong QW, 2021 (41)       | 30                 | 30            | 66.1 ± 7.2        | 64.8 ± 5.0        | 16S rDNA               | 2.11 ± 0.65       | 7.5              |                                 |           |
| Vascellari S, 2020 (42)  | 64                 | 51            | 71.39 ± 10.99     | 51.67 ± 12.42     | 16S rRNA               | /                 | 7.5              |                                 |           |
| Wallen ZD, 2022 (43)     | 158                | 51            | 68.7 ± 8.5        | 65.8 ± 8.8        | Metagenomic sequencing | /                 | 6.5              |                                 |           |
| Wang YI, 2022 (44)       | 30                 | 30            | 59.64 ± 5.7       | 61.28 ± 6.2       | 16S rRNA               | /                 | 7.5              |                                 |           |
| Zhang F, 2020 (45)       | 63                 | 74            | 64.0 ± 7.4        | 63.4 ± 6.6        | 16S rRNA               | 2.1 ± 0.8         | 8                |                                 |           |
| Zhang F, 2020 (46)       | 46                 | 46            | 63.6 ± 6.9        | 63.8 ± 7.0        | Metagenomic sequencing | /                 | 8                |                                 |           |
| Zhang LN, 2021 (47)      | 20                 | 20            | 67.80 ± 7.84      | 66.25 ± 7.04      | 16S rRNA               | /                 | 7.5              |                                 |           |
| Zhang TQ, 2019 (48)      | 38                 | 15            | 68.76 ± 7.343     | 69.80 ± 7.253     | 16S rRNA               | /                 | 8                |                                 |           |
| Zhao C, 2018 (49)        | 24                 | 14            | 73.75 ± 6.26      | 74.64 ± 5.57      | 16S rRNA               | /                 | 8                |                                 |           |
| Zhuo WY, 2018 (50)       | 52                 | 52            | 66.57 ± 11.82     | 65.33 ± 10.19     | 16S rDNA               | 2.53 ± 0.89       | 7.5              |                                 |           |

**Table 2. Basic information of the studies included in MPTP staging model**

| Included study      | Sample size |               | Detection method | Staging type     | SYRCLE score |
|---------------------|-------------|---------------|------------------|------------------|--------------|
|                     | PD group    | Control group |                  |                  |              |
| Aktas B, 2023 (51)  | 10          | 10            | 16S rRNA         | acute/subchronic | 8            |
| An YY, 2019 (52)    | 6           | 6             | 16S rRNA         | chronic          | 8            |
| An YY, 2019 (53)    | 6           | 6             | 16S rRNA         | chronic          | 8.5          |
| Chen XX, 2022 (54)  | 6           | 6             | 16S rDNA         | chronic          | 8.5          |
| Chen XX, 2022 (55)  | 6           | 6             | 16S rDNA         | chronic          | 8.5          |
| Dong XL, 2020 (56)  | 8           | 8             | 16S rRNA         | acute            | 8.5          |
| Jang JH, 2020 (57)  | 10          | 6             | 16S rRNA         | subchronic       | 7            |
| Jeon H, 2021 (58)   | 5           | 5             | 16S rRNA         | subchronic       | 6.5          |
| Liao JF, 2020 (59)  | 12          | 12            | 16S rRNA         | subchronic       | 7.5          |
| Liu MM, 2022 (60)   | 3           | 3             | 16S rRNA         | subchronic       | 7            |
| Liu X, 2021 (61)    | 8           | 8             | 16S rRNA         | subchronic       | 7.5          |
| Liu X, 2021 (62)    | 8           | 8             | 16S rRNA         | chronic          | 8            |
| Liu X, 2022 (63)    | 8           | 8             | 16S rRNA         | chronic          | 8.5          |
| Shi Y, 2021 (64)    | 10          | 10            | 16S rDNA         | acute            | 7.5          |
| Sun MF, 2018 (65)   | 15          | 15            | 16S rRNA         | subchronic       | 7.5          |
| Sun Z, 2022 (66)    | 12          | 12            | 16S rRNA         | subchronic       | 8.5          |
| Zhang LY, 2020 (67) | 12          | 12            | 16S rDNA         | subchronic       | 8.5          |

etc.), 9 orders of bacteria (*Actinomycetales*, *Erysipelotrichales*, *Lactobacillales*, etc.), 21 families of bacteria (*Bacteroidaceae*, *Lactobacillaceae*, *Prevotellaceae*, etc.), 25 genera of bacteria (*Bacteroides*, *Lachnospira*, *Parabacteroides*, etc.) and 52 species of bacteria (*Akkermansia muciniphila*, *Faecalibacterium prausnitzii*, *Parabacteroides gordonii*, etc.) between PD patients at different stages and healthy controls. In the two studies, the microbiomes with significant differences in expression between PD patients with different stages and healthy people are shown in the Table 4 (Online Table: <https://www.biosciencetrends.com/action/getSupplementalData.php?ID=234>).

### 3.4. Differences in intestinal microbiota abundance of MPTP models at different stages through meta-analysis

Through meta-analysis, we found that the MPTP models of different stages had different relative abundance of intestinal microbiota at different classification levels. We found that *Actinobacteriota*, *Bacteroidetes* and *Bacteroidales* increased significantly in the subchronic MPTP model. *Actinobacteriota*, *Firmicutes*, *Deferribacteraceae*, *Erysipelotrichaceae*, *Ruminococcaceae*, *Allobaculum* and *Oscillibacter* were significantly increased in the chronic MPTP model. *Bacteroidetes*, *Prevotellaceae*, *Blautia* and *Prevotellaceae UCG-001* decreased significantly in the chronic MPTP model. Forest plots and funnel plots of all the microbiota are shown in Supplemental data 2 (<https://www.biosciencetrends.com/action/getSupplementalData.php?ID=234>).

### 3.5. Rotenone induced motor and gastrointestinal dysfunction in PD rats at different stages

The rotenone-treated group presented yellow hair,

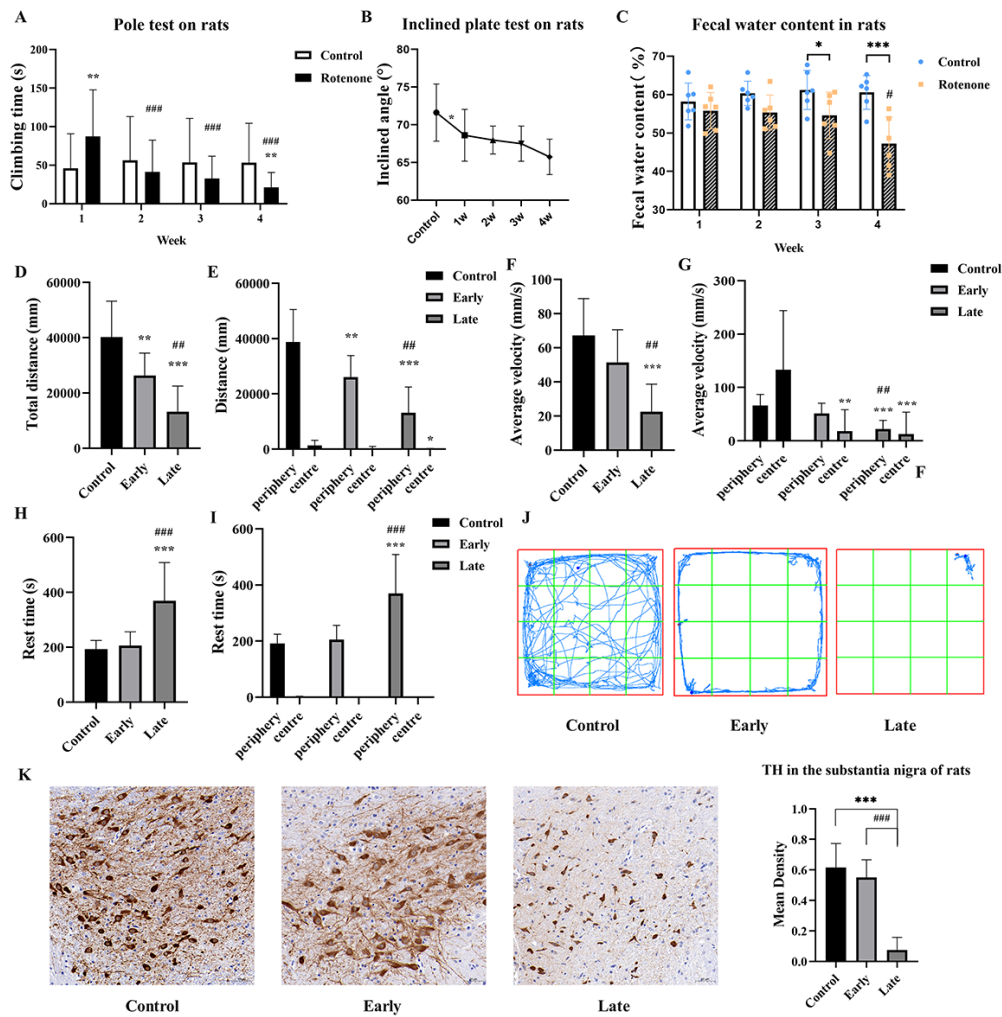
reduced activity, and slow movement at 7 days. The rotenone-treated rats presented dirtier hair, almost no activity, and unsteady gait at 28 days. The pole climbing time of rotenone-treated rats in the early group was significantly greater than that of the control group ( $P < 0.01$ ), and that of the late group was significantly lower than that of the control group ( $P < 0.01$ ). The inclined plate angle of the model rats gradually decreased, and the angle of the late group was lower than that of the early group. Compared with the control group, the movement distance of the rats in the early group was significantly lower ( $P < 0.01$ ), the movement distance and average movement speed of the rats in the late group were significantly lower ( $P < 0.001$ ,  $P < 0.001$ ), and the rest time of the rats in the late group was significantly increased ( $P < 0.001$ ). The distribution of different groups of rats in the central and peripheral areas of the open field also differed. The fecal water content of the late group was significantly lower than that of the control group ( $P < 0.001$ ). TH in the late group was significantly lower than that in the control group ( $P < 0.001$ ). These results are shown in Figure 2.

### 3.6. MPTP induced motor and gastrointestinal dysfunction in PD mice at different stages

Compared with the control group, slow movement was observed on the 7th day after MPTP induction. Compared with the control group, the pole climbing time of the MPTP-induced mice in the late group was significantly lower ( $P < 0.001$ ). The inclined plate angle of the late group was lower than that of the early group. Compared with the control group, the moving distance and average speed of the mice in the early and late groups were significantly lower ( $P < 0.05$ ). The distribution of different groups of mice in the central and peripheral areas of the open field also differed. The fecal

**Table 3. Intestinal microbiota with differential abundance between PD patients and healthy people**

| Phylum                  | Class                                     |                                       | Order                                     |                                       | Family                                    |                                       |   | Genus                                 |   | Species                               |  |
|-------------------------|---|---------------------------------------|---|---------------------------------------|---|---------------------------------------|---|---------------------------------------|---|---------------------------------------|--|
|                         | Dominant bacteria in health control group | Dominant bacteria in PD patient group | Dominant bacteria in health control group | Dominant bacteria in PD patient group | Dominant bacteria in health control group | Dominant bacteria in PD patient group | Dominant bacteria in health control group | Dominant bacteria in PD patient group | Dominant bacteria in health control group | Dominant bacteria in PD patient group |  |
| <i>Actinobacteriota</i> | <i>Bacteroidetes</i>                      | <i>Bacilli</i>                        | <i>Pasteurellales</i>                     | <i>Bifidobacteriaceae</i>             | <i>Prevotellaceae</i>                     | <i>Actinomycetes</i>                  | <i>Blautia</i>                            | <i>Akkermansia muciniphila</i>        | <i>Faecalibacterium prausnitzii</i>       |                                       |  |
| <i>Euryarchaeota</i>    | <i>Fusobacteria</i>                       | <i>Deltaproteobacteria</i>            | <i>Methanobacteriales</i>                 | <i>Christensenellaceae</i>            | <i>Micrococcaceae</i>                     | <i>Akkermansia</i>                    | <i>Faecalibacterium</i>                   | <i>Anaerotruncus colliformis</i>      | <i>Bacteroides stercoris</i>              |                                       |  |
| <i>Lentisphaerae</i>    | <i>Proteobacteria</i>                     | <i>Methanobacteria</i>                | <i>Verrucomicrobiales</i>                 | <i>Coriobacteriaceae</i>              | <i>Lachnospiraceae</i>                    | <i>Alistipes</i>                      | <i>Fusicatenibacter</i>                   | <i>Bifidobacterium adolescentis</i>   | <i>Bifidobacterium bifidum</i>            |                                       |  |
| <i>Synergistetes</i>    |   | <i>Synergistia</i>                    |   | <i>Corynebacteriaceae</i>             | <i>Fusobacteriaceae</i>                   | <i>Anaerotruncus</i>                  | <i>Fusobacterium</i>                      | <i>Bifidobacterium longum</i>         | <i>Bifidobacterium breve</i>              |                                       |  |
| <i>Verrucomicrobia</i>  |   | <i>Verrucomicrobiae</i>               |   | <i>Dehalobacteriaceae</i>             | <i>Comamonadaceae</i>                     | <i>Barnesiella</i>                    | <i>Lachnospira</i>                        | <i>Bifidobacterium longum</i>         | <i>Bifidobacterium longum</i>             |                                       |  |
|                         |   |                                       |   | <i>Desulfosporosporiaceae</i>         | <i>Alcaligenaceae</i>                     | <i>Bifidobacterium Bilophila</i>      | <i>Paraprevotella Prevotella</i>          | <i>Christensenella</i>                | <i>Roseburia</i>                          |                                       |  |
|                         |   |                                       |   | <i>Enterobacteriaceae</i>             | <i>Enterococcaceae</i>                    | <i>Enterococcus</i>                   | <i>Collinsella</i>                        | <i>Collinsella</i>                    | <i>asparagiforme Clostridium</i>          |                                       |  |
|                         |   |                                       |   |                                       | <i>Eubacteriaceae</i>                     | <i>Eubacterium</i>                    |   | <i>saccharolyticum</i>                | <i>Escherichia coli</i>                   |                                       |  |
|                         |   |                                       |   |                                       | <i>Lactobacillaceae</i>                   | <i>Corynebacterium</i>                |   | <i>Escherichia coli</i>               | <i>Eubacterium dolichum</i>               |                                       |  |
|                         |   |                                       |   |                                       | <i>Methanobacteriaceae</i>                | <i>Desulfovibrio</i>                  |   | <i>Gordonibacter</i>                  | <i>Gordonibacter pamelaeae</i>            |                                       |  |
|                         |   |                                       |   |                                       | <i>Mogibacteriaceae</i>                   | <i>Enterobacter</i>                   |   | <i>Lactobacillus</i>                  | <i>Lactobacillus salivarius</i>           |                                       |  |
|                         |   |                                       |   |                                       | <i>Oxalobacteraceae</i>                   | <i>Enterobacter</i>                   |   | <i>Megaspheara</i>                    | <i>Megaspheara elsdenii</i>               |                                       |  |
|                         |   |                                       |   |                                       | <i>Peptococcaceae</i>                     | <i>Escherichia</i>                    |   | <i>Parabacteroides distasonis</i>     | <i>Parabacteroides merdae</i>             |                                       |  |
|                         |   |                                       |   |                                       | <i>Porphyromonadaceae</i>                 | <i>Gordonibacter</i>                  |   | <i>Streptococcus anginosus</i>        | <i>Streptococcus thermophilus</i>         |                                       |  |
|                         |   |                                       |   |                                       | <i>Rikenellaceae</i>                      | <i>Lactobacillus</i>                  |   |                                       |   |                                       |  |
|                         |   |                                       |   |                                       | <i>Ruminococcaceae</i>                    | <i>Megaspheara</i>                    |   |                                       |   |                                       |  |
|                         |   |                                       |   |                                       | <i>Synergistaceae</i>                     | <i>Methanobrevibacter</i>             |   |                                       |   |                                       |  |
|                         |   |                                       |   |                                       | <i>Verrucomicrobiaceae</i>                | <i>Parabacteroides</i>                |   |                                       |   |                                       |  |
|                         |   |                                       |   |                                       |   | <i>Peptoniphilus</i>                  |   |                                       |   |                                       |  |
|                         |   |                                       |   |                                       |   | <i>Porphyromonas</i>                  |   |                                       |   |                                       |  |
|                         |   |                                       |   |                                       |   | <i>Scardovia</i>                      |   |                                       |   |                                       |  |
|                         |   |                                       |   |                                       |   | <i>Slackia</i>                        |   |                                       |   |                                       |  |
|                         |   |                                       |   |                                       |   | <i>Varibaculum</i>                    |   |                                       |   |                                       |  |



water content of mice in the late group was significantly lower than that of the control group ( $P < 0.001$ ). These results are shown in Figure 3.

### 3.7. The intestinal microbiota of rats and mice with PD at different stages changed significantly

We obtained the Amplicon Sequence Variants (ASVs) sequences and species abundance tables for each group of samples at different taxonomic levels. LefSe analysis showed significant differences in potential biomarkers among different groups, as shown in Figure 4. The Kruskal–Wallis test showed that 9 phyla, 12 classes, 17 orders, 23 families, 40 genera and 24 species of bacteria were significantly differentially expressed among the different groups of rats. There were 6 phyla, 6 classes, 8 orders, 14 families, 35 genera and 10 species of bacteria whose expression significantly differed

among the different groups of mice, as shown in the Supplemental data 3 (<https://www.biosciencetrends.com/action/getSupplementalData.php?ID=235>). There were significant differences in the diversity of the intestinal microbiota in PD rats and mice at different stages. Compared with the control group, the  $\alpha$  diversity indices of rats and mice in the early group showed significant differences. There were significant differences in  $\beta$  diversity among different groups of rats and mice. These results are shown in Supplemental data 4 (<https://www.biosciencetrends.com/action/getSupplementalData.php?ID=234>). The prediction results of intestinal microbial function in different groups showed that 156 pathways were significantly different between rats and 159 pathways were significantly different between mice, as shown in Figure 5.

### 3.8. Changes in the intestinal microbiota in PD patients

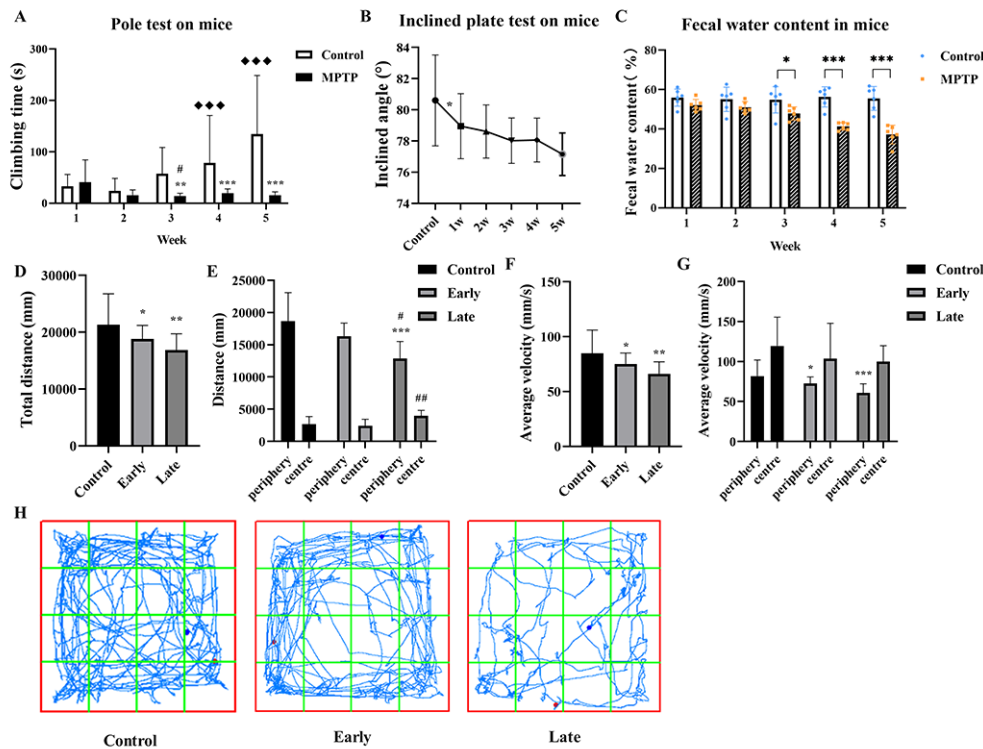


**Figure 3. MPTP induced motor and gastrointestinal dysfunction in PD mice at different stages.** (A) Pole climbing time of the mice in different groups ( $n = 10$ ). (B) Angle of the inclined plate of the mice in different groups ( $n = 10$ ). (C) Changes in the fecal water content of the mice in different groups over time ( $n = 6$ ). (D, E) Total distance and distance distributions of the mice in the open field in different groups ( $n = 10$ ). (F, G) Average velocity and distribution of the different groups of mice in the open field in different groups in the open field ( $n = 10$ ). (H) Movement tracks of the mice in different groups in the open field ( $n = 10$ ). Compared with the control group, \* $P < 0.05$ , \*\* $P < 0.01$ , \*\*\* $P < 0.001$ . Compared with the early group, # $P < 0.05$ , ## $P < 0.01$ . Compared with the 1-week control group, \*\*\* $P < 0.001$ .

and models at different stages

The results of the meta-analysis, bioinformatics analysis, and the rats and mice simulations revealed significant changes in the intestinal microbes at different stages of PD. Ultimately, we found that in the early PD, *Akkermansia*, *Alistipes*, *Anaerotruncus*, *Bilophila*, *Rikenellaceae*, *Verrucomicrobia* and *Verrucomicrobiae* were predominant. In the late PD, *Actinobacteriota* and *Erysipelotrichaceae* were predominant. The significant changes in these microbiomes across the different results are shown in Table 5.

#### 4. Discussion

Parkinson's disease is a chronic and progressive neurodegenerative disease. Clinically, PD patients are divided into different stages according to the degree of motor function impairment. However, the typical biomarkers of PD patients or models at different stages are not known, which presents a great challenge for the treatment and accurate diagnosis of PD at different stages. Many studies have focused on the role and changes in the intestinal microbiota in the course of PD, and the intestinal microbiota is considered one of the important factors regulating gut–brain interactions in the

course of PD (69). In this study, the intestinal microbiota distribution of PD patients or models at different stages was taken as the core object of study. We used meta-analysis to explore the differences in intestinal microbiota between PD patients and healthy people, PD staging model and control group, and bioinformatic analysis to explore the distribution characteristics of intestinal flora between PD patients with different stages and healthy people. PD models of different stages were established in rotenone-treated rats and MPTP-induced mice, and the intestinal flora of PD model rats or PD model mice at different stages were investigated.

We first used meta-analysis to screen case–control studies on PD patients and the gut microbiota. We found that there were significant differences between PD patients and healthy controls. On this basis, we screened the studies that could obtain the HY score and original sequence of the microbiota of each PD patient. We performed bioinformatics analysis in PRJEB30615 and PRJNA588035. The two studies included 47 patients with early PD, 26 patients with middle to late stage PD, and 64 healthy controls. In two studies, there were significant differences between PD patients at different stages and healthy controls. We then screened studies with closely related gut microbiota in PD models with different stages. We found significant differences in

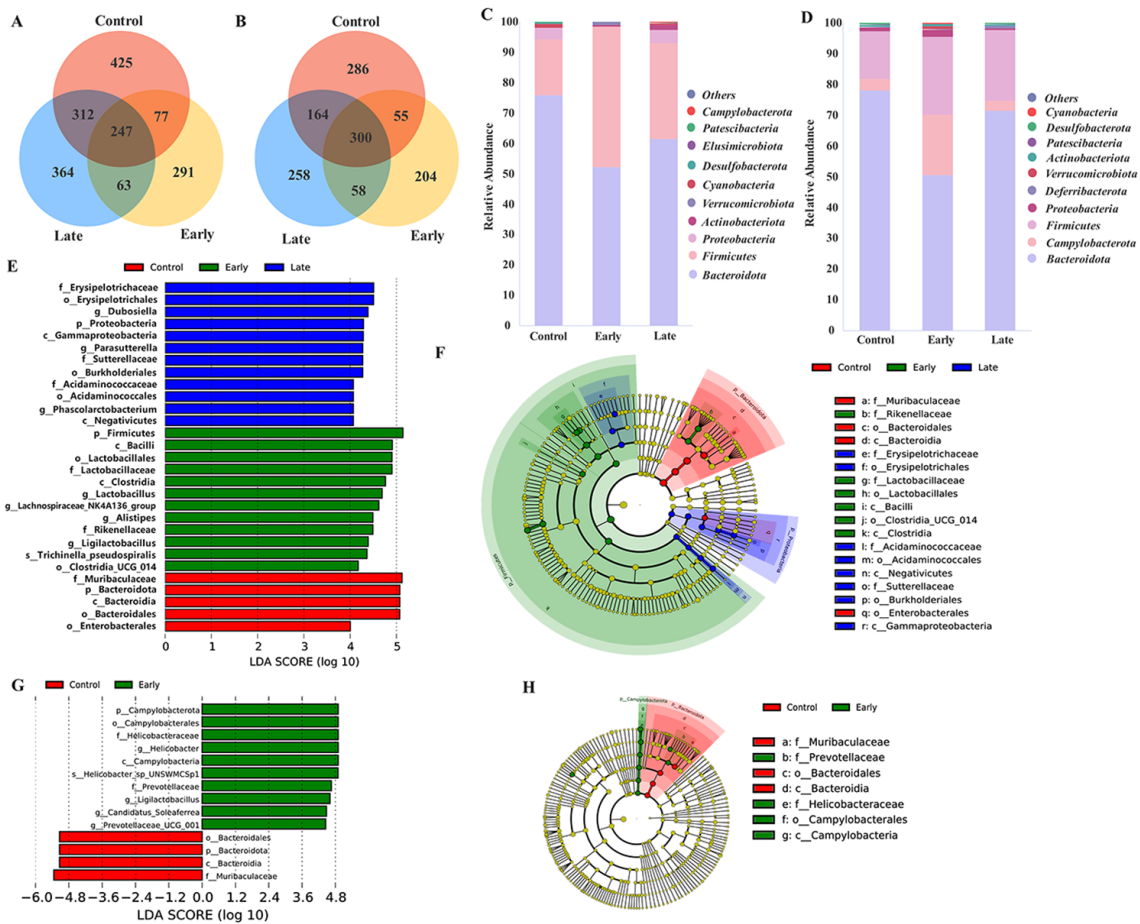


**Figure 4. Intestinal microbiota characteristics of rats and mice in different groups.** (A) Venn diagram of the number of ASVs in different groups of rats ( $n = 6$ ). (B) Venn diagram of the number of ASVs in different groups of mice ( $n = 6$ ). (C) Species abundance histogram of rats in different groups under phylum classification (top 10). (D) Species abundance histogram of mice in different groups under phylum classification (top 10). (E) LDA histogram of different microbiota in different groups of rats (red represents the control group, green represents the early group, and blue represents the late group, as are figures F, G, and H). (F) Evolutionary cladistics of different microbiota in different groups of rats. (G) LDA histogram of different microbiota in different groups of mice. (H) Evolutionary cladistics of different microbiota in different groups of mice.

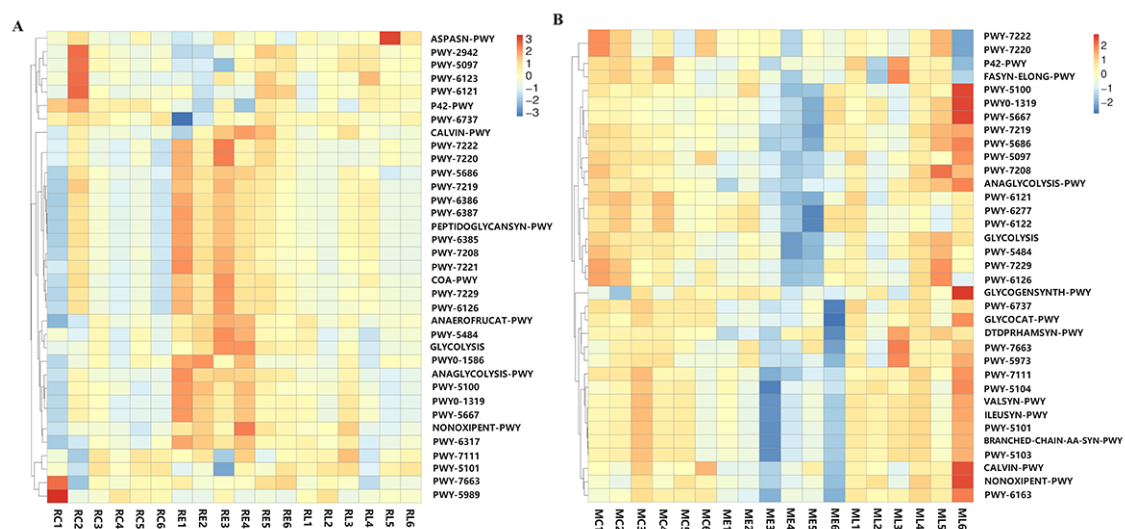


**Figure 5. Predictive functional clustering heatmaps of the intestinal microbiota in different groups of rats or mice.** (A) Predictive functional cluster heatmaps of samples from different groups of rats (control group of rats, RC; early group of rats, RE; late group of rats, RL). (B) Predictive functional cluster heatmaps of samples from different groups of mice (control group of mice, MC; early group of mice, ME; late group of mice, ML).

**Table 5. Intestinal microbiota with common changes between PD patients and models at different stages**

| Treatments                 | Meta 1 | Meta 2 | PRJEB30615 | PRJNA588035 | Rat     | Mice  |
|----------------------------|--------|--------|------------|-------------|---------|-------|
| <i>Akkermansia</i>         | PD     | /      | Early      | /           | /       | Early |
| <i>Alistipes</i>           | PD     | /      | /          | Early       | Early   | /     |
| <i>Anaerotruncus</i>       | PD     | /      | /          | Early       | /       | Early |
| <i>Bilophila</i>           | PD     | /      | /          | Early       | Control | Early |
| <i>Rikenellaceae</i>       | PD     | /      | /          | Early       | Early   | /     |
| <i>Verrucomicrobia</i>     | PD     | /      | Early      | /           | /       | Early |
| <i>Verrucomicrobiae</i>    | PD     | /      | Early      | /           | /       | Early |
| <i>Actinobacteriota</i>    | PD     | Late   | Late       | Late        | Late    | /     |
| <i>Erysipelotrichaceae</i> | /      | Late   | Late       | /           | Late    | /     |

Meta 1 represents the meta-analysis between PD patients and healthy controls. Meta 2 represents the meta-analysis of MPTP models at different stages. PD indicates that the bacteria are dominant in PD patients. Control indicates that the bacteria have a dominant expression in the control group. Early indicates that the bacteria have a dominant expression in the early stage of PD patients or models. Late indicates that the bacteria have a dominant expression in the late stage of PD patients or models. / indicates that no significant changes in the bacteria have been observed in this study.

the distribution of intestinal flora in acute, subchronic, chronic MPTP models and control mice.

At present, there is no model that can fully simulate PD, and each model has its own advantages and disadvantages (70). Rotenone can cause apoptosis of dopamine neurons and induce pathological features similar to PD in rats, but there is no staging model (71). It has the characteristics of short half-life, fast degradation and strong self-healing ability (72). Previous studies have shown that the change of the rotenone subcutaneous injection model first occurred at about 7 days, and extremely significant motor function loss occurred at about 28 days (73). Therefore, different stages of the PD rat model were simulated for 7 and 28 days. 1-Methyl-4-phenyl-1, 2, 3, 6-tetrahydropyridine (MPTP) is a neurotoxin that easily crosses the blood-brain barrier (74). MPTP-induced PD models can be divided into acute, subchronic and chronic models, among which the chronic models develop gradually and are more consistent with the clinical symptoms of PD patients (75,76). In this study, the changes in the intestinal microbiota of rats and mice were integrated, which was helpful for more comprehensively discovering the changes in PD models at different stages.

The results showed that the motor and gastrointestinal functions of PD rats and mice were significantly damaged, and the damage in the late group was more serious than that in the early group, which was consistent with the evolution of PD at different stages. There are still some problems that need to be considered; for example, the pole climbing time of early PD rats is significantly longer than that of the control group, and this may be related to damage to cognitive function, as these rats need more time to adapt to and understand pole climbing. In addition, as more tests were conducted, the control mice took significantly longer to climb the pole, even though they had learned how to leave the pole. In contrast, the climbing time of PD mice was significantly shorter, indicating that their motor function was impaired. Compared with the PD

mice, the damage of PD rats was more obvious with the increase of stage, and the simulation effect was better. Therefore, we investigated the TH expression of the substantia nigra in rats, and the TH expression in the late group showed a significant decrease.

The intestinal microbiota of the different groups of rats and mice significantly differed. The  $\alpha$  diversity indices of intestinal microbiota in the early PD was significantly affected. The results of  $\beta$  diversity analysis also revealed significant changes in the intestinal microbiota distribution among the different groups. In late PD, the damage was manifested by significant changes in the abundance of dominant species. Combined with all the results of this study, we found that *Akkermansia*, *Alistipes*, *Anaerotruncus*, *Bilophila*, *Rikenellaceae*, *Verrucomicrobia* and *Verrucomicrobiae* were significantly increased in early PD patients and models. *Actinobacteriota* and *Erysipelotrichaceae* significantly increased in late PD patients and models.

*Akkermansia* is the only representative member of *Verrucomicrobia* found in mammalian gastrointestinal samples (77). Previous studies and this meta-analysis have both confirmed the increase in the relative abundance of *Akkermansia* in PD patients (78). However, whether an increase in the relative abundance of *Akkermansia* is beneficial or harmful remains a matter of debate (79). Studies have shown that oral administration of *Akkermansia* can improve motor function and relieve neuroinflammation in PD mice (80). It has also been suggested that excessive enrichment of *Akkermansia* may alter mucin degradation processes, thereby impacting the intestinal barrier and inducing the secretion of inflammatory factors (81). This study suggests that *Akkermansia* is significantly increased in early PD. Its beneficial or harmful effects may be related to its expression, and it is likely to play different roles in different stages of PD, which is closely related to the regulation of neuroinflammation.

*Alistipes*, which belongs to *Rikenellaceae*, is found in the gut microbiota of healthy people and plays a role in inflammation and many diseases (82,83). Previous

studies have shown that *Alistipes* may be beneficial or harmful (84). In this study, the abundance of *Alistipes* significantly increased in early PD; coincidentally, it was also related to inflammation, similar to *Akkermansia*. In addition, previous studies have found an increase in *Rikenellaceae* in PD patients and models, but its increase in the early stage was the first to be found and requires further exploration (85-87). There have been few studies on *Anaerotruncus* and *Bilophila* in PD, but they have been found to be significantly increased in PD patients, consistent with the results of this study (31,88), and it is worthwhile to investigate their role in the early PD.

In this study, *Actinobacteriota* increased significantly in the late PD patients and models, and the changes were consistent with previous studies (89,90). Previous studies explored the role of five candidate bacterial biomarkers of the *Actinobacteriota* in PD patients and reported that they were associated with abnormal inflammation (91). These indicate that the increase in *Actinobacteriota* may be related to the severity of PD and can be considered as a biomarker for late PD. The expression of *Erysipelotrichaceae* has been reported to change over time in PD. In a longitudinal study, *Erysipelotrichaceae* UCG-003 was found to be differentially expressed in PD patients at 0, 6 and 12 months (92). Furthermore, the abundance of *Erysipelotrichaceae* in mice induced by MPTP for 3 weeks was significantly increased compared with that in those induced for 2 days (93). These are consistent with this study, indicating that *Erysipelotrichaceae* has great potential as a biomarker of late PD models.

This study also has some limitations. Although the included studies excluded factors such as probiotics and antibiotics, the vast majority of patients included in clinical studies had PD treatment history, which could also affect the intestinal microbiota. In addition, there is a great gap between the pathologically and pathophysiologically of PD patients and PD animal models, so the two cannot be simply confused, and ultimately there is no microbiota with absolutely consistent trends in all studies. But we screened for the more common ones, and at least these flora showed similar changes in both. It is worth taking them as follow-up research points and conducting research based on PD models, so as to provide some microbiota related treatment references for relieving the pain of PD patients.

In summary, this study explored the differences between PD patients at different stages and healthy people, and between PD models at different stages in terms of changes in the intestinal microbes at different classification levels. Subsequent research on early PD patients and models can be based on *Akkermansia*, *Alistipes*, *Anaerotruncus*, *Bilophila*, *Rikenellaceae*, *Verrucomicrobia* and *Verrucomicrobia*. Research on late PD patients and models may be based on the *Actinobacteriota* and *Erysipelotrichaceae*.

## Acknowledgements

The authors sincerely thank all participants and researchers for their invaluable cooperation in this study.

**Funding:** This research was supported by grants from the National Major Science and Technology Projects of China (2020071720300). The funding source had no involvement in the study design, data collection, analysis, interpretation of results, or manuscript preparation.

**Conflict of Interest:** The authors have no conflicts of interest to disclose.

## References

1. Hoehn MM, Yahr MD. Parkinsonism: onset, progression and mortality. *Neurology*. 1967; 17:427-442.
2. Goetz CG, Poewe W, Rascol O, Sampaio C, Stebbins GT, Counsell C, Giladi N, Holloway RG, Moore CG, Wenning GK, Yahr MD, Seidl L, Movement Disorder Society Task Force on Rating Scales for Parkinson's Disease. Movement Disorder Society Task Force report on the Hoehn and Yahr staging scale: status and recommendations. *Mov Disord*. 2004; 19:1020-1028.
3. Chinese Society of Parkinson's Disease and Movement Disorders, Parkinson's Disease and Movement Disorder Section of Neurologist Branch of Chinese Medical Doctor Association. Chinese guidelines for the treatment of Parkinson's disease (fourth edition). *Chinese Journal of Neurology*. 2020; 53:973-986. (in Chinese)
4. Zhuang M, Zhang X, Cai J. Microbiota-gut-brain axis: interplay between microbiota, barrier function and lymphatic system. *Gut Microbes*. 2024; 16:2387800.
5. Nuzum ND, Deady C, Kittel-Schneider S, Cryan JF, O'Mahony SM, Clarke G. More than just a number: the gut microbiota and brain function across the extremes of life. *Gut Microbes*. 2024; 16:2418988.
6. Domínguez Rojo N, Blanco Benítez M, Cava R, Fuentes JM, Canales Cortés S, González Polo RA. Convergence of neuroinflammation, microbiota, and Parkinson's disease: Therapeutic insights and prospects. *Int J Mol Sci*. 2024; 25:11629.
7. Zhao Z, Chen J, Zhao D, Chen B, Wang Q, Li Y, Chen J, Bai C, Guo X, Hu N, Zhang B, Zhao R, Yuan J. Microbial biomarker discovery in Parkinson's disease through a network-based approach. *NPJ Parkinsons Dis*. 2024; 10:203.
8. Zhu M, Liu X, Ye Y, Yan X, Cheng Y, Zhao L, Chen F, Ling Z. Gut microbiota: A novel therapeutic target for Parkinson's disease. *Front Immunol*. 2022; 13:937555.
9. Jackson-Lewis V, Przedborski S. Protocol for the MPTP mouse model of Parkinson's disease. *Nat Protoc*. 2007; 2:141-151.
10. Madiha S, Batool Z, Shahzad S, Tabassum S, Liaquat L, Afzal A, Sadir S, Sajid I, Mehdi BJ, Ahmad S, Haider S. Naringenin, a functional food component, improves motor and non-motor symptoms in animal model of parkinsonism induced by rotenone. *Plant Foods Hum Nutr*. 2023; 78:654-661.
11. Haider S, Madiha S, Batool Z. Amelioration of motor and non-motor deficits and increased striatal APoE levels highlight the beneficial role of pistachio supplementation

- in rotenone-induced rat model of PD. *Metab Brain Dis.* 2020; 35:1189-1200.
12. Sharma S, Kumar P, Deshmukh R. Neuroprotective potential of spermidine against rotenone induced Parkinson's disease in rats. *Neurochem Int.* 2018; 116:104-111.
  13. Liu X, Du ZR, Wang X, Luk KH, Chan CH, Cao X, Zhao Q, Zhao F, Wong WT, Wong KH, Dong XL. Colonic dopaminergic neurons changed reversely with those in the midbrain *via* gut microbiota-mediated autophagy in a chronic Parkinson's disease mice model. *Front Aging Neurosci.* 2021; 13:649627.
  14. Hu XM, Song LZ, Zhang ZZ, Ruan X, Li HC, Yu Z, Huang L. Electroacupuncture at ST25 corrected gut microbial dysbiosis and SNpc lipid peroxidation in Parkinson's disease rats. *Front Microbiol.* 2024; 15:1358525.
  15. Eo H, Yu SH, Choi Y, Kim Y, Kang YC, Lee H, Kim JH, Han K, Lee HK, Chang MY, Oh MS, Kim CH. Mitochondrial transplantation exhibits neuroprotective effects and improves behavioral deficits in an animal model of Parkinson's disease. *Neurotherapeutics.* 2024; 21:e00355.
  16. Gao L, Cao M, Du GH, Qin XM. Huangqin decoction exerts beneficial effects on rotenone-induced rat model of Parkinson's disease by improving mitochondrial dysfunction and alleviating metabolic abnormality of mitochondria. *Front Aging Neurosci.* 2022; 14:911924.
  17. Kerdiles O, Oye Mintsu Mi-Mba MF, Coulombe K, Tremblay C, Émond V, Saint-Pierre M, Rouxel C, Berthiaume L, Julien P, Cicchetti F, Calon F. Additive neurorestorative effects of exercise and docosahexaenoic acid intake in a mouse model of Parkinson's disease. *Neural Regen Res.* 2025; 20:574-586.
  18. Jiang W, Cheng Y, Wang Y, Wu J, Rong Z, Sun L, Zhou Y, Zhang K. Involvement of abnormal p- $\alpha$ -syn accumulation and TLR2-mediated inflammation of Schwann cells in enteric autonomic nerve dysfunction of Parkinson's disease: an animal model study. *Mol Neurobiol.* 2023; 60:4738-4752.
  19. Aho VTE, Pereira PAB, Voutilainen S, Paulin L, Pekkonen E, Auvinen P, Scheperjans F. Gut microbiota in Parkinson's disease: Temporal stability and relations to disease progression. *EBioMedicine.* 2019; 44:691-707.
  20. Babacan Yildiz G, Kayacan ZC, Karacan I, Sumbul B, Elibol B, Gelisin O, Akgul O. Altered gut microbiota in patients with idiopathic Parkinson's disease: an age-sex matched case-control study. *Acta Neurol Belg.* 2023; 123:999-1009.
  21. Barichella M, Severgnini M, Cilia R, *et al.* Unraveling gut microbiota in Parkinson's disease and atypical parkinsonism. *Mov Disord.* 2019; 34:396-405.
  22. Bi ZA. Analysis of gut microbiota in patients with Parkinson's disease. Nanjing Medical University. 2018. (in Chinese)
  23. Bolliri C, Fontana A, Cereda E, Barichella M, Cilia R, Ferri V, Caronni S, Calandrella D, Morelli L, Pezzoli G. Gut microbiota in monozygotic twins discordant for Parkinson's disease. *Ann Neurol.* 2022; 92:631-636.
  24. Cerroni R, Pietrucci D, Teofani A, Chillemi G, Liguori C, Pierantozzi M, Unida V, Selmani S, Mercuri NB, Stefani A. Not just a snapshot: An Italian longitudinal evaluation of stability of gut microbiota findings in Parkinson's disease. *Brain Sci.* 2022; 12:739.
  25. Chen H. Diversity of intestinal microflora in patients with Parkinson's disease. Jinan University. 2017. (in Chinese)
  26. Cirstea MS, Yu AC, Golz E, Sundvick K, Kliger D, Radisavljevic N, Foulger LH, Mackenzie M, Huan T, Finlay BB, Appel-Cresswell S. Microbiota composition and metabolism are associated with gut function in Parkinson's disease. *Mov Disord.* 2020; 35:1208-1217.
  27. Hill-Burns EM, Debelius JW, Morton JT, Wissemann WT, Lewis MR, Wallen ZD, Peddada SD, Factor SA, Molho E, Zabetian CP, Knight R, Payami H. Parkinson's disease and Parkinson's disease medications have distinct signatures of the gut microbiome. *Mov Disord.* 2017; 32:739-749.
  28. Li F, Wang P, Chen Z, Sui X, Xie X, Zhang J. Alteration of the fecal microbiota in North-Eastern Han Chinese population with sporadic Parkinson's disease. *Neurosci Lett.* 2019; 707:134297.
  29. Li KS. Multi-center Clinical observation of acupuncture intervention of Parkinson's disease and its effect on intestinal microbiome, short chain fatty acid. Shanghai University of Traditional Chinese Medicine. 2020. (in Chinese)
  30. Li T. The relationship between TCM syndrome and clinical stage, substantia nigra change and intestinal flora of Parkinson's disease. Beijing University of Chinese Medicine. 2020. (in Chinese)
  31. Li Y, Li RX, Du YT, Xu XJ, Xue Y, Gao D, Gao T, Sheng Z, Zhang LY, Tuo HZ. Features of gut microbiota in patients with idiopathic Parkinson's disease. *National Medical Journal of China.* 2020; 100:1017-1022. (in Chinese)
  32. Lin A, Zheng W, He Y, Tang W, Wei X, He R, Huang W, Su Y, Huang Y, Zhou H, Xie H. Gut microbiota in patients with Parkinson's disease in southern China. *Parkinsonism Relat Disord.* 2018; 53:82-88.
  33. Mao L, Zhang Y, Tian J, Sang M, Zhang G, Zhou Y, Wang P. Cross-Sectional study on the gut microbiome of Parkinson's disease patients in central China. *Front Microbiol.* 2021; 12:728479.
  34. Nakahara K, Nakane S, Ishii K, Ikeda T, Ando Y. Gut microbiota of Parkinson's disease in an appendectomy cohort: a preliminary study. *Sci Rep.* 2023; 13:2210.
  35. Pietrucci D, Cerroni R, Unida V, Farcomeni A, Pierantozzi M, Mercuri NB, Biocca S, Stefani A, Desideri A. Dysbiosis of gut microbiota in a selected population of Parkinson's patients. *Parkinsonism Relat Disord.* 2019; 65:124-130.
  36. Qian Y, Yang X, Xu S, Huang P, Li B, Du J, He Y, Su B, Xu LM, Wang L, Huang R, Chen S, Xiao Q. Gut metagenomics-derived genes as potential biomarkers of Parkinson's disease. *Brain.* 2020; 143:2474-2489.
  37. Ren T, Gao Y, Qiu Y, Jiang S, Zhang Q, Zhang J, Wang L, Zhang Y, Wang L, Nie K. Gut microbiota altered in mild cognitive impairment compared with normal cognition in sporadic Parkinson's disease. *Front Neurol.* 2020; 11:137.
  38. Scheperjans F, Aho V, Pereira PA, Koskinen K, Paulin L, Pekkonen E, Haapaniemi E, Kaakkola S, Eerola-Rautio J, Pohja M, Kinnunen E, Murros K, Auvinen P. Gut microbiota are related to Parkinson's disease and clinical phenotype. *Mov Disord.* 2015; 30:350-358.
  39. Tan AH, Chong CW, Lim SY, Yap IKS, Teh CSJ, Loke MF, Song SL, Tan JY, Ang BH, Tan YQ, Kho MT, Bowman J, Mahadeva S, Yong HS, Lang AE. Gut microbial ecosystem in Parkinson's disease: New clinicobiological insights from multi-omics. *Ann Neurol.* 2021; 89:546-559.
  40. Tetz G, Brown SM, Hao Y, Tetz V. Parkinson's disease and bacteriophages as its overlooked contributors. *Sci Rep.*

- 2018; 8:10812.
41. Tong QW, Chen YF, Wu SX, Zheng LF, Chen YY, Feng M, Ye H. Relationship between gut microbiota and clinical symptoms in patients with Parkinson's disease. *Zhejiang Medical Journal*. 2021; 43:1085-1090. (in Chinese)
  42. Vascellari S, Palmas V, Melis M, *et al.* Gut microbiota and metabolome alterations associated with Parkinson's disease. *mSystems*. 2020; 5:e00561-20.
  43. Wallen ZD, Demirkan A, Twa G, Cohen G, Dean MN, Standaert DG, Sampson TR, Payami H. Metagenomics of Parkinson's disease implicates the gut microbiome in multiple disease mechanisms. *Nat Commun*. 2022; 13:6958.
  44. Wang YJ. Alterations of intestinal flora and its relationship with intestinal features in Parkinson's disease patients. ZHENGZHOU UNIVERSITY. 2022. (in Chinese)
  45. Zhang F. Gut microbiota diversity analysis and biomarker identification in patients with Parkinson's disease. Hubei University of Medicine. 2020. (in Chinese)
  46. Zhang F, Fang X, Xu ML, Zhang Y, Gao P, Zhao Q, Sun XD, Sang M, Wang PQ. The changed abundance of intestinal *Prevotella\_copri* and its predictive value in patients with Parkinson's disease. *Journal of Medical Research & Combat Trauma Care*. 2020; 33:482-486. (in Chinese)
  47. Zhang LN, Ye M, Shi P, Yin L, Li QQ, Lu L. Structural characteristics of intestinal flora in patients with Parkinson's disease. *Diet Health*. 2021; 27:27. (in Chinese)
  48. Zhang TQ. The characteristics of intestinal flora in Parkinson's disease and the curative effect of Shengqing Jiangzhuo prescription on constipation. Beijing University of Chinese Medicine. 2019. (in Chinese)
  49. Zhao C, Yu HY, Li W, Shi J, Qin B. Structural changes of gut microbiota in patients with Parkinson's disease. *Chinese Journal of Neurology*. 2018; 51:498-503. (in Chinese)
  50. Zhuo WY. Changes of intestinal flora and SNCA gene polymorphism in patients with Parkinson's disease. Jinan University. 2018. (in Chinese)
  51. Aktas B. Gut microbial alteration in MPTP mouse model of Parkinson's disease is administration regimen dependent. *Cell Mol Neurobiol*. 2023; 43:2815-2829.
  52. An YY. Resveratrol ameliorates the symptoms of Parkinson's disease mouse and its effect on gut microbiota. Xinxiang Medical University. 2019. (in Chinese)
  53. An YY, Wu MN, Li PZ, Jing XR, Zhang JF, Xue HF, Deng BG, Zhong GS. Effect of oral administration of streptomycin sulfate on symptoms and gut microbiota of Parkinson's disease mice. *Acta Microbiologica Sinica*. 2019; 59:1636-1650. (in Chinese)
  54. Chen XX, Wang T, Zhang T. MPTP-induced intestinal flora and brain inflammation in a mouse model of chronic Parkinson's disease. *Chinese Journal of Gerontology*. 2022; 42:4031-4035. (in Chinese)
  55. Chen XX, Wang T, Zhang T. Effects of fecal bacteria transplantation on inflammation of substantia nigra in mice with chronic Parkinson's disease. *Chinese Journal of Gerontology*. 2022; 42:4778-4783. (in Chinese)
  56. Dong XL, Wang X, Liu F, Liu X, Du ZR, Li RW, Xue CH, Wong KH, Wong WT, Zhao Q, Tang QJ. Polymannuronic acid prevents dopaminergic neuronal loss *via* brain-gut-microbiota axis in Parkinson's disease model. *Int J Biol Macromol*. 2020; 164:994-1005.
  57. Jang JH, Yeom MJ, Ahn S, Oh JY, Ji S, Kim TH, Park HJ. Acupuncture inhibits neuroinflammation and gut microbial dysbiosis in a mouse model of Parkinson's disease. *Brain Behav Immun*. 2020; 89:641-655.
  58. Jeon H, Bae CH, Lee Y, Kim HY, Kim S. Korean red ginseng suppresses 1-methyl-4-phenyl-1,2,3,6-tetrahydropyridine-induced inflammation in the substantia nigra and colon. *Brain Behav Immun*. 2021; 94:410-423.
  59. Liao JF, Cheng YF, You ST, Kuo WC, Huang CW, Chiou JJ, Hsu CC, Hsieh-Li HM, Wang S, Tsai YC. *Lactobacillus plantarum* PS128 alleviates neurodegenerative progression in 1-methyl-4-phenyl-1,2,3,6-tetrahydropyridine-induced mouse models of Parkinson's disease. *Brain Behav Immun*. 2020; 90:26-46.
  60. Liu MM, Zhou N, Jiang N, Lu KM, Wu CF, Bao JK. Neuroprotective effects of oligosaccharides from *Periplaneta Americana* on Parkinson's disease models *in vitro* and *in vivo*. *Front Pharmacol*. 2022; 13:936818.
  61. Liu X, Liu S, Tang Y, Pu Z, Xiao H, Gao J, Yin Q, Jia Y, Bai Q. Intragastric administration of casein leads to nigrostriatal disease progressed accompanied with persistent nigrostriatal-intestinal inflammation activated and intestinal microbiota-metabolic disorders induced in MPTP mouse model of Parkinson's disease. *Neurochem Res*. 2021; 46:1514-1539.
  62. Liu X, Du ZR, Wang X, Luk KH, Chan CH, Cao X, Zhao Q, Zhao F, Wong WT, Wong KH, Dong XL. Colonic dopaminergic neurons changed reversely with those in the midbrain *via* gut microbiota-mediated autophagy in a chronic Parkinson's disease mice model. *Front Aging Neurosci*. 2021; 13:649627.
  63. Liu X, Du ZR, Wang X, Sun XR, Zhao Q, Zhao F, Wong WT, Wong KH, Dong XL. Polymannuronic acid prebiotic plus *Lactocaseibacillus rhamnosus* GG probiotic as a novel synbiotic promoted their separate neuroprotection against Parkinson's disease. *Food Res Int*. 2022; 155:111067.
  64. Shi Y. 5-HT4 receptor antagonist exacerbates neuropathology *via* gut-brain axis in Parkinson's disease mice. JIANGNAN UNIVERSITY. 2021. (in Chinese)
  65. Sun MF, Zhu YL, Zhou ZL, Jia XB, Xu YD, Yang Q, Cui C, Shen YQ. Neuroprotective effects of fecal microbiota transplantation on MPTP-induced Parkinson's disease mice: Gut microbiota, glial reaction and TLR4/TNF- $\alpha$  signaling pathway. *Brain Behav Immun*. 2018; 70:48-60.
  66. Sun Z, Gu P, Xu H, Zhao W, Zhou Y, Zhou L, Zhang Z, Wang W, Han R, Chai X, An S. Human umbilical cord mesenchymal stem cells improve locomotor function in Parkinson's disease mouse model through regulating intestinal microorganisms. *Front Cell Dev Biol*. 2022; 9:808905.
  67. Zhang LY. Based on gut microbes to study the effect of "anti-Parkinson granule" on improving the behavior and constipation of Parkinson's model mice. SHUTCM. 2020. (in Chinese)
  68. Weis S, Schwirtz A, Unger MM, Becker A, Faßbender K, Ratering S, Kohl M, Schnell S, Schäfer KH, Egert M. Effect of Parkinson's disease and related medications on the composition of the fecal bacterial microbiota. *NPJ Parkinsons Dis*. 2019; 5:28.
  69. Feng W. Research progress on the involvement of intestinal microbes in the occurrence and development of Parkinson's disease. *Chinese Journal of Practical Nervous Diseases*. 2024; 27:504-507. (in Chinese)
  70. Akyazı O, Korkmaz D, Cevher SC. Experimental Parkinson models and green chemistry approach. *Behav Brain Res*. 2024; 471:115092.

71. Bisbal M, Sanchez M. Neurotoxicity of the pesticide rotenone on neuronal polarization: a mechanistic approach. *Neural Regen Res.* 2019; 14:762-766.
72. Meng JL, Liang JF, Zhang XB, Wen MJ, Deng XY. Research progress and evaluation on animal models of Parkinson's disease. *Acta Laboratorium Animalis Scientia Sinica.* 2021; 29:399-404. (in Chinese)
73. Mao ML, Guan YR, Yan YM, Li T, Wang D. Discussion on the best modeling method of rotenone-induced Parkinson's disease model. *Chinese Journal of Integrative Medicine on Cardio-Cerebrovascular Disease.* 2022; 20:1611-1616. (in Chinese)
74. Dovonou A, Bolduc C, Soto Linan V, Gora C, Peralta Iii MR, Lévesque M. Animal models of Parkinson's disease: bridging the gap between disease hallmarks and research questions. *Transl Neurodegener.* 2023; 12:36.
75. Zhang QS, Heng Y, Mou Z, Huang JY, Yuan YH, Chen NH. Reassessment of subacute MPTP-treated mice as animal model of Parkinson's disease. *Acta Pharmacol Sin.* 2017; 38:1317-1328.
76. Han X, Liu Y, Dai Y, Xu T, Hu Q, Yi X, Rui L, Hu G, Hu J. Neuronal SH2B1 attenuates apoptosis in an MPTP mouse model of Parkinson's disease *via* promoting PLIN4 degradation. *Redox Biol.* 2022; 52:102308.
77. Davey LE, Malkus PN, Villa M, Dolat L, Holmes ZC, Letourneau J, Ansaldo E, David LA, Barton GM, Valdivia RH. A genetic system for *Akkermansia muciniphila* reveals a role for mucin foraging in gut colonization and host sterol biosynthesis gene expression. *Nat Microbiol.* 2023; 8:1450-1467.
78. Bonnechère B, Amin N, van Duijn C. What are the key gut microbiota involved in neurological diseases? A systematic review. *Int J Mol Sci.* 2022; 23:13665.
79. Chiantera V, Laganà AS, Basciani S, Nordio M, Bizzarri M. A critical perspective on the supplementation of *Akkermansia muciniphila*: benefits and harms. *Life (Basel).* 2023; 13:1247.
80. Qiao CM, Huang WY, Zhou Y, Quan W, Niu GY, Li T, Zhang MX, Wu J, Zhao LP, Zhao WJ, Cui C, Shen YQ. *Akkermansia muciniphila* is beneficial to a mouse model of Parkinson's disease, *via* alleviated neuroinflammation and promoted neurogenesis, with involvement of SCFAs. *Brain Sci.* 2024; 14:238.
81. Khan S, Waliullah S, Godfrey V, Khan MAW, Ramachandran RA, Cantarel BL, Behrendt C, Peng L, Hooper LV, Zaki H. Dietary simple sugars alter microbial ecology in the gut and promote colitis in mice. *Sci Transl Med.* 2020; 12:eaay6218.
82. Shkorporov AN, Chaplin AV, Khokhlova EV, Shcherbakova VA, Motuzova OV, Bozhenko VK, Kafarskaia LI, Efimov BA. *Alistipes inops* sp. nov. and *Coprobacter secundus* sp. nov., isolated from human faeces. *Int J Syst Evol Microbiol.* 2015; 65:4580-4588.
83. Kaur H, Das C, Mande SS. *In silico* analysis of putrefaction pathways in bacteria and its implication in colorectal cancer. *Front Microbiol.* 2017; 8:2166.
84. Parker BJ, Wearsch PA, Veloo ACM, Rodriguez-Palacios A. The Genus *Alistipes*: Gut bacteria with emerging implications to inflammation, Cancer, and Mental Health. *Front Immunol.* 2020; 11:906.
85. Bai F, You L, Lei H, Li X. Association between increased and decreased gut microbiota abundance and Parkinson's disease: A systematic review and subgroup meta-analysis. *Exp Gerontol.* 2024; 191:112444.
86. Li J, Ni Y, Huang L, Yu X, Zhu J. Er-Bai-Tang decoction improved the movement disorders and neuronal injury in the Parkinson's disease model rats *via* decreasing p38 MAPK pathway and improving the composition of intestinal flora. *Acta Cir Bras.* 2023; 37:e371104.
87. Qian Y, Yang X, Xu S, Wu C, Song Y, Qin N, Chen SD, Xiao Q. Alteration of the fecal microbiota in Chinese patients with Parkinson's disease. *Brain Behav Immun.* 2018; 70:194-202.
88. Li Z, Liang H, Hu Y, *et al.* Gut bacterial profiles in Parkinson's disease: A systematic review. *CNS Neurosci Ther.* 2023; 29:140-157.
89. Zhang H. Correlation analysis between Parkinson's disease and intestinal flora. Henan University. 2023. (in Chinese)
90. Zhao ZF. The study of brain dopamine transporter, the level of proBDNF in serum and intestinal flora's changes in patients with Parkinson's disease. Army Medical University. 2019. (in Chinese)
91. Li Z, Lu G, Li Z, *et al.* Altered actinobacteria and firmicutes phylum associated epitopes in patients with Parkinson's disease. *Front Immunol.* 2021; 12:632482.
92. Lubomski M, Xu X, Holmes AJ, Muller S, Yang JYH, Davis RL, Sue CM. The gut microbiome in Parkinson's disease: A longitudinal study of the impacts on disease progression and the use of device-assisted therapies. *Front Aging Neurosci.* 2022; 14:875261.
93. Lai F, Jiang R, Xie W, Liu X, Tang Y, Xiao H, Gao J, Jia Y, Bai Q. Intestinal pathology and gut microbiota alterations in a methyl-4-phenyl-1,2,3,6-tetrahydropyridine (MPTP) mouse model of Parkinson's disease. *Neurochem Res.* 2018; 43:1986-1999.

Received October 31, 2025; Revised January 16, 2025; Accepted January 22, 2025.

\*Address correspondence to:

Jinli Shi, School of Chinese Materia Medica, Beijing University of Chinese Medicine, No. 11, Bei San Huan Dong Lu, Chaoyang District, Beijing 100029, China.  
E-mail: shijl@vip.sina.com

Released online in J-STAGE as advance publication January 25, 2025

# $N^5$ -((perfluorophenyl)amino)glutamine regulates BACE1, tau phosphorylation, synaptic function, and neuroinflammation in Alzheimer's disease models

Jun-Sik Kim<sup>1,§</sup>, Yongeun Cho<sup>1,§</sup>, Jeongmi Lee<sup>1,§</sup>, Heewon Cho<sup>1</sup>, Sukmin Han<sup>2</sup>,  
Yeongyeong Lee<sup>1</sup>, Yeji Jeon<sup>1</sup>, Tai Kyoung Kim<sup>3</sup>, Ju-Mi Hong<sup>3</sup>, Jeonghyeong Im<sup>1</sup>,  
Minshik Chae<sup>1</sup>, Yujeong Lee<sup>1</sup>, Hyunwook Kim<sup>4</sup>, Sang Yoon Park<sup>4</sup>, Sung Hyun Kim<sup>2,5</sup>,  
Joung Han Yim<sup>3,\*</sup>, Dong-Gyu Jo<sup>1,6,7,8,\*</sup>

<sup>1</sup> School of Pharmacy, Sungkyunkwan University, Suwon, Korea;

<sup>2</sup> Department of Neuroscience, Graduate School, Kyung Hee University, Seoul, Korea;

<sup>3</sup> Division of Polar Life Sciences, Korea Polar Research Institute, Incheon, Korea;

<sup>4</sup> Bio Research Dept, Ahngook Pharmaceutical Co., Gwacheon, Korea;

<sup>5</sup> Department of Physiology, School of Medicine, Kyung Hee University, Seoul, Korea;

<sup>6</sup> Samsung Advanced Institute for Health Sciences and Technology, Sungkyunkwan University, Seoul, Korea;

<sup>7</sup> Biomedical Institute for Convergence, Sungkyunkwan University, Suwon, Korea;

<sup>8</sup> Institute of Quantum Biophysics, Sungkyunkwan University, Suwon, Korea.

**SUMMARY:** Alzheimer's disease (AD) is the most common type of dementia. Its incidence is rising rapidly as the global population ages, leading to a significant social and economic burden. AD involves complex pathologies, including amyloid plaque accumulation, synaptic dysfunction, and neuroinflammation. This study explores the therapeutic potential of  $N^5$ -((perfluorophenyl)amino)glutamine (RA-PF), a derivative of  $\gamma$ -glutamyl- $N'$ -(2-hydroxyphenyl)hydrazide (Ramalin), a compound with antioxidant and anti-inflammatory properties. Administration of RA-PF to 5xFAD mice decreases BACE1, reduces A $\beta$  plaque deposition, inhibits microglial activation, restores synaptic transmission, and improves mitochondrial motility, leading to the recovery of cognitive function. Additionally, RA-PF treatment in 3xTg-AD mice alleviates anxiety-like behaviors, tau phosphorylation via inactivating GSK-3 $\beta$ , and BACE1 expression. Further transcriptomic analysis reveals RA-PF treatment in AD mice models recovers phagosome, inflammation, NOD-like receptor, presynaptic membrane, and postsynaptic membrane related signaling pathways. These findings suggest that RA-PF effectively targets multiple aspects of AD pathology, offering a novel multi-target approach for AD treatment.

**Keywords:** Alzheimer's disease (AD), ramalin, RA-PF, BACE1, tau, synaptic function

## 1. Introduction

Alzheimer's disease (AD) is a degenerative brain disorder and the most prevalent form of dementia (1-3). The pathological features of AD include the accumulation of  $\beta$ -amyloid (A $\beta$ ) and tau proteins, neuroinflammation, and neuronal death, leading to a reduction in brain volume that is directly related to memory impairment (4-6). Beta-site amyloid precursor protein cleaving enzyme 1 (BACE1) is a key player in the production of A $\beta$ , which has been identified as a primary target for AD treatment (7-11). Neuroinflammation also plays a crucial role in the AD pathogenesis. Inflammatory responses accelerate AD progression, and they are activated even before the onset of symptoms (12,13). Inhibition of neuroinflammation

has been reported to show pre-clinical results in preventing AD onset (14,15).

Here, we introduce  $\gamma$ -glutamyl- $N'$ -(2-hydroxyphenyl)hydrazide (Ramalin) derivative showing pre-clinical efficacy on AD progression. Ramalin, isolated from the Antarctic lichen *Ramalina terebrata*, is known for its potent antioxidant, anti-inflammatory, and antibacterial effects (16,17). To enhance these therapeutic potentials, we designed and synthesized derivatives of ramalin by replacing its phenyl ring with various structural groups. From these derivatives,  $N^5$ -((perfluorophenyl)amino)glutamine (RA-PF) was identified through toxicity screening as exhibiting the lowest *in vivo* toxicity. And it is bioavailable and capable of penetrating the blood-brain barrier. In this study, we demonstrated RA-PF's

therapeutic effects on 5xFAD (10,11) and 3xTg-AD mice (10,11), which express mutations associated with familial AD (5xFAD: human APP (Swedish, Florida, London mutations) and PSEN1 (M146L and L286V mutations) and 3xTg: APP (Swedish), MAPT (P301L), and PSEN1 (M146V)). It reduces A $\beta$  plaque deposition by regulating BACE1 expression, inhibits tau phosphorylation, restores hippocampal neuronal transmission, and ameliorates neuroinflammatory responses in AD models. These findings highlight the potential of ramalin derivative, RA-PF as a therapeutic strategy for AD.

## 2. Materials and Methods

### 2.1. Animals

This study used 3xTg-AD (B6;129-Tg(APP<sup>Swe</sup>, tauP301L)1Lfa *Psen1*<sup>tm1Mpm</sup>/Mmjax) and 5xFAD (B6.Cg-Tg(APP<sup>Swe</sup>FILon, PSEN1\*<sup>M146L</sup>\*L286V)6799Vas/Mmjax) for AD animal models. All mice were kept in a 12-hour light/dark cycle with unrestricted access to food and water. 3xTg-AD mice were administered with 20 mg/kg of RA-PF once a day orally for 1.5 months and 5xFAD mice were treated with 20 mg/kg of RA-PF once a day orally for 2 months, respectively. After treatment, the mice underwent behavioral tests. All animal experimental procedures were approved by the Institutional Animal Care and Use Committee of Sungkyunkwan University (SKKUIACUC2022-10-41-1).

### 2.2. Synthesis method of RA-PF

Synthesis of benzyl *N*<sup>2</sup>-((benzyloxy)carbonyl)-*N*<sup>5</sup>-((perfluorophenyl)amino)glutamate (p-Glu-PF-Hyd): A 250 mL round-bottom flask fitted with a magnetic stir bar was charged with (*S*)-5-(benzyloxy)-4-(((benzyloxy)carbonyl)amino)-5-oxopentanoic acid (2.0 g, 5.39 mmol) dissolved in 50 mL of dichloromethane (DCM). The reaction mixture was cooled to 0°C, and then triethylamine (TEA) (1.2 equivalents, 6.47 mmol, 902  $\mu$ L) was added gradually. After 10 minutes, ethyl chloroformate (ECF) (1.2 equivalents, 6.47 mmol, 615  $\mu$ L) was introduced dropwise over 1 hour. The mixture was stirred at 0°C for 4 hours. In a separate 100 mL pear-shaped flask, (perfluorophenyl)hydrazine (1.2 equivalents, 6.47 mmol, 1.28 g) was dissolved in 10 mL of DCM. This solution was then added slowly to the primary reaction flask over 1 hour while maintaining the temperature at 0°C. After the hydrazine was added, the reaction mixture was allowed to reach RT and stirred for an additional 16 hours. Upon completion, the organic layer was washed sequentially with distilled water, 1 N HCl, 0.5 N NaHCO<sub>3</sub>, and distilled water again, before being separated and collected. The organic phase was dried over sodium sulfate (Na<sub>2</sub>SO<sub>4</sub>) and concentrated using a rotary evaporator. The target product was purified

by recrystallization from a mixture of ethyl acetate and n-hexane (1:5). The synthesis yield of p-Glu-PF-Hyd is 92% (4.96 g).

Synthesis of *N*<sup>5</sup>-((perfluorophenyl)amino)glutamine (RA-PF): A 500 mL round-bottom flask with a magnetic stir bar was loaded with the p-Glu-PF-Hyd (3.6 mmol, 2.0 g) and palladium on carbon (10 wt.%, 200 mg) in methanol (400 mL). The reaction mixture was stirred under hydrogen atmosphere (1 atm, using a hydrogen balloon) for 16 h. Once the reaction was complete, the mixture was passed through a 0.4  $\mu$ m glass microfiber filter. The filtrate was then concentrated using a rotary evaporator, followed by purification through recrystallization from a 1:5 mixture of methanol and ethyl acetate. The synthesis yield of RA-PF is 80 % (940 mg).

### 2.3. Morris water maze

The Morris water maze test (MWM) was conducted to examine the spatial memory and learning abilities of the mice. The MWM was carried out as previously described with minor modifications (18). A pool with a diameter of 100 cm was used. Before the experiments began, the pool was filled with water to a level 1 cm higher than the platform, and non-toxic white pigment was added to prevent the mice from seeing the platform. The training sessions were conducted for 8 consecutive days, and mice were placed in three different locations each day. The escape latency and swimming speed were recorded by a camera. Each trial lasted for 60 seconds and if the mouse found the hidden platform within 60 seconds and stayed on it for 5 seconds, the mouse was returned to the cage. If the mouse did not find the platform within 60 seconds, it was put on the hidden platform and allowed to observe the surroundings for 10 seconds. All experimental data was recorded and analyzed by Ethovision software (Noldus).

### 2.4. Elevated plus maze test

The elevated plus maze test (EPM) is a widely used behavioral test to assess the anxiety of the mice (19). Briefly, the mouse was placed in the center of the elevated plus maze facing an open arm and allowed to explore for 5 minutes. Behavioral patterns were recorded and analyzed by Ethovision software (Noldus).

### 2.5. Brain tissue preparation

After behavioral tests, mice were sacrificed, and brain samples of mice were collected. Mice were anesthetized using Zoletil (Virbac) and Rompun (Bayer) and then perfused with phosphate-buffered saline (PBS). The two hemispheres of the brain were separated. One hemisphere was stored in 4% paraformaldehyde and the other was dissected into cortex and hippocampus. Dissected

samples were then snap-frozen in liquid nitrogen and stored at -80 °C until further analysis.

#### 2.6. Microsomal stability assay

The metabolic stability of RA-PF was assessed using liver microsomes derived from humans and various animal species including mice, rats, dogs, and monkeys. This test was conducted by SP MED Co., Ltd (Republic of Korea). A 1 µM of RA-PF was incubated with liver microsomes at 37 °C for 30 minutes in the presence or absence of NADPH. The reaction was terminated by adding acetonitrile containing an internal standard. Samples were then centrifuged, and the supernatants were further analyzed by LC-MS/MS. The percentage of RA-PF remaining was calculated by comparing the quantified amount of RA-PF at 30 minutes to that at 0 minutes. This provided the % remaining value, which reflects the compound's metabolic stability under the test conditions.

#### 2.7. Cytochrome P450 inhibitory assay

The inhibitory potential of RA-PF on key cytochrome P450 (CYP) isoforms (CYP1A2, CYP2C9, CYP2C19, CYP2D6, and CYP3A) was evaluated. This test was conducted by SP MED Co., Ltd (Republic of Korea). Human liver microsomes were incubated with phosphate buffer (pH 7.4), each CYP substrate (phenacetin for CYP1A2, diclofenac for CYP2C9, S-mephenytoin for CYP2C19, dextromethorphan for CYP2D6, and midazolam for CYP3A), and 10 µM of RA-PF in the presence of NADPH. The reaction was terminated by the addition of an acetonitrile containing an internal standard. Samples were then centrifuged, and the supernatant was analyzed by LC-MS/MS to quantify the amount of metabolites of each substrate drug.

#### 2.8. Pharmacokinetic study

Pharmacokinetic parameters of RA-PF were measured using Sprague-Dawley rats by NeuroVis (Republic of Korea). Animals received 10 mg/kg of RA-PF *via* either oral administration or intravenous injection. Blood collection was performed using the BASi Culex ABS (Automated Blood Sampling) system. After catheter insertion into the jugular vein and carotid artery, the system was programmed to collect 200 µL blood samples at predetermined time points (0, 0.25, 0.5, 1, 2, and 7 hours). Blood samples were then centrifuged at 12,000 x rpm for 10 minutes, and the resulting plasma was immediately stored at -80 °C. For brain pharmacokinetics analysis, 10 mg/kg of RA-PF was orally administered to Sprague-Dawley rats. Blood and brain tissue samples were collected post-administration. Samples were mixed with ofloxacin, an internal standard, and centrifuged at 13,000 x rpm for 5 minutes at 4 °C. Supernatants were

mixed with 50% methanol and analyzed by LC-MS/MS.

#### 2.9. Mutagenicity assay (Ames test)

To evaluate whether RA-PF causes DNA mutation, the Ames test was performed using *Salmonella typhimurim* TA98, TA100, TA1535, TA1537 and *Escherichia coli* WP2uvrA (pKM101). 6 doses of RA-PF (50, 100, 500, 1,000, 2,500, and 5,000 µg/plate) were tested. RA-PF was incubated with S9 mix, each bacterial suspension, and top agar specific to each bacterium, followed by vortexing. The resulting suspensions were then overlaid onto minimum glucose agar plates, which were subsequently left at RT. After top agar solidified, plates were incubated at 37 °C for 48 hours. Following incubation, revertant colonies were then counted visually.

#### 2.10. Cell culture

Human neuroblastoma cell line, SH-SY5Y, and mouse microglial cell line, BV-2 were maintained in DMEM (Hyclone) media supplemented with 10 % fetal bovine serum (Gibco) and 1 % penicillin/streptomycin (Capricorn) at 37 °C in a humidified atmosphere containing 5 % CO<sub>2</sub> (v/v). For the BV-2 cell line culture, heat-inactivated FBS was used. SH-SY5Y cells were treated with 5 µM and 10 µM of RA-PF for 24 hours. Then, cells were exposed to 200 µM of hydrogen peroxide (Sigma) for 2 hours. BV-2 cells were incubated with 5 µM and 10 µM of RA-PF for 24 hours and then treated with 0.1 µg/mL of lipopolysaccharide (Sigma) for 2 hours.

#### 2.11. Primary neuron culture

Hippocampal CA1-CA3 regions were isolated from postnatal (0-3 day old) 5xFAD transgenic mice and plated on poly-ornithine-coated coverslips. Neurons were transfected 7 days after plating and further incubated for 14–21 days in a culture medium. All results are from at least three independent primary cultures. Animal treatments in this study were carried out in accordance with Animal Care and Use Guidelines, and all experiments were approved by the Animal Care Committee of Kyung Hee University (KHSASP-24-266).

#### 2.12. *In vitro* optical imaging

For optical imaging, vGlut1-pHluorin (vG-pH) was transfected to primary cultured hippocampal neurons using the Ca<sup>2+</sup> phosphate precipitation method, as previously described (20). Briefly, vG-pH was incubated with 2x HeBS (273 mM NaCl, 9.5 mM KCl, 1.4 mM Na<sub>2</sub>HPO<sub>4</sub>·PO<sub>2</sub>O, 15 mM D-glucose, 42 mM HEPES, pH 7.10) containing 2 mM Ca<sup>2+</sup>, subsequently, the mixture was applied to hippocampal neurons cultured for 8 days *in vitro* (DIV8). Live-cell imaging was conducted

on neurons at DIV14-21 neurons, which had been transfected with vG-pH 7 days post-plating. Neurons were present with 10  $\mu$ M of RA-PF for 6 h. Coverslips containing neurons were mounted in a laminar-flow-perfused stimulation chamber on the stage of a custom-built, laser-illuminated epifluorescence microscope (Zeiss Observer). Live-cell images were captured using an Andor iXon Ultra 897 (Model #DU-897U-CS0-#BV) back-illuminated EMCCD camera. A diode-pumped OBIS 488 laser (Coherent) is used as the light source, with its TTL on/off synchronized with the EMCCD camera during image acquisition. Fluorescence excitation/emission and collection were performed using a 40 $\times$ Fluar Zeiss objective lens (1.3 NA) along with 500–550 nm emission and 498 nm dichroic filters (Chroma). Action potentials (APs) were induced by passing a 1-ms current pulse *via* platinum-iridium electrodes using an isolated current stimulator (World Precision Instruments). Neurons were perfused with Tyrode's buffer containing 119 mM NaCl, 2.5 mM KCl, 2 mM CaCl<sub>2</sub>, 2 mM MgCl<sub>2</sub>, 25 mM HEPES, 30 mM glucose, 10  $\mu$ M 6-cyano-7-nitroquinoxaline-2,3-dione (CNQX), and D, L-2-amino-5-phosphonovaleric acid (AP5), with the pH adjusted to 7.4. All experiments were conducted at 30 °C. All images were captured at 2 Hz with a 50-ms exposure.

### 2.13. *In vitro* imaging for mitochondria motility

For recording mitochondria motility, neurons were transfected with Mito-red plasmids at DIV7 and further incubated until 14-21 DIV. Live-cell imaging was carried out using a custom-built, laser-illuminated epifluorescence microscope (Zeiss Observer). Neurons expressing Mito-red were illuminated with a 561 nm laser and images were acquired every 3 seconds for 5 min. For analyzing mitochondria motility, the total number of Mito-red positive puncta were counted at the axon, and during the imaging period (5 min), more than 1  $\mu$ m moving Mito-red is defined as motility of mitochondria.

### 2.14. Image analysis

All images were analyzed using Image J (<http://rsb.info.nih.gov/ij>) with the plugin Time Series Analyzer which is available at <https://imagej.nih.gov/ij/plugins/time-series.html>. Synaptic boutons were selected as oval regions of interest (diameter, 10 pixels), and the intensity of fluorescence at synapses was measured. Fluorescence traces were analyzed using Origin Pro (ver. 2020).

### 2.15. Western blot analysis

Cells were lysed with T-PER™ Tissue Protein Extraction Reagent (Thermo Scientific) supplemented with the protease/phosphatase inhibitor cocktail (Thermo Scientific) and incubated at 4°C for 10 minutes. The

samples were then centrifuged at 13,000 x rpm for 10 minutes at 4°C. The supernatant was used for western blot analysis. Mouse brain tissue samples were homogenized with RIPA lysis buffer (Merck) supplemented with the protease/phosphatase inhibitor cocktail. The homogenate was incubated at 4°C for 20 minutes and the lysed samples were then centrifuged at 13,000 $\times$ rpm for 20 minutes at 4°C. The supernatant was used for western blot analysis. Protein concentrations of lysed samples were quantified using Pierce™ BCA Protein Assay Kits (Thermo Scientific). Equal amounts of protein samples were combined with NuPAGE™ LDS Sample Buffer (Invitrogen) containing 5% 2-mercaptoethanol (Sigma) and heated at 95 °C for 5 minutes. Subsequently, 8-10  $\mu$ g of each sample was loaded onto SDS-polyacrylamide gels and subjected to electrophoresis until the protein bands were fully separated. Following SDS-PAGE, the proteins were transferred to 0.45  $\mu$ m polyvinylidene fluoride (PVDF) membranes (Millipore). The PVDF membranes were then blocked with 5% non-fat skim milk for 1 hour at RT. Following blocking, the membranes were incubated overnight at 4°C with primary antibodies against APP (6E10) (BioLegend), AT180 (Invitrogen), BACE1 (Cell Signaling Technology), Actin (Sigma), and NLRP3 (Cell Signaling Technology). The membranes were then washed with tris-buffered saline with Tween-20 (TBS-T) and incubated with HRP-conjugated anti-mouse or anti-rabbit secondary antibodies (Millipore) for 1 hour at RT. Protein bands were visualized using enhanced chemiluminescence solution (Cytiva) and quantified using ImageJ 1.54f (NIH). All unedited blots and experimental repeats were presented in Supplementary Figure S1 and S2 (<https://www.biosciencetrends.com/action/getSupplementalData.php?ID=233>).

### 2.16. RNA extraction and real-time quantitative PCR

Total RNA was extracted from brain tissues using RNAiso Plus (Takara) according to the manufacturer's instructions. Equal amounts of RNA were then used to synthesize cDNA with the PrimeScript™ RT Reagent Kit with gDNA Eraser (Takara), following the provided protocol. The synthesized cDNA was diluted 10-fold with RNase-free water. PCR amplification was conducted using TB Green® Premix Ex Taq™ II (Takara) on a CFX Connect (Bio-rad). Relative gene expression was calculated using the housekeeping gene (*Hprt*). The primers used for real-time quantitative PCR were as follows: mouse *Il-1 $\beta$*  forward 5'-agttgacggaccacaaaag-3', mouse *Il-1 $\beta$*  reverse 5'-agctggatgctctcatcagg-3', mouse *Iba1* forward 5'-atctgcctccaaactga-3', mouse *Iba1* reverse 5'-ctagtggtggtcttgggaacc-3', mouse *Tnf- $\alpha$*  forward 5'-tcttctcattcctgcttggg-3', mouse *Tnf- $\alpha$*  reverse 5'-ggtctgggcatagaactga-3', mouse *Hprt* forward 5'-cctcctcagaccgctttt-3', and mouse *Hprt* reverse 5'-aacctggtcatcagctaa-3'.

### 2.17. Brain tissue frozen section

Brain tissues preserved in 4% paraformaldehyde were sequentially soaked in 10%, 20%, and 30% sucrose solutions (Junsei), each for one day at 4°C. The tissues were then embedded in FSC 22 Frozen Section Media (Leica) and frozen. The frozen brain samples were sectioned at a thickness of 30 µm using a cryotome (Leica) and stored in a cryoprotectant solution (Biosolution).

### 2.18. Immunohistochemistry (IHC)

Serially sectioned brain slices were blocked at PBS containing Triton-X 100 solution and 3 % donkey serum (Bio-Rad). Following the blocking step, the slices were incubated overnight at 4 °C with the primary antibodies against IBA1 (Wako) and APP (6E10) (BioLegend). On the next day, the slices were washed and incubated with fluorescently labeled secondary antibodies for 1 hour at RT. Subsequently, the slices were washed again and mounted using VECTASHIELD® Antifade Mounting Medium with DAPI (Vector Laboratories). Images were acquired using a confocal microscope (Leica). Analysis of Aβ plaques and IBA1 was performed using the "Surfaces" function in IMARIS software.

### 2.19. Thioflavin S staining

Brain slices were floated in PBS and stained with 1% thioflavin S (Sigma) dissolved in 50% ethanol for 8 minutes. The tissue samples were then washed with 80 % ethanol twice followed by washing with PBS three times. After washing, the samples were mounted onto slide glass using VECTASHIELD® Antifade Mounting Medium with DAPI (Vector Laboratories).

### 2.20. RNA sequencing analysis

The procedure was conducted following the previously described method (21). Total RNA from mouse cortical tissue was used for mRNA sequencing analysis. Purity and concentration of total RNA were measured using Take 3 (BioTek). RNA integrity was determined using the 2100 Bioanalyzer Instrument (Agilent). Preparation of mRNA library and transcriptome analysis with data quality control was conducted by Novogene Co., LTD (Hong Kong). For quality control, fastq files for all RNA-seq samples were filtered, and the adapters were trimmed. The reads were then aligned to the mouse reference genome GRCm38 by the STAR Aligner. Genes with Fold change > 1.3 and *p*-value < 0.05 were regarded as differentially expressed.

### 2.21. Statistical analysis

Graphs were created and statistical analyses were

conducted using Prism 8 software (GraphPad Software). Data were analyzed using unpaired two-tailed *t*-tests, one-way ANOVA with Dunnett's multiple comparisons test, or two-way ANOVA with Dunnett's multiple comparisons test. All data are presented as mean ± standard deviation (SD) or standard error of the mean (SEM). For optical imaging analysis, Origin Pro was utilized for statistical analysis.

### 2.22. Data Availability

The data that support the findings and materials of this study are available upon request to the corresponding author.

## 3. Results

### 3.1. RA-PF reduces BACE1 expression and inflammation in *in vitro* systems.

Among the ramalin derivatives, RA-PF (Figure 1A) demonstrated low toxicity in the Ames test (Figure 1B-C), metabolic stability (Table 1, upper panel), and minimal CYP inhibitory interaction (Table 2, lower panel). It is orally bioavailable (Figure 1D; Table 2, upper panel) and capable of penetrating the blood-brain barrier (Figure 1E; Table 2, lower panel). Previously we demonstrated the BACE1 inhibitory and anti-inflammatory effects of ramalin (16,17,22). To evaluate the efficacy of RA-PF on the regulation of BACE1 expression levels in an *in vitro* system, we induced BACE1 under oxidative stress conditions using hydrogen peroxide (H<sub>2</sub>O<sub>2</sub>) treatment (23). H<sub>2</sub>O<sub>2</sub> treatment to SH-SY5Y cells, the human neuroblastoma cell line, induced BACE1 expression, while treatment with 5, and 10 µM of RA-PF restored BACE1 expression (Figure 2A, C). We then investigated the effects of RA-PF on neuroinflammation using BV-2, the mouse microglial cell line. Lipopolysaccharide (LPS) treatment induced the NLR family pyrin domain containing 3 (NLRP3) levels and treatment with 10 µM of RA-PF significantly recovered NLRP3 levels (Figure 2B, D).

### 3.2. Administration of RA-PF restores the synaptic transmission function in primary hippocampal neurons of 5xFAD.

Given ramalin's positive effects in an AD model, we investigated whether RA-PF also possesses therapeutic potential for synaptic dysfunction in an AD model. To monitor synaptic function, particularly synaptic transmission, we employed a pHluorin-based assay. This assay involves pHluorin conjugated to the luminal region of synaptic vesicle membrane proteins such as vesicular glutamate transporter 1 (vGlut1, vG-pH). 10 µM of RA-PF was administered to hippocampal neurons derived from 5xFAD mice. These 5xFAD hippocampal neurons

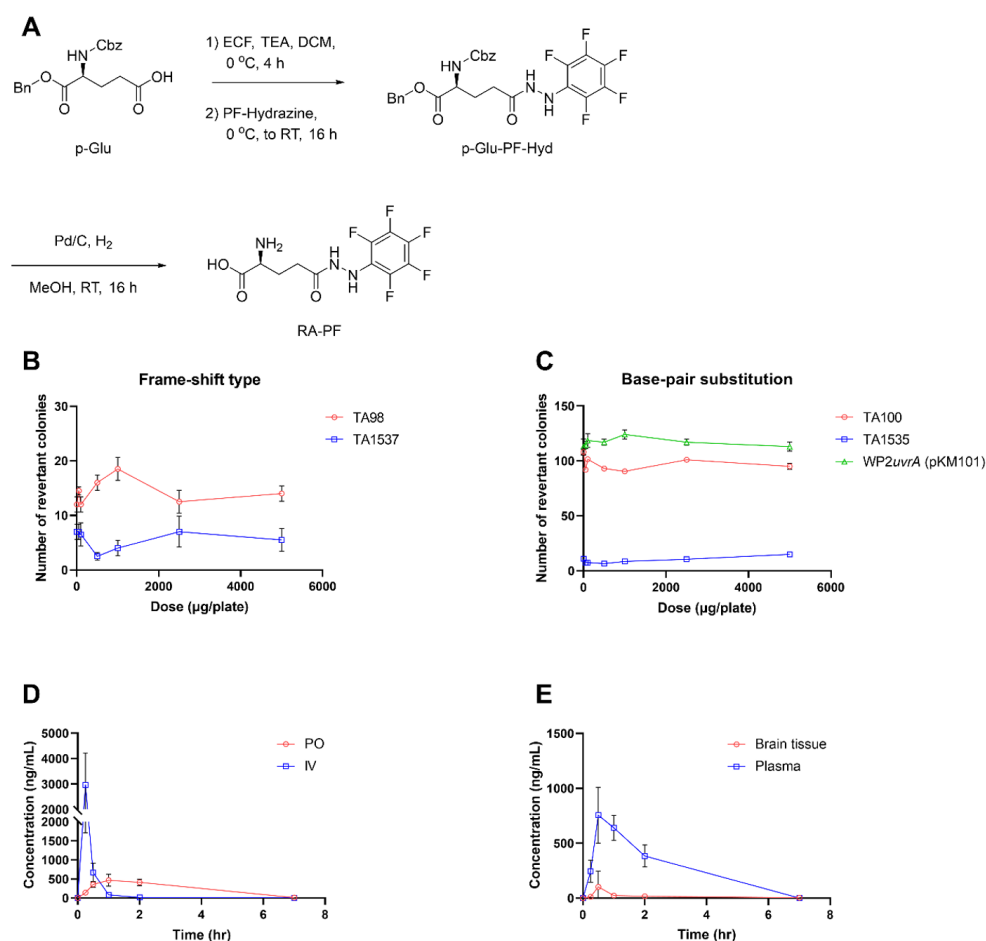


**Figure 1. RA-PF has low toxicity and can penetrate the blood-brain barrier via oral administration.** (A) Scheme showing the synthesis of RA-PF. ECF (Ethyl chloroformate), TEA (Triethyl amine), DCM (Dichloromethane), Pd/C (Palladium on carbon 10 wt. %), MeOH (Methanol), RT (room temperature). (B and C) Ames test to evaluate the mutagenicity effect of RA-PF. (B) represents frame-shift mutagenicity and (C) represents base-pair substitution mutagenicity. (D) Plasma concentration of RA-PF after IV 10 mg/kg and PO 10 mg/kg injection into Sprague-Dawley rats ( $n = 6$ ). (E) Brain tissue and plasma concentration of RA-PF after PO 10mg/kg injection into Sprague-Dawley rats ( $n = 3$ ).

**Table 1. Metabolic stability of RA-PF and CYP inhibitory interaction of RA-PF**

| Mean remaining (%)        |        |         |        |       |
|---------------------------|--------|---------|--------|-------|
| HLM                       | MLM    | RLM     | DLM    | MkLM  |
| 100.7                     | 99.2   | 94.4    | 98.1   | 100.0 |
| Mean control activity (%) |        |         |        |       |
| CYP1A2                    | CYP2C9 | CYP2C19 | CYP2D6 | CYP3A |
| 95.2                      | 89.8   | 88.5    | 90.7   | 98.1  |

HLM: human liver microsomes, MLM: mouse liver microsomes, RLM: rat liver microsomes, DLM: dog liver microsomes, MkLM: monkey liver microsomes.

expressing vG-pH were stimulated with 100 action potentials (AP) at 10 Hz, and fluorescence intensity was measured to quantify synaptic transmission. In wild-type (WT) neurons, the average synaptic transmission following 100 APs was approximately 20%. However, in 5xFAD neurons, synaptic transmission was significantly impaired, decreasing to about 11%. Remarkably, 5xFAD neurons treated with RA-PF exhibited almost complete restoration of synaptic transmission to normal levels (Figure 3A-C), suggesting that RA-PF may have

**Table 2. In vivo pharmacokinetic parameters of RA-PF**

|                        | PO, 10 mg/kg           | IV, 10 mg/kg            |           |
|------------------------|------------------------|-------------------------|-----------|
| $T_{max}$ (hr)         | $1.25 \pm 0.612$       | 0.25                    |           |
| $C_{max}$ (ng/mL)      | $480.320 \pm 144.594$  | $2966.155 \pm 1251.925$ |           |
| $T_{1/2}$ (hr)         | $1.062 \pm 0.457$      | $1.314 \pm 0.251$       |           |
| $AUC_{inf}$ (ng*h/mL)  | $1279.059 \pm 241.783$ | $987.859 \pm 358.449$   |           |
|                        | Plasma                 | Brain                   | B/P ratio |
| $C_{max}$ (ng/mL)      | 855.981                | 105.368                 | 0.123     |
| $AUC_{0-7h}$ (ng*h/mL) | 1337.037               | 111.379                 | 0.083     |

therapeutic effects on synaptic dysfunction in the AD model.

Additionally, we investigated whether RA-PF affects mitochondrial motility, as alterations in mitochondrial trafficking are closely related to AD pathology (24). To measure mitochondrial motility, we employed live-cell imaging by introducing Mito-red plasmids into the neurons. In WT neurons, approximately 20% of mitochondria were motile. In contrast, the motility rate in 5xFAD neurons decreased to about 10%. Consistent

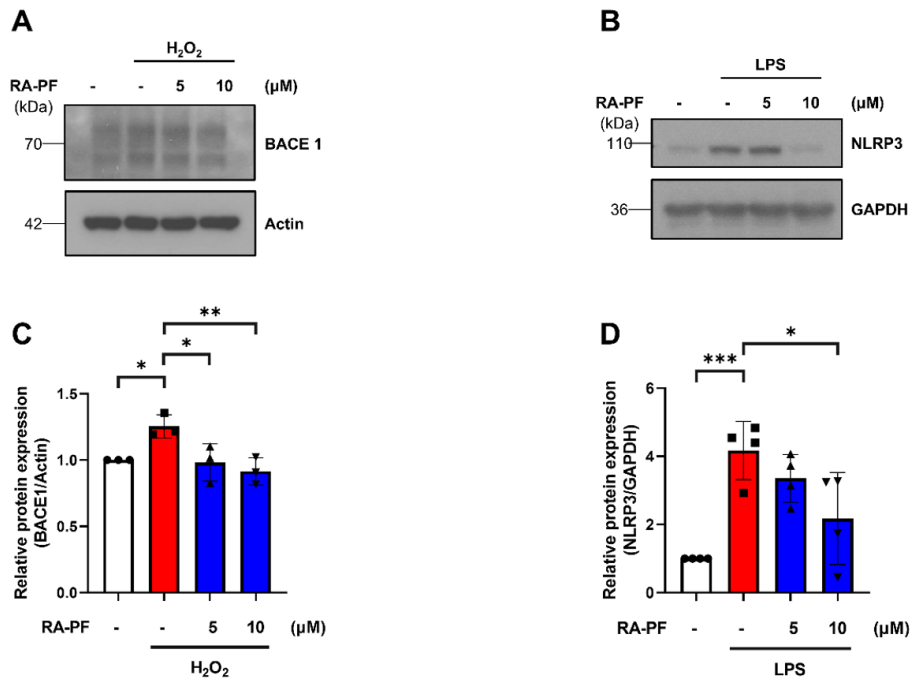


**Figure 2. RA-PF ameliorates BACE1 induced by oxidative stress and suppresses LPS-induced inflammatory responses.** (A) Western blot analysis of BACE1 and Actin following induction with 200 μM of H<sub>2</sub>O<sub>2</sub> for 2 hours in SH-SY5Y cells. Cells were pre-treated with RA-PF or vehicle and incubated for 24 hours before H<sub>2</sub>O<sub>2</sub> exposure (*n* = 3). (B) Western blot analysis of NLRP3 and GAPDH. Cells were treated with RA-PF or vehicle for 24 hours followed by LPS induction for 2 hours (*n* = 4). (C) Quantification of BACE1 expression in (A) (*n* = 3). (D) Quantification of NLRP3 expression in (B) (*n* = 4). Values are presented as means ± SD. \**p* < 0.05, \*\**p* < 0.01, and \*\*\**p* < 0.001 versus H<sub>2</sub>O<sub>2</sub> or LPS-induced and vehicle pre-treated group; one-way ANOVA with Dunnett's test (C-D).

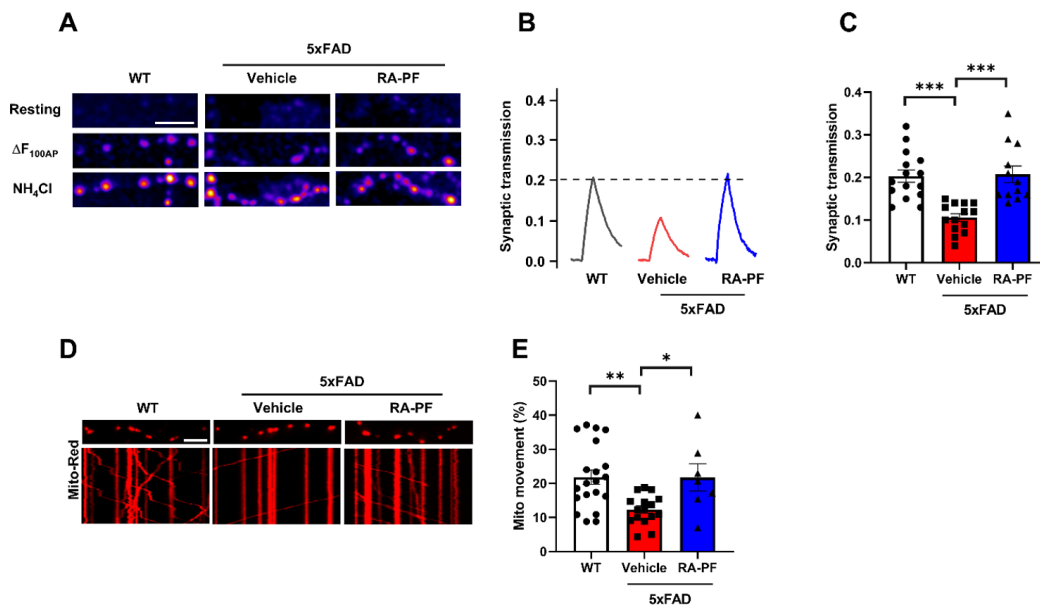


**Figure 3. Treatment of RA-PF restores synaptic function and mitochondria movement in 5xFAD hippocampal neurons.** (A) Representative images of vG-pH at resting (left), 100 AP (middle), and NH<sub>4</sub>Cl (right) neurons (Scale bar, 5 mm). (B) Representative ensemble average traces of vG-pH in response to 100AP in WT, vehicle treated 5xFAD, and RA-PF treated 5xFAD neurons. Neurons expressed with vG-pH were stimulated at 10Hz 10s with or without RA-PF. Intensities were normalized to the maximal value of NH<sub>4</sub>Cl response. (C) Mean values of amplitudes of 100AP responses in WT, vehicle treated 5xFAD, and RA-PF-treated 5xFAD neurons. (*n* = 12 - 15). (D) Representative image of mitochondria (Top) and its kymograph (Bottom) in WT (left), 5xFAD (middle), and RA-PF-treated 5xFAD (right) neuron (Scale bar, 5 μm). (E) Mean values of mitochondria motility rate in WT, 5xFAD, and RA-PF treated 5xFAD neurons. (*n* = WT: 20, Vehicle treated 5xFAD: 16, RA-PF treated 5xFAD: 7). Values are presented as means ± SEM. \**p* < 0.05, \*\**p* < 0.01, \*\*\**p* < 0.001 versus vehicle treated 5xFAD group; one-way ANOVA with Dunnett's test (C and E).

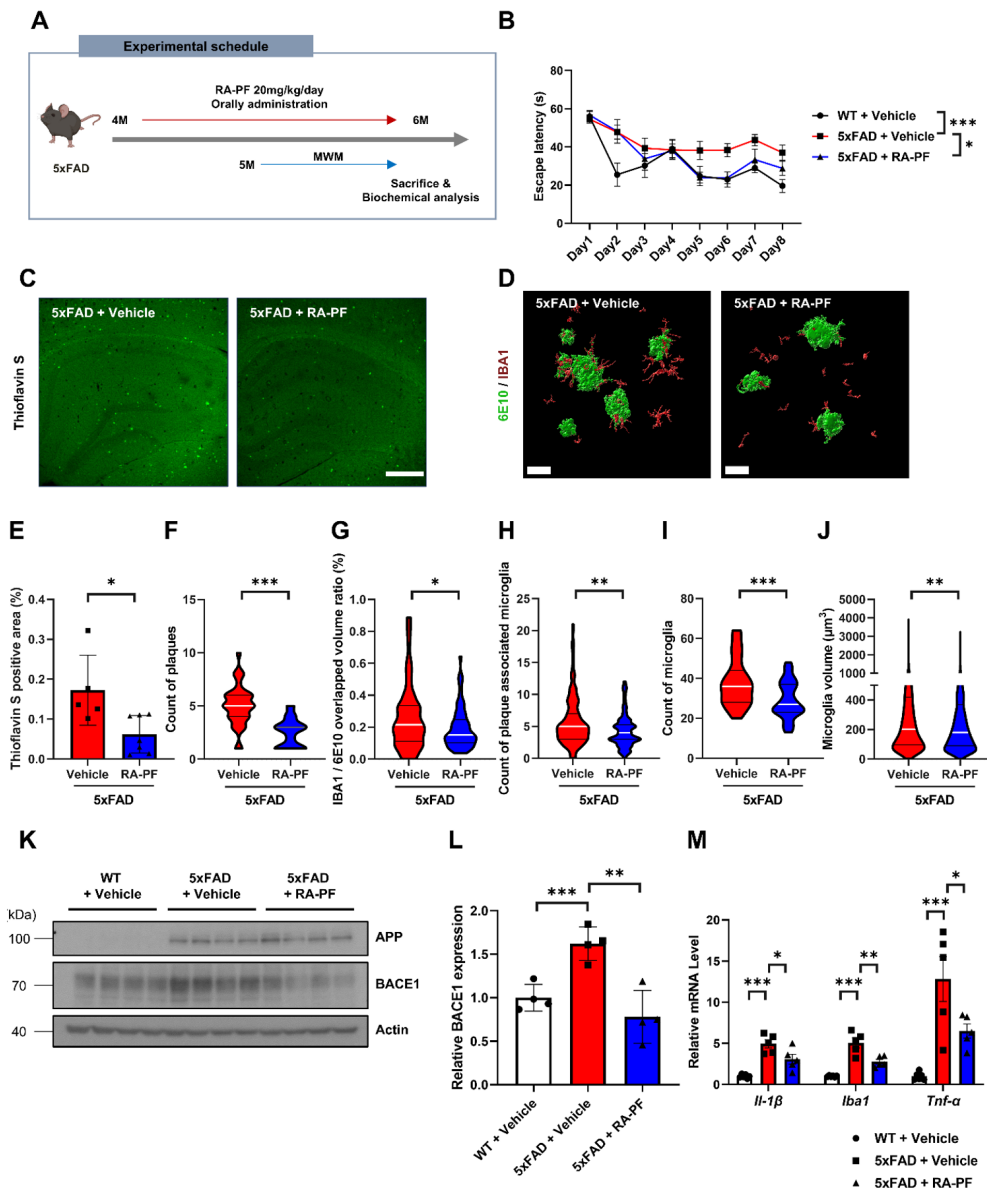


**Figure 4. Administration of RA-PF alleviates BACE1 activation, A $\beta$  deposition, inflammatory responses, and cognitive dysfunction in 5xFAD mice.** (A) A schematic diagram of the experimental design. Created with Biorender.com. (B) Escape latency was recorded during the MWM training trials of indicated groups ( $n = 6 - 12$ ). (C) Representative thioflavin S staining images of the hippocampal region. (D and E) Quantification of thioflavin S positive area (%) in (C) ( $n = 5 - 7$ ). (F-J) IMARIS-based quantification of plaque count in field of view (F) ( $n = 25 - 34$ ), IBA1 and 6E10 overlapped volume ratio percentage (G) ( $n = 62 - 172$ ), count of plaque associated microglia (H) ( $n = 62 - 172$ ), microglial count in field of view (I) ( $n = 35 - 45$ ), and microglia volume ( $n = 1309 - 1332$ ) (J) (K) Western blot analysis of APP, BACE1, and Actin using the hippocampal samples of 5xFAD ( $n = 4$ ). (L) Quantification of BACE1 expression in (G). (M) mRNA expression levels of *Il-1 $\beta$* , *Iba1*, and *Tnf- $\alpha$*  in the hippocampal samples ( $n = 6$ ). Values are presented as means  $\pm$  SEM. \* $p < 0.05$ , \*\* $p < 0.01$ , \*\*\* $p < 0.001$ , versus 5xFAD + Vehicle; two-way ANOVA with Dunnett's  $t$ -test (B), two-tailed Student's  $t$ -test (E-J), one-way ANOVA with Dunnett's test (L-M).

with restoring synaptic function, 5xFAD neurons treated with RA-PF showed recovery of mitochondrial motility in the axon (Figure 3D-E). These results collectively suggest that RA-PF positively impacts synaptic function and mitochondrial motility in the AD model, indicating its potential as a therapeutic agent.

3.3. *In vivo* RA-PF administration ameliorates cognitive impairment, BACE1 expression, A $\beta$  plaque deposition, and microglial activation in a 5xFAD mouse model.

To evaluate the therapeutic effects of RA-PF in 5xFAD mice, 20 mg/kg of RA-PF was administered for 2-month to 4-month-old 5xFAD female mice, followed by behavior study and biochemical analysis at 6 months of age (Figure 4A). As a result, cognitive impairment was observed in the 5xFAD mice in the Morris water maze test, but this impairment was alleviated in the RA-PF administered group (Figure 4B). Additionally, thioflavin S-positive plaques observed in the 5xFAD hippocampus were found to be reduced following

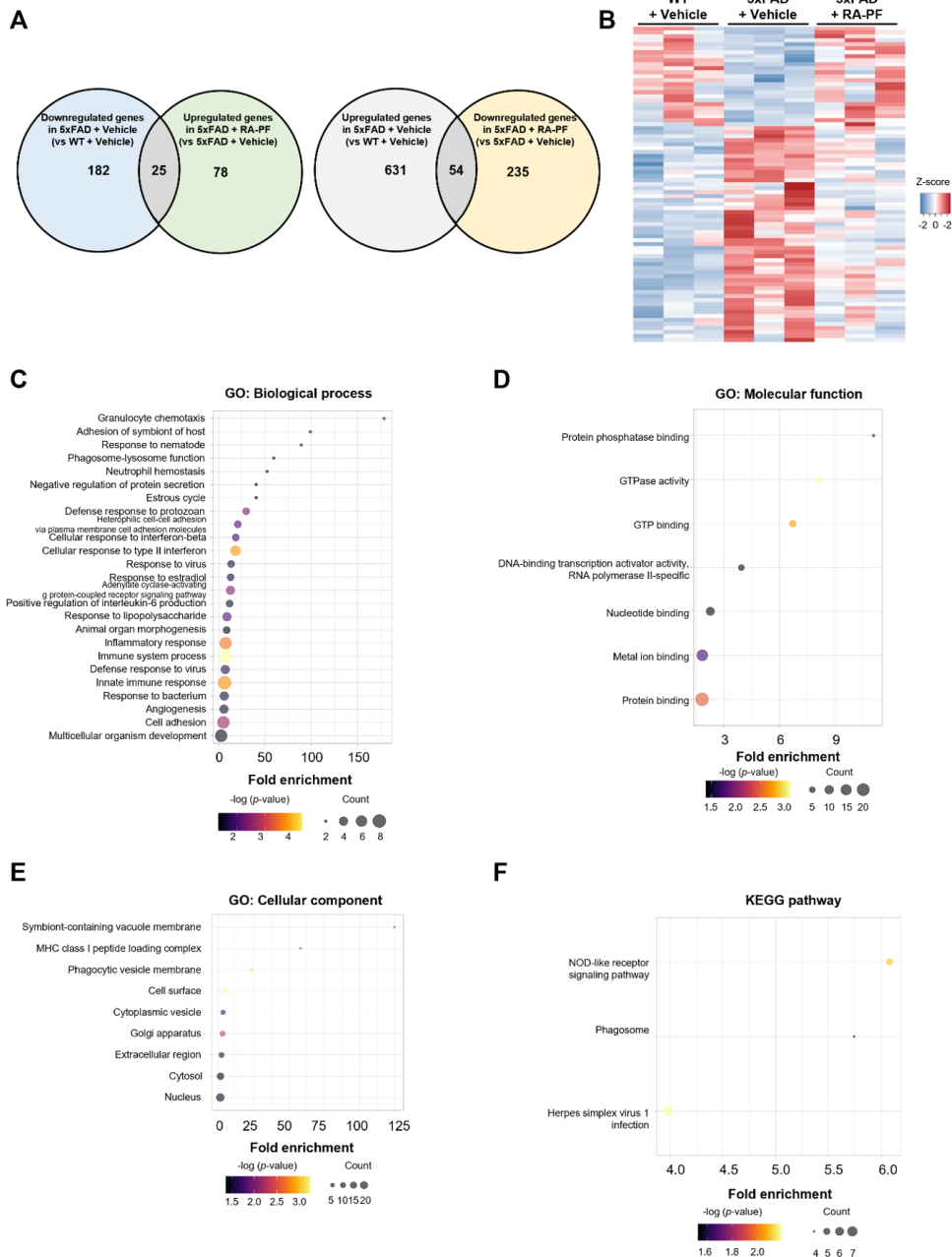


**Figure 5. Gene profiling analysis in RA-PF treated 5xFAD mouse model.** (A) Venn diagrams of DEGs between groups. (B) Heatmap panels of 79 DEGs in three groups (WT + Vehicle, 5xFAD + Vehicle, and 5xFAD + RA-PF). (C) Gene ontology analysis in biological process category using 79 DEGs. (D) Gene ontology analysis in molecular function category using 79 DEGs. (E) Gene ontology analysis in cellular component category using 79 DEGs. (F) KEGG pathway analysis using 79 DEGs revealed 'NOD-like receptor signaling pathway', 'phagosome', and 'herpes simplex virus 1 infection' pathway-related genes were altered.

RA-PF administration (Figure 4C, E). The 3D image analysis program IMARIS was used to investigate the relationship between A $\beta$  plaque and microglia (Figure 4D). The analysis cross-confirmed that RA-PF treatment reduced the number of plaques (Figure 4F), alongside a decrease in plaque-associated microglia and the overlapped area of 6E10 and IBA1 (Figure 4G-H). Additionally, the number and volume of microglia was significantly reduced (Figure 4I-J). It was also confirmed that the BACE1 upregulation observed in 5xFAD mice

was ameliorated by RA-PF treatment (Figure 4K-L) and that the inflammatory response was reduced at the mRNA level of *Il-1 $\beta$* , *Iba1*, and *Tnf- $\alpha$*  following RA-PF administration (Figure 4M).

### 3.4. Gene expression profiles following *in vivo* RA-PF administration in 5xFAD mouse model.

To investigate the gene expression changes by RA-PF administration, we conducted the RNA-sequencing using

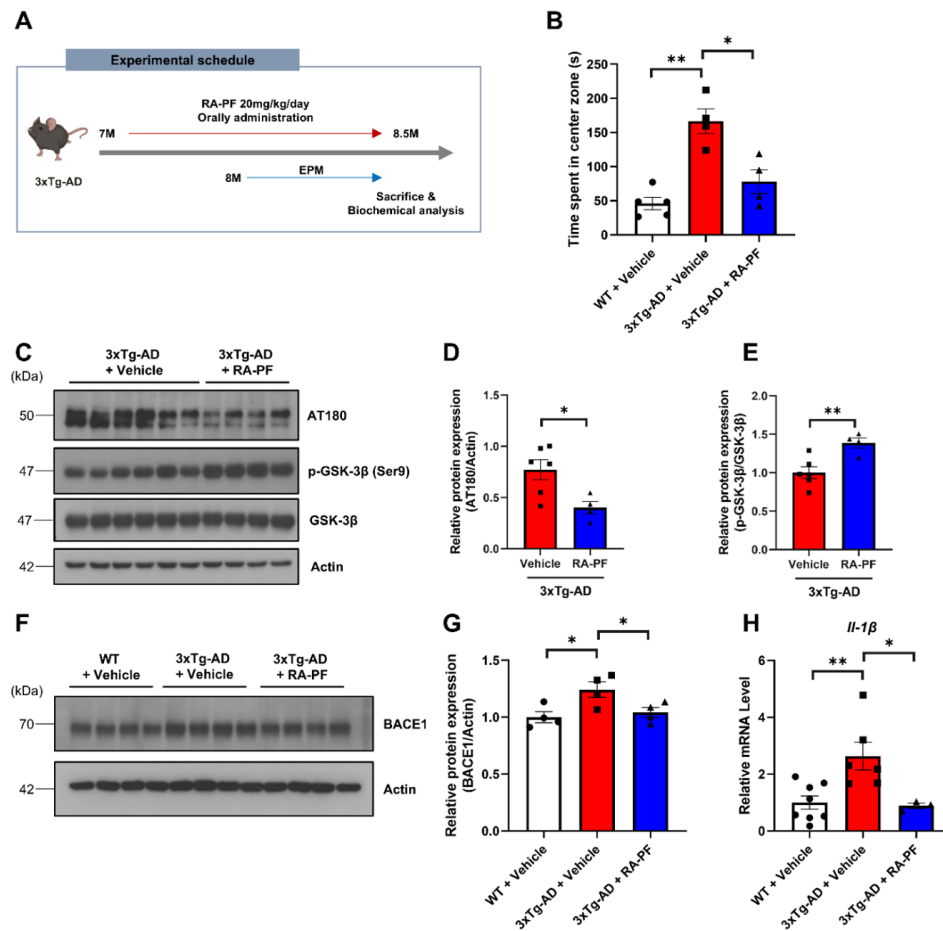


**Figure 6. Administration of RA-PF ameliorates BACE1 expression, tau phosphorylation, neuroinflammation, and anxiety in 3xTg-AD mice.** (A) A schematic diagram of the experimental design. Created with Biorender.com. (B) Time spent in the center zone of indicated groups in elevated plus maze test ( $n = 4 - 6$ ). (C) Western blot analysis of AT180 (phospho-Tau Thr231), phospho-GSK-3 $\beta$  Ser9, GSK-3 $\beta$ , and Actin using the cortical samples of indicated groups ( $n = 4 - 6$ ). (D-E) Quantification of AT180 (D) and phospho-GSK-3 $\beta$  Ser9 (E) expression in (C) ( $n = 4 - 6$ ). (F) Western blot analysis of BACE1 and Actin using the cortical samples of indicated groups ( $n = 4$ ). (G) Quantification of BACE1 expression in (E) ( $n = 4$ ). (H) mRNA expression levels of *Il-1 $\beta$*  in the cortical samples of indicated groups ( $n = 3 - 6$ ). Values are presented as means  $\pm$  SEM. \* $p < 0.05$  and \*\* $p < 0.01$ , versus 3xTg-AD + Vehicle; two-tailed Student's *t*-test (D-E), versus 3xTg-AD + Vehicle; one-way ANOVA with Dunnett's test (B, G, and H).

mRNA isolated from the cortice of mice. As a result, there were 25 genes overlapped between downregulated genes in 5xFAD + Vehicle (vs WT + Vehicle) and upregulated genes in 5xFAD + RA-PF (vs 5xFAD + Vehicle) and 54 genes overlapped between upregulated genes in 5xFAD + Vehicle (vs WT + Vehicle) and downregulated genes in 5xFAD + RA-PF (vs 5xFAD + Vehicle) (Figure 5A-B). Gene ontology (GO) analysis using these 79 differentially expressed genes (DEGs) revealed that 'phagosome-lysosome function', 'response to lipopolysaccharide', and 'inflammatory response'-related genes were significantly enriched in biological process (Figure 5C). In the molecular function category, 'protein phosphatase binding', 'nucleotide binding', and 'protein binding'-related genes were enriched and 'phagocytic vesicle membrane', 'cytoplasmic vesicle', and 'nucleus'-related genes were enriched in cellular component category (Figure 5D-E). Kyoto Encyclopedia of Genes and Genomes (KEGG) pathway analysis revealed that significant enrichment in 'NOD-like

receptor signaling pathway', 'phagosome', and 'herpes simplex virus 1 infection' pathway (Figure 5F).

### 3.5. *In vivo* RA-PF administration ameliorates BACE1 expression, tau phosphorylation, and anxiety in 3xTg-AD mouse model.

To further investigate the effects of RA-PF on AD, we orally administered 20 mg/kg of RA-PF to 7-month-old 3xTg-AD, a widely used AD model (Figure 6A). In the elevated plus maze test, 3xTg-AD mice spent more time in the center zone than other groups and RA-PF administration significantly recovered time spent in the center zone compared to 3xTg-AD + Vehicle (Figure 6B). Biochemical analysis revealed a significant reduction in tau phosphorylation following RA-PF administration (Figure 6C-D). GSK-3 $\beta$  is a key regulator of tau phosphorylation at the Thr231 site (25), and its inactive form, phosphorylated GSK-3 $\beta$  at the Ser9 site, was upregulated following RA-PF treated group

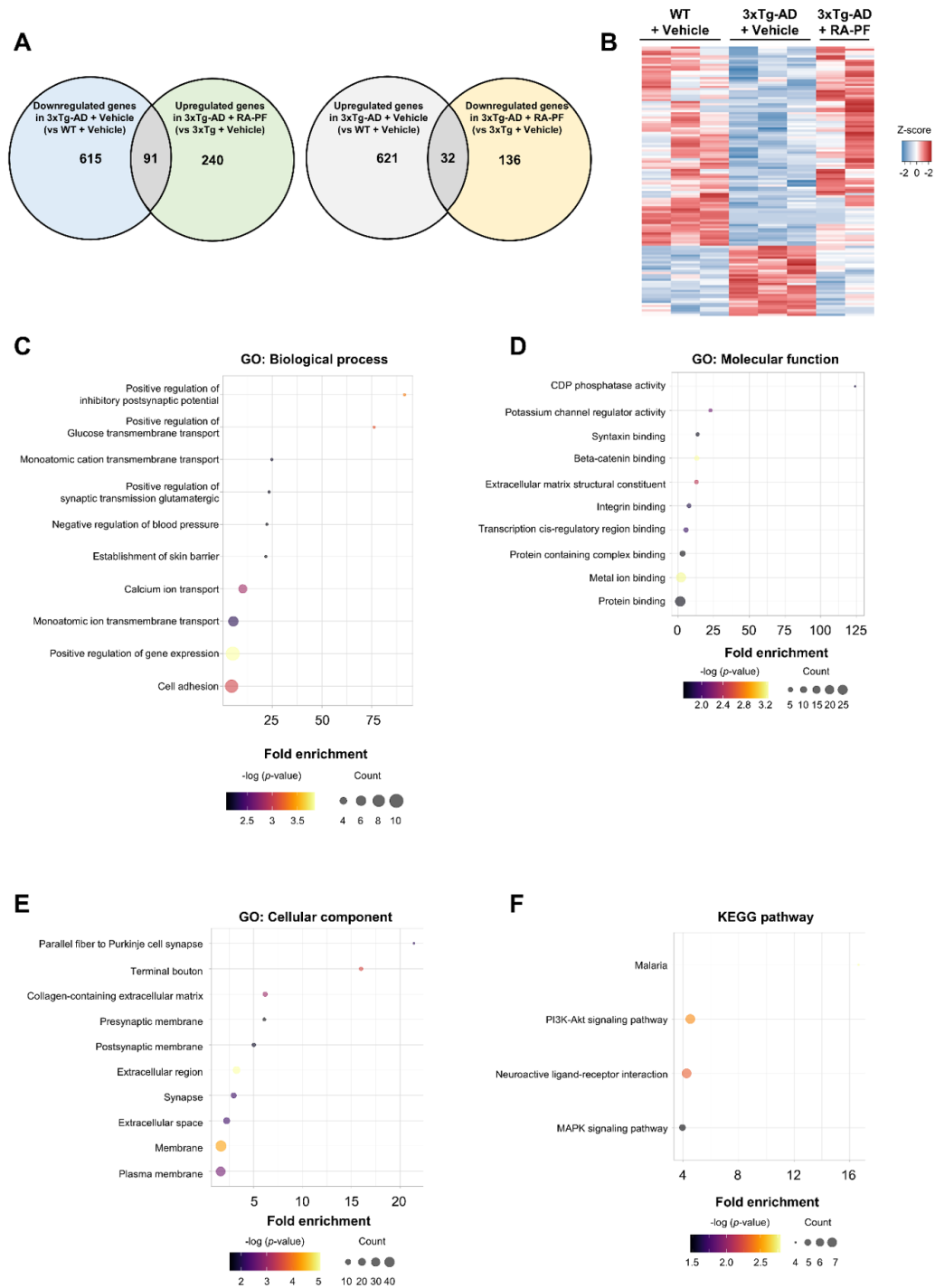


**Figure 7. Gene profiling analysis in RA-PF treated 3xTg-AD mice.** (A) Venn diagrams of DEGs between groups. (B) Heatmap panels of 123 DEGs in three groups (WT + Vehicle, 3xTg-AD + Vehicle, and 3xTg-AD + RA-PF). (C) Gene ontology analysis in biological process category using 123 DEGs. (D) Gene ontology analysis in molecular function category using 123 DEGs. (E) Gene ontology analysis in cellular component category using 123 DEGs. (F) KEGG pathway analysis using 123 DEGs revealed 'malaria', 'PI3K-Akt signaling pathway', 'neuroactive ligand-receptor interaction', and 'MAPK signaling pathway'-related genes were altered.

(Figure 6C, E). Additionally, BACE1 expression in 3xTg-AD mice also recovered (Figure 6F-G) and the neuroinflammation marker, *Il-1β* was reduced at the mRNA level after RA-PF treatment (Figure 6H).

3.6. Gene expression profiles following RA-PF *in vivo* administration in the 3xTg-AD mouse model.

To examine RA-PF efficacy on 3xTg-AD, we further evaluated the gene expression profile of the cortical region. 91 genes were overlapped between downregulated genes in 3xTg-AD + Vehicle (vs WT + Vehicle) and upregulated genes in 3xTg + RA-PF (vs 3xTg-AD + Vehicle), and 32 genes were overlapped between upregulated genes in 3xTg-AD + Vehicle (vs

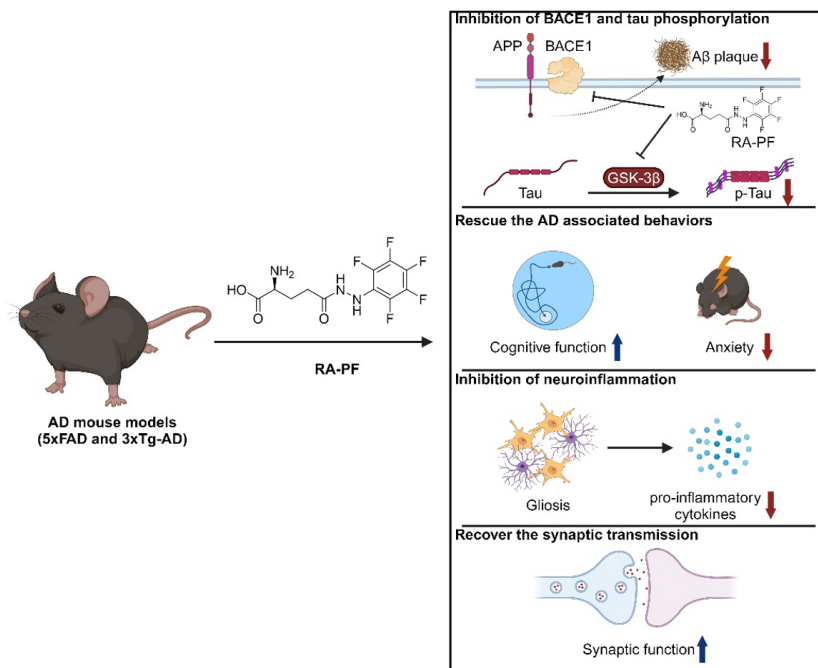


**Figure 8. Schematic illustration of RA-PF's therapeutic effect of RA-PF on AD mouse models.** Orally administered RA-PF crosses the blood-brain barrier and reduces A $\beta$  plaques by BACE1 inhibition, alongside decreasing tau phosphorylation *via* GSK-3 $\beta$  inactivation. Additionally, RA-PF alleviates neuroinflammation and enhances synaptic transmission. These effects improve AD-associated behaviors, including cognitive function and anxiety. Created with Biorender.com.

WT + Vehicle) and downregulated genes in 3xTg-AD + RA-PF (vs 3xTg + Vehicle) (Figure 7A-B). Using these 123 DEGs, we further analyzed functional annotations and found that 'positive regulation of inhibitory postsynaptic potential', 'positive regulation of synaptic transmission glutamatergic', and 'calcium ion transport'-related genes were significantly enriched in biological process (Figure 7C). 'Potassium channel regulator activity', 'syntaxin binding', and 'protein binding' were enriched in molecular function category (Figure 7D) and we further identified significant enrichment in 'presynaptic membrane', 'postsynaptic membrane' and 'synapse' in cellular component category (Figure 7E). KEGG pathway analysis revealed that 'PI3K-Akt signaling pathway', 'neuroactive ligand-receptor interaction', and 'MAPK signaling pathway' were significantly enriched (Figure 7F).

#### 4. Discussion

This study highlights the therapeutic potential of RA-PF in modulating AD pathogenesis. While the therapeutic potential of ramalin and its derivatives for AD has been proposed (17,22), their *in vivo* efficacy has not yet been reported. To enhance the therapeutic potential of ramalin, we designed and synthesized several derivatives by substituting its phenyl ring with different structural groups. Among them, RA-PF was identified through toxicity screening as having the lowest *in vivo* toxicity, being orally bioavailable, and capable of

penetrating the blood-brain barrier (Figure 1B-E; Table 1-2). Our results demonstrate that RA-PF significantly reduces BACE1 expression and neuroinflammation in the AD models. Targeting BACE1 has long been proposed as a therapeutic approach for AD. However, many studies have failed because BACE1 has numerous binding partners and full BACE1 inhibitors have been unsuccessful in drug development due to toxicity (26). Nevertheless, BACE1 remains an attractive target for AD therapy, and new approaches to its inhibition are being explored, including partial BACE1 inhibitors and indirect BACE1 regulators (10,11). These alternatives offer safety advantages over full BACE1 inhibitors or BACE1 knockout approaches while effectively reducing A $\beta$  plaque deposition. In this context, it restores BACE1 levels to normal under various AD conditions, leading to cognitive improvement and reduced plaque deposition.

In AD condition, microglia become hyperactivated around A $\beta$  plaques leading to neuroinflammation. Our RNA-seq data revealed that terms related to phagocytosis, such as 'phagosome-lysosome function' (Figure 5C), 'phagocytic vesicle membrane' (Figure 5E), and 'phagosome' (Figure 5F) were dysregulated in 5xFAD group, while effectively normalized by RA-PF administration. Based on these findings, we focused on the relationship between plaques and microglia. Microglial activation (27) and plaque-associated microglia observed in 5xFAD were mitigated by RA-PF treatment (Figure 4G-J), which was associated

with neuroinflammation (Figure 4M). Paradoxically, this process also resulted in a reduction in A $\beta$  plaque levels (Figure 4E-F), which we interpret as a complex phenomenon mediated by RA-PF's regulation of BACE1 (Figure 4K-L). To further evaluate the impact of RA-PF beyond the regulation of BACE1 and neuroinflammation, we utilized the 3xTg-AD model to investigate its effects on tau. In this model, RA-PF administration reduced tau phosphorylation, accompanied by the suppression of GSK-3 $\beta$  activity, a key regulator of tau hyperphosphorylation (Figure 6C-E). AD pathogenesis does not follow a single specific pathogenesis. It involves multiple pathogenic processes, including the accumulation of misfolded proteins, neuroinflammation, and mitochondrial dysfunction. Targeting these multiple processes is advantageous for treating diseases with complex pathogenesis (28,29). RA-PF not only regulates BACE1 expression but also inhibits neuroinflammation, and tau phosphorylation and restores synaptic function making it a more effective treatment for AD.

In conclusion, this study demonstrated that RA-PF targets multiple aspects of AD pathogenesis. The findings highlight the potential of RA-PF as a therapeutic agent addressing the complex pathologies involved in AD progression, introducing a novel compound for AD treatment (Figure 8). However, it remains unclear how RA-PF regulates BACE1 expression, ameliorates neuroinflammation, and restores synaptic functions. Further studies are needed to elucidate the detailed mechanism underlying these effects. Moreover, this study is based on pre-clinical models, it remains uncertain whether the observed effects will translate effectively to clinical settings. For clinical application, a comprehensive risk-benefit assessment will be essential.

**Funding:** This work was supported by Korea Institute of Marine Science & Technology Promotion (KIMST) grant funded by the Ministry of Oceans and Fisheries (RS-2021-KS211513).

**Conflict of Interest:** Kim H and Park SY are employees of Ahngook Pharmaceutical Co.. The other authors have no conflicts of interest in this work.

## References

1. Cho Y, Bae HG, Okun E, Arumugam TV, Jo DG. Physiology and pharmacology of amyloid precursor protein. *Pharmacol Ther.* 2022; 235:108122.
2. Deng Y, Wang H, Gu K, Song P. Alzheimer's disease with frailty: Prevalence, screening, assessment, intervention strategies and challenges. *Biosci Trends.* 2023; 17:283-292.
3. Peng Y, Song P, Karako T, Asakawa T. Blocking progression from intervenable mild cognitive impairment to irreversible dementia, what can we do? *Biosci Trends.* 2024; 18:409-412.
4. Park J, Lai MKP, Arumugam TV, Jo DG. O-GlcNAcylation as a therapeutic target for Alzheimer's disease. *Neuromolecular Med.* 2020; 22:171-193.
5. Ma YN, Hu X, Karako K, Song P, Tang W, Xia Y. Exploring the multiple therapeutic mechanisms and challenges of mesenchymal stem cell-derived exosomes in Alzheimer's disease. *Biosci Trends.* 2024.
6. Hong S, Baek S-H, Lai MKP, Arumugam TV, Jo D-G. Aging-associated sensory decline and Alzheimer's disease. *Molecular Neurodegeneration.* 2024; 19:93.
7. Vassar R. BACE1 inhibitor drugs in clinical trials for Alzheimer's disease. *Alzheimers Res Ther.* 2014; 6:89.
8. Ghosh AK, Brindisi M, Tang J. Developing  $\beta$ -secretase inhibitors for treatment of Alzheimer's disease. *J Neurochem.* 2012; 120 Suppl 1:71-83.
9. Ugbaja SC, Lawal IA, Abubakar BH, Mushebenge AG, Lawal MM, Kumalo HM. Allosteric inhibition of BACE1 by psychotic and meroterpenoid drugs in Alzheimer's disease therapy. *Molecules.* 2022; 27:4372.
10. Bahn G, Park J-S, Yun UJ, *et al.* NRF2/ARE pathway negatively regulates BACE1 expression and ameliorates cognitive deficits in mouse Alzheimer's models. *Proc Natl Acad Sci U S A.* 2019; 116:12516-12523.
11. Han J, Sul JH, Lee J, Kim E, Kim HK, Chae M, Lim J, Kim J, Kim C, Kim JS, Cho Y, Park JH, Cho YW, Jo DG. Engineered exosomes with a photoinducible protein delivery system enable CRISPR-Cas-based epigenome editing in Alzheimer's disease. *Sci Transl Med.* 2024; 16:eadi4830.
12. Leng F, Edison P. Neuroinflammation and microglial activation in Alzheimer disease: Where do we go from here? *Nat Rev Neurol.* 2021; 17:157-172.
13. Hu X, Ma YN, Xia Y. Association between abnormal lipid metabolism and Alzheimer's disease: New research has revealed significant findings on the APOE4 genotype in microglia. *Biosci Trends.* 2024; 18:195-197.
14. Larson KC, Martens LH, Marconi M, Dejesus C, Bruhn S, Miller TA, Tate B, Levenson JM. Preclinical translational platform of neuroinflammatory disease biology relevant to neurodegenerative disease. *J Neuroinflammation.* 2024; 21:37.
15. Gao C, Jiang J, Tan Y, Chen S. Microglia in neurodegenerative diseases: Mechanism and potential therapeutic targets. *Signal Transduct Target Ther.* 2023; 8:359.
16. Paudel B, Bhattarai HD, Koh HY, Lee SG, Han SJ, Lee HK, Oh H, Shin HW, Yim JH. Ramalin, a novel nontoxic antioxidant compound from the Antarctic lichen *Ramalina terebrata*. *Phytomedicine.* 2011; 18:1285-1290.
17. Kim TK, Cho Y, Kim J, Lee J, Hong JM, Cho H, Kim JS, Lee Y, Kim KH, Kim IC, Han SJ, Oh H, Jo DG, Yim JH. Synthesis and evaluation of chloride-substituted ramalin derivatives for Alzheimer's disease treatment. *Molecules.* 2024; 29:3701.
18. Park J, Ha H-J, Chung ES, *et al.* O-GlcNAcylation ameliorates the pathological manifestations of Alzheimer's disease by inhibiting necroptosis. *Sci Adv.* 2021; 7:eabd3207.
19. Walf AA, Frye CA. The use of the elevated plus maze as an assay of anxiety-related behavior in rodents. *Nat Protoc.* 2007; 2:322-328.
20. Bae JR, Lee W, Jo YO, Han S, Koh S, Song WK, Kim SH. Distinct synaptic vesicle recycling in inhibitory nerve terminals is coordinated by SV2A. *Prog Neurobiol.* 2020; 194:101879.
21. Kim J-S, Jun JH, Lee J, *et al.* HDAC6 mediates NLRP3 inflammasome activation in the pathogenesis of diabetic

- retinopathy. *Metabolism*. 2024; 164:156108.
22. Kim TK, Hong JM, Kim KH, Han SJ, Kim IC, Oh H, Yim JH. Potential of ramalin and its derivatives for the treatment of Alzheimer's disease. *Molecules*. 2021; 26:6445.
  23. Mouton-Liger F, Paquet C, Dumurgier J, Bouras C, Pradier L, Gray F, Hugon J. Oxidative stress increases BACE1 protein levels through activation of the PKR-eIF2 $\alpha$  pathway. *Biochim Biophys Acta*. 2012; 1822:885-896.
  24. Correia SC, Perry G, Moreira PI. Mitochondrial traffic jams in Alzheimer's disease - pinpointing the roadblocks. *Biochim Biophys Acta*. 2016; 1862:1909-1917.
  25. Cho JH, Johnson GV. Primed phosphorylation of tau at Thr231 by glycogen synthase kinase 3 $\beta$  (GSK3 $\beta$ ) plays a critical role in regulating tau's ability to bind and stabilize microtubules. *J Neurochem*. 2004; 88:349-358.
  26. Mullard A. BACE failures lower AD expectations, again. *Nat Rev Drug Discov*. 2018; 17:385.
  27. Chan TE, Grossman YS, Bloss EB, Janssen WG, Lou W, McEwen BS, Dumitriu D, Morrison JH. Cell-type specific changes in glial morphology and glucocorticoid expression during stress and aging in the medial prefrontal cortex. *Front Aging Neurosci*. 2018; 10:146.
  28. Gong CX, Dai CL, Liu F, Iqbal K. Multi-targets: An unconventional drug development Strategy for Alzheimer's disease. *Front Aging Neurosci*. 2022; 14:837649.
  29. Jun JH, Kim JS, Palomera LF, Jo DG. Dysregulation of histone deacetylases in ocular diseases. *Arch Pharm Res*. 2024; 47:20-39.
- Received November 11, 2024; Revised December 30, 2024; Accepted January 22, 2025.
- §These authors contributed equally to this work.  
\*Address correspondence to:  
Joung Han Yim, Division of Polar Life Sciences, Korea Polar Research Institute, Incheon 21990, Korea.  
E-mail: jhyim@kopri.re.kr
- Dong-Gyu Jo, School of Pharmacy, Sungkyunkwan University, Suwon 16419, Korea.  
E-mail: jodg@skku.edu
- Released online in J-STAGE as advance publication January 25, 2025.

# Plasma extracellular vesicle pathognomonic proteins as the biomarkers of the progression of Parkinson's disease

Chien-Tai Hong<sup>1,2,3</sup>, Chen-Chih Chung<sup>1,2,3</sup>, Yi-Chen Hsieh<sup>4</sup>, Lung Chan<sup>1,\*</sup>

<sup>1</sup>Department of Neurology, Shuang Ho Hospital, Taipei Medical University, New Taipei City, Taiwan;

<sup>2</sup>Department of Neurology, School of Medicine, College of Medicine, Taipei Medical University, Taipei, Taiwan;

<sup>3</sup>Taipei Neuroscience Institute, Taipei Medical University, Taipei, Taiwan;

<sup>4</sup>Ph.D in Medical Neuroscience, College of Medical Science and Technology, Taipei Medical University, Taipei, Taiwan.

**SUMMARY:** Parkinson's disease (PD) is a progressive neurodegenerative disorder for which reliable blood biomarkers to predict disease progression remain elusive. Plasma extracellular vesicles (EVs) have gained attention as a promising biomarker platform due to their stability and ability to cross the blood-brain barrier. This study explored the potential of EV-cargo proteins, specifically  $\alpha$ -synuclein, tau, and  $\beta$ -amyloid, as biomarkers of PD progression. A cohort of 55 people with PD (PwP) and 58 healthy controls (HCs) underwent annual assessments of plasma EV proteins, cognition, and motor symptoms. EVs were isolated and validated using standardized methods, with pathognomonic proteins quantified *via* immunomagnetic reduction assays. Associations between biomarker changes and clinical symptom progression were analyzed. Over an average of 3.96 visits for PwP and 2.25 visits for HCs, PwP exhibited a distinct pattern of plasma EV protein changes linked to motor symptom progression, particularly in the Unified PD Rating Scale (UPDRS) part II score. Notably, changes in plasma EV  $\alpha$ -synuclein levels were significantly correlated with changes in motor and cognitive symptoms, suggesting its central role in disease progression. These findings highlight the potential of plasma EV biomarkers, especially  $\alpha$ -synuclein, as indicators of ongoing pathogenesis and as candidates for evaluating  $\alpha$ -synuclein-targeted therapies in PD.

**Keywords:** sodium glucose transporter 2 inhibitors, type-2 diabetes mellitus, cype-2 diabetes mellitus, canagliflozin, sodium glucose transporter 2 inhibitors

## 1. Introduction

Parkinson's disease (PD) is a challenging neurodegenerative disease regarding the diagnosis and prognosis prediction (1). The progression characteristics of PD results in severe disability in the people at advanced stage of disease. However, the speed of deterioration varies. The urgent need for reliable biomarkers for PD is underscored by the potential of early predicting the disease prognosis and the development of disease modification therapies (2,3). However, the quest for definitive blood biomarkers has been fraught with inconsistencies (4) and the results were mixed (5,6). The instability of free-form proteins and nucleic acids in the blood are vulnerable to spontaneous degradation in the blood or storage, which can significantly alter their concentration and detectability (7-9). The blood-brain barrier (BBB) also poses a significant obstacle, and the selective permeability of BBB limited the accurate reflection of brain pathology in the bloodstream for neurological disease (10). Conversely, cerebrospinal fluid

(CSF) is an optimal source of providing more accurate biomarkers, but the invasive procedure to obtain CSF limited its widespread application (11,12).

Recent advances in the development of blood extracellular vesicle (EV) biomarkers offer a promising avenue for improving the diagnosis and monitoring the progression of PD (11-14). EVs are small, membrane-bound, cell-derived carrying with proteins, lipids, and nucleic acids (15). One of the key advantages of EV-contained protein biomarkers is their enhanced stability compared to free-form proteins and nucleic acids (16-18). Moreover, EVs possess the remarkable ability to cross the BBB (19). This capability enhances the potential of EVs to serve as reliable indicators of neurological conditions like PD.

$\alpha$ -Synuclein, tau, and  $\beta$ -amyloid (A $\beta$ ) play critical pathological roles in the development and progression of PD, making them key targets for biomarker research (20-22).  $\alpha$ -Synuclein is the main component of Lewy bodies, a pathological hallmark of PD.  $\alpha$ -Synuclein aggregates disrupt cellular function, leading to neuronal death and

the characteristic motor symptoms of PD (23). The progression of Lewy bodies from the brainstem to the cortex, as described by Braak staging (24), underscores the association between the progression of  $\alpha$ -synuclein pathology and clinical deterioration. Tau is the main component of neurofibrillary tangles, which disrupt the normal functioning of neurons, contributing to neurodegeneration and cognitive decline, one of the main progression indicators in PD (25). A $\beta$  forms extracellular plaques that contribute to neuroinflammation and oxidative stress, exacerbating neuronal damage. The presence of A $\beta$  plaques in PwP suggests a complex interplay between different proteinopathies in the disease's pathology (26,27). The associations between these pathognomonic proteins and the progression of clinical manifestations of PD position them as promising candidates for prognostic biomarkers, targets for disease-modifying treatments, and parameters for neuroprotective clinical trials.

Previous studies have explored these proteins as blood biomarkers for PD, but results have been inconsistent (28). Recent research has shifted focus to blood EVs as carriers of these pathognomonic proteins. Encapsulated within EVs,  $\alpha$ -synuclein, tau, and A $\beta$  are protected from degradation, making them more stable and detectable in blood samples. Elevated levels of EV-associated  $\alpha$ -synuclein have been observed in PwP, offering a more reliable biomarker due to the vesicles' ability to cross the blood-brain barrier and reflect central nervous system pathology (29). Similarly, EV-associated tau and A $\beta$  levels have shown potential as biomarkers, correlating with disease severity and progression (13,14). These findings underscore the promise of blood EV pathognomonic proteins as accurate and non-invasive biomarkers for diagnosing and monitoring PD, representing a significant advancement in neurodegenerative disease research. This study hypothesizes that in a longitudinal PD cohort, blood EV pathognomonic proteins — namely  $\alpha$ -synuclein, tau, and A $\beta$  — could serve as biomarkers

of PD progression, particularly in relation to motor and cognitive aspects.

## 2. Materials and Methods

### 2.1. Study population

The first PD cohort was established in November 2016, led by Dr. C.T. Hong (approval of Joint Institutional Review Board of Taipei Medical University with approval no. N201609017), and the second PD cohort, led by Dr. C.C. Chung (approval of Joint Institutional Review Board of Taipei Medical University with approval no. N201801043) at the same institute, was established in May 2018. Subsequently, the two cohorts collaborated. Study participants were followed annually with assessments including the Unified Parkinson's Disease Rating Scale (UPDRS) (motor function in PD), Mini-Mental State Examination (MMSE) and the Montreal Cognitive Assessment (MoCA) (cognitive function in PD), and blood sampling for plasma EV analysis.

However, the COVID-19 pandemic significantly impacted participants' willingness to undergo follow-up assessments, as these required extended hospital visits. Consequently, we terminated the two cohorts. In 2022, after the pandemic, a third PD cohort (approval of Joint Institutional Review Board of Taipei Medical University with approval no. N202205008) was launched. Participants from the first two cohorts were invited to resume follow-up assessments as part of the third cohort. The data from all three cohorts were then integrated. The study protocol was illustrated in Figure 1.

PD was diagnosed according to the UK Parkinson's Disease Society Brain Bank Diagnostic Criteria (30). Participants with PD were limited to those in the early to mid-stages, defined by Hoehn and Yahr stages I~III. The HCs were free from significant neurodegenerative diseases and disabilities, and were regularly monitored in outpatient clinics for chronic conditions such as

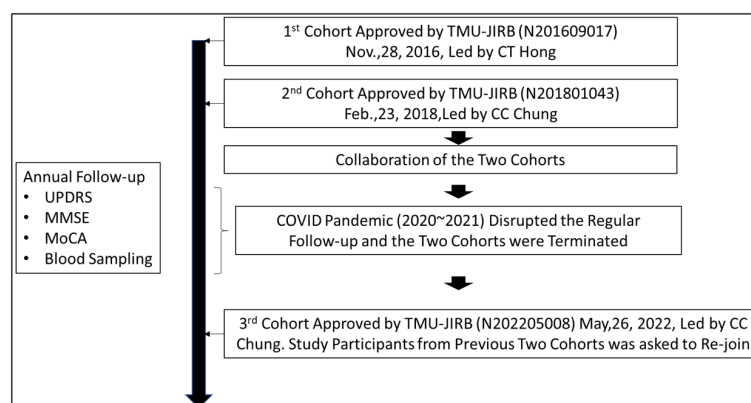


**Figure 1.** The diagram of the establishment of the study cohort and the assessment of the study participants during the visit. UPDRS, Unified Parkinson's Disease Rating Scale; MMSE, mini-mental status exams; MoCA, Montreal Cognitive Assessments, MoCA.

hypertension, diabetes, hyperlipidemia, headaches, or vertigo. In total, 140 PwP and 66 HCs completed their initial visit. The dropout rate and non-compliance with annual follow-ups were significant during the COVID-19 pandemic, leading to variations in the number of cases over the follow-up period.

Given that this cohort had previously examined the cross-sectional and 1-year follow-up results of plasma EV biomarkers in PD (13,14), this study now focuses on longer-term follow-up. As a result, the current analysis includes only PwP with three or more visits and HCs with two or three visits in the cohort.

## 2.2. Clinical assessment

Each participant underwent an interview to gather baseline demographic information. Trained nurses assessed the cognitive function of all participants using the Taiwanese versions of the MMSE and the MoCA. Additionally, all participants were evaluated using Parts I, II, and III of the UPDRS during an outpatient visit. The interval between the last dose of anti-PD medication and the UPDRS Part III assessment was not documented; therefore, it was assumed that PwP were in their "on" state. Tremor, akinetic rigidity (AR), and postural instability and gait disturbance (PIGD) subscores were derived from the subitems in UPDRS Part III and calculated according to modifications from the previous study (31).

## 2.3. Plasma EV isolation and validation

The details of plasma EV isolation and validation have been published previously (14). Venous blood samples were collected from all study participants during clinic visit, and plasma isolation was performed within 3 hours after venous blood sampling. Later on, storage plasma EV was isolated using the exoEasy Maxi kit according to the manufacturer's instructions. The isolated EVs were validated based on the presence of surface markers, such as CD63, CD9, and CD81; their morphology was determined using transmission electron microscopy; and particle size analysis was conducted through nanoparticle tracking.

## 2.4. Immunomagnetic reduction assay for quantifying $\alpha$ -synuclein, tau, and $\beta$ -amyloid

The details of the immunomagnetic reduction assay for quantifying plasma EV  $\alpha$ -synuclein, tau, and  $\beta$  have been described previously<sup>2</sup>; these analyses were conducted by MagQu Co (New Taipei, Taiwan). According to their instructions, the assay limit of detection was 1.39, 26, and 77 fg/mL for  $\alpha$ -synuclein, tau, and  $\beta$ , respectively.

## 2.5. Statistical analysis

All statistical analyses were performed using IBM SPSS, version 26 (IBM, Armonk, NY, USA). Generalized estimating equations evaluated associations between clinical symptom progression and plasma EV biomarkers. Spearman correlation assessed the relationship between biomarkers and age- and sex-adjusted clinical symptoms in PwP. The adjusted UPDRS, MMSE and MoCA scores have been standardized to Z scores to account for variations in age and gender across different visits. This standardization process involves calculating the mean and standard deviation of UPDRS, MMSE and MoCA scores within each age and gender group, and then converting individual scores to Z scores. A Z score indicates how many standard deviations an individual's score is from the mean of their age and gender group. Positive Z scores signify scores above the group mean, while negative Z scores indicate scores below the group mean. *P* value < 0.05 was considered statistically significant.

## 3. Results

### 3.1. Demographic data

In total, the clinical and plasma EV biomarkers data from 55 PwP who had three or more visits and 58 HCs with two or three visits were analyzed. There was no significant difference of age, gender distribution and baseline cognition (MMSE and MoCA) between two groups (Table 1). Regarding the progression of disease, for PwP, the UPDRS III remained stable between 1<sup>st</sup> to 3<sup>rd</sup> visits, and substantially deteriorated at 4<sup>th</sup> and 5<sup>th</sup> follow-up. In terms of cognition, there was no significant change of MMSE for PwP during the follow-up. At baseline, there was no significant difference of plasma EV  $\alpha$ -synuclein, tau, and  $\beta$  between PwP and HCs, despite a trend of lower of these plasma EV pathognomonic proteins in PwP. During follow-up, the change of plasma EV  $\alpha$ -synuclein, tau, and  $\beta$  was significantly different between PwP and HCs with the adjustment of age and sex. In general, an increase tendency was noted in PwP whereas the levels of plasma EV  $\alpha$ -synuclein, tau, and  $\beta$  were variable without substantial difference in HCs during the follow-up period of time (Table 1).

### 3.2. Association between the change of plasma EV $\alpha$ -synuclein, tau, and $\beta$ with changes in clinical motor and cognition symptoms during the whole course of follow-up

Considering only PwP, Figure 2 demonstrated the dynamic change of the clinical parameters and plasma EV pathognomonic proteins during the whole course of follow-up. In general, the increase trend was observed in all plasma EV pathognomonic proteins, in parallel with the change of UPDRS part II and III. The changes of cognitive parameters (MMSE and MoCA) were not

**Table 1. Baseline demographic data of study participants (with completed baseline and follow-up)**

|                     | HCs, n = 58  |              |             |   |   | PwP, n = 55  |              |              |              |              | p-value            |
|---------------------|--------------|--------------|-------------|---|---|--------------|--------------|--------------|--------------|--------------|--------------------|
|                     | 1            | 2            | 3           | 4 | 5 | 1            | 2            | 3            | 4            | 5            |                    |
| Age (y/o)           | 66.05 ± 7.06 |              |             |   |   | 68.11 ± 6.67 |              |              |              |              | 0.11*              |
| Female              | 22           |              |             |   |   | 25           |              |              |              |              | 0.45*              |
|                     | Visit        |              |             |   |   | Visit        |              |              |              |              |                    |
|                     | 1            | 2            | 3           | 4 | 5 | 1            | 2            | 3            | 4            | 5            |                    |
| Clinical Parameters |              |              |             |   |   |              |              |              |              |              |                    |
| MMSE                | 27.09 ± 3.55 | 27.16 ± 3.72 | -           | - | - | 26.55 ± 3.21 | 26.50 ± 4.16 | 26.23 ± 4.23 | 28.37 ± 1.42 | 27.82 ± 1.82 | 0.40*              |
| MoCA                | 23.21 ± 4.64 | 24.21 ± 5.28 | -           | - | - | 22.25 ± 4.76 | 22.92 ± 5.15 | 22.33 ± 5.48 | 25.53 ± 3.53 | 25.18 ± 3.86 | 0.95*              |
| UPDRS-II            | -            | -            | -           | - | - | 7.13 ± 4.62  | 10.04 ± 5.36 | 11.46 ± 6.61 | 8.26 ± 5.37  | 10.77 ± 5.18 |                    |
| UPDRS-III           | -            | -            | -           | - | - | 21.67 ± 8.86 | 20.08 ± 7.84 | 20.13 ± 9.08 | 27.58 ± 7.93 | 29.32 ± 8.42 |                    |
| Plasma EV Proteins  |              |              |             |   |   |              |              |              |              |              |                    |
| α-synuclein (fg/mL) | 80.9 ± 31.6  | 68.2 ± 27.6  | 75.4 ± 30.2 | - | - | 56.0 ± 35.6  | 73.0 ± 27.6  | 69.8 ± 26.0  | 76.0 ± 12.8  | 82.2 ± 16.6  | 0.012 <sup>§</sup> |
| Tau (pg/mL)         | 4.65 ± 1.99  | 5.16 ± 2.32  | 5.75 ± 2.21 | - | - | 3.55 ± 2.24  | 5.78 ± 2.41  | 5.17 ± 2.25  | 6.02 ± 3.55  | 5.23 ± 3.21  | 0.017 <sup>§</sup> |
| Aβ (pg/mL)          | 1.37 ± 0.50  | 1.41 ± 0.36  | 1.52 ± 0.22 | - | - | 1.13 ± 0.46  | 1.49 ± 0.33  | 1.25 ± 0.37  | 1.33 ± 0.58  | 1.53 ± 0.51  | 0.001 <sup>§</sup> |

Aβ, β-amyloid; EV, extracellular vesicle; HC, healthy control; PwP, people with Parkinson's disease; MMSE, Mini-Mental State Examination; MoCA, Montreal cognitive assessment; UPDRS, unified Parkinson's disease rating scale. Data was presented as mean ± standard deviation. \*, p value was obtained from the comparison at visit 1. <sup>§</sup>, p-value was obtained from the generalized estimated equation to compare the trend of change with the adjustment of age and sex.

substantial. The regression model with the adjustment of age and sex further delineated the association between the plasma EV pathognomonic proteins with clinical parameters (Table 2). IT was found that plasma EV α-synuclein and Aβ levels from baseline to the end of the follow-up were significantly associated with changes in UPDRS II scores during the same period, reflecting alterations in daily functional activity over the follow-up period. This association suggests that increases in plasma EV α-synuclein and Aβ could serve as indicators of worsening daily functional activity in PwP. However, no association was found between changes in plasma EV α-synuclein, tau, or Aβ levels from baseline to the end of the follow-up with changes in UPDRS III, MMSE, or MoCA scores during the same period (Table 2).

### 3.3. Correlation of changes in plasma EV α-synuclein, tau, and Aβ with changes in clinical motor and cognition severity at each follow-up time-point

To thoroughly delineate the association between changes in plasma EV α-synuclein, tau, and Aβ and clinical progression, correlation analysis was performed at each follow-up time point. The severity of motor and cognitive symptoms was adjusted for age and sex, then normalized and presented as changes in Z scores. A significant association was found between changes in plasma EV α-synuclein and changes in age- and sex-adjusted UPDRS II and MMSE scores at each follow-up time point (Table 3 and Figure 3). These associations suggest that plasma EV α-synuclein could serve as a real-time indicator of changes in the severity of motor and cognitive function in PwP.

## 4. Discussion

The present study demonstrated that PwP exhibited a distinct pattern of changes in plasma EV proteins compared to HCs, which were significantly associated with alterations in PD-related daily functioning. Furthermore, changes in plasma EV α-synuclein levels showed a significant correlation with changes in UPDRS-II scores and cognitive function. These findings suggest that blood EV pathognomonic proteins may reflect the progression of brain pathology in PD, with changes in plasma EV α-synuclein levels serving as an indicator of clinical disease progression.

In the pathogenesis of PD, α-synuclein, tau, and Aβ play crucial roles. Misfolded α-synuclein aggregates disrupt neuronal function, leading to neurodegeneration (23). Hyperphosphorylated tau forms neurofibrillary tangles that impair axonal transport and synaptic function (32). Aβ is also implicated in PD by contributing to neuroinflammation and oxidative stress through amyloid plaque formation (26,33). Research has increasingly focused on the potential of these proteins as biomarkers for PD (34). Decreased levels of CSF α-synuclein

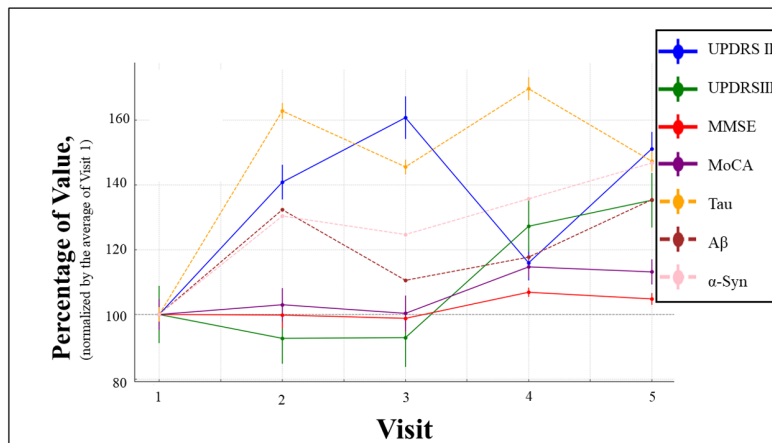


**Figure 2.** The dynamic change of motor symptoms (assessed by total score of Unified Parkinson's Disease Rating Scale, UPDRS part II and III), cognition (assessed by mini-mental status exams, MMSE and Montreal Cognitive Assessments, MoCA) and plasma extracellular vesicle pathognomonic proteins (Tau,  $\beta$ -amyloid [A $\beta$ ] and  $\alpha$ -synuclein [ $\alpha$ -Syn] in people with Parkinson's disease during 1<sup>st</sup> to 5<sup>th</sup> visits. Data of each parameter was normalized by the average of 1<sup>st</sup> visit and presented as percentage with standard deviation.

**Table 2.** Regression models for the association between the changes in plasma extracellular vesicle (EV) pathognomonic proteins with the changes in clinical assessments in people with Parkinson's disease during the whole course of follow-up after adjustment of age and sex. Data are presented as standardized beta value ( $\beta$  value)

|            | Changes in Plasma EV |                |                     |
|------------|----------------------|----------------|---------------------|
|            | Tau                  | A $\beta$      | $\alpha$ -synuclein |
| Changes in |                      |                |                     |
| UPDRS-II   | 0.23 (0.854)         | 2.05** (0.008) | 0.04** (0.001)      |
| UPDRS-III  | -0.09 (0.686)        | 0.33 (0.727)   | 0.02 (0.287)        |
| MMSE       | 0.01 (0.825)         | -0.50 (0.218)  | -0.02 (0.954)       |
| MoCA       | 0.004 (0.954)        | 0.05 (0.916)   | -0.01 (0.553)       |

MMSE, Mini-Mental State Examination; MoCA, Montreal cognitive assessment; UPDRS, Unified Parkinson's Disease Rating Scale. \*,  $p < 0.05$ ; \*\*,  $p < 0.01$ .

**Table 3.** Association between the changes in plasma extracellular vesicle (EV) pathognomonic proteins with the changes in age, sex-normalized clinical parameters in people with Parkinson's disease at each point of visit. Data are presented as correlation coefficient ( $\rho$ ) and  $p$  value

| Change of Plasma EV Protein | Change of age & sex-normalized clinical parameters |          |        |        |        |          |        |
|-----------------------------|--|----------|--------|--------|--------|----------|--------|
|                             | UPDRSII  | UPDRSIII | Tremor | AR     | PIGD   | MMSE     | MoCA   |
| $\alpha$ -synuclein         |  |          |        |        |        |          |        |
| $\rho$                      | 0.211*   | 0.041    | 0.086  | 0.001  | 0.059  | -0.275** | -0.079 |
| $p$ -value                  | 0.026  | 0.673    | 0.372  | 0.994  | 0.537  | 0.004    | 0.411  |
| Tau                         |  |          |        |        |        |          |        |
| $\rho$                      | 0.106  | -0.053   | -0.053 | -0.018 | -0.112 | 0.000    | 0.043  |
| $p$ -value                  | 0.269  | 0.584    | 0.580  | 0.853  | 0.242  | 0.997    | 0.657  |
| A $\beta$                   |  |          |        |        |        |          |        |
| $\rho$                      | 0.152  | 0.012    | 0.069  | -0.003 | -0.043 | -0.067   | 0.025  |
| $p$ -value                  | 0.112  | 0.899    | 0.473  | 0.978  | 0.657  | 0.484    | 0.795  |

A $\beta$ ,  $\beta$ -amyloid; AR, akinetic rigidity; MMSE, Mini-Mental State Examination; MoCA, Montreal cognitive assessment; PIGD, postural instability and gait disturbance; UPDRS, Unified Parkinson's Disease Rating Scale. \*,  $p < 0.05$ ; \*\*,  $p < 0.01$ .

and A $\beta$  have been noted in PD, while higher levels of phosphorylated tau in CSF have been associated with cognitive impairment in PwP (35). Our group has previously published findings highlighting the association between elevated levels of tau and A $\beta$  in plasma EVs and cognitive decline in PwP (14). Additionally, we observed that PwP exhibit a distinct pattern of increased levels of  $\alpha$ -synuclein, tau, and A $\beta$  within blood EVs compared to

controls in a short-term follow-up period of time (13). These findings support the potential of EV-associated proteins as biomarkers for PD progression, emphasizing the need for further research to validate their clinical utility and understand the underlying mechanisms. In the present study, we observed no significant baseline differences in the levels of  $\alpha$ -synuclein, tau, and A $\beta$  between PwP and HCs. However, the trend of these

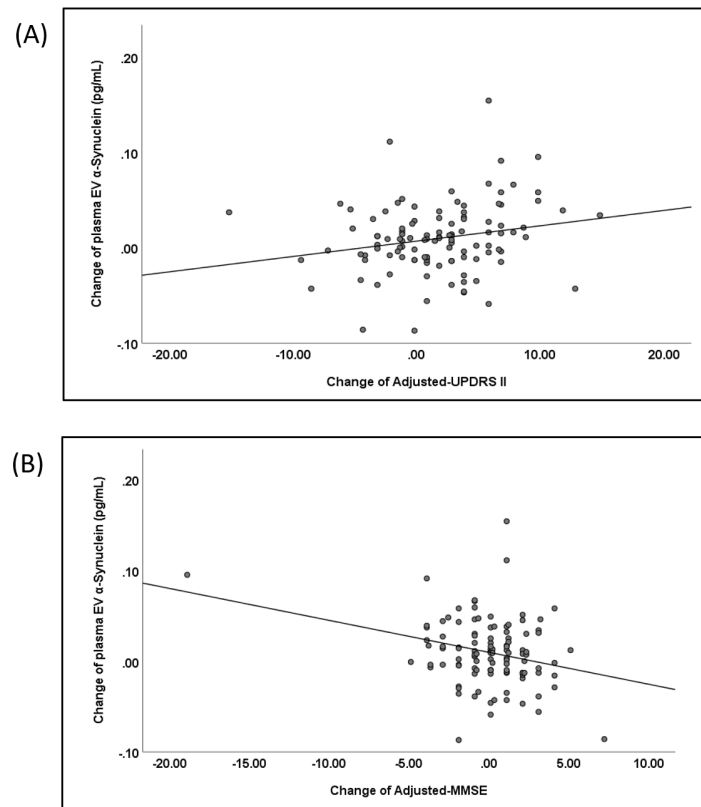


**Figure 3.** The association between the change of plasma extracellular vesicle (EV)  $\alpha$ -synuclein with the change of adjusted Unified Parkinson's Disease Rating Scale, (UPDRS) part II (A), and the change of adjusted Mini-Mental Status Examination (MMSE) (B).

proteins over the follow-up period revealed significant differences. Specifically, while the levels of these proteins tended to remain stable in HCs, there was a noticeable increase in PwP over time. This trend suggests a progressive accumulation of these proteins in PwP, which aligns with the disease's neurodegenerative nature. These findings supported the hypothesis that blood EV $\alpha$ -synuclein, tau, and A $\beta$  could serve as biomarkers of PD progression.

Previous studies had identified several blood biomarkers, including neurofilament light chain (36), uric acid (37) and inflammatory cytokines (38), as potential indicators of PD progression. Among these, the most extensively studied biomarker is  $\alpha$ -synuclein. Elevated baseline levels of plasma ser129-phosphorylated  $\alpha$ -synuclein have been associated with a higher risk of motor symptom progression (39). However, it has also been observed that plasma total  $\alpha$ -synuclein levels increase over time, up to 20 years of follow-up, while phosphorylated  $\alpha$ -synuclein levels remain constant during the same period (40). Overall, studies on blood  $\alpha$ -synuclein as a biomarker for PD progression have yielded inconsistent results, likely due to variations in quantification methods and contamination from red blood cells. For blood exosomal  $\alpha$ -synuclein, a small-scale study demonstrated that longitudinally increases in  $\alpha$ -synuclein, rather than baseline levels, were associated with a higher risk of motor symptom

progression in PD (41). However, this association was not confirmed in other study (42). Furthermore, the relationship between blood free  $\alpha$ -synuclein and blood EV  $\alpha$ -synuclein has yet to be investigated in PD. In the present study, the changes in the levels of plasma EV  $\alpha$ -synuclein, tau, and A $\beta$  were significantly correlated with the progression in the UPDRS part II scores, reflecting the daily functional abilities of PwP. This association underscores the potential of these proteins as biomarkers for monitoring disease progression and daily functional decline in PD. These findings are consistent with previous research indicating that increases in these protein levels, particularly within blood extracellular vesicles, are associated with PD motor progression (41). This study further supports the utility of monitoring these biomarkers longitudinally to better understand and predict the trajectory of PD. We also identified a significant association between changes in blood EV  $\alpha$ -synuclein levels and age- and sex-adjusted changes in UPDRS-II and MMSE scores. Notably, it was the change in blood EV  $\alpha$ -synuclein, rather than its absolute value, that predicted disease progression. This suggests that the dynamic change in  $\alpha$ -synuclein levels correlates with the progression of PD pathology and its clinical manifestations. This relationship highlights the potential of blood EV  $\alpha$ -synuclein as a sensitive biomarker for monitoring PD progression and evaluating therapeutic efficacy, particularly for  $\alpha$ -synuclein-targeted treatments.

The correlation between the progression of  $\alpha$ -synuclein pathology and clinical disease markers supports its use as a more nuanced biomarker compared to traditional motor symptom scores. This could significantly enhance the precision of therapeutic monitoring and the assessment of novel treatments aimed at reducing  $\alpha$ -synuclein pathology. These insights provide a valuable framework for future research and clinical applications, emphasizing the importance of longitudinal biomarker monitoring in PD management.

The present study demonstrated that PwP exhibited a distinct pattern of changes in plasma EV proteins compared to HCs, which were significantly associated with alterations in PD-related daily functioning. Furthermore, changes in plasma EV  $\alpha$ -synuclein levels showed a significant correlation with changes in UPDRS-II scores and cognitive function. These findings suggest that blood EV pathognomonic proteins may reflect the progression of brain pathology in PD, with changes in plasma EV  $\alpha$ -synuclein levels serving as an indicator of clinical disease progression. This aligns with the understanding that  $\alpha$ -synuclein pathology is central to PD, while tau and A $\beta$  are more strongly associated with the cognitive aspects of PD (22). The cerebral multimorbidity hypothesis, which posits the coexistence of mixed pathologies in neurodegenerative diseases, supports the presence of tau and A $\beta$  in PwP (43). However, our findings indicated that each neurodegenerative disease maintains distinct pathological patterns and preferences. This underscores the complexity of neurodegenerative diseases and the necessity for disease-specific biomarkers and treatment strategies. The lack of significant findings for tau and A $\beta$  suggests that while these proteins contribute to the broader landscape of neurodegeneration,  $\alpha$ -synuclein remains the primary marker for PD. This distinction is crucial for developing targeted therapies and improving patient outcomes in PD.

Despite its strengths, this study has several limitations that warrant discussion. First, the study design excluded participants who deteriorated too rapidly or severely to return for follow-up visits. This exclusion likely introduced a bias, resulting in a cohort that may represent slower disease progression. Furthermore, the COVID-19 pandemic significantly affected participant retention, particularly among healthy controls, leading to a higher dropout rate and reduced sample size. Second, the study utilized total plasma EVs as biomarkers rather than neuron-derived exosomes, which are more specific to neuronal changes associated with PD. Neuron-derived exosomes could provide a higher degree of specificity and sensitivity, and future studies should explore this approach to enhance biomarker detection. Third, assessments of motor symptoms using the UPDRS were conducted during the PwP's "on" medication state, potentially masking the full extent of motor dysfunction. This methodological limitation

may have influenced the observed associations between biomarkers and clinical parameters. Fourth, while the statistical methods employed provided valuable insights, the study did not integrate artificial intelligence (AI)-based analyses. AI approaches could uncover complex, non-linear relationships between biomarkers and disease progression, improving predictive accuracy and enhancing biomarker utility. Incorporating AI in future studies could address this gap and provide more nuanced interpretations of the data. Finally, the relatively short follow-up period, despite being supplemented by data from integrated cohorts, limits the ability to fully capture the long-term dynamics of disease progression. Future studies with extended follow-up durations and more frequent assessments will be critical to validate and expand upon these findings.

## 5. Conclusion

In conclusion, while our study provides valuable insights into the potential of plasma EV  $\alpha$ -synuclein as a biomarker for PD progression, which was associated with cognition and daily functional activity, these limitations highlight the need for cautious interpretation of the results and underscore the importance of designing more robust and comprehensive studies in the future.

*Funding:* This study was funded by Ministry of Science and Technology, Taiwan (MOST 110-2314-B-038-096), and National Science and Technology Council (NSTC 111-2314-B-038 -136).

*Conflict of Interest:* The authors have no conflicts of interest to disclose.

## References

1. Tolosa E, Garrido A, Scholz SW, Poewe W. Challenges in the diagnosis of Parkinson's disease. *Lancet Neurol.* 2021; 20:385-397.
2. Le W, Dong J, Li S, Korczyn AD. Can Biomarkers Help the Early Diagnosis of Parkinson's Disease? *Neurosci Bull.* 2017; 33:535-542.
3. T Tönges L, Buhmann C, Klebe S, Klucken J, Kwon EH, Müller T, Pedrosa DJ, Schröter N, Riederer P, Lingor P. Blood-based biomarker in Parkinson's disease: potential for future applications in clinical research and practice. *J Neural Transm (Vienna).* 2022; 129:1201-1217.
4. Morris HR. Blood based biomarkers for movement disorders. *Acta Neurol Scand.* 2022; 146:353-361.
5. Cova I, Priori A. Diagnostic biomarkers for Parkinson's disease at a glance: where are we? *J Neural Transm (Vienna).* 2018; 125:1417-1432.
6. Delenclos M, Jones DR, McLean PJ, Uitti RJ. Biomarkers in Parkinson's disease: Advances and strategies. *Parkinsonism Relat Disord.* 2016; 22 Suppl 1:S106-110.
7. Wang C, Liu H. Factors influencing degradation kinetics of mRNAs and half-lives of microRNAs, circRNAs, lncRNAs in blood *in vitro* using quantitative PCR. *Sci Rep.* 2022; 12:7259.

8. Paulovich AG, Whiteaker JR, Hoofnagle AN, Wang P. The interface between biomarker discovery and clinical validation: The tar pit of the protein biomarker pipeline. *Proteomics Clin Appl.* 2008; 2:1386-1402.
9. Rifai N, Gillette MA, Carr SA. Protein biomarker discovery and validation: the long and uncertain path to clinical utility. *Nat Biotechnol.* 2006; 24:971-983.
10. Thambisetty M, Lovestone S. Blood-based biomarkers of Alzheimer's disease: challenging but feasible. *Biomark Med.* 2010; 4:65-79.
11. Howell JC, Parker MW, Watts KD, Kollhoff A, Tsvetkova DZ, Hu WT. Research Lumbar Punctures among African Americans and Caucasians: Perception Predicts Experience. *Front Aging Neurosci.* 2016; 8:296.
12. Tsvetkova DZ, Bergquist SH, Parker MW, Jarrett TL, Howell JC, Watts KD, Kollhoff A, Roberts DL, Hu WT. Fear and Uncertainty Do Not Influence Reported Willingness to Undergo Lumbar Punctures in a U.S. Multi-Cultural Cohort. *Front Aging Neurosci.* 2017; 9:22.
13. Chan L, Chung CC, Hsieh YC, Wu RM, Hong CT. Plasma extracellular vesicle tau,  $\beta$ -amyloid, and  $\alpha$ -synuclein and the progression of Parkinson's disease: a follow-up study. *Ther Adv Neurol Disord.* 2023; 16:17562864221150329.
14. Chung CC, Chan L, Chen JH, Bamodu OA, Chiu HW, Hong CT. Plasma extracellular vesicles tau and  $\beta$ -amyloid as biomarkers of cognitive dysfunction of Parkinson's disease. *FASEB J.* 2021; 35:e21895.
15. Yáñez-Mó M, Siljander PR, Andreu Z. *et al.* Biological properties of extracellular vesicles and their physiological functions. *J Extracell Vesicles.* 2015; 4:27066.
16. Boukouris S, Mathivanan S. Exosomes in bodily fluids are a highly stable resource of disease biomarkers. *Proteomics Clin Appl.* 2015; 9:358-367.
17. J Jin Y, Chen K, Wang Z. *et al.* DNA in serum extracellular vesicles is stable under different storage conditions. *BMC Cancer.* 2016; 16:753.
18. Ge Q, Zhou Y, Lu J, Bai Y, Xie X, Lu Z. miRNA in plasma exosome is stable under different storage conditions. *Molecules.* 2014; 19:1568-1575.
19. Haqqani AS, Delaney CE, Tremblay TL, Sodja C, Sandhu JK, Stanimirovic DB. Method for isolation and molecular characterization of extracellular microvesicles released from brain endothelial cells. *Fluids Barriers CNS.* 2013; 10:4.
20. Noguchi-Shinohara M, Ono K. The Mechanisms of the Roles of  $\alpha$ -Synuclein, Amyloid- $\beta$ , and Tau Protein in the Lewy Body Diseases: Pathogenesis, Early Detection, and Therapeutics. *Int J Mol Sci.* 2023; 24:10215.
21. Sengupta U, Kaye R. Amyloid  $\beta$ , Tau, and  $\alpha$ -Synuclein aggregates in the pathogenesis, prognosis, and therapeutics for neurodegenerative diseases. *Prog Neurobiol.* 2022; 214:102270.
22. Compta Y, Parkkinen L, Kempster P, Selikhova M, Lashley T, Holton JL, Lees AJ, Revesz T. The Significance of  $\alpha$ -Synuclein, Amyloid- $\beta$  and Tau Pathologies in Parkinson's Disease Progression and Related Dementia. *Neurodegenerative Diseases* 13, 154-156 (2013).
23. Calabresi P, Mechelli A, Natale G, Volpicelli-Daley L, Di Lazzaro G, Ghiglieri V. Alpha-synuclein in Parkinson's disease and other synucleinopathies: from overt neurodegeneration back to early synaptic dysfunction. *Cell Death Dis.* 2023; 14:176.
24. Braak H, Ghebremedhin E, Rüb U, Bratzke H, Del Tredici K. Stages in the development of Parkinson's disease-related pathology. *Cell Tissue Res.* 2004; 318:121-134.
25. Pan L, Meng L, He M, Zhang Z. Tau in the pathophysiology of Parkinson's disease. *J Mol Neurosci.* 2021; 71:2179-2191.
26. Lim EW, Aarsland D, Ffytche D, Taddei RN, van Wamelen DJ, Wan YM, Tan EK, Ray Chaudhuri K; Kings Parcog group MDS Nonmotor study group. Amyloid- $\beta$  and Parkinson's disease. *J Neurol.* 2019; 266:2605-2619.
27. Hepp DH, Vergoossen DL, Huisman E, Lemstra AW; Netherlands Brain Bank; Berendse HW, Rozemuller AJ, Foncke EM, van de Berg WD. Distribution and load of amyloid- $\beta$  pathology in Parkinson disease and dementia with lewy bodies. *J Neuropathol Exp Neurol.* 2016; 75:936-945.
28. Parnetti L, Gaetani L, Eusebi P, Paciotti S, Hansson O, El-Agnaf O, Mollenhauer B, Blennow K, Calabresi P. CSF and blood biomarkers for Parkinson's disease. *Lancet Neurol.* 2019; 18:573-586.
29. Xylaki M, Chopra A, Weber S, Bartl M, Outeiro TF, Mollenhauer B. Extracellular vesicles for the diagnosis of Parkinson's disease: Systematic review and meta-analysis. *Mov Disord.* 2023; 38:1585-1597.
30. Marsden CD. Parkinson's disease. *J Neurol Neurosurg Psychiatry.* 1994; 57:672-681.
31. Eggers C, Kahraman D, Fink GR, Schmidt M, Timmermann L. Akinetic-rigid and tremor-dominant Parkinson's disease patients show different patterns of FP-CIT single photon emission computed tomography. *Mov Disord.* 2011; 26:416-423.
32. Honson NS, Kuret J. Tau aggregation and toxicity in tauopathic neurodegenerative diseases. *J Alzheimers Dis.* 2008; 14:417-422.
33. Roy RG, Mandal PK, Maroon JC. Oxidative stress occurs prior to amyloid A $\beta$  plaque formation and tau phosphorylation in Alzheimer's disease: Role of glutathione and metal ions. *ACS Chem Neurosci.* 2023; 14:2944-2954.
34. Coughlin DG, Irwin DJ. Fluid and biopsy based biomarkers in Parkinson's disease. *Neurotherapeutics.* 2023; 20:932-954.
35. Shi M, Zhang J. CSF  $\alpha$ -synuclein, tau, and amyloid  $\beta$  in Parkinson's disease. *Lancet Neurol.* 2011; 10:681; author's reply 681-3.
36. Lin CH, Li CH, Yang KC, Lin FJ, Wu CC, Chieh JJ, Chiu MJ. Blood NfL: A biomarker for disease severity and progression in Parkinson disease. *Neurology.* 2019; 93:e1104-e1111.
37. Chahine LM, Stern MB, Chen-Plotkin A. Blood-based biomarkers for Parkinson's disease. *Parkinsonism Relat Disord.* 2014; 20 Suppl 1:S99-103.
38. Joo J, Jeong J, Park HJ. Blood Biomarkers in Patients with Parkinson's Disease: A Review in Context of Anesthetic Care. *Diagnostics (Basel).* 2023; 13:693.
39. Lin CH, Liu HC, Yang SY, Yang KC, Wu CC, Chiu MJ. Plasma pS129- $\alpha$ -Synuclein Is a Surrogate Biofluid Marker of Motor Severity and Progression in Parkinson's Disease. *J Clin Med.* 2019; 8:1601.
40. Foulds PG, Diggle P, Mitchell JD, Parker A, Hasegawa M, Masuda-Suzukake M, Mann DM, Allsop D. A longitudinal study on  $\alpha$ -synuclein in blood plasma as a biomarker for Parkinson's disease. *Sci Rep.* 2013; 3:2540.
41. Niu M, Li Y, Li G, Zhou L, Luo N, Yao M, Kang W, Liu J. A longitudinal study on  $\alpha$ -synuclein in plasma neuronal exosomes as a biomarker for Parkinson's disease development and progression. *Eur J Neurol.* 2020 ;27:967-

- 974.
42. Zhao ZH, Chen ZT, Zhou RL, Zhang X, Ye QY, Wang YZ. Increased DJ-1 and  $\alpha$ -Synuclein in Plasma Neural-Derived Exosomes as Potential Markers for Parkinson's Disease. *Front Aging Neurosci.* 2019; 10:438
  43. Attems J, Jellinger K. Neuropathological correlates of cerebral multimorbidity. *Curr Alzheimer Res.* 2013; 10:569-577.

Received November 23, 2024; Revised January 24, 2025;

Accepted January 29, 2025.

*\*Address correspondence to:*

Lung Chan, Department of Neurology, Shuang Ho Hospital, Taipei Medical University, No. 291, Zhongzheng Rd, Zhonghe District, New Taipei City, 235, Taiwan.

E-mail: cjustinmd@tmu.edu.tw

Released online in J-STAGE as advance publication February 9, 2025.

# Multimodal optimal matching and augmentation method for small sample gesture recognition

Wenli Zhang<sup>1,\*</sup>, Bo Liu<sup>1</sup>, Tingsong Zhao<sup>1</sup>, Shuyan Qie<sup>2</sup>

<sup>1</sup> Faculty of Information Science and Technology, Beijing University of Technology, Beijing, China;

<sup>2</sup> Department of Rehabilitation, Beijing Rehabilitation Hospital Capital Medical University, Beijing, China.

**SUMMARY:** In human-computer interaction, gesture recognition based on physiological signals offers advantages such as a more natural and fast interaction mode and less constrained by the environment than visual-based. Surface electromyography-based gesture recognition has significantly progressed. However, since individuals have physical differences, researchers must collect data multiple times from each user to train the deep learning model. This data acquisition process can be particularly burdensome for non-healthy users. Researchers are currently exploring transfer learning and data augmentation techniques to enhance the accuracy of small-sample gesture recognition models. However, challenges persist, such as negative transfer and limited diversity in training samples, leading to suboptimal recognition performance. Therefore, We introduce motion information into sEMG-based recognition and propose a multimodal optimal matching and augmentation method for small sample gesture recognition, achieving efficient gesture recognition with only one acquisition per gesture. Firstly, this method utilizes the optimal matching signal selection module to select the most similar signals from the existing data to the new user as the training set, reducing inter-domain differences. Secondly, the similarity calculation augmentation module enhances the diversity of the training set. Finally, the Modal-type embedding enhances the information interaction between each mode signal. We evaluated the effectiveness on Self-collected Stroke Patient, the Ninapro DB1 dataset and the Ninapro DB5 dataset and achieved accuracies of 93.69%, 91.65% and 98.56%, respectively. These results demonstrate that the method achieved performance comparable to traditional recognition models while significantly reducing the collected data.

**Keywords:** Neuro-robotics, gesture recognition, small sample, rehabilitation therapy, signal similarity

## 1. Introduction

With the advancement of sensor and deep learning technology, gesture recognition based on physiological signals has been widely applied in human-computer interaction. It finds applications in various areas, such as sign language recognition, robot control, virtual reality, and prosthetic control (1-4). Utilizing physiological signals to capture gestures is a more natural and immersive interaction, offering advantages such as low latency and computational requirements. Among physiological signals, surface electromyography (sEMG) signals are particularly suitable for capturing muscle activities. By placing electrodes on the skin's surface in the region of interest, muscle action potentials can be measured without causing harm to the human body. Consequently, acquiring and recognizing gestures from sEMG signals have become a hot research topic in related fields (5).

In previous research, we proposed a long-short-

term feature fusion network called LST-EMG-Net for sEMG gesture recognition (6). The network is entirely designed based on attention mechanisms. LST-EMG-Net extracts long-term and short-term features separately and employs a feature cross-attention module to fuse them, addressing the mismatch between the extracted feature information and the information required for gesture recognition. On the DB2 E2, Ninapro DB5 E3, and CapgMyo DB-C datasets, LST-EMG-Net achieved accuracies of 81.47%, 88.24%, and 98.80%, respectively. Compared to the state-of-the-art methods in the literature, it improved the accuracy by 2.70%, 4.49%, and 0.42% for the respective datasets, enhancing the accuracy and stability of gesture recognition across various classes. However, the challenge of a heavy user data collection burden still exists:

The datasets used by traditional gesture recognition models such as LST-EMG-Net are obtained under ideal conditions, where each participant has sufficient data

to train individual recognition models. For example, in the Ninapro public dataset (7-10), each sub-dataset gesture typically requires patients to repeat it 6 to 10 times. Each participant must perform continuous arm movements for approximately half an hour when collecting over a dozen gestures. Prolonged data collection leads to muscle fatigue in the participants and affects the data quality (11). This data collection burden, particularly in stroke or disabled patients, imposes significant physical and time costs on the patients. Moreover, there exist differences among participants in terms of height, weight, body mass index (BMI), and the amount of fat in the superficial muscles. Even when performing the same gesture, individuals exhibit significant variations in signal distribution (12). As a result, personalized small-sample signal-based models and models trained on signals from other individuals struggle to achieve the desired recognition accuracy.

Related researchers generally propose small-sample gesture recognition methods in terms of either transfer learning (TL) or signal augmentation to reduce the user's acquisition burden.

Transfer learning Small-sample gesture recognition methods typically use existing user data as the source domain and the new user data as the target domain. Researchers design transfer strategies from the perspectives of data, features, or models to effectively recognize the target domain (13-20).

Kanoga *et al.* (13) proposed a transfer framework that projects the source domain data onto the target domain data distribution through linear projection. Azab *et al.* (14) introduced a data transfer method based on Kullback-Leibler (K-L) divergence measurement. Wang *et al.* (15) presented a multi-source integration transfer learning (MSITL) approach to explore cross-user gesture recognition. It involves training recognition models for each source domain (user) and fine-tuning them using the target domain (new user) data evaluation scores. Colli Alfaro *et al.* (16) introduced IMU data to the existing EMG signals of subjects. Multiple pre-trained prediction models are created for each source data and fine-tuned using an adaptive least squares support vector machine (LS-SVM) to select the model with the highest accuracy. Sheng *et al.* (17) proposed a general framework called the common spatial-spectral analysis (CSSA) framework. Campbell *et al.* (18) introduced an Adaptive Domain Adversarial Neural Network (ADANN), which freezes certain layers and fine-tunes others when adding new subjects. Tsinganos *et al.* (19) proposed a new convolutional neural network (TSNet) that combines both temporal and spatial features, as well as an improved version of AtzoriNet denoted as AtzoriNet\*. They trained the network models using data from multiple participants (source domain) and then fine-tuned the model weights using data from the target domain to recognize gestures performed by new users. Yu *et al.* (20) employed a similar approach, utilizing the

source domain data to train an improved CNN model and fine-tuning the fully connected layers with target domain data for recognizing gestures from new subjects. We summarize the relevant studies on transfer learning for small sample recognition from the perspectives of methodology, datasets, number of subjects, types of gestures, signal types, and accuracy, as shown in Table 1.

In summary, applying transfer learning to small sample gesture recognition can somewhat improve recognition performance. However, due to the inherent differences in the physical characteristics of physiological signals such as sEMG signals among different individuals and the influence of factors such as environmental noise and body posture, there are significant differences in the feature distributions of signals between the source and target domains. Consequently, knowledge learned in the source domain may not be applicable to the target domain, resulting in a performance decline when the knowledge or model learned from the source domain data is applied to the target domain data. This can lead to the problem of negative transfer (21), which affects the model's recognition performance.

In addition to the methods mentioned above, in tasks such as emotion recognition (22-25), researchers have employed multimodal data fusion methods to combine data from different types of sensors. The method aims to obtain comprehensive, accurate, and reliable physiological information, thereby improving the recognition accuracy and generalization of the models. Although the application of multimodal data fusion methods in small-sample gesture recognition is currently limited, this approach provides valuable insights. It allows us to complement the general physiological information of gesture movements, reduce inter-user domain differences, and enhance the accuracy of small-sample gesture recognition.

Based on the above problems and research status, in order to maximize the accuracy of small-sample gesture recognition we propose a multimodal optimal matching and augmentation method for Small sample gesture recognition. The method can effectively address the negative transfer problem and enhance the diversity of signals in the training set. With only one data collection for each gesture, this method achieves comparable accuracy to traditional gesture recognition models based on individual data. The main contributions of this paper are as follows: In response to the negative transfer problem caused by the significant domain differences between the source and target domains, we analyze the characteristics of signals from different individuals for the same gesture. We propose an optimal matching signal selection module that calculates the similarity between existing and new user signals from a time-frequency perspective. This module selects high-similarity signals to form the optimal matching signal training set, enhancing the similarity between the source

**Table 1. Summary of Related Research on Transfer Learning-Based Small-Sample Gesture Recognition**

| References                   | Methods            | Dataset   | Number of Participants  | Types of Gestures                 | Signal Types | Accuracy   |
|------------------------------|--------------------|---|---|-----------------------------------|--------------|--|
| Kanoga <i>et al.</i> (13)    | SVM                | 1-DoF<br>2-DoFs   | 25 Intact Subjects  | 8                                 | EMG          | 91.96 ± 5.75%<br>63.28 ± 10.43%  |
| Wang <i>et al.</i> (15)      | MSITL              | NinaPro DB1<br>CapgMyo DB-a<br>CapgMyo DB-b<br>CapgMyo DB-c<br>Self-collected dataset<br>Self-collected dataset | 27 Intact Subjects<br>18 Intact Subjects<br>10 Intact Subjects<br>10 Intact Subjects<br>22 Intact Subjects<br>7 Intact Subjects | 8<br>8<br>8<br>12<br>7<br>11<br>9 | EMG          | 69.93% ± 4.33%<br>86.62% ± 5.68%<br>88.35% ± 4.67%<br>74.61% ± 5.45%<br>84.6% ± 7.3%<br>63.83%<br>72.84% |
| Campbell <i>et al.</i> (18)  | ADANN              | Intact-limb and amputee datasets  | 10 Intact Subjects<br>5 amputees  | 10<br>10                          | EMG<br>EMG   | 86.03%<br>86.8 – 96.2%<br>64.1 – 84.2%   |
| Tsinganos <i>et al.</i> (19) | TsNet<br>AtzorNet* | NinaPro DB7   | 20 Intact Subjects  | 17                                | EMG          | 91.93% ± 4.29%<br>90.57% ± 4.43%   |
| Yu <i>et al.</i> (20)        | CNN                | CapgMyo DB-a<br>CapgMyo DB-c<br>NinaPro DB1   | 18 Intact Subjects<br>10 Intact Subjects<br>27 Intact Subjects  | 8<br>12<br>12                     | EMG          | 86.7%<br>84.47%<br>74.7%   |

and target domains and avoiding the occurrence of negative transfer phenomena.

## 2. Materials and Method

The overall framework of the proposed multimodal optimal matching and augmentation method is depicted in Figure 1. The framework consists of three main components: the optimal matching signal selection module, the similarity calculation augmentation module, and the multimodal LST-EMG-Net.

**Optimal matching signal selection module:** This module calculates the similarity between new user-calibrated gestures signals and the database's signals. After adaptive selection based on multimodal signals, it outputs the optimal matching signals as part of the training set.

*Signal augmentation module:* This module utilizes Variational Autoencoder (VAE) to expand the multimodal signal samples of new user calibrated gestures by using a reconstruction loss based on time-domain similarity calculation to compute the difference between the generated samples and the original samples to optimize the generation of samples. The enhanced samples are then outputted as another part of the training set.

*Multimodal LST-EMG-Net:* This network inputs the training set consisting of the optimal matching signal and augmentation samples. The sEMG and motion signals in each sample are separated with Modal-type embedding and fed into the LST-EMG-Net to extract features for gesture recognition.

The application process of the multimodal optimal matching and augmentation gesture recognition method consists of two stages:

*Model training stage:* The stage involves organizing the multimodal signals of existing users into a multimodal signal database based on the number of gesture repetitions. A single repetition of the gesture signal from a new user is collected as the calibration gesture signal. Once the data collection is complete, the new user's calibration gesture dataset and the multimodal signal database are inputted into the optimal matching signal screening module and the signal enhancement module based on signal similarity calculation. The obtained training set is then inputted into the Multimodal LST-EMG-Net for training, constructing a gesture recognition model.

*Online gesture recognition stage:* The user wears the collection device to capture real-time multimodal signals. These signals are then input into the trained Multimodal LST-EMG-Net to obtain the gesture category.

### 2.1. Multimodal Datasets

We evaluate our small-sample gesture recognition using

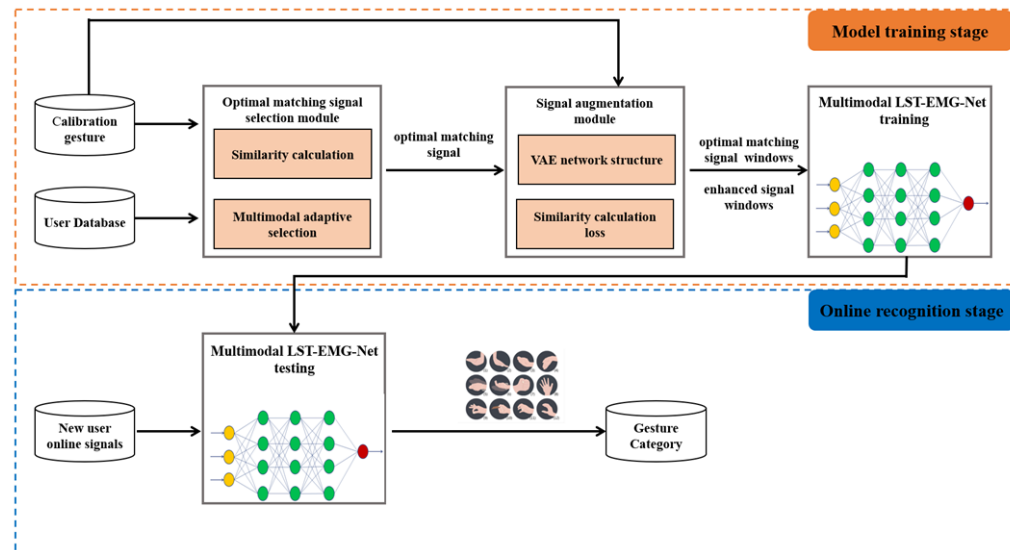


Figure 1. Overall framework of multimodal optimal matching and augmentation method.

the self-collected stroke patient dataset, the public dataset Ninapro DB1 and the public dataset Ninapro DB5.

*Self-collected Stroke Patient Dataset:* This dataset was obtained from 6 stroke patients (5 males, 1 female, aged 57–68 years) at the Beijing rehabilitation hospital. Under the guidance of professional rehabilitation physicians, the patients used an MYO armband (as shown in Figure 2) to collect multimodal signals of 7 commonly used hand gestures on their unaffected side, which are beneficial for muscle recovery in daily activities. Each hand gesture was recorded six times, with a duration of 5 seconds per repetition and a 3-second rest period. A 30-second rest interval was provided between consecutive hand gestures. Before data collection, participants received detailed explanations about the experiment, and their informed consent was obtained. The study adhered to the principles of the Helsinki Declaration and obtained ethical approval from the ethics committee (*This work involved human subjects in its research. Approval of all ethical and experimental procedures and protocols was granted by the Ethics Committee of Beijing Rehabilitation Hospital Affiliated with Capital Medical University No. 2022bkky-048*).

*Ninapro DB1 Dataset:* We selected Ninapro DB1 Exercise C's 7 dynamic gestures (as shown in Figure 3(b)) that are beneficial for muscle recovery training. The DB1 dataset was collected from 27 participants using ten electrodes (Otto Bock MyoBock 13E200) and a data glove, capturing 10 channels of sEMG signals and 22 channels of hand and finger joint motion information. The sampling rate for each electrode was 100Hz. In Ninapro DB1 Exercise C, each hand gesture was repeated 10 times, with a 5-second duration for each active signal collection and a 3-second rest interval between each collection.



Figure 2. MYO ring acquisition signal schematic. The 7 hand gestures include fist grip, holding a cellphone, palm-to-palm exercise (cupping), cylindrical grip (holding a water cup), finger opposition exercise (thumb and index finger gripping a pen), single finger extension (extending index finger to touch the screen), and lateral thumb pinch (pinching a key, etc.) (as shown in Figure 3(a)). The multimodal signals include 8-channel sEMG signal, 3-channel arm acceleration signal, 3-channel angular velocity signal, 4-channel quaternion signal. Acceleration, angular velocity, and quaternion are inertial measurement units (IMU).

*Ninapro DB5 Dataset:* We selected Ninapro DB5 Exercise C's 7 dynamic gestures (as shown in Figure 3(c)) which differ from those selected in Ninapro DB1 Exercise Cg. The DB5 dataset was collected from 10 healthy participants using two Myo armbands (Thalmic Labs Myo) and a data glove, capturing 16 channels of sEMG signals and 22 channels of hand and finger joint motion information. The sampling rate for each electrode was 200Hz. In Ninapro DB5 Exercise C, each hand gesture was repeated six times, with a 5-second duration for each active signal collection and a 3-second rest interval between each collection.

In each dataset experiment, for the sEMG signals, a fourth-order Butterworth bandpass filter (20 Hz–500 Hz) was first applied to remove motion artifacts and high-frequency noise, preserving useful motion information. Subsequently, the sEMG signals were standardized using a min-max normalization algorithm. For motion signals, the min-max normalization method was similarly used to map the data to the range of 0–1,

facilitating subsequent processing.

### 2.2. Optimal matching signal selection module

In gesture recognition tasks, when using existing signals to recognize new user signals in the target domain, it is important to select training data from existing signals similar to the target domain. This enables knowledge transfer learning. However, determining the similarity between signals directly through observation can be challenging. When two individuals have different muscle activity patterns, their sEMG and other physiological signals often differ significantly. In such cases, selecting inappropriate source domain signals can lead to negative transfer, resulting in a decline in the performance of the recognition model.

Therefore, we propose an optimal matching signal

selection module to select highly similar signals to the target domain, enabling better transfer learning between users. The optimal matching signal selection module consists of signal similarity calculation and multimodal signal adaptation selection, as shown in Figure 4. Specifically, this method first constructs a multimodal signal database, "user1, user2, ..., user n," based on existing user data. Then, the calibration gestures of the new user obtained are compared with the signals in the database using the signal similarity calculation part to calculate the similarity of each modality. Finally, multimodal signal adaptation selection combines highly similar modal data to form the optimally matched signals, creating a new user training set. As shown in Figure 4.

*Signal Similarity Calculation:* Signal similarity assessment typically involves describing the differences

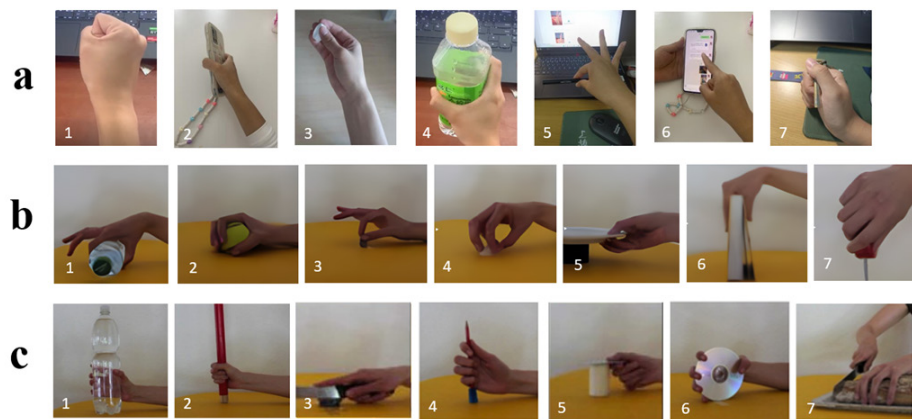


**Figure 3. Types of gestures in this paper:** (a) 7 gestures in the self-harvested stroke patient; (b) 7 dynamic gestures in the Ninapro DB1 Exercise C. (c) 7 dynamic gestures in the Ninapro DB5 Exercise C.

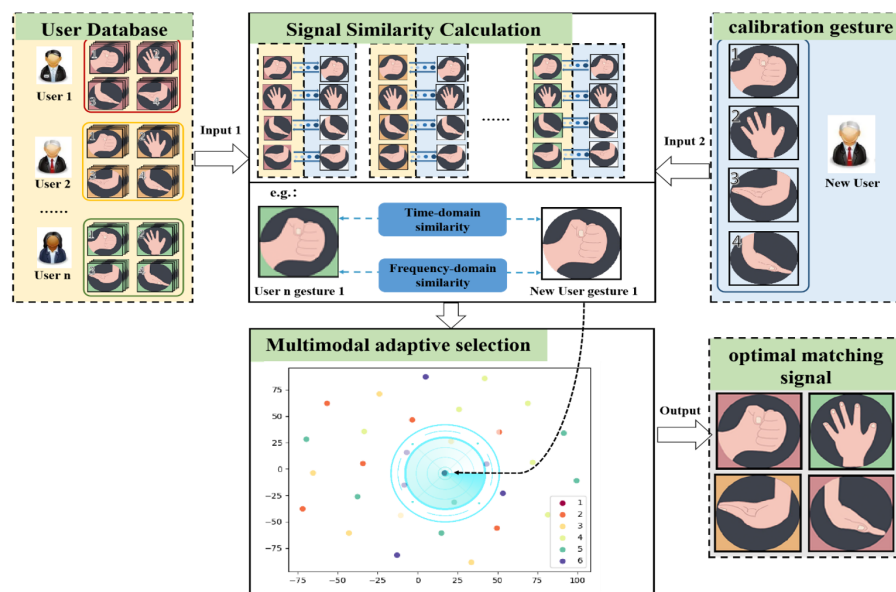


**Figure 4. Optimal matching signal selection module.**

in shape, spectrum, amplitude, and other features between two signals. Traditional methods mainly focus on time-domain calculations (26), but this approach has some limitations. Firstly, it lacks sufficient consideration of the differences in signal spectrum features. Secondly, traditional similarity measurements often use Euclidean distance or Pearson correlation coefficient, which may overlook some important features. Additionally, traditional methods cannot effectively compute the similarity between signals of inconsistent lengths. To overcome these issues, this paper proposes a new method for signal similarity calculation. This method comprehensively and accurately describes the similarity between two signals. Specifically, we consider the similarity between gesture single-cycle signals from both time and frequency domains to comprehensively evaluate their shape, spectrum, and other features. Figure 5 illustrates the detailed similarity calculation process.

Firstly, in terms of time-domain similarity calculation, this paper adopts the Dynamic Time Warping (DTW) algorithm (27) to compute the similarity  $d_{DTW}$  between two-time series. The time-domain similarity calculation  $d_{DTW}$  between two-time series  $x = \{x_1, x_2, x_3, \dots, x_n\}$  and  $y = \{y_1, y_2, y_3, \dots, y_m\}$  is calculated as shown in Equation (1):

$$d_{DTW} = -\gamma \log(\sum_{A \in A_{m,n}} e^{-(A \Delta(x,y)) / \gamma}) \quad (1)$$

Here,  $\gamma$  represents the smoothing parameter used to select the smoothness of the path, in this study, the default value of  $\gamma$  is set to 1.  $\gamma = 1$  indicates a moderate strength of the smoothing factor, which makes the path selection of DTW more focused on the optimal path while still allowing a certain degree of suboptimal paths to contribute to the weight calculation, and  $A_{m,n}$  represents the set of alignment matrices, indicating all possible paths that can be selected.  $\Delta(x,y)$  is the cost matrix composed of distance values between corresponding points of the two time series. This method effectively overcomes the potential issues caused by inconsistent lengths of time series in describing signal time-domain similarity.

In terms of frequency-domain similarity calculation, we first apply Fast Fourier Transform (FFT) to transform two time series into the frequency domain. Then, we compute the Mean Squared Error (MSE) between the amplitudes of the two frequency-domain signals to calculate the frequency-domain similarity  $d_{MSE}$ . The calculation of frequency-domain similarity  $d_{MSE}$  between two signals is as shown in Equation (2):

$$d_{MSE} = \frac{1}{len} \sum_{i=0}^{len-1} |FFT(x_i) - FFT(y_j)|^2 \quad (2)$$

Here,  $len = \min(n,m)$ , representing the length of the shorter sequence.

Next, since we aim to fully consider both the time-domain and frequency-domain information of the signals in the final similarity value, it is necessary to scale the obtained time-domain similarity value  $d_{DTW}$  and frequency-domain similarity value  $d_{MSE}$ . The scaled time-domain similarity value is denoted as  $D_{TD}$  and the scaled frequency-domain similarity value is denoted as  $D_{FD}$ . The scaling process is illustrated in Equation (3) and Equation (4):

$$D_{TD} = \frac{d_{DTW} - \text{avg}(d_{DTW_1}, \dots, d_{DTW_{i-1}}, \dots, d_{DTW_N \times L})}{\max(d_{DTW_1}, \dots, d_{DTW_{i-1}}, \dots, d_{DTW_N \times L}) - \min(d_{DTW_1}, \dots, d_{DTW_{i-1}}, \dots, d_{DTW_N \times L})} \times \sigma \quad (3)$$

$$D_{FD} = \frac{d_{MSE} - \text{avg}(d_{MSE_1}, \dots, d_{MSE_{i-1}}, \dots, d_{MSE_N \times L})}{\max(d_{MSE_1}, \dots, d_{MSE_{i-1}}, \dots, d_{MSE_N \times L}) - \min(d_{MSE_1}, \dots, d_{MSE_{i-1}}, \dots, d_{MSE_N \times L})} \times \sigma \quad (4)$$

$\sigma$  is the scaling factor used to measure the importance of time-frequency domain similarity, in this study, the scaling factor  $\sigma$  is set to 0.5, indicating that temporal information and frequency information are considered equally important for similarity calculation.

Finally, the scaled time-domain similarity value  $D_{TD}$  and frequency-domain similarity value  $D_{FD}$  are combined using Equation (5) to obtain the final signal similarity value, denoted as  $SSV$ . The signal similarity value ( $SSV$ ) represents the temporal and spectral distance between two signals, with smaller values indicating a smaller temporal and spectral distance and higher similarity between the two signals.

$$SSV = \sqrt{D_{TD}^2 + D_{FD}^2} \quad (5)$$

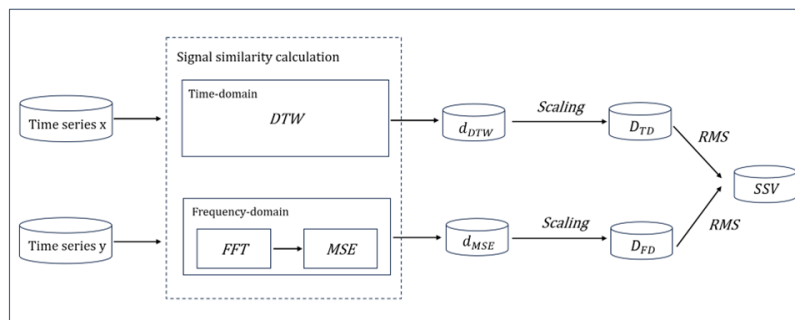


Figure 5. Signal similarity calculation process.

The input of the entire signal similarity calculation section consists of two parts. The first part is the existing user database  $D$ , which contains  $N$  users, each with  $M$  gestures, and each gesture repeated  $L$  times.  $D = \{G_1 \{R_{11}, \dots, R_{1j}, \dots, R_{1L}\}, \dots, G_k \{R_{k1}, \dots, R_{kj}, \dots, R_{kL}\}, \dots, G_M \{R_{M1}, \dots, R_{Mj}, \dots, R_{ML}\}\}$ , where  $G_k$  represents the  $k_{th}$  gesture, and  $R_{ij}$  in  $G_k$  represents the  $j_{th}$  repetition data of the  $i_{th}$  user. The second part is the calibration gesture set  $D_0$  for the new user, which includes only one new user with  $M$  gestures, each repeated once.  $D_0 = \{G_1 \{R_{01}\}, \dots, G_k \{R_{01}\}, \dots, G_M \{R_{01}\}\}$ , where  $R_{01}$  in  $G_k$  represents the single calibration gesture data of the new user.

The final output is a set  $W$  containing the similarity values between each calibration gesture data of the new user and all the repetitive data for that gesture in the database.  $W = \{G_1 \{S_{11}, \dots, S_{1j}, \dots, S_{1L}\}, \dots, G_k \{S_{k1}, \dots, S_{kj}, \dots, S_{kL}\}, \dots, G_M \{S_{M1}, \dots, S_{Mj}, \dots, S_{ML}\}\}$ , where  $S_{ij}$  in  $G_k$  represents the similarity value between the single calibration gesture data  $R_{01}$  of the new user and the  $j_{th}$  repetition data  $R_{ij}$  of the  $i_{th}$  user in the database. The pseudocode for the overall signal similarity calculation process is illustrated in Figure 6.

In the above pseudocode, the similarity calculation

is performed on the signals corresponding to the complete execution of a single gesture. This approach captures the global information within the entire time series of the gesture, accurately and intuitively reflecting the similarity between signals from both the time and frequency domains. It enables sorting the similarity between the signals in the database and the calibration gesture.

*Multimodal signal adaptation selection:* After completing the signal similarity calculation section and obtaining the similarity value set  $W$  for each modality signal in the database, the next step is to select the optimal matching signals to construct the training set based on the sorting of similarities in  $W$ . Considering the influence of data quality in the database, relying solely on the average or median of similarity indicators as a threshold and selecting all signals below this threshold as the optimal matching signals cannot guarantee the accurate selection of the optimal signals. Especially when the behavioral patterns of patients in the database are close to those of the new user, there may be a large amount of similar data, while such data may be scarce when the behavioral patterns are

---

**Algorithm 1** Optimal matching signal screening algorithm

---

**Input:** User database  $D = \{S_1, S_2, \dots, S_i, \dots, S_N\}$ , New user single calibration gesture signal  $S_0$

**Output:** Database similarity sorting set  $W$

- 1:  $S_i = \{G_1, G_2, \dots, G_i, \dots, G_M\}$  // There are  $M$  gestures per user in the database
- 2: **for**  $m = 1 \rightarrow M$  **do** //  $m$  indicates the type of gesture
- 3:      $FFT[S_0G_m] = \sum^{N-1} x(n)W_N^k$  // Calculate the FFT of the  $m$  gesture of the new user transform
- 4:     **for**  $n = 1 \rightarrow N$  **do** //  $n$  indicates the user number
- 5:          $S_nG_m = \{R_1, R_2, \dots, R_i, \dots, R_L\}$  // user  $S_n$  has a total of  $L$  repetitions of the gesture  $G_m$
- 6:         **for**  $l = 1 \rightarrow L$  **do** //  $l$  indicates gesture repetition number
- 7:              $FFT[S_0R_mG_l] = \sum^{N-1} x(n)W_N^k$  // Compute the FFT of the  $l_{th}$   $R_m$  gesture of the user  $S_n$
- 8:              $d_{MSE} = \frac{1}{N} \sum_{n=0}^{N-1} |FFT[S_0R_m] - FFT[S_0R_mG_l]|^2$  // Calculate the frequency domain similarity
- 9:              $d_{DTW} = |D[S_0R_m] - FFT[S_0R_mG_l]|^2$  // Calculate time domain similarity
- 10:         **end for**
- 11:     **end for**
- 12:     **for**  $i = 1 \rightarrow N * L$  **do**
- 13:          $d_{FD_i} = \frac{d_{MSE_i} - \text{avg}(d_{MSE_1}, \dots, d_{MSE_i}, \dots, d_{MSE_{N*L}})}{\max(d_{MSE_1}, \dots, d_{MSE_i}, \dots, d_{MSE_{N*L}}) - \min(d_{MSE_1}, \dots, d_{MSE_i}, \dots, d_{MSE_{N*L}})} \times \sigma$  // Frequency domain similarity scaling
- 14:          $d_{TD_i} = \frac{d_{DTW_i} - \text{avg}(d_{DTW_1}, \dots, d_{DTW_i}, \dots, d_{DTW_{N*L}})}{\max(d_{DTW_1}, \dots, d_{DTW_i}, \dots, d_{DTW_{N*L}}) - \min(d_{DTW_1}, \dots, d_{DTW_i}, \dots, d_{DTW_{N*L}})} \times \sigma$  // Time domain similarity scaling
- 15:     **end for**
- 16:      $d_{FD} = \{d_{FD_1}, d_{FD_2}, \dots, d_{FD_i}, \dots, d_{FD_{N*L}}\}$  // Frequency domain similarity set
- 17:      $d_{TD} = \{d_{TD_1}, d_{TD_2}, \dots, d_{TD_i}, \dots, d_{TD_{N*L}}\}$  // Time domain similarity set
- 18:      $\{D_{TD_1}, D_{FD_1}\}, \dots, \{D_{TD_L}, D_{FD_L}\}$  // Establish a similarity diagram with the time domain similarity as the horizontal coordinate and the frequency domain similarity as the vertical coordinate
- 19:      $W_m = \sqrt{d_{TD}^2 + d_{FD}^2}$  // Calculate the final similarity value of the database gesture  $m$
- 20: **end for**
- 21: **return**  $W = \{W_1, W_2, \dots, W_i, \dots, W_M\}$  // output results

---

Figure 6. Pseudo-code for signal similarity calculation.

further apart. Therefore, to adaptively select similar data and reduce the domain gap between the training set and the new user, this paper proposes an adaptive selection method for the optimal signals. This method can automatically select high-similarity signals from the database as the optimal matching signals adaptively, denoted as  $Q$  representing the number of adaptively selected optimal matching signals. The specific steps are as follows:

**Selecting and combining the top  $Q$  similar signals:** After obtaining the similarity rankings of various modality signals from the signal similarity calculation module, the value of  $Q$  is set.  $Q$  is initialized to 1, and  $Q$  signals are selected from each modality in ascending order of similarity values. After corresponding with each modality signal one by one, they are combined to create the training set.

**Train model:** The training set obtained from the previous step trains LST-EMG-Net. The model's average recognition accuracy is calculated.

**Determination of the optimal matching signals:** Increment  $Q$  by 1, then repeat steps (1) and (2). The range of  $Q$  is from 1 to  $N \times L$ . Additionally, to reduce the time required to determine the optimal  $Q$  value during model training, we stipulate that if  $Q = n$ , and the recognition accuracy  $Accuracy_n$  is greater than  $Accuracy_{n+1}$  and  $Accuracy_{n+2}$ , then it is considered that the signal similarity is higher at this point, and  $n$  is considered the optimal value. The first  $n$  similar data points are considered the optimal matching data.

The above steps demonstrate that the adaptive selection of multimodal signals allows for identifying and filtering data from the database, improving recognition accuracy. This approach mitigates the negative transfer caused by significant differences between the source and target domain signals.

### 2.3. Signal Augmentation Module

Considering the impact of the size of the database on the recognition accuracy of the model by the optimal Match Signal Selection Module, to maximize the recognition rate of the model, this paper adopts the Variational Autoencoder (VAE) (28) as an augmentation

network to generate new signal samples and enrich the training set.

The basic architecture of the VAE encoder-decoder consists of three parts: the encoder, latent variable generation, and decoder, as shown in Figure 7. The encoder uses a fully connected layer to map the input data to a latent space distribution, which is used to calculate the low-dimensional mean  $\mu$  and variance  $\sigma$  of each input sEMG signal. The latent variable generation part computes the probability density function  $Z = \{Z_1, Z_2, Z_3, \dots, Z_n\}$  by performing mathematical operations with random noise  $e$  and the mean  $\mu$  and variance  $\sigma$ . Finally, the decoder generates more diverse sEMG signals. The initial learning rate of the VAE is set to 0.0001, with the Adam optimizer used and a batch size of 100. The VAE loss function consists of two components: the reconstruction error loss and the KL divergence loss. To minimize the reconstruction error, this study employs Soft-DTW, a gradient-calculable variation of DTW similarity, as the reconstruction loss function to measure the difference between the original input data and the generated data, thereby enhancing the learning of signal temporal dependencies.

This signal augmentation method used in this study effectively doubles the quantity of sEMG signals, thereby enriching the multi-modal training samples and further contributing to improving the model's recognition accuracy.

### 2.4. Multimodal LST-EMG-Net

In the linear projection of the model LST-EMG-Net (6) that we studied previously, the sEMG segments were transformed into patch tokens and combined with Position Embedding and classification token as input to the sub-encoder, as shown in Figure 8. However, when dealing with multi-modal tasks, the sub-encoder fails to differentiate the modalities of the patch tokens. The self-attention makes capturing the continuity between different modalities challenging and hampers the information interaction between modalities.

Therefore, for multimodal tasks, we introduce a Modal-type embedding as shown by the gray vector in Figure 9. Modal-type embedding was initially

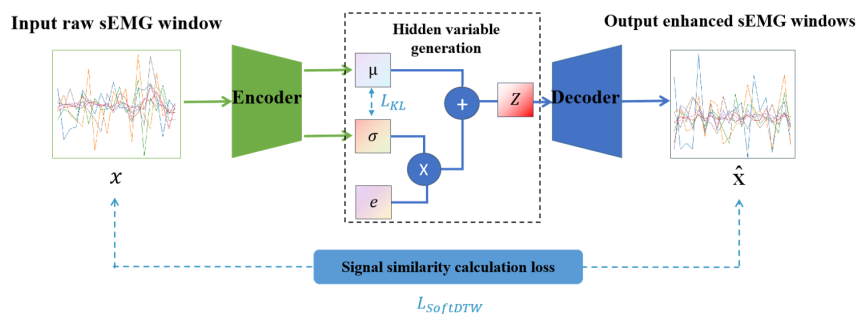


Figure 7. Structure and loss function of variational autoencoder network.

introduced by Kim *et al.* (29) in 2021 as part of a multimodal model to separately label image and text tokens, enhancing interaction between images and text. In this paper, Modal-type embedding is utilized to label sEMG and motion signals, concatenating with slice and position marker vectors. This allows the embedding of two modalities into different vector spaces of the same dimensionality, facilitating the interaction learning of category information by the encoder. The value "1" represents that the patch token is from the sEMG signal, while "2" represents that the patch token is from the motion signal.

The Modal-type embedding allows distinguishing which type of signal the patch token originates from. The Modal-type embedding is concatenated with the patch tokens and Position Embedding and then input to the sub-encoder. Multimodal LST-EMG-Net facilitates the learning of temporal characteristics within the same type of signals and promotes interaction between different modal signals.

### 3. Results

This study utilized deep learning frameworks on a computer platform for model training and testing. The computer hardware configuration used is shown in Table 2: Intel Core i7-10700K CPU (64GB RAM), GeForce GTX 3090 GPU (24GB VRAM), operating

system Ubuntu 18.04.5 LTS, and programming language Python 3.6.5. The network model was built, trained, and validated using the PyTorch 1.8.0 deep learning framework.

In the validation of the algorithm, each patient in the dataset is taken in turn as a new user and remaining data from other users in the dataset as the database. By repeating this process, we obtained recognition accuracy for each user and calculated the average recognition accuracy. The experiments were divided into three parts:

*Optimal matching signal selection experiment* : This part presents the results of signal similarity in the time-frequency domain for each modality and demonstrates the change in recognition accuracy when selecting the top N similar signals. Taking the multimodal dataset of patients as an example, it explains the process of selecting the optimal matching signals.

*Comparison experiments*: This part of the experiment compares the method in this paper with several of the more effective small-sample gesture recognition algorithms that we have summarised, in order to demonstrate the effectiveness of the method proposed in this paper by exploring the differences in the performance of the various algorithms when dealing with small-sample gesture recognition problems.

*Ablation experiment*: This part of the experiment is divided into two parts, the first part of the experiment are divided into two scenarios based on the composition of the training set. The first scenario involves not using new user data in the training set, while the second scenario involves using new user calibration gestures in the small sample data. The effectiveness of the optimal matching signal selection module, multimodal LST-EMG-Net, and similarity calculation augmentation module are validated sequentially. In the second part of the experiments, we use three different types of data, namely sEMG, IMU, and sEMG + IMU, to verify that multimodal signals yield better results compared to

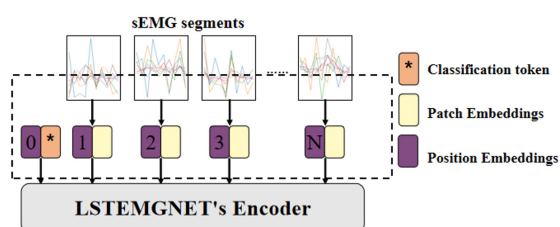


Figure 8. LST-EMG-Net Linear Projection module.

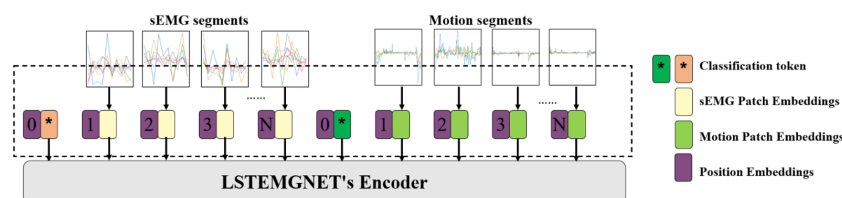


Figure 9. Multimodal LST-EMG-Net Linear Projection module.

Table 2. Computer development environment

| Hardware environment                        | Software environment                   |
|---|--|
| CPU: Intel(R) Core(TM) i7-10700K CPU 3.8GHz | Programming language: Python 3.6.5     |
| RAM: 64.00GB                                | Deep learning framework: Pytorch 1.8.0 |
| System: Ubuntu 18.04.5 LTS                  | Development tool: JetBrains Pycharm    |
| GPU: NVIDIA Geforce GTX 3090                |  |

single-modal signals.

### 3.1. Optimal matching signal selection experiment

First, we evaluated the effectiveness of the optimal matching signal selection module on the self-collected stroke patient dataset:

The 6 patients are denoted as Subject 1 to Subject 6 (S1-S6). Each patient performed 7 gestures labeled Gesture 1 to Gesture 7 (G1-G7). Each gesture had 6 repetitions labeled as Repetition 1 to Repetition 6 (R1- R6). One of the repetitions R1, R3, R4, or R6 of a gesture was randomly selected as the calibration gesture, and the repetitions R2 and R5 of the same gesture were used as the test set.

Taking S1 as the new user and R1 as the calibration gesture as an example, we used DTW (Dynamic Time Warping) and FFT (Fast Fourier Transform) to calculate the time-frequency domain distances between the user's gestures in the database and the sEMG and IMU (Inertial Measurement Unit) signals of Gesture 1 as the calibration gesture. These distances represented the similarity values between the signals, as shown in Table 3.

Table 3 shows the DTW and MSE distance as time-frequency domain similarities for each modality that Gesture 1 corresponds to a fist-clenching action. Except

for Subject 5, the sEMG signals of the other subjects show similar time-frequency domain similarities to the sEMG signal of Subject 1's calibration gesture. However, there are significant differences in the similarity of the IMU signals. This demonstrates that the muscle activation patterns are similar among the subjects for Gesture 1, but there are significant variations in the movement trajectories during fist-clenching. Therefore, cross-user recognition may rely more on the information contained in the sEMG signals. The time-frequency domain similarities from the graph above are then scaled using the multimodal signal-adaptive selection module, resulting in the sEMG and IMU similarity maps shown in Figure 10.

Each point in the graph represents one repetition of Gesture 1, and the point's color indicates the patient's identifier. The point labeled "1" represents the calibration gesture of the new user, while the other points represent the data of each patient in the database. Each patient has six points corresponding to the six repetitions of Gesture 1.

We sequentially select the data based on the distance between each point and the calibration gesture point. The point with the shortest distance is considered the most similar sEMG/IMU signal, the second closest point is the second most similar sEMG/IMU signal, and so on. We select the top N similar data points

**Table 3. Time-frequency domain similarity of sEMG and IMU for Gesture 1**

| Calibration gesture | Patient ID | Database | sEMG time domain similarity | sEMG frequency domain similarity | IMU time domain similarity | IMU frequency domain similarity |
|---------------------|------------|----------|-----------------------------|----------------------------------|----------------------------|---------------------------------|
| SIG1R1              | S2         | G1R1     | 19857                       | 87764                            | 24820                      | 136687                          |
|                     |            | G1R2     | 17113                       | 81258                            | 18848                      | 113217                          |
|                     |            | G1R3     | 17664                       | 87163                            | 28720                      | 163913                          |
|                     |            | G1R4     | 15901                       | 76296                            | 3658                       | 27274                           |
|                     |            | G1R5     | 14336                       | 79550                            | 1679                       | 16066                           |
|                     |            | G1R6     | 14099                       | 72952                            | 2336                       | 20250                           |
|                     | S3         | G1R1     | 15355                       | 70516                            | 5442                       | 19040                           |
|                     |            | G1R2     | 14253                       | 67061                            | 12605                      | 100635                          |
|                     |            | G1R3     | 14375                       | 66950                            | 2339                       | 8545                            |
|                     |            | G1R4     | 14664                       | 70103                            | 1566                       | 7007                            |
|                     |            | G1R5     | 15043                       | 69187                            | 1047                       | 11653                           |
|                     |            | G1R6     | 14684                       | 69802                            | 844                        | 4373                            |
|                     | S4         | G1R1     | 16142                       | 71191                            | -522                       | 4498                            |
|                     |            | G1R2     | 13512                       | 59287                            | -342                       | 5393                            |
|                     |            | G1R3     | 13201                       | 57734                            | -202                       | 6011                            |
|                     |            | G1R4     | 12773                       | 52954                            | 900                        | 10988                           |
|                     |            | G1R5     | 12829                       | 54230                            | -505                       | 2837                            |
|                     |            | G1R6     | 12899                       | 51904                            | 1064                       | 12723                           |
|                     | S5         | G1R1     | 34228                       | 209840                           | 10158                      | 14845                           |
|                     |            | G1R2     | 37123                       | 227054                           | 8867                       | 30776                           |
|                     |            | G1R3     | 32275                       | 194394                           | 10997                      | 38618                           |
|                     |            | G1R4     | 32814                       | 208064                           | 8233                       | 24182                           |
|                     |            | G1R5     | 24403                       | 141499                           | 10582                      | 49617                           |
|                     |            | G1R6     | 37392                       | 235632                           | 7279                       | 20191                           |
|                     | S6         | G1R1     | 15439                       | 69035                            | 4422                       | 11588                           |
|                     |            | G1R2     | 14413                       | 64632                            | 3776                       | 12296                           |
|                     |            | G1R3     | 15617                       | 64293                            | 3036                       | 10492                           |
|                     |            | G1R4     | 14855                       | 64446                            | 3006                       | 14249                           |
|                     |            | G1R5     | 14084                       | 60028                            | 2666                       | 14510                           |
|                     |            | G1R6     | 15025                       | 61445                            | 2246                       | 15820                           |

for each gesture, N refers to the number of the top N most similar data points to the current calibration gesture data, selected after sorting all the data based on similarity, repeating this process until all gestures have been used to create the training set. The recognition accuracy is evaluated using the LST-EMG-Net model, and the results are shown in Table 4 as N increases.

Table 4 shows that the average recognition accuracy initially increases and decreases as N increases. When N is less than 3, the training dataset is not saturated, and the selected data is closest to the new user. In this case, increasing N significantly improves the accuracy. As N increases to 3-5, the selected data has moderate similarity with the new user, and the average recognition accuracy fluctuates within a certain range. When N is greater than 5, the selected data have lower similarity with the new user, resulting in negative transfer effects and decreased recognition accuracy. Based on the table, in this experiment on the self-collected multimodal dataset of stroke patients, selecting N=5 achieves the highest average accuracy of

75.20%. This indicates that the selected data at this N value represents the optimal matching data.

In addition, we visualized the best-match signal screening experiments on Ninapro DB5 following the above procedure, as shown in Figure 11.

The graph illustrates that the value of N and the maximum average accuracy are related to the amount of user data in the database. In theory, as the data volume increases, more similar data are in the database, and the N value that achieves the maximum recognition accuracy will shift to the right. Therefore, for the Ninapro DB5, when N is equal to 9, the average recognition accuracy is 91.00%, both N=10 and N=11 have accuracies lower than 91.00%. Hence, for the Ninapro DB5 dataset, N=9 is considered the optimal matching signals.

### 3.2. Comparison experiments

In Table 1, we have quantitatively summarized existing literature and selected ADANN, TSnet, and AtzoriNet\*

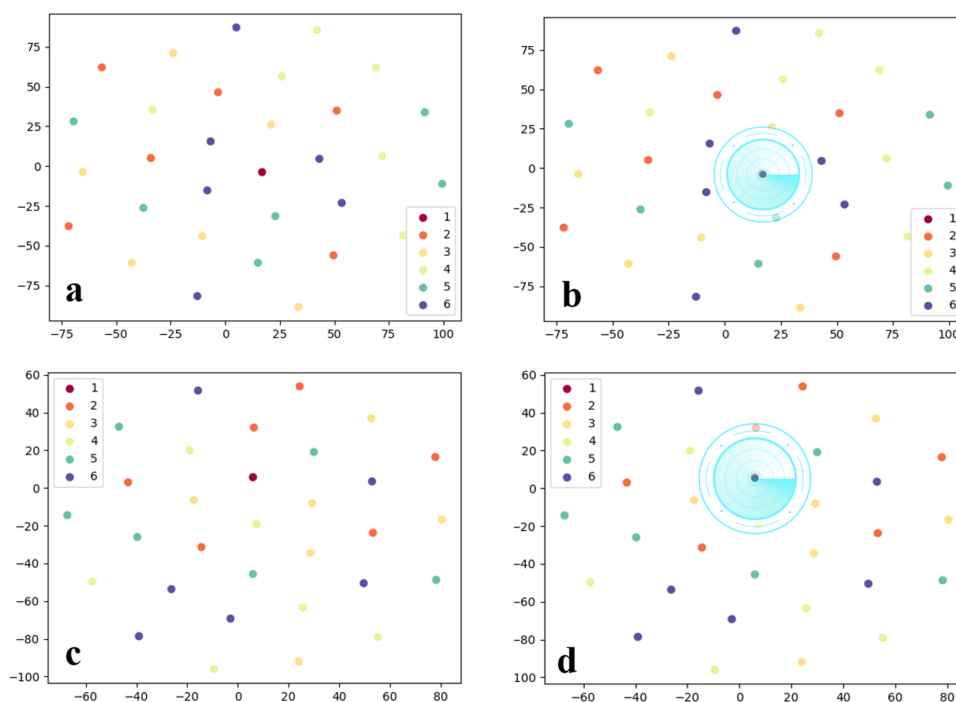


**Figure 10. Gesture 1 Similarity Graphs:** (a) sEMG Similarity Graph (b) Selection of Nearest Gestures based on sEMG Calibration Gesture (c) IMU Similarity Graph (d) Selection of Nearest Gestures based on IMU Calibration Gesture.

**Table 4. Recognition Accuracy of Subjects at Different N Values**

| Selecting Signals N | S1     | S2     | S3     | S4     | S5     | S6     | Average recognition |
|---------------------|--------|--------|--------|--------|--------|--------|---------------------|
| 1                   | 51.97% | 64.21% | 67.05% | 48.56% | 65.90% | 80.46% | 63.03%              |
| 2                   | 63.25% | 71.30% | 76.38% | 61.63% | 79.37% | 79.27% | 71.87%              |
| 3                   | 74.09% | 71.80% | 89.89% | 55.84% | 71.46% | 83.09% | 74.36%              |
| 4                   | 74.43% | 63.16% | 87.73% | 61.99% | 68.04% | 88.99% | 74.06%              |
| 5                   | 85.95% | 61.03% | 89.48% | 64.01% | 79.26% | 77.18% | 75.20%              |
| 6                   | 76.09% | 61.35% | 85.97% | 58.28% | 68.09% | 81.60% | 71.90%              |
| 7                   | 75.32% | 59.08% | 82.25% | 55.34% | 65.20% | 78.03% | 69.20%              |

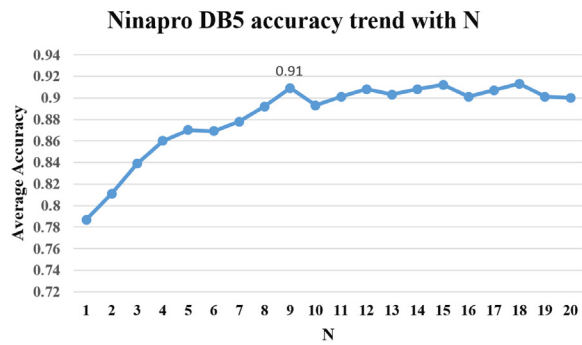


Figure 11. Average recognition accuracy of Ninapro DB5 dataset with N value.

as the three best-performing methods for comparison. In this section, we conduct comparative experiments on our self-collected stroke patient dataset, Ninapro DB1 dataset, and Ninapro DB5 dataset. Table 5 presents the average accuracy values of each comparative algorithm across the three datasets.

From Table 5, it can be observed that our method achieved an average accuracy of 93.69% on the self-collected stroke patient dataset, 98.56% on the Ninapro DB5 dataset, and 91.56% on the Ninapro DB1 dataset. This represents an improvement over ADANN by 18.42%, 5.74%, and 6.42%, respectively, over TSNet by 27.37%, 34.75%, and 4.61%, respectively, and over AtzoriNet\* by 19.41%, 33.4%, and 17.96%, respectively. Compared to the comparative algorithms ADANN, TSNet, and AtzoriNet\*, our method consistently maintains a relatively high and stable level of average accuracy across all three datasets. This is primarily attributed to the optimal signal matching module, which selects signals most similar to the new user from the existing data as the training set, thereby reducing domain differences to a large extent. Additionally, our proposed LST-EMG-Net effectively learns features from sEMG signals, resulting in excellent performance in small-sample gesture recognition.

We believe the poorer performance of the comparison algorithms compared to the proposed method may be due to two main factors. First, regarding the network architecture design, the proposed method uses a Transformer architecture, while the comparison algorithms use convolutional architectures. Compared to convolutional architectures, Transformers have significant advantages, particularly in modeling long-range dependencies in sequential data, dynamic feature extraction, efficient parallelization, and context-awareness. These advantages are especially evident when dealing with complex, multi-dimensional, long-time series data. In contrast, convolutional architectures focus on local feature extraction, limiting their ability to model complex global interactions. Secondly, in terms of data volume, the proposed method utilizes data

Table 5. Average Accuracy Values of Comparative Algorithms on Each Dataset

| Model      | Dataset         | Average recognition |
|------------|-----------------|---------------------|
| ADANN      | Stroke patients | 0.7527              |
|            | Ninapro DB5     | 0.9282              |
| AtzoriNet* | Ninapro DB1     | 0.8523              |
|            | Stroke patients | 0.7428              |
| TSNet      | Ninapro DB5     | 0.6516              |
|            | Ninapro DB1     | 0.7369              |
|            | Stroke patients | 0.6632              |
| Ours       | Ninapro DB5     | 0.6381              |
|            | Ninapro DB1     | 0.8704              |
|            | Stroke patients | 0.9369              |
|            | Ninapro DB5     | 0.9856              |
|            | Ninapro DB1     | 0.9165              |

augmentation techniques, and the enriched data volume is crucial for improving accuracy.

### 3.3. Ablation experiments

The aim is to verify whether the proposed multimodal optimal matching and augmentation method can achieve effective recognition with reduced data collection. In this section, two approaches are evaluated for recognizing new users: (1) not using new user data in the training set (Experiments 1-4) and (2) using small-sample data of the new user's calibration gesture (CG) (Experiments 5-8). Furthermore, the effectiveness of the optimal matching signal screening module (OMSS), the MM-LSTEMGNet, and the similarity calculation augmentation module (SCA) is gradually evaluated in both approaches using the self-collected stroke patient and the Ninapro DB5 dataset, as shown in Table 6.

Experiment 2 demonstrated that using the Optimal Matching Signal Screening module allows for selecting data from the database similar to the new user, effectively avoiding negative transfer. This resulted in an improvement of 19.42% and 18.77% in accuracy on the two datasets, respectively, compared to Experiment 1, where the entire database was used as the training set. The similarity calculation augmentation module effectively utilized the signals' temporal characteristics. Particularly, in Experiment 4, where calibration gesture data (CG data) was not used, there was a 9.42% increase in accuracy on the stroke patient dataset, significantly increasing the diversity of signals.

Experiment 4 showed that a model trained only on the optimal matching data achieved an accuracy of 85.85% and 93.76% on the two datasets, respectively, meeting basic rehabilitation needs. Experiment 8 demonstrated that our method using only the single repeat calibration gesture data, the accuracy reached 93.69% and 98.56% on the two datasets. This achieved results comparable to models trained on individual data while greatly reducing the burden of data collection. It makes the intelligent rehabilitation device more user-friendly and beneficial for practical application.

**Table 6. Multimodal optimal matching and augmentation method ablation experiments**

| Experiment   | CG data | OMSS | MM-LSTEMGNet | SCA | Stroke patients dataset | Ninapro DB5 dataset |
|--------------|---------|------|--------------|-----|-------------------------|---------------------|
| Experiment 1 |         |      |              |     | 55.78%                  | 72.53%              |
| Experiment 2 |         | √    |              |     | 75.20%                  | 91.30%              |
| Experiment 3 |         | √    | √            |     | 76.41%                  | 92.00%              |
| Experiment 4 |         | √    | √            | √   | <b>85.83%</b>           | <b>93.76%</b>       |
| Experiment 5 | √       |      |              |     | 88.28%                  | 95.68%              |
| Experiment 6 | √       | √    |              |     | 89.62%                  | 97.17%              |
| Experiment 7 | √       | √    | √            |     | 91.08%                  | 97.06%              |
| Experiment 8 | √       | √    | √            | √   | <b>93.69%</b>           | <b>98.56%</b>       |

To validate whether using multimodal data can improve gesture recognition accuracy, in this section, we conducted ablation experiments using two different types of data: sEMG alone + IMU alone and sEMG + IMU (IMU signals include 3 channels of arm acceleration signals, 3 channels of angular velocity signals, and 4 channels of quaternion signals). These experiments were conducted on the self-collected stroke patient dataset, Ninapro DB1 dataset, and Ninapro DB5 dataset. The results of the ablation experiments on the three datasets are shown in Table 7.

Table 7 shows that on our self-collected stroke patient dataset, using only sEMG signals resulted in an average accuracy increase of 3.15% compared to using only IMU signals. Similarly, on the Ninapro DB1 dataset and Ninapro DB5 dataset, using only IMU signals led to average accuracy improvements of 12.91% and 7.89%, respectively, compared to using only sEMG signals. Furthermore, utilizing multimodal signals achieved an average accuracy increase of 24.02% and 18.74% compared to using only sEMG signals and only IMU signals, respectively, across all three datasets. These results indicate that using multimodal signals yields higher accuracy compared to using single-modal signals.

#### 4. Discussion

To alleviate the burden of data collection in gesture recognition, we propose a new approach to address small-sample gesture recognition. This method selects the optimal matching signals with high similarity to the new user from the existing users' multimodal data, which are then used as the training set. This reduces the domain differences between the signals of the target user and the training data, thereby avoiding the negative transfer issue that can affect the model's recognition accuracy. Additionally, the method generates enhanced data, which expands the diversity of the training set signals.

Currently, research teams have publicly released large-scale datasets(30,31) such as Ninapro, Csl-hdemg, and Capgmyo, which contain multimodal information, including sEMG signals, IMU, and motion information collected from various devices. These datasets also include a substantial number of subjects and a wide

**Table 7. Results of Ablation Experiments**

| Dataset         | Sensor     | Average recognition |
|-----------------|------------|---------------------|
| Stroke patients | sEMG       | 0.7958              |
|                 | IMU        | 0.7463              |
| Ninapro DB5     | sEMG + IMU | 0.9369              |
|                 | sEMG       | 0.6938              |
|                 | IMU        | 0.7727              |
| Ninapro DB1     | sEMG + IMU | 0.9856              |
|                 | sEMG       | 0.6287              |
|                 | IMU        | 0.7578              |
|                 | sEMG + IMU | 0.9165              |

variety of gestures. Therefore, it is relatively easy to obtain a large amount of multimodal public data to build small-sample databases, providing strong support for the portable use of our method.

However, in the adaptive selection of the optimal signal, the method proposed in this paper still relies on evaluating the model accuracy to screen the optimal matching signals, which requires a certain amount of computational resources. Because the time required for the optimal matching signal selection process is influenced by the number of users in the database. The more users in the database, the more similarity calculations are needed between the new user's data and the existing user data, ultimately increasing the time required for the optimal matching signal selection, we are considering, as a potential avenue for future research, the development of a method for extracting common features of user gestures. This method would aim to extract common features from all users in the database for a specific action. By comparing the gesture data features of new users with the common features of relevant actions in the database, this approach can identify the type of gesture performed by the new user. Such a method would reduce the time overhead associated with an increasing number of users in the database, thereby making the gesture recognition method more effective in practical applications.

In addition, an increase in the number of users does not necessarily lead to more training cycles, as it depends on whether there is beneficial similar data in the dataset. Currently, the entire system in practical applications consists of three main components: user data collection, model training, and model usage. The time required to collect user samples has been reduced

from 6 collections in traditional algorithms to just 1, resulting in an efficiency improvement of 83.3%. The entire model training process takes approximately 15 minutes, and these two steps only need to be performed once. After that, the main focus during model usage is the inference time. The model inference time proposed in this paper is only 4-6 milliseconds, which fully meets the real-time usage needs of new users.

As this study is conducted in the context of hand rehabilitation training for stroke patients, the gestures used are predefined as part of the rehabilitation program. In contrast to random gestures performed in daily life, the gestures in this study exhibit low uncertainty. However, in real-life scenarios, patients' movements entail randomness and uncertainty. To address these issues, we plan to harness the potential of graph structure learning, such as leveraging methods like "EGNN: Graph structure learning based on evolutionary computation" (32), for further improvement and enhancement. We believe that graph-based learning can be applied to small-sample cross-user recognition for sEMG signals. In cross-user recognition tasks, the nodes in the graph network can represent the signal features or muscle activity patterns of different users, while the edges represent the similarity or dependency of signals between different users. This approach creates a shared feature space across users, enabling model transfer learning or knowledge sharing between users.

In summary, the multimodal optimal matching and augmentation method effectively improves small-sample gesture recognition accuracy. When using only a single calibration gesture, it achieves 93.69%, 91.65% and 98.56% accuracy on the multimodal dataset of stroke patients, the publicly available Ninapro DB1 dataset and the publicly available Ninapro DB5 dataset, respectively, comparable to the performance of traditional recognition models trained on personal data. In the future, our method will be applied to active hand rehabilitation treatment for stroke patients.

**Funding:** This work was supported by a grant from the Special Project on Scientific Research and Development of Beijing Rehabilitation Hospital Affiliated with Capital Medical University (2022-001). Beijing Municipal Science and Technology Program: Research and Translational Application of Clinical Characteristic Diagnostic and Treatment Techniques in the Capital City (Project No. Z221100007422113).

**Conflict of Interest:** The authors have no conflicts of interest to disclose.

## References

- Amin MS, Rizvi STH, Hossain MM. A comparative review on applications of different sensors for sign language recognition. *Journal of Imaging*. 2022; 8:98.
- Yadav D, Veer K. Recent trends and challenges of surface electromyography in prosthetic applications. *Biomedical Engineering Letters*. 2023; 13:353-373.
- Tong L, Zhang M, Ma H, Wang C, Peng L. sEMG-based gesture recognition method for coal mine inspection manipulator using multistream CNN. *IEEE Sensors Journal*. 2023; 23:11082-11090.
- Mahmud A, Heidari O, Schoen MP. sEMG based Real-Time Motion Classification using Virtual Reality and Artificial Neural Networks. *Journal of Electrical Engineering*. 2022; 4:241-256.
- Li W, Shi P, Yu H. Gesture recognition using surface electromyography and deep learning for prostheses hand: state-of-the-art, challenges, and future. *Frontiers in neuroscience*. 2021; 15:621885.
- Zhang W, Zhao T, Zhang J, Wang Y. LST-EMG-Net: Long short-term transformer feature fusion network for sEMG gesture recognition. *Frontiers in Neurobotics*. 2023; 17:1127338.
- Atzori M, Gijsberts A, Castellini C, Caputo B, Hager A-GM, Elsig S, Giatsidis G, Bassetto F, Müller H. Electromyography data for non-invasive naturally-controlled robotic hand prostheses. *Scientific data*. 2014; 1:1-13.
- Atzori M, Gijsberts A, Kuzborskij I, Elsig S, Hager A-GM, Deriaz O, Castellini C, Müller H, Caputo B. Characterization of a benchmark database for myoelectric movement classification. *IEEE transactions on neural systems and rehabilitation engineering*. 2014; 23:73-83.
- Gijsberts A, Atzori M, Castellini C, Müller H, Caputo B. Measuring movement classification performance with the movement error rate. *IEEE Trans Neural Syst Rehabil Eng*. 2014; 89621:735-744.
- Atzori M, Gijsberts A, Heynen S, Hager A-GM, Deriaz O, Van Der Smagt P, Castellini C, Caputo B, Müller H. Building the Ninapro database: A resource for the biorobotics community. In: 2012 4th IEEE RAS & EMBS International Conference on Biomedical Robotics and Biomechanics (BioRob) (IEEE, 2012; pp. 1258-1265.
- Rampichini S, Vieira TM, Castiglioni P, Merati G. Complexity analysis of surface electromyography for assessing the myoelectric manifestation of muscle fatigue: A review. *Entropy*. 2020; 22:529.
- He J, Jiang N. Biometric from surface electromyogram (sEMG): Feasibility of user verification and identification based on gesture recognition. *Frontiers in bioengineering and biotechnology*. 2020; 8:58.
- Kanoga S, Hoshino T, Asoh H. Semi-supervised style transfer mapping-based framework for sEMG-based pattern recognition with 1-or 2-DoF forearm motions. *Biomedical Signal Processing and Control*. 2021; 68:102817.
- Azab AM, Mihaylova L, Ang KK, Arvaneh M. Weighted transfer learning for improving motor imagery-based brain-computer interface. *IEEE Transactions on Neural Systems and Rehabilitation Engineering*. 2019; 27:1352-1359.
- Wang K, Chen Y, Zhang Y, Yang X, Hu C. Multi-source integration based transfer learning method for cross-user semg gesture recognition. In: 2022 International Joint Conference on Neural Networks (IJCNN) (IEEE, 2022; pp. 1-8.

16. Colli Alfaro JG, Trejos AL. User-independent hand gesture recognition classification models using sensor fusion. *Sensors*. 2022; 22:1321.
  17. Sheng X, Lv B, Guo W, Zhu X. Common spatial-spectral analysis of EMG signals for multiday and multiuser myoelectric interface. *Biomedical Signal Processing and Control*. 2019; 53:101572.
  18. Campbell E, Phinyomark A, Scheme E. Deep cross-user models reduce the training burden in myoelectric control. *Frontiers in Neuroscience*. 2021; 15:657958.
  19. Tsinganos P, Cornelis J, Cornelis B, Jansen B, Skodras A. Transfer learning in semg-based gesture recognition. In: 2021 12th International Conference on Information, Intelligence, Systems & Applications (IISA) (IEEE, 2021); pp. 1-7.
  20. Yu Z, Zhao J, Wang Y, He L, Wang S. Surface EMG-based instantaneous hand gesture recognition using convolutional neural network with the transfer learning method. *Sensors*. 2021; 21:2540.
  21. Novick LR. Analogical transfer, problem similarity, and expertise. *Journal of Experimental Psychology: Learning, memory, and cognition*. 1988; 14:510.
  22. Abdullah SMSA, Ameen SYA, Sadeeq MA, Zeebaree S. Multimodal emotion recognition using deep learning. *Journal of Applied Science and Technology Trends*. 2021; 2:73-79.
  23. Liu W, Qiu JL, Zheng WL, Lu BL. Multimodal Emotion Recognition Using Deep Canonical Correlation Analysis. 2019.
  24. Yan M, Deng Z, He B, Zou C, Wu J, Zhu Z. Emotion classification with multichannel physiological signals using hybrid feature and adaptive decision fusion. *Biomedical Signal Processing and Control*. 2022; 71:103235.
  25. Gandhi A, Adhvaryu K, Poria S, Cambria E, Hussain A. Multimodal sentiment analysis: A systematic review of history, datasets, multimodal fusion methods, applications, challenges and future directions. *Information Fusion*. 2023; 91:424-444.
  26. Singh MK, Singh N, Singh A. Speaker's voice characteristics and similarity measurement using Euclidean distances. In: 2019 International Conference on Signal Processing and Communication (ICSC) (IEEE, 2019); pp. 317-322.
  27. Müller M. Information Retrieval for Music and Motion. *Information Retrieval for Music and Motion*. 2007.
  28. Kingma DP, Welling M. An introduction to variational autoencoders. *Foundations and Trends® in Machine Learning*. 2019; 12:307-392.
  29. Kim W, Son B, Kim I. Vilt: Vision-and-language transformer without convolution or region supervision. In: International conference on machine learning (PMLR, 2021); pp. 5583-5594.
  30. Geng W, Du Y, Jin W, Wei W, Hu Y, Li J. Gesture recognition by instantaneous surface EMG images. *Scientific reports*. 2016; 6:36571.
  31. Dai Q, Li X, Geng W, Jin W, Liang X. CAPG-MYO: a muscle-computer interface supporting user-defined gesture recognition. In: Proceedings of the 9th International Conference on Computer and Communications Management (2021); pp. 52-58.
  32. Liu Z, Yang D, Wang Y, Lu M, Li R. EGNN: Graph structure learning based on evolutionary computation helps more in graph neural networks. *Applied Soft Computing*. 2023; 135:110040.
- Received November 23, 2024; Revised January 5, 2025; Accepted January 21, 2025.
- \*Address correspondence to:*  
Wenli Zhang, Faculty of Information Science and Technology, Beijing University of Technology, Beijing, 100124, China  
E-mail: zhangwenli@bjut.edu.cn
- Released online in J-STAGE as advance publication January 25, 2025.



## Guide for Authors

### 1. Scope of Articles

*BioScience Trends* (Print ISSN 1881-7815, Online ISSN 1881-7823) is an international peer-reviewed journal. *BioScience Trends* devotes to publishing the latest and most exciting advances in scientific research. Articles cover fields of life science such as biochemistry, molecular biology, clinical research, public health, medical care system, and social science in order to encourage cooperation and exchange among scientists and clinical researchers.

### 2. Submission Types

**Original Articles** should be well-documented, novel, and significant to the field as a whole. An Original Article should be arranged into the following sections: Title page, Abstract, Introduction, Materials and Methods, Results, Discussion, Acknowledgments, and References. Original articles should not exceed 5,000 words in length (excluding references) and should be limited to a maximum of 50 references. Articles may contain a maximum of 10 figures and/or tables. Supplementary Data are permitted but should be limited to information that is not essential to the general understanding of the research presented in the main text, such as unaltered blots and source data as well as other file types.

**Brief Reports** definitively documenting either experimental results or informative clinical observations will be considered for publication in this category. Brief Reports are not intended for publication of incomplete or preliminary findings. Brief Reports should not exceed 3,000 words in length (excluding references) and should be limited to a maximum of 4 figures and/or tables and 30 references. A Brief Report contains the same sections as an Original Article, but the Results and Discussion sections should be combined.

**Reviews** should present a full and up-to-date account of recent developments within an area of research. Normally, reviews should not exceed 8,000 words in length (excluding references) and should be limited to a maximum of 10 figures and/or tables and 100 references. Mini reviews are also accepted, which should not exceed 4,000 words in length (excluding references) and should be limited to a maximum of 5 figures and/or tables and 50 references.

**Policy Forum** articles discuss research and policy issues in areas related to life science such as public health, the medical care system, and social science and may address governmental issues at district, national, and international levels of discourse. Policy Forum articles should not exceed 3,000 words in length (excluding references) and should be limited to a maximum of 5 figures and/or tables and 30 references.

**Communications** are short, timely pieces that spotlight new research findings or policy issues of interest to the field of global health and medical practice that are of immediate importance. Depending on their content, Communications will be published as "Comments" or "Correspondence". Communications should not exceed 1,500 words in length (excluding references) and should be limited to a maximum of 2 figures and/or tables and 20 references.

**Editorials** are short, invited opinion pieces that discuss an issue of immediate importance to the fields of global health, medical practice, and basic science oriented for clinical application. Editorials should not exceed 1,000 words in length (excluding references) and should be limited to a maximum of 10 references. Editorials may contain one figure or table.

**News** articles should report the latest events in health sciences and medical research from around the world. News should not exceed 500 words in length.

**Letters** should present considered opinions in response to articles published in *BioScience Trends* in the last 6 months or issues of general interest. Letters should not exceed 800 words in length and may contain a maximum of 10 references. Letters may contain one figure or table.

### 3. Editorial Policies

For publishing and ethical standards, *BioScience Trends* follows the Recommendations for the Conduct, Reporting, Editing, and Publication of Scholarly Work in Medical Journals issued by the International Committee of Medical Journal Editors (ICMJE, <https://icmje.org/recommendations>), and the Principles of Transparency and Best Practice in Scholarly Publishing jointly issued by the Committee on Publication Ethics (COPE, <https://publicationethics.org/resources/guidelines-new/principles-transparency-and-best-practice-scholarly-publishing>), the Directory of Open Access Journals (DOAJ, <https://doaj.org/apply/transparency>), the Open Access Scholarly Publishers Association (OASPA, <https://oaspa.org/principles-of-transparency-and-best-practice-in-scholarly-publishing-4>), and the World Association of Medical Editors (WAME, <https://wame.org/principles-of-transparency-and-best-practice-in-scholarly-publishing>).

*BioScience Trends* will perform an especially prompt review to encourage innovative work. All original research will be subjected to a rigorous standard of peer review and will be edited by experienced copy editors to the highest standards.

**Ethical Approval of Studies and Informed Consent:** For all manuscripts reporting data from studies involving human participants or animals, formal review and approval, or formal review and waiver, by an appropriate institutional review board or ethics committee is required and should be described in the Methods section. When your manuscript contains any case details, personal information and/or images of patients or other individuals, authors must obtain appropriate written consent, permission and release in order to comply with all applicable laws and regulations concerning privacy and/or security of personal information. The consent form needs to comply with the relevant legal requirements of your particular jurisdiction, and please do not send signed consent form to *BioScience Trends* to respect your patient's and any other individual's privacy. Please instead describe the information clearly in the Methods (patient consent) section of your manuscript while retaining copies of the signed forms in the event they should be needed. Authors should also state that the study conformed to the provisions of the Declaration of Helsinki (as revised in 2013, <https://wma.net/what-we-do/medical-ethics/declaration-of-helsinki>). When reporting experiments on animals, authors should indicate whether the institutional and national guide for the care and use of laboratory animals was followed.

**Reporting Clinical Trials:** The ICMJE (<https://icmje.org/recommendations/browse/publishing-and-editorial-issues/clinical-trial-registration.html>) defines a clinical trial as any research project that prospectively assigns people or a group of people to an intervention, with or without concurrent comparison or control groups, to study the relationship between a health-related intervention and a health outcome. Registration of clinical trials in a public trial registry at or before the time of first patient enrollment is a condition of consideration for publication in *BioScience Trends*, and the trial registration number will be published at the end of the Abstract. The registry must be independent of for-profit interest and publicly accessible. Reports of trials must conform to CONSORT 2010 guidelines (<https://consort-statement.org/consort-2010>). Articles reporting the results of randomized trials must include the CONSORT flow diagram showing the progress of patients throughout the trial.

**Conflict of Interest:** All authors are required to disclose any actual or potential conflict of interest including financial interests or relationships with other people or organizations that might raise questions of bias

in the work reported. If no conflict of interest exists for each author, please state "There is no conflict of interest to disclose".

**Submission Declaration:** When a manuscript is considered for submission to *BioScience Trends*, the authors should confirm that 1) no part of this manuscript is currently under consideration for publication elsewhere; 2) this manuscript does not contain the same information in whole or in part as manuscripts that have been published, accepted, or are under review elsewhere, except in the form of an abstract, a letter to the editor, or part of a published lecture or academic thesis; 3) authorization for publication has been obtained from the authors' employer or institution; and 4) all contributing authors have agreed to submit this manuscript.

**Initial Editorial Check:** Immediately after submission, the journal's managing editor will perform an initial check of the manuscript. A suitable academic editor will be notified of the submission and invited to check the manuscript and recommend reviewers. Academic editors will check for plagiarism and duplicate publication at this stage. The journal has a formal recusal process in place to help manage potential conflicts of interest of editors. In the event that an editor has a conflict of interest with a submitted manuscript or with the authors, the manuscript, review, and editorial decisions are managed by another designated editor without a conflict of interest related to the manuscript.

**Peer Review:** *BioScience Trends* operates a single-anonymized review process, which means that reviewers know the names of the authors, but the authors do not know who reviewed their manuscript. All articles are evaluated objectively based on academic content. External peer review of research articles is performed by at least two reviewers, and sometimes the opinions of more reviewers are sought. Peer reviewers are selected based on their expertise and ability to provide quality, constructive, and fair reviews. For research manuscripts, the editors may, in addition, seek the opinion of a statistical reviewer. Every reviewer is expected to evaluate the manuscript in a timely, transparent, and ethical manner, following the COPE guidelines ([https://publicationethics.org/files/cope-ethical-guidelines-peer-reviewers-v2\\_0.pdf](https://publicationethics.org/files/cope-ethical-guidelines-peer-reviewers-v2_0.pdf)). We ask authors for sufficient revisions (with a second round of peer review, when necessary) before a final decision is made. Consideration for publication is based on the article's originality, novelty, and scientific soundness, and the appropriateness of its analysis.

**Suggested Reviewers:** A list of up to 3 reviewers who are qualified to assess the scientific merit of the study is welcomed. Reviewer information including names, affiliations, addresses, and e-mail should be provided at the same time the manuscript is submitted online. Please do not suggest reviewers with known conflicts of interest, including participants or anyone with a stake in the proposed research; anyone from the same institution; former students, advisors, or research collaborators (within the last three years); or close personal contacts. Please note that the Editor-in-Chief may accept one or more of the proposed reviewers or may request a review by other qualified persons.

**Language Editing:** Manuscripts prepared by authors whose native language is not English should have their work proofread by a native English speaker before submission. If not, this might delay the publication of your manuscript in *BioScience Trends*.

The Editing Support Organization can provide English proofreading, Japanese-English translation, and Chinese-English translation services to authors who want to publish in *BioScience Trends* and need assistance before submitting a manuscript. Authors can visit this organization directly at <https://www.iacmhr.com/iac-eso/support.php?lang=en>. IAC-ESO was established to facilitate manuscript preparation by researchers whose native language is not English and to help edit works intended for international academic journals.

**Copyright and Reuse:** Before a manuscript is accepted for publication in *BioScience Trends*, authors will be asked to sign a transfer of copyright agreement, which recognizes the common

interest that both the journal and author(s) have in the protection of copyright. We accept that some authors (e.g., government employees in some countries) are unable to transfer copyright. A JOURNAL PUBLISHING AGREEMENT (JPA) form will be e-mailed to the authors by the Editorial Office and must be returned by the authors by mail, fax, or as a scan. Only forms with a hand-written signature from the corresponding author are accepted. This copyright will ensure the widest possible dissemination of information. Please note that the manuscript will not proceed to the next step in publication until the JPA Form is received. In addition, if excerpts from other copyrighted works are included, the author(s) must obtain written permission from the copyright owners and credit the source(s) in the article.

#### 4. Cover Letter

The manuscript must be accompanied by a cover letter prepared by the corresponding author on behalf of all authors. The letter should indicate the basic findings of the work and their significance. The letter should also include a statement affirming that all authors concur with the submission and that the material submitted for publication has not been published previously or is not under consideration for publication elsewhere. The cover letter should be submitted in PDF format. For an example of Cover Letter, please visit: <https://www.biosciencetrends.com/downcentre> (Download Centre).

#### 5. Submission Checklist

The Submission Checklist should be submitted when submitting a manuscript through the Online Submission System. Please visit Download Centre (<https://www.biosciencetrends.com/downcentre>) and download the Submission Checklist file. We recommend that authors use this checklist when preparing your manuscript to check that all the necessary information is included in your article (if applicable), especially with regard to Ethics Statements.

#### 6. Manuscript Preparation

Manuscripts are suggested to be prepared in accordance with the "Recommendations for the Conduct, Reporting, Editing, and Publication of Scholarly Work in Medical Journals", as presented at <https://www.ICMJE.org>.

Manuscripts should be written in clear, grammatically correct English and submitted as a Microsoft Word file in a single-column format. Manuscripts must be paginated and typed in 12-point Times New Roman font with 24-point line spacing. Please do not embed figures in the text. Abbreviations should be used as little as possible and should be explained at first mention unless the term is a well-known abbreviation (e.g. DNA). Single words should not be abbreviated.

**Title page:** The title page must include 1) the title of the paper (Please note the title should be short, informative, and contain the major key words); 2) full name(s) and affiliation(s) of the author(s), 3) abbreviated names of the author(s), 4) full name, mailing address, telephone/fax numbers, and e-mail address of the corresponding author; 5) author contribution statements to specify the individual contributions of all authors to this manuscript, and 6) conflicts of interest (if you have an actual or potential conflict of interest to disclose, it must be included as a footnote on the title page of the manuscript; if no conflict of interest exists for each author, please state "There is no conflict of interest to disclose").

**Abstract:** The abstract should briefly state the purpose of the study, methods, main findings, and conclusions. For articles that are Original Articles, Brief Reports, Reviews, or Policy Forum articles, a one-paragraph abstract consisting of no more than 250 words must be included in the manuscript. For Communications, Editorials, News, or Letters, a brief summary of main content in 150 words or fewer should be included in the manuscript. For articles reporting clinical trials, the trial registration number should be stated at the end of the Abstract. Abbreviations must be kept to a minimum and non-standard

abbreviations explained in brackets at first mention. References should be avoided in the abstract. Three to six key words or phrases that do not occur in the title should be included in the Abstract page.

**Introduction:** The introduction should provide sufficient background information to make the article intelligible to readers in other disciplines and sufficient context clarifying the significance of the experimental findings

**Materials/Patients and Methods:** The description should be brief but with sufficient detail to enable others to reproduce the experiments. Procedures that have been published previously should not be described in detail but appropriate references should simply be cited. Only new and significant modifications of previously published procedures require complete description. Names of products and manufacturers with their locations (city and state/country) should be given and sources of animals and cell lines should always be indicated. All clinical investigations must have been conducted in accordance Materials/Patients and Methods.

**Results:** The description of the experimental results should be succinct but in sufficient detail to allow the experiments to be analyzed and interpreted by an independent reader. If necessary, subheadings may be used for an orderly presentation. All Figures and Tables should be referred to in the text in order, including those in the Supplementary Data.

**Discussion:** The data should be interpreted concisely without repeating material already presented in the Results section. Speculation is permissible, but it must be well-founded, and discussion of the wider implications of the findings is encouraged. Conclusions derived from the study should be included in this section.

**Acknowledgments:** All funding sources (including grant identification) should be credited in the Acknowledgments section. Authors should also describe the role of the study sponsor(s), if any, in study design; in the collection, analysis, and interpretation of data; in the writing of the report; and in the decision to submit the paper for publication. If the funding source had no such involvement, the authors should so state.

In addition, people who contributed to the work but who do not meet the criteria for authors should be listed along with their contributions.

**References:** References should be numbered in the order in which they appear in the text. Citing of unpublished results, personal communications, conference abstracts, and theses in the reference list is not recommended but these sources may be mentioned in the text. In the reference list, cite the names of all authors when there are fifteen or fewer authors; if there are sixteen or more authors, list the first three followed by *et al.* Names of journals should be abbreviated in the style used in PubMed. Authors are responsible for the accuracy of the references. The EndNote Style of *BioScience Trends* could be downloaded at **EndNote** ([https://ircabssagroup.com/examples/BioScience\\_Trends.ens](https://ircabssagroup.com/examples/BioScience_Trends.ens)).

Examples are given below:

*Example 1 (Sample journal reference):*

Inagaki Y, Tang W, Zhang L, Du GH, Xu WF, Kokudo N. Novel aminopeptidase N (APN/CD13) inhibitor 24F can suppress invasion of hepatocellular carcinoma cells as well as angiogenesis. *Biosci Trends*. 2010; 4:56-60.

*Example 2 (Sample journal reference with more than 15 authors):*

Darby S, Hill D, Auvinen A, *et al.* Radon in homes and risk of lung cancer: Collaborative analysis of individual data from 13 European case-control studies. *BMJ*. 2005; 330:223.

*Example 3 (Sample book reference):*

Shalev AY. Post-traumatic stress disorder: Diagnosis, history and life course. In: *Post-traumatic Stress Disorder, Diagnosis, Management and Treatment* (Nutt DJ, Davidson JR, Zohar J, eds.). Martin Dunitz, London, UK, 2000; pp. 1-15.

*Example 4 (Sample web page reference):*

World Health Organization. The World Health Report 2008 – primary health care: Now more than ever. [http://www.who.int/whr/2008/whr08\\_en.pdf](http://www.who.int/whr/2008/whr08_en.pdf) (accessed September 23, 2022).

**Tables:** All tables should be prepared in Microsoft Word or Excel and should be arranged at the end of the manuscript after the References section. Please note that tables should not in image format. All tables should have a concise title and should be numbered consecutively with Arabic numerals. If necessary, additional information should be given below the table.

**Figure Legend:** The figure legend should be typed on a separate page of the main manuscript and should include a short title and explanation. The legend should be concise but comprehensive and should be understood without referring to the text. Symbols used in figures must be explained. Any individually labeled figure parts or panels (A, B, *etc.*) should be specifically described by part name within the legend.

**Figure Preparation:** All figures should be clear and cited in numerical order in the text. Figures must fit a one- or two-column format on the journal page: 8.3 cm (3.3 in.) wide for a single column, 17.3 cm (6.8 in.) wide for a double column; maximum height: 24.0 cm (9.5 in.). Please make sure that the symbols and numbers appeared in the figures should be clear. Please make sure that artwork files are in an acceptable format (TIFF or JPEG) at minimum resolution (600 dpi for illustrations, graphs, and annotated artwork, and 300 dpi for micrographs and photographs). Please provide all figures as separate files. Please note that low-resolution images are one of the leading causes of article resubmission and schedule delays.

**Units and Symbols:** Units and symbols conforming to the International System of Units (SI) should be used for physicochemical quantities. Solidus notation (*e.g.* mg/kg, mg/mL, mol/mm<sup>2</sup>/min) should be used. Please refer to the SI Guide [www.bipm.org/en/si/](http://www.bipm.org/en/si/) for standard units.

**Supplemental data:** Supplemental data might be useful for supporting and enhancing your scientific research and *BioScience Trends* accepts the submission of these materials which will be only published online alongside the electronic version of your article. Supplemental files (figures, tables, and other text materials) should be prepared according to the above guidelines, numbered in Arabic numerals (*e.g.*, Figure S1, Figure S2, and Table S1, Table S2) and referred to in the text. All figures and tables should have titles and legends. All figure legends, tables and supplemental text materials should be placed at the end of the paper. Please note all of these supplemental data should be provided at the time of initial submission and note that the editors reserve the right to limit the size and length of Supplemental Data.

## 5. Submission Checklist

The Submission Checklist will be useful during the final checking of a manuscript prior to sending it to *BioScience Trends* for review. Please visit Download Centre and download the Submission Checklist file.

## 6. Online Submission

Manuscripts should be submitted to *BioScience Trends* online at <https://www.biosciencetrends.com/login>. Receipt of your manuscripts submitted online will be acknowledged by an e-mail from Editorial Office containing a reference number, which should be used in all future communications. If for any reason you are unable to submit a file online, please contact the Editorial Office by e-mail at [office@biosciencetrends.com](mailto:office@biosciencetrends.com)

## 8. Accepted Manuscripts

**Page Charge:** Page charges will be levied on all manuscripts accepted for publication in *BioScience Trends* (Original Articles / Brief Reports / Reviews / Policy Forum / Communications: \$140 per page for black white pages, \$340 per page for color pages; News / Letters: a total cost of \$600). Under exceptional circumstances, the author(s) may apply to the editorial office for a waiver of the publication charges by stating the reason in the Cover Letter when the manuscript online.

**Misconduct:** *BioScience Trends* takes seriously all allegations of potential misconduct and adhere to the ICMJE Guideline (<https://icmje.org/recommendations>) and COPE Guideline ([https://publicationethics.org/files/Code\\_of\\_conduct\\_for\\_journal\\_editors.pdf](https://publicationethics.org/files/Code_of_conduct_for_journal_editors.pdf)). In cases of

suspected research or publication misconduct, it may be necessary for the Editor or Publisher to contact and share submission details with third parties including authors' institutions and ethics committees. The corrections, retractions, or editorial expressions of concern will be performed in line with above guidelines.

(As of December 2022)

**BioScience Trends**  
Editorial and Head Office  
Pearl City Koishikawa 603,  
2-4-5 Kasuga, Bunkyo-ku,  
Tokyo 112-0003, Japan.

E-mail: [office@biosciencetrends.com](mailto:office@biosciencetrends.com)



